

**LIME MORTAR AND PLASTER
CHARACTERISTICS OF SOME BYZANTINE
PERIOD BUILDINGS IN KADIKALESİ (ANAIA)
AND AYASULUK HILL**

**A Thesis Submitted to
the Graduate School of Engineering and Sciences of
İzmir Institute of Technology
in Partial Fulfillment of the Requirements for the Degree of**

MASTER OF SCIENCE

in Architectural Restoration

**by
Tuğçe IŞIK**

**July 2022
İZMİR**

ACKNOWLEDGMENTS

I would like to extend my deepest gratitude to my supervisor, Assoc. Prof. Dr. Elif Uğurlu Sağın for her scientific guidance, spectacular contributions, and invaluable support during this thesis. I am incredibly grateful to her because of different perspectives she adds to the subjects broaden my horizon. She provided deep and effective traces for my educational perspective thanks to her competence in the field. I would also like to mention that it has been an honor for me to be one of her first master's students.

I should also appreciate Prof. Dr. Başak İpekoğlu for always supporting and contributing to laying the foundations of the study by collaboration with the excavation team. I am extremely grateful to Prof. Dr. Hasan Böke for outstanding advises and encouragement for the research. I must also thank Inst. Dr. Kerem Şerifaki for conveying his wide experience, especially in interpreting the SEM images and guidance for the research. I must also like to thank Res. Assist. Ayşen Etlacakuş for her cheerfulness and helpfulness.

I would like to pay my special regards to Prof. Dr. Zeynep Mercangöz, and Assoc. Prof. Dr. Sinan Mimaroglu for their hospitality, valuable contributions to thesis and precious advises. I must also thank to excavation team of Kadıkalesi and Ayasuluk for their companionship, and helpfulness.

I am very grateful to jury members Prof. Dr. Mine Turan, and Assoc. Prof. Dr. Sinan Mimaroglu for their participation to thesis jury.

I am also thankful to Integrated Research Centers, where SEM-EDS, XRD, and TGA analyses were done. I would like to recognize the invaluable assistance of especially Zehra Sinem Yılmaz for her tolerance, unlimited help, and conveying information about SEM-EDS. I would also like to extend my sincere thanks to Dr. Taygun Uzelli for his helpfulness, precious contributions to the thesis, and unlimited support, especially in identifying raw material provenances.

I wish also thank to my dearest friends Hatice Ayşegül Demir, Tuğçe Tekin, Nihan Bulut, Zeynep Özkaya and Rabia Nur Bilekli to make this study easier by providing a lot of fun. I would like to especially thank to my dear friend Elif Çam for the good and amusing times we spent together during the fieldwork and laboratory process. She was always there for me and provided all kinds of support afterwards.

I owe my special thanks to my beloved Sait Aydinalp, who has stood by me through all the challenges I faced. He always encouraged me and never stopped believing in me. The thesis would not have been possible without the unlimited support, encouragement, and infinite love of my beloved parents Bircan Yerli, Ergün Yulu, my aunt Eda Çetin, my uncles Can Yerli, Veliyetdin Çetin, and my lovely grandmother Güldöne Yerli. This study is dedicated to those who make everything meaningful.

ABSTRACT

LIME MORTAR AND PLASTER CHARACTERISTICS OF SOME BYZANTINE PERIOD BUILDINGS IN KADIKALESİ (ANAIA) AND AYASULUK HILL

In this study, characteristics of lime mortars and plasters from Kadıkalesi and Ayasuluk were evaluated by considering the sites, construction periods, function, contained aggregate types. Results compared with Byzantine lime mortar studies. For this purpose, basic physical properties, raw material compositions, geological features, mineralogical and chemical compositions, hydraulic and microstructural properties were determined by RILEM standard test methods, SEM-EDS, XRD and TGA. Also, possible raw material provenances used in the production of mortars and plasters were determined.

According to results, pure lime and pozzolanic aggregates were used in the production of these mortars and plasters. Lime/aggregate ratios may have differed as a result of the geological origins of aggregates and raw material resources. The mortars and plasters had hydraulic properties due to the pozzolanic aggregates.

Natural aggregates consisted of different types of rocks with angular forms were obtained from breccia sources found in the Menderes Massif units. The differences in mineralogical and chemical compositions revealed that different raw material sources were used in Kadıkalesi and Ayasuluk. Natural aggregates of Kadıkalesi mortars may have been obtained from the mountain slopes of Büyük Menderes containing mostly carbonate rock fragments, while those Ayasuluk's may have been obtained from the mountain slopes of Küçük Menderes containing a high percentage of volcanic particles. Brick aggregates were produced at firing temperatures between 800–900°C using clay with low Ca content.

In both sites, the physical properties, chemical, mineralogical compositions and hydraulic properties of lime mortars and plasters did not change significantly according to different construction periods and location of use in the building. The differences determined in their chemical and mineralogical compositions resulted from the type of aggregates used and the diversity of raw material sources. The use of mortars and plasters with similar properties in different periods revealed that the production technology had been transferred and maintained over the centuries, also suitable sources had been consciously chosen to produce hydraulic lime mortars and plasters.

ÖZET

KADIKALESİ (ANAİA) VE AYASULUK TEPEŞİ'NDEKİ BAZI BİZANS DÖNEMİ YAPILARININ KİREÇ HARÇ VE SIVA ÖZELLİKLERİ

Bu çalışmada, Kadıkalesi (Anaia) ve Ayasuluk'tan alınan kireç harç ve sıvaların özellikleri; örneklerin alındığı alanlar, inşa dönemleri, fonksiyonları, içerdikleri agrega türleri dikkate alınarak değerlendirilmiştir. Sonuçlar, Bizans kireç harcı çalışmaları ile karşılaştırılmıştır. Bu amaçla, temel fiziksel özellikler, hammadde kompozisyonları, jeolojik özellikleri, mineralojik ve kimyasal kompozisyonlar, hidrolik ve mikroyapısal özellikleri; RILEM standart test yöntemleri, SEM-EDS, XRD ve TGA ile saptanmıştır. Harç ve sıvaların üretimlerinde kullanılmış olası hammadde kaynakları da belirlenmiştir.

Analiz sonuçlarına göre, tuğla agregalı kireç harç ve sıvaları, doğal agregalılara göre daha gözenekli ve daha az yoğun malzemelerdir. Kireç/agrega oranları, agregaların jeolojik kökenleri ve hammadde kaynaklarına bağlı olarak farklılık göstermiş olabilir. Bu harç ve sıvaların üretiminde, yüksek kalsiyumlu kireç ve puzolanik agregalar kullanılmıştır. Böylece harç ve sıvalar hidrolik nitelik kazanmışlardır.

Doğal agregalarda bulunan farklı tipteki kayaç kırıkları ve köşeli formları dolayısıyla Menderes Masifi birimlerinden elde edilmiş breş kaynaklarının kullanıldığı belirlenmiştir. Mineralojik ve kimyasal kompozisyonlarında görülen farklılıklar Kadıkalesi ve Ayasuluk'ta farklı hammadde kaynaklarının kullanıldığı göstermiştir. Kadıkalesi harçlarının doğal agregaları daha çok karbonatlı kayaç kırıntıları içeren Büyük Menderes dağ eteklerinden, Ayasuluk harçlarının doğal agregaları ise yüksek oranda volkanik parçacık içeren Küçük Menderes dağ eteklerinden elde edilmiş olabilir. Tuğla agregalar ise düşük kalsiyumlu kil kullanılarak 800–900°C arasında üretilmiştir.

Her iki alanda da kireç harç ve sıvalarının fiziksel özellikleri, kimyasal, mineralojik kompozisyonları ve hidrolik özellikleri farklı inşa dönemlerine ve yapıdaki kullanım yerlerine göre anlamlı bir değişiklik göstermemiştir. Kimyasal ve mineralojik kompozisyonlarında belirlenen farklılıklar ise kullanılan agregaların türünden ve hammadde kaynaklarının çeşitliliğinden kaynaklanmıştır. Farklı dönemlerde benzer özelliklerde harç ve sıva kullanımı, üretim teknolojisinin yüzyıllar içinde sürekliliğini koruduğunu, hidrolik kireç harç ve sıva üretebilmek için uygun kaynakların bilinçle seçildiğini ortaya koymuştur.

TABLE OF CONTENTS

LIST OF FIGURES	viii
LIST OF TABLES.....	xii
CHAPTER 1. INTRODUCTION	1
1.1. Problem Definition.....	2
1.2. Aim and Scope of the Study	3
1.3. Methodology	3
1.4. Content of the Study	4
CHAPTER 2. HISTORICAL LIME MORTARS AND PLASTERS	6
2.1. Characteristics of Lime Mortars and Plasters	6
2.2. Recent Studies on Byzantine Lime Mortars and Plasters	12
2.2.1. Basic Physical Properties	13
2.2.2. Raw Material Compositions.....	14
2.2.3. Chemical and Mineralogical Compositions	18
2.2.4. Microstructural Properties.....	21
2.2.5. Pozzolanic Properties of Aggregates.....	26
2.2.6. Hydraulic Properties of Mortars and Plasters	27
CHAPTER 3. KADIKALESİ (ANAIA) AND AYASULUK	31
3.1. Kadıkalesi (Anaia)	33
3.1.1. Historical Background of Kadıkalesi (Anaia).....	34
3.1.2. Architectural Features and Material Characteristics of Kadıkalesi and Anaia Church	36
3.2. Ayasuluk Hill and St. Jean Church	43
3.2.1. Historical Background of Ayasuluk.....	44
3.2.2. Architectural Features and Material Characteristics of Ayasuluk and St. Jean Church.....	47

CHAPTER 4. EXPERIMENTAL METHODS	52
4.1. Sampling	52
4.1.1. Kadıkalesi (Anaia).....	54
4.1.2. Ayasuluk.....	60
4.2. Experimental Studies	66
4.2.1. Determination of Basic Physical Properties.....	66
4.2.2. Determination of Raw Material Compositions	68
4.2.3. Determination of Mineralogical Compositions.....	70
4.2.4. Determination of Chemical Compositions.....	70
4.2.5. Determination of Microstructural Properties	71
4.2.6. Determination of Pozzolanic Activities of Aggregates.....	71
4.2.7. Determination of Hydraulic Properties	72
 CHAPTER 5. RESULTS AND DISCUSSION.....	 73
5.1. Basic Physical Properties.....	73
5.2. Raw Material Compositions	79
5.3. Possible Provenance of Natural Aggregates	92
5.4. Characteristics of Fine Aggregates	96
5.4.1. Characteristics of Fine Natural Aggregates	96
5.4.2. Characteristics of Fine Brick Aggregates.....	107
5.5. Characteristics of Lime Used as Binding Material	121
5.6. Characteristics of Binders	125
5.6.1. Characteristics of Binders with Natural Aggregates.....	126
5.6.2. Characteristics of Binders with Brick Aggregates	138
 CHAPTER 6. CONCLUSION	 146
 REFERENCES	 149

LIST OF FIGURES

<u>Figure</u>	<u>Page</u>
Figure 2.1. Restorated lime kiln in AlmaVerde.....	8
Figure 2.2. Schematic drawing of a lime kiln from Campania.....	9
Figure 2.3. Description of lime kiln.....	9
Figure 2.4. Constituents and classification of lime mortars and plasters	11
Figure 3.1. Location of Kadıkalesi (Anaia) and Ayasuluk.....	31
Figure 3.2. Kadıkalesi (Anaia) and Ayasuluk.....	32
Figure 3.3. Plans of Anaia Church, Kadıkalesi fortification walls and St. Jean Church, Gate of persecution of Ayasuluk in different Byzantine periods.....	33
Figure 3.4. Aerial image of Kadıkalesi (Anaia).....	33
Figure 3.5. Aerial image of Anaia Church.....	35
Figure 3.6. Plan showing the spaces and construction periods of Anaia Church.....	37
Figure 3.7. a: Ambo in naos as the characteristic of Early Byzantine period,..... b: Substructure).....	38
Figure 3.8. Mural paintings in substructure.....	38
Figure 3.9. Early Byzantine baptistery of Anaia Church.....	39
Figure 3.10. Bonding differences and discontinuity in joints between the naos walls and narthex buttresses	40
Figure 3.11. a: Recessed brick technique, b: Plastering the joints.....	41
Figure 3.12. Kadıkalesi fortification wall.....	42
Figure 3.13. Horizontal and vertical ornaments on brick-lime plaster	43
Figure 3.14. Aerial image of Ayasuluk.....	44
Figure 3.15. Aerial image of St. Jean Church.....	45
Figure 3.16. Schematic layout plan of Ayasuluk(Ephesus)during the Beyliks Period ..	46
Figure 3.17. Plan showing the spaces and construction periods of St. Jean Church	47
Figure 3.18. Baptistery in St. Jean Church(a:Baptistery,b:Apsidal hall with tesserae)..	48
Figure 3.19. Treasure room in St. Jean Church, a: East facing part of the treasure room, b: West wall of the treasure room.....	49
Figure 3.20. West side of naos in the St. Jean Church	50

<u>Figure</u>	<u>Page</u>
Figure 3.21. a: Discontinuity of the nave and transept walls, b: Monograms of Justinian (B) and Theodora (A) (Source: Karydis 2015).....	50
Figure 4.1 Site plan of Kadıkalesi (Anaia) and Anaia Church with the photographs of the relevant areas	54
Figure 4.2. The plan of the Kadıkalesi, Anaia Church and the Substructure showing the locations of samples	55
Figure 4.3. Site plan of Ayasuluk and St. Jean Church with the photographs of the relevant areas.....	60
Figure 4.4. Plan of St. Jean Church, its Substructure and Gate of Persecution	61
Figure 4.5. a: Weighing the dry and saturated samples by precision balance, b: The samples in vacuum oven to saturated them entirely	67
Figure 4.6. Measurement of Archimedes weight.....	67
Figure 4.7. a: Filtering of the insoluble parts while washing with distilled water, b: Shaking the aggregates and so eliminating them from series of sieves... ..	69
Figure 4.8. Roundness scale	70
Figure 4.9. a: Magnetic stirrer to mix the Ca(OH) ₂ and fine aggregate, b: Electrical conductivity analysis by conductivity meter.....	72
Figure 5.1. Particle size distributions of aggregates from Kadıkalesi (Anaia) and Ayasuluk Hill	89
Figure 5.2. Distribution of the aggregates from coarse to fine in samples indicated in Figure 5.3 and 5.4	89
Figure 5.3. Natural aggregates used in lime mortars from Kadıkalesi (Anaia) and Ayasuluk	90
Figure 5.4. Brick aggregates used in lime mortars from Kadıkalesi (Anaia) and Ayasuluk	91
Figure 5.5. Geological map of the Kadıkalesi (Anaia), and Ayasuluk environs	92
Figure 5.6. Macro-observations of natural aggregates from Kadıkalesi (Anaia) (a) and Ayasuluk (b).....	93
Figure 5.7. Schematic determination of the possible places of natural aggregate sources.....	94
Figure 5.8. Possible sediment transportation and accumulation directions of Büyük and Küçük Menderes rivers	95

<u>Figure</u>	<u>Page</u>
Figure 5.9. Ternary Diagram ($\text{SiO}_2 + \text{Al}_2\text{O}_3 - \text{CaO} + \text{MgO} - \text{Na}_2\text{O} + \text{K}_2\text{O} + \text{TiO}_2 + \text{Fe}_2\text{O}_3$) of chemical compositions of natural aggregate.....	100
Figure 5.10. Total Alkali Silica (TAS) diagram showing the geochemical origins of fine aggregates	101
Figure 5.11. XRD patterns of natural aggregates in lime mortars from Kadıkalesi (Anaia)	104
Figure 5.12. XRD patterns of natural aggregates in lime mortars from Ayasuluk.....	105
Figure 5.13. The existence of amorphous silicates with a diffuse band between the 20-30 °2θ in XRD pattern	105
Figure 5.14. SEM images showing the angular forms of natural aggregates within the mortar matrix from Kadıkalesi (Anaia).....	106
Figure 5.15. Less porous structure of the natural aggregates and strong adhesion between binder and the aggregate from Ayasuluk.....	106
Figure 5.16. SEM image and EDS analysis of breccia in lime mortar (KNM3) from Kadıkalesi (Anaia)	107
Figure 5.17. SiO_2 and Fe_2O_3 contents of brick aggregates	108
Figure 5.18. Ternary plot showed the $\text{Fe}_2\text{O}_3 - \text{MgO} - \text{Al}_2\text{O}_3$ compositions of brick aggregates	109
Figure 5.19. XRD patterns of brick aggregates in lime plasters from Kadıkalesi.....	114
Figure 5.20. XRD patterns of brick aggregates in lime mortars and plasters from Ayasuluk	115
Figure 5.21. The porous structure of the brick aggregates from Kadıkalesi (Anaia) ...	117
Figure 5.22. Precipitated calcite crystals in the pores of brick aggregate from Kadıkalesi (Anaia)	118
Figure 5.23. Clay layers of brick aggregates from Ayasuluk	119
Figure 5.24. Hematite existence in the brick aggregates from Ayasuluk.....	120
Figure 5.25. XRD patterns of lime lumps.....	121
Figure 5.26. The hydraulicity ranges of the lime lumps.....	123
Figure 5.27. SEM images of lime lumps from Ayasuluk	124
Figure 5.28. SEM images of lime lumps from Kadıkalesi (Anaia)	125
Figure 5.29. $(\text{CaO} + \text{MgO}) - (\text{Al}_2\text{O}_3 + \text{Fe}_2\text{O}_3) - \text{SiO}_2$ diagram representing the composition of the binders with natural aggregates.....	128

<u>Figure</u>	<u>Page</u>
Figure 5.30. SiO ₂ + Al ₂ O ₃ + Fe ₂ O ₃ / CaO+ MgO diagrams of binder and lime lumps in the lime mortars of Kadıkalesi(Anaia).....	129
Figure 5.31. XRD patterns of the binders with natural aggregates from Kadıkalesi....	131
Figure 5.32. XRD patterns of the binders with natural aggregates from Ayasuluk.....	132
Figure 5.33. Binder matrix of Kadıkalesi (Anaia) and Ayasuluk.....	133
Figure 5.34. SEM images of CSH and CAH formations detected in Ayasuluk binders.....	134
Figure 5.35. SEM images of CSH and CAH formations detected in Kadıkalesi	134
Figure 5.36. SEM images that showed the dedolomitization of dolomitic aggregate in lime mortar sample of Kadıkalesi (Anaia).....	137
Figure 5.37. SiO ₂ + Al ₂ O ₃ + Fe ₂ O ₃ / CaO+ MgO diagrams of binder and lime lumps in the lime mortars of Ayasuluk.....	140
Figure 5.38. XRD patterns of binders with brick aggregates from Kadıkalesi	141
Figure 5.39. XRD patterns of binders with brick aggregates from Ayasuluk	142
Figure 5.40. SEM images showed the strong adhesion between pozzolans and lime detected in lime mortar sample from Ayasuluk.....	143
Figure 5.41. SEM images of CSH/CAH formations specified in Kadıkalesi (Anaia) lime plaster.....	144
Figure 5.42. SEM images of CSH/CAH formations determined in Ayasuluk lime mortar.....	145

LIST OF TABLES

<u>Table</u>	<u>Page</u>
Table 2.1. Lime classification combined according to Vicat and Davey	7
Table 2.2. Methods used for the determination of basic physical properties and raw material compositions of mortars and plasters used in different Byzantine period buildings by recent studies.....	16
Table 2.3. Methods used for the determination of chemical, mineralogical compositions and microstructural properties of mortars and plasters used in different Byzantine period buildings by recent studies.....	24
Table 2.4. Methods used for the determination of hydraulic and pozzolanic properties of mortars and plasters used in different Byzantine period buildings by recent studies.....	29
Table 3.1. MSK-64 Intensity scale with its definition.....	40
Table 4.1. Distribution of collected samples according to the sites, periods, and aggregate types.....	53
Table 4.2. Abbreviations used for labeling the collected samples.....	53
Table 4.3. Samples of lime mortars and plasters from Kadıkalesi (Anaia).....	56
Table 4.4. Samples of lime mortar and plaster samples from Ayasuluk	62
Table 5.1. Basic physical properties of lime mortars and plasters from Kadıkalesi.....	75
Table 5.2. Basic physical properties of lime mortars and plasters from Ayasuluk	76
Table 5.3. Basic physical properties of mortars and plasters used in different Byzantine period buildings	77
Table 5.4. Lime and aggregate percentages and lime/aggregate ratios of lime mortars and plasters from Kadıkalesi (Anaia)	81
Table 5.5. Lime and aggregate percentages and lime/aggregate ratios of lime mortars and plasters from Ayasuluk	82
Table 5.6. Comparison of the raw material compositions with the literature.....	83
Table 5.7. Particle size distributions, mean roundness of aggregates and maximum aggregate size from Kadıkalesi (Anaia).....	86
Table 5.8. Particle size distributions, mean roundness of aggregates and maximum aggregate size from Ayasuluk.....	87

<u>Table</u>	<u>Page</u>
Table 5.9. Comparison of the raw material compositions with the literature.....	88
Table 5.10. Chemical compositions and pozzolanic activities of the natural aggregates in Kadıkalesi (Anaia) and Ayasuluk.....	98
Table 5.11. Comparison of chemical compositions and pozzolanic activity of natural aggregates with the literature.....	99
Table 5.12. Chemical compositions and pozzolanic activities of the brick aggregates in Kadıkalesi (Anaia) and Ayasuluk.....	111
Table 5.13. Comparison of chemical compositions of brick aggregates with the literature.....	112
Table 5.14. Comparison of mineralogical compositions of brick aggregates with the literature.....	116
Table 5.15. Chemical composition of the brick aggregate in ABM matrix.....	121
Table 5.16. The chemical compositions (%), hydraulic (H.I.) and cementation indices (C.I.) of lime lumps.....	122
Table 5.17. Chemical compositions of the binders with natural aggregates in Kadıkalesi (Anaia) and Ayasuluk.....	127
Table 5.18. Chemical compositions of CSH and CAH formations observed in ATM2 and KNM1 mortar matrices.....	135
Table 5.19. Chemical compositions of binders with brick aggregates in Kadıkalesi (Anaia) and Ayasuluk.....	139

CHAPTER 1

INTRODUCTION

Lime mortars have been one of the most prevalent binding materials for centuries which were used for structural, protective, or adhesive purposes in buildings of different scales and programs.

One of the earliest known use of lime mortars was as a terrazzo floor covering discovered in Çayönü excavations (Diyarbakır), which dates back to 6000 BC (Oates 1998; Adam 2005; Özdoğan 2007; Öztan 2009). Similarly, another of the earliest examples of lime mortar found was the floor covering Lepinski Vir, dated to 6000 BC (Oates 1998). In the following periods, it is known that lime mortars were used for non-structural purposes as lime stuccos and plasters in Egyptian architecture (Cowper 1998; Vicat 1837). In Greek architecture, lime mortars were generally used as plasters for wall paintings, stuccos, and claddings (Adam 2005). Greek lime mortars were generally considered as the predecessors of the technology of Roman lime mortars (Macdonald 1965). In fact, each generation added its practical experience and the knowledge was developed by trials and errors until the last century of Roman Republic (Macdonald 1965; Ward-Perkins 1970). The remarkable accomplishment of the Romans was mixing pozzolans, either obtained from local volcanic sands (*pozzolana*) or heated ceramic materials, with lime for mortar production which resulted in gaining property of setting under water and higher mechanical strength (Ward-Perkins 1970; Oates 1998). With these superior properties, lime mortars began to be used for structural purposes and thus enabled bonding of rubble masonry and invention of vaulted constructions (Macdonald 1965; Adam 2005). The Roman lime mortar technology was influenced and transferred by several civilizations such as Byzantines, Seljuks and Ottomans by using their local raw material sources and craftsmanship (Akman, Güner, and Aksoy 1986). This production technology was continued to be used until about early 20th century, while modern cement became widespread.

The lime mortars and plasters, which were developed for centuries by different civilizations, are historical documents that shed light on technical knowledge, construction and material technique, experience, skills and craftsmanship of the era and

geography they belonged to (ICOMOS 2013). To conserve the historical, aesthetic, technical, and documentary values of historical lime mortars and plasters and transfer them to future generations, their characteristics, possible raw material sources and production technologies should be fully investigated and elicited. These historical documents should be conserved and repaired with determining original materials, in case of need, using all science and techniques (ICOMOS 1964).

This study focuses on Byzantine lime mortars and plasters used in Western Anatolia, whose properties are less known than those used in the Byzantine imperial center.

1.1. Problem Definition

The Byzantines, who had important settlements in Western Anatolia, continued to use the Roman period lime mortar and plaster technology. Studies on Byzantine lime mortar and plaster are very limited and generally focused on the monumental structures in and around the imperial capital, Constantinople (İstanbul), and only a few of the studies; Serapis Temples in Pergamon, Kyme in İzmir, St. Jean Church in Manisa and Stratonikeia in Muğla, were conducted around Western Anatolia (Aslan Özkaya 2005; Miriello et al. 2011; Oğuz Kılıç et al. 2004; Caner and Güney 2018).

Due to these limited studies, it is not known whether the characteristics and production technologies of lime mortars and plasters used in the Byzantine period has changed according to the spaces, architectural elements of the buildings over the centuries. Besides, the production and craft knowledge were similar in nearby Byzantine settlements or that each area had its own skill and craftsmanship is unknown. The raw materials used in this production should be obtained from local sources as a consequence of logistical difficulties of the period and the need for rapid constructions that especially on the defense lines. Although these local provenances can be determined by the comparison of the characterization data, studies on this subject are very limited.

Consequently, there is a knowledge deficiency about material characteristics and provenance of raw materials of Byzantine lime mortars and plasters from Western Anatolia.

1.2. Aim and Scope of the Study

The study aims to identify the characteristics of Byzantine lime mortars and plasters in Western Anatolia, composed of natural and brick aggregates to better understand the material technique and continuity of the lime mortar technology. The study also aims to specify the possible provenances of raw materials.

Within this aim, Byzantine seaports in Western Anatolia namely; Anaia in Kuşadası, Aydın and Ayasuluk in Selçuk, İzmir, were selected due to their vicinity, historical importance and resemblance in terms of being archbishopric centers of Ephesus. In addition, these structures have similar construction periods dated to different centuries in terms of Early and Middle Byzantine periods, including the addition of new spaces and architectural elements and the repairs of damages caused by earthquakes. The study also intends to compare the characteristics of lime mortar and plasters produced in different centuries and used for different functions in the constructions and hereby to determine whether mortar technology and raw material sources had been changed over centuries in terms of the functions and selected areas. The results will also be compared with Byzantine lime mortar studies in the literature to determine whether the technology was changed according to the different regions.

Thus, it will contribute to the existing literature about Byzantine period lime mortars and plasters which mostly focused on monumental structures in and around the imperial capital, as well as the characteristics and possible raw material sources of lime mortars and plasters to be used in future conservation studies of the sites.

1.3. Methodology

This is a case study on the characteristics of Byzantine period lime mortars and plasters through field survey, literature review, experimental studies, evaluation of the results and comparison within the case areas and recent Byzantine period studies. The selected case areas were Kadıkalesi (Anaia) in Kuşadası, Aydın and Ayasuluk in Selçuk, İzmir.

The measured drawings of the areas were obtained from the excavation archives. The field survey was conducted in July 2020. During the field survey, sampling was

carried out according to the periods determined by the excavation team, by collecting lime mortar and plaster samples from different periods, and locations of the Byzantine monuments. Also, the structure and the sample locations were documented by photographs.

Experimental studies were carried out between September 2020 and January 2022. The samples were analyzed in Material Conservation Laboratory of Izmir Institute of Technology (IZTECH), Conservation and Restoration of Cultural Heritage Department, and in the Center of Materials Research of IZTECH.

The data collection was done by using standard test methods, scanning electron microscopy coupled with energy-dispersive X-ray spectrometry (SEM-EDX), X-ray diffraction (XRD), and thermogravimetric analysis (TGA). Macroscopic observations and geological evaluations were done on the aggregates to specify the possible provenances. The results were given and discussed considering the sites, construction periods, their location, function, and aggregate types used in lime mortars and plasters. Also, according to the results obtained, the lime mortars and plasters from Kadıkalesi and Ayasuluk were compared within themselves and with other Byzantine period studies. The data were evaluated to investigate the continuity of lime mortar technology over centuries and the possible provenance of raw materials.

1.4. Content of the Study

The thesis is composed of six chapters; introduction, historical lime mortars and plasters, Kadıkalesi (Anaia) and Ayasuluk, experimental methods, results and discussion and conclusion.

In the second chapter, the history and manufacturing techniques of the lime mortars and plasters were explained, and the results of recent studies on Byzantine lime mortars were given.

In the third chapter, general information about the historical background, architectural characteristics, and material use of the two outstanding Byzantine settlements, Kadıkalesi (Anaia) and Ayasuluk were presented.

In the fourth chapter, sampling of the lime mortars and plasters and experimental studies and tools to determine basic physical properties, raw material compositions, and

hydraulic properties of lime mortars and plasters; mineralogical and chemical compositions, microstructural properties of aggregates, limes, and binders; and pozzolanic activities of aggregates were defined.

In the fifth chapter, basic physical properties, raw material compositions, and hydraulic properties of lime mortars and plasters; possible provenance of natural aggregates; mineralogical and chemical compositions, microstructural properties of aggregates, limes and binders; pozzolanic activities of aggregates were determined by using RILEM test methods, XRD, SEM-EDX and TGA. Also, the possible provenances of aggregates were discussed.

In the sixth chapter, all results were summarized and evaluated by considering the sites, construction periods, function and aggregate types used in lime mortars and plasters.

CHAPTER 2

HISTORICAL LIME MORTARS AND PLASTERS

In this chapter, the development of lime mortar and plasters throughout history and their manufacturing techniques were examined. In addition, the results of recent studies on the characterization of Byzantine lime mortars were given.

2.1. Characteristics of Lime Mortars and Plasters

Historical lime mortars and plasters were manufactured by mixing lime as bonding agent and natural and/or brick aggregates.

Limestones, which are sedimentary rocks mainly consisted of calcium carbonate (CaCO_3), are the raw materials for lime manufacturing (Lazell 1915; Davey 1961). There are various classifications of limes according to their hydraulic properties, chemical compositions and characteristics of limestones (Vicat 1837; Eckel 1905; Lazell 1915; Davey 1961; Cowper 1998; Zacharopoulou 1998). Among these classifications, classifications of Vicat (1837) and Davey (1961) were the most commonly accepted approaches in the literature.

According to Vicat, the main classification of lime was consisted of five major groups in terms of their chemical compositions (Table 2.1) (Vicat 1837):

- Rich or fat limes: Containing less than ~5% of inert impurities such as alumina, silica, iron etc., can rapidly slake.
- Poor or lean limes: Including ~5–30% inert impurities, slake slowly
- Slightly or Feebly Hydraulic Limes: Consisting of <12% active clay etc.
- Moderately Hydraulic Limes: Composed of 12–18% active clay etc.
- Eminently Hydraulic Limes: Involving 18-25% active clay etc.

Davey classified limes according to limestone provenance, mineralogical and chemical compositions and mainly grouped them as non-hydraulic and hydraulic (Davey 1961) (Table 2.1):

- Non-hydraulic limes: Carboniferous and pure oolitic limestone (CaCO_3) including $<5\%$ MgO, or magnesian (dolomitic) limestone (MgCO_3) containing $>5\%$ MgO.
- Hydraulic limes: Grey chalks, siliceous, argillaceous limestones or magnesian limestones containing SiO_2 (4–16%), Al_2O_3 (1–8%), Fe_2O_3 (0.3–6%), and $\text{CaO} + \text{MgO}$ (78–92%).

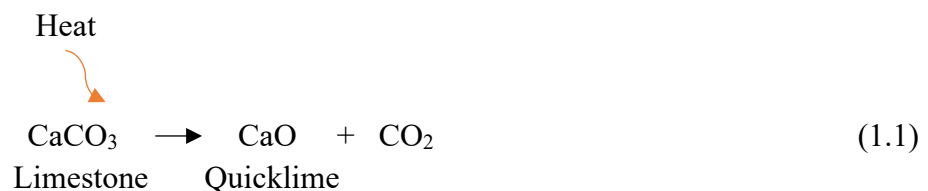
Table 2.1. Lime classification combined according to Vicat and Davey

(Source: Vicat 1837; Davey 1961)

Classification		Raw Materials	Composition
Non-hydraulic Limes	Fat/Rich limes	Carboniferous limestone Pure oolitic limestone ($<5\%$ MgO)	$>94\%$ CaO, MgO
		Magnesian (dolomitic) limestone ($>5\%$ MgO)	
	Lean/Poor limes	Carboniferous limestone Pure oolitic limestone ($<5\%$ MgO)	$>70\%$ CaO, MgO Residue inert
		Magnesian (dolomitic) limestone ($>5\%$ MgO)	
Hydraulic Limes	Slightly or Feebly Moderately Eminently	Grey chalks Siliceous limestones Argillaceous limestones	SiO_2 (4–16%) Al_2O_3 (1–8%) Fe_2O_3 (0.3–6%)

The manufacturing of lime starts with extracting limestones from the quarries. Vitruvius, recommended the use of white and less porous limestones for mortars of structural purposes (Vitruvius 1960).

In the second step, limestones (CaCO_3) are generally heated at moderate temperatures around $900\text{--}1200^\circ\text{C}$, during heating carbon dioxide (CO_2) is released and quicklime (calcium oxide (CaO)) is obtained (1.1) (Lazell 1915; Boynton 1966; Oates 1998; Adam 2005). The pores of the quicklime increases by releasing CO_2 .



In the traditional lime kilns, the used fuel was wood and charcoal, so they could reach the temperatures of approximately 900°C. Lower calcination temperatures (~900°C) lead the formation of higher specific surface area and more reactive quicklime. Therefore, the limes may have been produced in a higher quality (Moropoulou, Bakolas, and Aggelakopoulou 2001).

In historical lime production, the calcination process was mostly carried out in lime kilns which were often close to the limestone quarry so that the kiln could be operated with minimum labor (Figure 2.1–2.3) (Davey 1961; Oates 1998). On the other side, some lime kilns were built near important buildings such as fortification walls, basilicas etc. and especially marble elements of earlier periods monuments were used as raw materials during Byzantine Period (Adam 2005).

During calcination, limestone lost its weight. Therefore, at the end of this process transportation of quicklime to the construction site became easier.



Figure 2.1. Restorated lime kiln in AlmaVerde
(Source: Tranmer 2015)

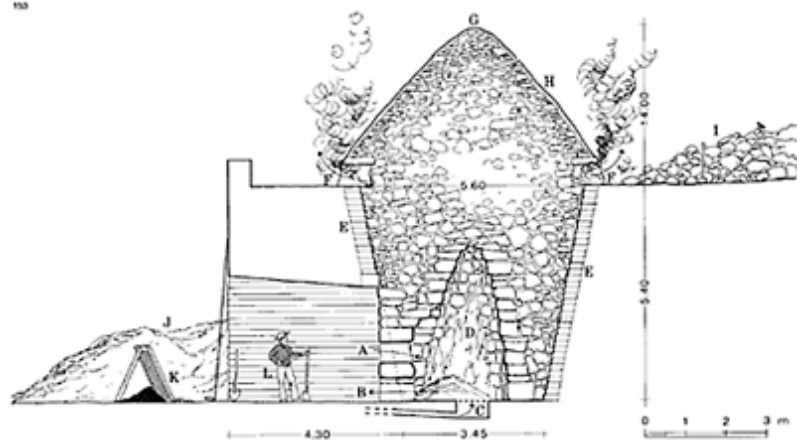


Figure 2.2. Schematic drawing of a lime kiln from Campania
(Source: Adam 2005, 121)

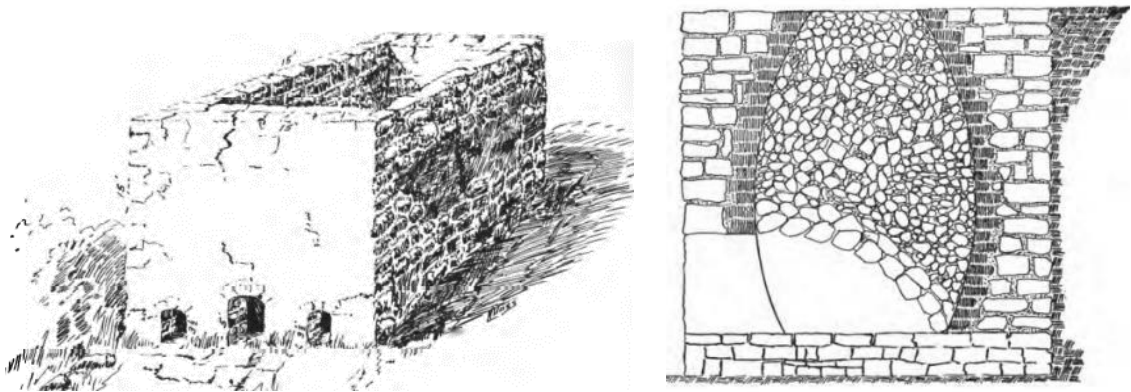
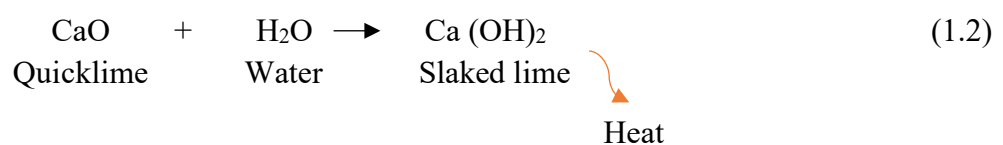


Figure 2.3. Description of lime kiln
(Source: Lazell 1915, 25-26)

Calcination process is followed by the slaking of quicklime by adding water (H_2O), and result in slaked lime/lime putty (calcium hydroxide ($Ca(OH)_2$)) (1.2) (Lazell 1915; Davey 1961; Boynton 1966; Oates 1998; Adam 2005). In the slaking process, water penetrates the quicklime's open pores. After it cools off, the heat is released (Vitruvius 1960). The existence of other chemically reactive substances can alter the slaking process and effect the hydraulicity of the product (Adam 2005). If excess water is used for hydration, the resultant hydrate would be in paste form (Lazell 1915).



Ancient masters recommended the use of aged lime (at least three years) for preparing lime mortars and plasters (Vitruvius 1960; Adam 2005). Using aged lime increases the plasticity of lime and carbonation rate by decreasing size of the calcite crystals (Cowper 1998; Rodriguez-Navarro, Hansen, and Ginell 1998; Zamba et al. 2007). In the production of lime mortars and plasters, quicklime or slaked lime were used as binding agent.

The quality of historical lime mortars and plasters were dependent on the properties of lime, the nature and the proportion of the aggregates, and homogeneous mixing of the lime and aggregates (Adam 2005).

Due to the pozzolanic properties of the aggregates, lime mortars and plasters gain hydraulic properties and higher strength (Moropoulou, Bakolas, and Bisbikou 1995; Moropoulou et al. 2002). On the other hand, proportion of the lime/ aggregate is essential for providing a good adhesion between them (Pasley 1997).

Vitruvius mentioned that 1 part of slaked lime and 3 parts of quarry sand or 2 parts of river sand would be correct proportions for mortar production. He also suggested the mixing of 1 part of lime, 2 parts of river sand and 1 part of broken tile fragments (Vitruvius 1960).

In general, lime mortars and plasters are classified according to their hydraulic properties as non-hydraulic lime mortars and hydraulic lime mortars (Figure 2.4). Non-hydraulic lime mortars can be produced by using non-hydraulic lime with inert aggregates whereas hydraulic lime mortars can be produced by using hydraulic lime with inert aggregates or non-hydraulic lime with pozzolanic aggregates. Historical lime mortars and plasters were generally in the group of non-hydraulic lime and pozzolanic aggregates. The pozzolanic aggregates can be classified as natural and artificial pozzolans.

Natural pozzolans, which are mostly the clasts or dusts of volcanic origin, were first discovered in the Puteoli region in the Bay of Naples by Romans (Oates 1998; Davey 1961; Ward-Perkins 1970; Adam 2005). Vitruvius recommended the use of volcanic sands found in Baiae (north of the Bay of Naples which is a volcanic area) as natural pozzolans with the sentence “*This powder mixed with lime and broken stones makes the masonry so hard that it hardens, not only in ordinary buildings but also under water.*” (Vitruvius 1960).

Although natural pozzolans were first discovered in the Puteoli region, local volcanic sources were consciously selected and used in the production of lime mortars in

wide geographies (Degryse, Elsen, and Waelkens 2002; Columbu, Sitzia, and Ennas 2017).

Artificial pozzolans, on the other hand, are terracotta-based materials such as bricks, tiles, and ceramic shards. When raw materials containing high amounts of clay are fired at low temperatures between 600-900°C, the crystal structure of clay minerals are lost and pozzolanic amorphous substances are formed (Davey 1961; Cowper 1998). At high firing temperatures (>900°C), pozzolanic activity is lost due to the formation of high temperature minerals and disappearance of amorphous substances (Lee, Kim, and Moon 1999; Cardiano et al. 2004).

In the presence of water, amorphous silica and alumina in the structure of pozzolans react with lime, and form calcium silicate hydrate (CSH) and calcium aluminate hydrates (CAH) (1.3) (Figure 2.4). These products provide hydraulic properties to mortars and plasters.



Lime

CAH

CSH

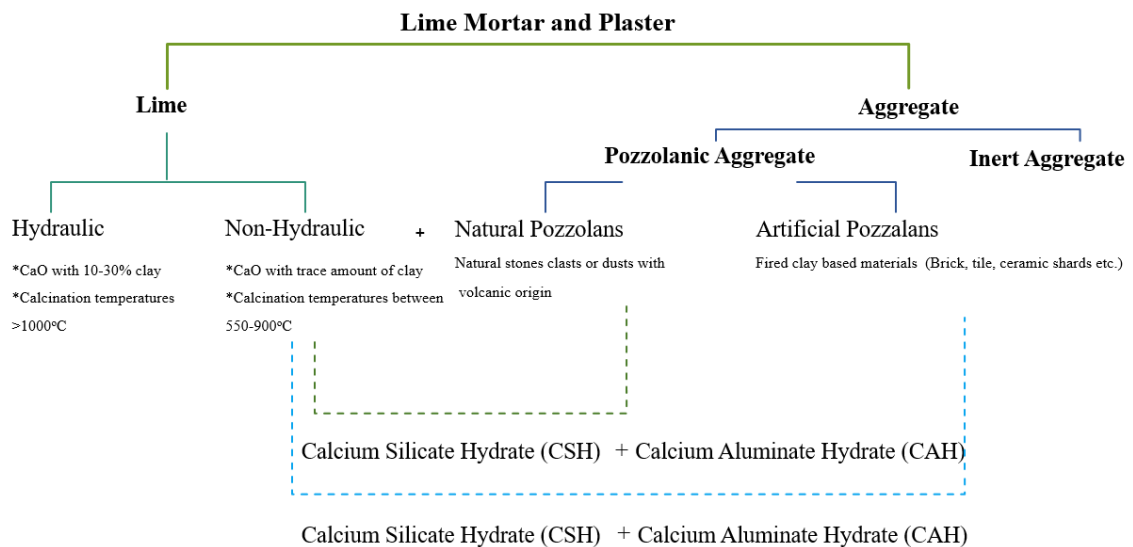


Figure 2.4. Constituents and classification of lime mortars and plasters

Different civilizations, such as the Romans, Byzantines, and Ottomans, appreciated the hydraulic, mechanical, and microstructural properties of lime mortars produced with pozzolanic aggregates. Hydraulic lime mortars provided stability and durability especially to water-related structures throughout centuries until the invention of modern cement (Davey 1961; Ward-Perkins 1970; Oates 1998; Baronio and Binda 1997; Adam 2005).

2.2. Recent Studies on Byzantine Lime Mortars and Plasters

Historical mortar characterization has been in the interest of scientific studies for about three decades. Several studies had been carried out on the characterization of lime mortars from different archaeological sites and historical buildings. Since, the Romans had a pioneer role in the development of the technology of lime mortars, and their reign continued for a long period in the history and in a very wide geography, the number of the studies on Roman period lime mortars constituted nearly the majority of the recent literature. The literature review was limited by including only the Roman period lime mortars and plasters from Turkey due to the case study subject includes examples from there.

The studies conducted on the lime mortars focused on Roman structures in Ankara (Güleç and Tulun 1996), Sagalassos in Burdur (Degryse, Elsen, and Waelkens 2002), Pergamon in İzmir (Özkaya and Böke 2009), Kyme in İzmir (Miriello et al. 2011), Kayseri (Kozlu and Ersen 2011), Andriake in Antalya (Oğuz, Türker, and Koçkal 2015), Lycia region (Taşcı and Böke 2018), Aigai in Manisa and Nysa in Aydın (Uğurlu Sağın, Duran, and Böke 2021), and Western Anatolia (Taşcı 2021).

However, there are fewer studies on the Byzantine period lime mortars, the successors of the Romans. These studies were generally carried out on the lime mortars and plasters of the monumental structures in and around the Imperial center, Istanbul (Güleç and Tulun 1996; Bakolas et al. 1998; Moropoulou, Çakmak, and Lohvyn 2000; Moropoulou et al. 2002; Gürdal, Kahraman Altaş, and Acun Özgünler 2011; Acun Özgünler, Ersen, and Güleç 2013; Kahraman Altaş, Acun Özgünler, and Gürdal 2013; Nežerka et al. 2015; Ulukaya et al. 2017). Also, some of the studies focused on the lime mortars and plasters from St. Jean Church in Manisa (Oğuz Kılıç et al. 2004), Pergamon

in Izmir (Aslan Özkaya 2005), Kiev (Moropoulou, Çakmak, and Lohvyn 2000; Moropoulou et al. 2007), Kayseri (Kozlu and Ersen 2011), Cilicia (Polat Pekmezci 2012), Stratonikeia in Muğla (Caner and Güney 2018) and Greece (Stefanidou et al. 2014; Maria 2016). In these works, generally lime mortars and plasters with brick aggregates were studied, and there were a few studies on lime mortars consisted of natural aggregates (Oğuz Kılıç et al. 2004; Aslan Özkaya 2005; Miriello et al. 2011; Kozlu and Ersen 2011; Polat Pekmezci 2012; Stefanidou et al. 2014; Oğuz, Türker, and Koçkal 2015).

In these mentioned studies, the physical, chemical, microstructural, hydraulic properties and raw material compositions of lime mortars were investigated. However, the provenance of their raw materials was not extensively defined and discussed.

The results of the recent studies on Byzantine lime mortars and plasters were given in the subheadings.

2.2.1. Basic Physical Properties

Basic physical properties of the Byzantine period lime mortars and plaster were frequently determined in the studies. These properties were defined by their density (g/cm^3) and total porosity (%) values by RILEM test methods (Oğuz Kılıç et al. 2004; Aslan Özkaya 2005; Gürdal, Kahraman Altaş, and Acun Özgünler 2011; Kurugöl and Güleç 2012; Polat Pekmezci 2012; Kahraman Altaş, Acun Özgünler, and Gürdal 2013; Stefanidou et al. 2014; Ulukaya et al. 2017; Caner and Güney 2018), TS EN 1936 (Kozlu and Ersen 2011; Oğuz, Türker, and Koçkal 2015), TS 699 and ASTM standards (Acun Özgünler, Ersen, and Güleç 2013) and porosimeter (Moropoulou, Çakmak, and Lohvyn 2000) (Table 2.2).

The porosity values of lime mortars and plasters with natural aggregates from Serapis Temple (Aslan Özkaya 2005), St. Basilius Monastery, St. Nicholas Church, Erdemli Church and Gereme Panagia Church from Kayseri (Kozlu and Ersen 2011), Fortification Wall of Adana and Kozan Castle in Cilicia (Polat Pekmezci 2012) Synagogue from Andriake Harbour (Oğuz, Türker, and Koçkal 2015) were found 48%, 32–54%, 24–30% and 33–41%, respectively. On the contrary, the porosity values of the lime mortars and plasters consisted of brick aggregates were found 48% in Serapis Temple (Aslan Özkaya 2005), between 34–45% in St. Jean Church in Manisa (Oğuz Kılıç et al. 2004), 42–46% in Sophia Cathedral, the Church of St. Michael, the Tithe Church of

the Assumption of the Virgin, the Cathedral of Assumption of the Virgin in Kiev (Moropoulou, Çakmak, and Lohvyn 2000), 32–48% in Hagia Sophia, Hagia Eirine, St. Mary of Chalkoprateia, Church of St. Euphemia, Monastery of Stoudios, Martyrion of Karpos and Papylos, Church of St. Polyeuctus (Gürdal, Kahraman Altaş, and Acun Özgünler 2011), 28–35% in Yoros Castle in Istanbul (Kurugöl and Güleç 2012), 54% in Middle Byzantine Chapel in Istanbul (Ulukaya et al. 2017), and between 40–48% in Early Byzantine Church in Stratonikeia in Muğla (Caner and Güney 2018).

The density values of the lime mortars and plasters with natural aggregates were found 1.7 g/cm³ by Aslan Özkaya (2005), between 1.75–1.94 g/cm³ by Polat Pekmezci (2012), 1.45–1.67 g/cm³ by Oğuz, Türker and Koçkal (2015), and 1.08–1.70g/cm³ by Kozlu and Ersen (2011). On the other hand, the lime mortars and plasters consisted of brick aggregates were found 1.3 g/cm³ by Aslan Özkaya, between 1.49–1.51 g/cm³ Moropoulou, Çakmak and Lohvyn (2000), 1.4–1.6 g/cm³ by Oğuz Kılıç et al. (2004), 1.23–1.66 g/cm³ by Gürdal, Kahraman Altaş and Acun Özgünler (2011), 1.55–1.83 g/cm³ by Kurugöl and Güleç (2012), 1.2 g/cm³ by Ulukaya et al. (2017), and 1.04–1.21 g/cm³ by Caner and Güney (2018).

2.2.2. Raw Material Compositions

The raw material compositions were defined by lime/aggregate ratios and particle size distributions. In the most of the studies, the lime/aggregate ratios were examined by acid loss analysis which is dissolving the mortar and plaster by using dilute hydrochloric acid to obtain acid soluble (lime) and acid insoluble (aggregate) parts by weight (Oğuz Kılıç et al. 2004; Aslan Özkaya 2005; Kozlu and Ersen 2011; Gürdal, Kahraman Altaş, and Acun Özgünler 2011; Kurugöl and Güleç 2012; Kahraman Altaş, Acun Özgünler, and Gürdal 2013; Oğuz, Türker, and Koçkal 2015; Ulukaya et al. 2017; Caner and Güney 2018) (Table 2.2). The other method is the examination of mortar and plaster samples, which prepared as thin sections, under optical microscope and calculating the percentage areas of the aggregates and binders (Moropoulou, Çakmak, and Lohvyn 2000; Miriello et al. 2011; Polat Pekmezci 2012; Nežerka et al. 2015) (Table 2.2). The particle size distributions were determined almost in all studies by sieve analysis on acid insoluble parts after dissolving the mortar and plasters (Oğuz Kılıç et al. 2004; Aslan Özkaya 2005; Kozlu and Ersen 2011; Gürdal, Kahraman Altaş, and Acun Özgünler 2011; Polat

Pekmezci 2012; Kurugöl and Güleç 2012; Kahraman Altaş, Acun Özgünler, and Gürdal 2013; Oğuz, Türker, and Koçkal 2015; Ulukaya et al. 2017; Caner and Güney 2018) (Table 2.2).

The lime/aggregate ratios obtained from lime mortars consisted of natural aggregates were found 1/5 in Serapis Temple (Aslan Özkaya 2005) and between 1/3–2/3 in Fortification Wall of Adana and Kozan Castle in Cilicia (Polat Pekmezci 2012).

The lime/aggregate ratios of the lime mortars and plasters produced by using brick aggregates were found as 1/1 in St. Jean Church in Manisa (Oğuz Kılıç et al. 2004), 1/2.6 in Serapis Temple (Aslan Özkaya 2005), 1/2–1/4 in Hagia Sophia, Hagia Eirine, St. Mary of Chalkoprateia, Church of St. Euphemia, Monastery of Stoudios, Martyrion of Karpos and Papylos, Church of St. Polyeuctus (Gürdal, Kahraman Altaş, and Acun Özgünler 2011), 1/2–1/3 in Yoros Castle in Istanbul (Kurugöl and Güleç 2012), 1/3 in Istanbul Land Walls and Theodosian Walls (Kahraman Altaş, Acun Özgünler, and Gürdal 2013), 2/3 in Middle Byzantine Church in Istanbul (Nežerka et al. 2015), 1/4–1/5 in Middle Byzantine Chapel in Istanbul (Ulukaya et al. 2017), and around 1/3 by volume in Sophia Cathedral, the Church of St. Michael, the Tithe Church of the Assumption of the Virgin, the Cathedral of Assumption of the Virgin in Kiev (Moropoulou, Çakmak, and Lohvyn 2000). According to these similar results, the aggregate type did not affect the lime/aggregate ratio.

Since wide range of particle sizes may enhance the mechanical strength of mortars (Lanas et al. 2004; Pavía and Toomey 2008), particle size distribution of aggregates were evaluated as another significant factor in defining the raw material compositions of lime mortars and plasters. Byzantine lime mortars with natural and brick aggregates indicated wide range of particle sizes and their largest fraction were found to be greater than 1000 µm (Oğuz Kılıç et al. 2004; Aslan Özkaya 2005; Gürdal, Kahraman Altaş, and Acun Özgünler 2011; Polat Pekmezci 2012; Kurugöl and Güleç 2012; Kahraman Altaş, Acun Özgünler, and Gürdal 2013; Ulukaya et al. 2017).

In the studies, the roundness scale of the aggregates was not analyzed. Only in archeological site of Kyme, the aggregates were found in sub-angular form, but its reason was, not specified (Miriello et al. 2011).

Table 2.2. Methods used for the determination of basic physical properties and raw material compositions of mortars and plasters used in different Byzantine period buildings by recent studies

Area & Reference	Period	Mortar/ Plaster	Aggregate Type	Basic Physical Properties	Raw Material Compositions	
					Lime/Aggregate Ratio	Particle Size Distributions
Fortification Wall of Adana and Kozan Castle in Cilicia (Polat Pekmezci 2012)	Early Byzantine	Mortar	Natural	RILEM test methods	Optical microscope	Sieve analysis on acid insoluble parts
Synagogue from Andriake Harbour (Oğuz, Türker, and Koçkal 2015)	Byzantine	Mortar	Natural	TS EN 1936 standard	Acid loss analysis	Sieve analysis on acid insoluble parts
Archeological Site of Kyme (Miriello et al. 2011)	Early Byzantine	Mortar	Natural	x	Optical microscopy	x
Serapis Temple/ Kızıl Avlu (Aslan Özkaya 2005)	Early Byzantine	Mortar	Natural	RILEM test methods	Acid loss analysis	Sieve analysis on acid insoluble parts
		Plaster	Brick			
Monastery and Churches from Kayseri (Kozlu and Ersen 2011)	Early– Middle Byzantine (4–11 th centuries)	Mortar	Natural	TS EN 1936 standard	Acid loss analysis	x
		Plaster	Natural			
Byzantine Bath of Thessaloniki and Castle of Servia (Stefanidou et al. 2014)	Middle Byzantine (10-13 th centuries)	Mortar Plaster	Natural	RILEM test methods	x	x
Esekap Madrasah (Güleç and Tulun 1996)	Middle Byzantine (11 th century)	Mortar	Natural	x	x	x
Land Walls of Yedikule in Istanbul (Acun Özgünler, Ersen, and Güleç 2013)	Early Byzantine (5 th century)	Mortar	Brick	TS 699 ASTM standards	Acid loss analysis	Sieve analysis on acid insoluble parts
Early Byzantine Church in Stratonikeia in Muğla (Caner and Güney 2018)	Early Byzantine (5–7 th centuries)	Mortar	Brick	RILEM test methods	Acid loss analysis	Sieve analysis on acid insoluble parts
		Plaster	Brick			

(cont. on next page)

Table 2.2. (cont.)

Area & Reference	Period	Mortar/ Plaster	Aggregate Type	Basic Physical Properties	Raw Material Compositions	
					Lime/Aggregate Ratio	Particle Size Distributions
Hagia Sophia Basilica (Bakolas et al. 1998)	Early Byzantine (6th century)	Mortar	Brick	x	x	x
St. Jean Church in Manisa (Oğuz Kılıç et al. 2004)	Early Byzantine (6th century)	Mortar	Brick	RILEM test methods	Acid loss analysis	Sieve analysis on acid insoluble parts
St. Katherines Hospice in Rhodes (Moropoulou, Bakolas, and Bisbikou 2000)	Early– Late Byzantine (6–14 th centuries)	Mortar	Brick	x	x	x
Religious Buildings in Istanbul (Gürdal, Kahraman Altaş, and Acun Özgünler 2011)	Early Byzantine	Mortar	Brick	RILEM test methods	Acid loss analysis	Sieve analysis on acid insoluble parts
Defense Structures in Istanbul (Kahraman Altaş, Acun Özgünler, and Gürdal 2013)	Early Byzantine	Mortar	Brick	RILEM test methods	Acid loss analysis	Sieve analysis on acid insoluble parts
Middle Byzantine Church in Istanbul (Nežerka et al. 2015)	Middle Byzantine (9 th centuries)	Mortar	Brick	x	Optical microscopy	x
Middle Byzantine Monuments in Kiev (Moropoulou, Çakmak, and Lohvyn 2000)	Middle Byzantine (11-13 th centuries)	Mortar	Brick	Porosimeter	Optical microscopy	x
Middle Byzantine Chapel in Istanbul (Ulukaya et al. 2017)	Middle Byzantine (11–12 th centuries)	Mortar	Brick	RILEM test methods	Acid loss analysis	Sieve analysis on acid insoluble parts
Yoros Castle in Istanbul (Kurugöl and Güleç 2012)	Late Byzantine (13–14 th centuries)	Mortar	Brick	RILEM test methods	Acid loss analysis	Sieve analysis on acid insoluble parts

2.2.3. Chemical and Mineralogical Compositions

Chemical and mineralogical composition analyses were generally carried out in three aspects in the recent studies. These were:

- Binders which were the fine parts of mortars composed of small grain-sized silica and carbonated lime (Güleç and Tulun 1996; Miriello et al. 2011; Polat Pekmezci 2012; Kurugöl and Güleç 2012; Acun Özgünler, Ersen, and Güleç 2013; Ulukaya et al. 2017),
- Aggregates, natural or brick, and generally with sizes finer than 53 μm (Baronio and Binda 1997; Aslan Özkaya 2005; Miriello et al. 2011; Polat Pekmezci 2012; Stefanidou et al. 2014; Ulukaya et al. 2017)
- Lime lumps which were accepted as the representative parts of the lime used in the production of mortars (Miriello et al. 2011)

The most common method used to determine major elements were using a scanning electron microscope coupled with an X-ray energy dispersive system (SEM-EDS) by calculating the averages of the data obtained from three distinct areas of the pellet samples (Table 2.3). For determining the major, minor, and trace element compositions, X-ray fluorescence spectroscopy (XRF) (Miriello et al. 2011; Oğuz, Türker, and Koçkal 2015; Ulukaya et al. 2017) and Inductively coupled plasma emission spectroscopy (ICP) (Kurugöl and Güleç 2012; Acun Özgünler, Ersen, and Güleç 2013) analyses were carried out in a few of the studies (Table 2.3).

In all the studies, X-ray diffraction (XRD) analyses were used to examine the mineralogical compositions (Table 2.3). Additionally, Fourier transformed infrared spectroscopy (FTIR), optical microscopy, polarizing microscope, and differential thermal analysis (DTA) were used in some of the studies (Table 2.3).

Binders in mortar and plaster:

The chemical compositions of the binders from archeological site of Kyme were consisted of larger amounts of SiO_2 (41.3–53.0%), moderate amounts of CaO (13.1–24.7%), MgO (1.37–2.4 %), Al_2O_3 (7.9–10.1%), and smaller amounts of Fe_2O_3 (1.9–2.4 %), K_2O (2.2–2.6 %), Na_2O (0.5–1.2 %), and TiO_2 (0.4–0.5 %) (Miriello et al. 2011). On the other hand, the major oxides of the Esekap Madrasah were mainly CaO (50.0–78.0%), SiO_2 (15.0–32.0%) and partly MgO (0.0–1.0 %), Al_2O_3 (1.4–7.2%), Fe_2O_3 (0.6–3.4 %),

K₂O (1.3–3.1 %), Na₂O (0.6 %), TiO₂ (0.0–0.4 %) (Güleç and Tulun 1996), and the major oxides of Fortification Wall of Adana and Kozan Castle in Cilicia were consisted of bigger amount CaO (51.7–75.0%), MgO (27.05 %), SiO₂ (11.2–18.7%) and smaller amount of Al₂O₃ (5.0–6.6%), Fe₂O₃ (1.2–2.6 %), and K₂O (0.8 %) (Polat Pekmezci 2012).

The lime mortars with natural aggregates from Archeological site of Kyme were composed of quartz, calcite, anorthite, muscovite, geothite, heulandite, actinolite and vaterite minerals (Miriello et al. 2011), whereas in Byzantine Church in Negev were consisted of quartz, calcite, dolomite, muscovite, clibozoisite, halite, gypsum, and kaolinite (Freidin and Meir 2005). The binders with natural aggregates of Esekap Madrasah were consisted of calcite, quartz, anorthite, muscovite and traces of gypsum minerals (Güleç and Tulun 1996), while in Fortification Wall of Adana and Kozan Castle in Cilicia, the binders were composed of calcite, quartz, glauconite (mica) and traces of gypsum minerals (Polat Pekmezci 2012).

Binders with brick aggregates from Yoros Castle in Istanbul were comprised of larger amounts of CaO (25.4–29.8%), SiO₂ (28.0–35.2%), and smaller amounts of MgO (1.0 %), Al₂O₃ (7.1–8.0%), Fe₂O₃ (1.6–2.4 %), K₂O (0.6–0.8 %), Na₂O (0.8–1.2 %), and TiO₂ (0.1–0.2 %) (Kurugöl and Güleç 2012), while the major oxide compositions of the binders with brick aggregates from Land walls of Yedikule in Istanbul contained of mainly CaO (15.9–31.5%), SiO₂ (32.6–52.7%), and partially MgO (0.5–1.3 %), Al₂O₃ (3.1–6.7%), Fe₂O₃ (1.2–2.8 %), K₂O (1.0–1.5 %), Na₂O (0.9–2.0 %), and TiO₂ (0.2–0.3 %)(Acun Özgünler, Ersen, and Güleç 2013). Similarly to Yoros Castle and Land Walls of Yedikule, the chemical compositions of Middle Byzantine Chapel in Istanbul were involved larger amounts of CaO (36.1–36.7%), SiO₂ (22.3–23.0%), and smaller amounts of MgO (2.0–2.2 %), Al₂O₃ (6.0–6.5%), Fe₂O₃ (2.1–2.5 %), K₂O (0.2–0.3 %), and Na₂O (0.1 %) (Ulukaya et al. 2017).

The lime mortars with brick aggregates from defense structures and religious buildings in Istanbul were composed of quartz and calcite, but religious buildings also had orthoclase minerals (Gürdal, Kahraman Altaş, and Acun Özgünler 2011; Kahraman Altaş, Acun Özgünler, and Gürdal 2013). St. Katherines Hospice in Rhodes of lime mortars with brick aggregates were consisted of quartz, calcite, muscovite, tobermorite and montmorillonite. Hydraulic components also observed in these peaks. The presence of hydraulic components and tobermorite might be caused by the crystallization of portlandite from lime due to the environmental conditions or construction techniques (Moropoulou, Bakolas, and Bisbikou 2000). In FTIR analyses of the Middle Byzantine

Chapel mortar, calcite bands at 713, 875, 1420, 1795 cm^{-1} and quartz band at 966 cm^{-1} were determined (Ulukaya et al. 2017). Any organic matter did not detected in the bands (Ulukaya et al. 2017).

Aggregates:

The major oxide compositions of the natural aggregates in lime mortars from archeological site of Kyme were mainly composed of large amounts of SiO_2 (60.3–76.7 %), moderate amounts of Al_2O_3 (12.6–21.4%), and smaller amounts of Fe_2O_3 (0.1–5.2 %), MgO (0.9–2.8 %), K_2O (2.8–4.8 %), Na_2O (1.8–5.0 %), CaO (1.0–5.9%) and TiO_2 (0.1–0.9 %), likewise the major oxides of the natural aggregates from Fortification Wall of Adana and Kozan Castle in Cilicia were mostly included SiO_2 (41.8–51.8 %), Al_2O_3 (21.8–25.5%) moderate amounts of, CaO (6.5–11.2 %), Fe_2O_3 (8.7–10.8 %) and in trace amounts of MgO (2.9–4.3 %), K_2O (3.8–7.4%), Na_2O (1.42%), and TiO_2 (0.00 %). The chemical compositions of the natural aggregates from Serapis Temple were consisted of higher amount of SiO_2 (80.1–83.9 %), and lower amounts of Al_2O_3 (5.6–6.8%), Fe_2O_3 (6.8–11.4 %), MgO (1.4–2.1 %), K_2O (1.0–1.1 %), Na_2O (1.3–2.3 %), and TiO_2 (0.7–1.3 %). Stefanidou et al. (2014) were determined the $\text{SiO}_2 + \text{Al}_2\text{O}_3 + \text{Fe}_2\text{O}_3$ (40.8–54.02%) and CaO (16.4–31.0%) to indicate the pozzolanic property (Stefanidou et al. 2014).

The natural aggregates in lime mortars from Serapis Temple composed of quartz, albite, feldspar and muscovite minerals (Aslan Özkaya 2005). In Esekap Madrasah, the natural aggregates in lime mortars were consisted of quartz, calcite, anorthite, muscovite, microcline, andesine, orthoclase and gypsum (Güleç and Tulun 1996).

Similar to the chemical compositions of natural aggregates, the brick aggregates in lime mortar from Middle Byzantine Chapel were mostly consisted of large amounts of SiO_2 (48.4–49.5%), moderate amounts of Al_2O_3 (14.0–14.4%), and smaller amounts of Fe_2O_3 (7.7–8.2 %), MgO (2.4–2.7 %), K_2O (2.0–2.3 %), Na_2O (1.1–1.3 %), CaO (23.1–23.9 %) and TiO_2 (0.00 %) (Ulukaya et al. 2017). The brick aggregates in lime plaster were consisted of mainly SiO_2 (50.5%) and partially Al_2O_3 (6.7%), Fe_2O_3 (3.9 %), MgO (1.6 %), K_2O (0.9 %), Na_2O (0.0 %), CaO (1.1 %) and TiO_2 (0.00 %). In the different studies, the use of local sources for brick aggregates was probably a common practice in the Byzantine period (Binda, Baronio, and Tedeschi 1999; Aslan Özkaya 2005; Stefanidou et al. 2014; Ulukaya et al. 2017; Taranto et al. 2019; Pérez-Monserrat et al. 2022).

The brick aggregates in lime mortars from Monuments in Kiev were consisted of calcite, quartz, feldspar, hematite and dolomite (Moropoulou, Çakmak, and Lohvyn 2000) while lime plasters from Serapis Temple had quartz, albite, feldspar, muscovite and hematite minerals (Özkaya and Böke 2009). In St. Jean Church in Manisa, the brick aggregates were composed of quartz, feldspars, calcite and illite minerals (Oğuz Kılıç et al. 2004). Amorphous phase also was detected (Oğuz Kılıç et al. 2004). The brick aggregates in lime mortar from Early Byzantine Church in Southwest Anatolia was composed of quartz, calcite, albite and illite minerals (Caner and Güney 2018) when Middle Byzantine Chapel in Istanbul had quartz, anorthite and muscovite minerals (Ulukaya et al. 2017).

Lime lumps:

The chemical compositions of the lime lumps obtained from Byzantine lime mortars and plasters were examined in a very few studies. The chemical compositions of Byzantine buildings in Kyme were defined and the lime lumps mainly comprised of CaO (91.52-95.82 %) and smaller amounts of SiO₂ (0.68-3.47 %), MgO (0.89-1.16 %), Na₂O (0.20-1.09 %), Al₂O₃ (0.41-1.51 %), K₂O (0.00-0.24 %), TiO₂ (0.09-0.27 %), Fe₂O₃ (0.22-0.62 %). In addition to this, the hydraulic index were calculated in the study with the Boynton formula and exhibiting hydraulic indices were between 0.01-0.06 which revealed that the lime was non-hydraulic (Miriello et al. 2011).

The mineralogical composition of the lime lump of Byzantine lime mortar were only observed in Middle Byzantine Chapel in Istanbul. The mineralogical composition of lime lumps showed only calcite peaks that originated to carbonation of slaked air lime (Ulukaya et al. 2017).

2.2.4. Microstructural Properties

The microstructural properties were examined most of the Byzantine lime mortar and plaster studies. They were generally focused on the mortar matrices, aggregates, the bonding and reactions between lime and pozzolanic aggregates, and shapes and sizes of calcite crystals by using SEM-EDS at different magnifications (80x, 200x, 350x, 500x), optical microscope, and polarizing microscope (Table 2.3).

In the optical microscopy images of lime mortar from St. Katherine's Hospice in Rhodes, crushed bricks were observed. The mortar matrix had a compact structure and

had reaction rims which surround the ceramic fragments. These reaction rims indicated were filled the discontinuities and vacancies in the mortar itself (Moropoulou, Bakolas, and Bisbikou 2000). The St. Jean Church in Manisa, the SEM images of lime mortar matrix had homogenous structure free from pores and cracks. At the brick-lime interface, calcium silicate hydrate (CSH) and calcium aluminate hydrate (CAH), which might be the indicators of hydraulic character of the mortar, were identified (Oğuz Kılıç et al. 2004). The brick-lime interface from Middle Byzantine Church were defined by SEM-EDS mapping analysis (Nežerka et al. 2015). The elemental maps showed that the interface was rich in aluminum and silica as a result of hydraulic reactions of brick and lime. In the reaction rim, calcium was also presented in relatively high amounts since CaO filled the pores of the boundaries of the brick fragments (Nežerka et al. 2015).

The petrographic analysis was performed by polarized microscopy and SEM in some of the studies in order to specify the minerals and aggregate types (Table 2.3). Miriello et al. (2011) determined that Byzantine mortars from Ancient city of Kyme were composed of mostly brick, volcanic rock fragments and a few of them had metamorphic rock fragments in a lower concentration. Some of the minerals, which were quartz, muscovite and calcite identified in XRD peaks, were also observed (Miriello et al. 2011). In lime mortars from Byzantine Church in Negev, quartz, kaolin, dolomite, calcite, gypsum and charcoal minerals were identified. The charcoal existence was attributed to the burnt wood (Freidin and Meir 2005). In the SEM images of Esekap Madrasah, quartz, calcite, anorthite, feldspar and muscovite minerals were observed in addition to the brick and sand fragments (Güleç and Tulun 1996). The brick aggregates from St. Jean Church in Manisa had porous structure in which pore sizes were less than 10 μm , and they were composed of large amounts of SiO_2 and Al_2O_3 determined via EDS. In the matrix, quartz and felspar minerals and sodium and potassium crystals were detected (Oğuz et al. 2003; Oğuz Kılıç et al. 2004).

The properties of lime lumps were examined by SEM images at different magnifications in a limited number of studies. The lime lumps from ancient city of Kyme were found in all Byzantine lime mortars in the size of 40–1000 μm (Miriello et al. 2011). The calcite existence and its recrystallization phenomena were also specified (Miriello et al. 2011).

In the lime mortars and plasters from Esekap Madrasah, the lime was finely grounded revealing the quality of the workmanship. The lime plasters were composed of higher amount of binder matrix than the lime mortars, and thus they had higher calcium

content (Güleç and Tulun 1996). In Early Byzantine Church in Stratonikeia, the SEM-EDS analysis were done on lime lumps (Caner and Güney 2018). Small sized calcite crystals were detected in the SEM images and the EDS analysis showed that the lime was pure lime (Caner and Güney 2018).

Table 2.3. Methods used for the determination of chemical, mineralogical compositions and microstructural properties of mortars and plasters used in different Byzantine period buildings by recent studies

Area & Reference	Period	Mortar/ Plaster	Aggregate Type	Chemical Compositions	Mineralogical Compositions	Microstructural Properties
Fortification Wall of Adana and Kozan Castle in Cilicia (Polat Pekmezci 2012)	Early Byzantine	Mortar	Natural	SEM-EDS	XRD Polarizing microscope Optical microscope	SEM-EDS
Synagogue from Andriake Harbour (Oğuz, Türker, and Koçkal 2015)	Byzantine	Mortar	Natural	XRF SEM-EDS	XRD	SEM-EDS Polarizing microscope
Archeological Site of Kyme (Miriello et al. 2011)	Early Byzantine	Mortar	Natural	XRF SEM-EDS	XRD	Polarizing microscope
Serapis Temple/ Kızıl Avlu (Aslan Özkaya 2005)	Early Byzantine	Mortar	Natural	SEM-EDS	XRD	SEM-EDS
		Plaster	Brick			
Monastery and Churches from Kayseri (Kozlu and Ersen 2011)	Early– Middle Byzantine (4–11 th centuries)	Mortar	Natural	x	x	x
		Plaster	Natural			
Byzantine Bath of Thessaloniki and Castle of Servia (Stefanidou et al. 2014)	Middle Byzantine (10-13 th centuries)	Mortar Plaster	Natural	SEM-EDS	x	SEM-EDS Optical microscope
Esekap Madrasah (Güleç and Tulun 1996)	Middle Byzantine (11 th century)	Mortar	Natural	SEM-EDA	XRD	SEM-EDA
Land Walls of Yedikule in Istanbul (Acun Özgünler, Ersen, and Güleç 2013)	Early Byzantine (5 th century)	Mortar	Brick	ICP	XRD DTA	SEM-EDS
Early Byzantine Church in Stratonikeia in Muğla (Caner and Güney 2018)	Early Byzantine (5–7 th centuries)	Mortar	Brick	SEM-EDS	XRD FTIR	SEM-EDS Polarizing microscope
		Plaster	Brick			

(cont. on next page)

Table 2.3. (cont.)

Area & Reference	Period	Mortar/ Plaster	Aggregate Type	Chemical Compositions	Mineralogical Compositions	Microstructural Properties
Hagia Sophia Basilica (Bakolas et al. 1998)	Early Byzantine (6th century)	Mortar	Brick	x	x	x
St. Jean Church in Manisa (Oğuz Kılıç et al. 2004)	Early Byzantine (6th century)	Mortar	Brick	x	XRD	SEM-EDS
St. Katherines Hospice in Rhodes (Moropoulou, Bakolas, and Bisbikou 2000)	Early– Late Byzantine (6–14 th centuries)	Mortar	Brick	x	XRD	SEM-EDS & TEM Optical microscope
Religious Buildings in Istanbul (Gürdal, Kahraman Altaş, and Acun Özgünler 2011)	Early Byzantine	Mortar	Brick	x	XRD	SEM-EDS Polarizing microscope
Defense Structures in Istanbul (Kahraman Altaş, Acun Özgünler, and Gürdal 2013)	Early Byzantine	Mortar	Brick	x	XRD	SEM-EDS Polarizing microscope
Middle Byzantine Church in Istanbul (Nežerka et al. 2015)	Middle Byzantine (9 th centuries)	Mortar	Brick	SEM-EDS	x	SEM-EDS Polarizing microscope
Middle Byzantine Monuments in Kiev (Moropoulou, Çakmak, and Lohvyn 2000)	Middle Byzantine (11-13 th centuries)	Mortar	Brick	x	XRD Optical microscopy	Optical microscopy
Middle Byzantine Chapel in Istanbul (Ulukaya et al. 2017)	Middle Byzantine (11–12 th centuries)	Mortar	Brick	XRF	XRD & FTIR	Polarizing microscope
Yoros Castle in Istanbul (Kurugöl and Güleç 2012)	Late Byzantine (13–14 th centuries)	Mortar	Brick	ICP	XRD & Polarizing microscope	Polarizing microscope

2.2.5. Pozzolanic Properties of Aggregates

Pozzolanic activities were not determined in all of the studies, but it was stated that the hydraulic properties of the mortars, which determined by TGA or loss of ignition, or the CSH, CAH formations observed in SEM images were attributed to existence of pozzolanic aggregates (Gürdal, Kahraman Altaş, and Acun Özgünler 2011; Kahraman Altaş, Acun Özgünler, and Gürdal 2013; Stefanidou et al. 2014; Ulukaya et al. 2017) (Table 2.4). While the defined pozzolanic properties were generally determined by the electrical conductivity method, the Frattini test method was also used in few studies. The ASTM C618-03 standard that defines the pozzolanic values of aggregates regarding their $\text{SiO}_2 + \text{Al}_2\text{O}_3 + \text{Fe}_2\text{O}_3$ content was not used even in the studies that determine the chemical properties of aggregates.

The electrical conductivities of saturated calcium hydroxide solution ($\text{Ca}(\text{OH})_2$) were measured before and after the addition of fine aggregates ($<53\mu\text{m}$) (Luxan, Madruga, and Saavedra 1989). The calculation found higher than 1.2 mS/cm showed the pozzolanic property of aggregates (Luxan, Madruga, and Saavedra 1989). The electrical conductivity differences of lime mortar with natural aggregates from Serapis Temple were 7.72 mS/cm. The differences were found in lime plasters and mortars with brick aggregates between 4.43–5.93 mS/cm in St. Jean Church in Manisa (Oğuz Kılıç et al. 2004), 3.23–5.90 mS/cm in Serapis Temple (Aslan Özkaya 2005), 0.4–1.2 mS/cm in Hagia Sophia, Hagia Eirine, St. Mary of Chalkoprateia, Church of St. Euphemia, Monastery of Stoudios, Martyrion of Karpos and Papylos, Church of St. Polyeuctus (Gürdal, Kahraman Altaş, and Acun Özgünler 2011), 0.4–1.2 mS/cm in Istanbul Land Walls and Theodosian Walls (Kahraman Altaş, Acun Özgünler, and Gürdal 2013), and 3.1–5.7 mS/cm in Early Byzantine Church in Southwest Anatolia (Caner and Güney 2018).

The Frattini test done by mixing in a certain amount of cement, test material and distilled water and kept 8 days in an oven at approximately 40°C. Then, the samples filter and the filtrates were analyzed for $[\text{OH}^-]$ and $[\text{Ca}^{2+}]$ ions by titration by means of indicators and solutions consisting in the EN 196-5 standard. When the $[\text{Ca}^{2+}]$ and $[\text{OH}^-]$ ions in the solution is down the solubility isotherm, calcined clay is considered as active pozzolan. Due to the Frattini test applied on Middle Byzantine Chapel in Istanbul, the brick aggregates showed pozzolanic property.

2.2.6. Hydraulic Properties of Mortars and Plasters

Determination of hydraulic properties for historical lime mortars and plasters has an important place in the literature to specify their characteristics and production technique. In most of the studies about Byzantine lime mortars and plasters, their hydraulic properties were examined via using thermogravimetric analysis (TGA) (Bakolas et al. 1998; Moropoulou, Çakmak, and Lohvyn 2000; Moropoulou, Bakolas, and Bisbikou 2000; Kurugöl and Güleç 2012), loss of ignition (Gürdal, Kahraman Altaş, and Acun Özgünler 2011; Polat Pekmezci 2012; Kahraman Altaş, Acun Özgünler, and Gürdal 2013; Acun Özgünler, Ersen, and Güleç 2013) and hydraulic and cementation index by Boynton formula (Miriello et al. 2011; Kurugöl and Güleç 2012; Stefanidou et al. 2014) (Table 2.4). In the thermogravimetric analysis or loss of ignition, the hydraulicity were determined by measuring the weight losses due to the loss of chemically bound water (H₂O) of hydraulic products between 200-600°C (H₂O) and the release of carbon dioxide (CO₂) during decomposition of calcium carbonate (CaCO₃) between 600-900°C (CO₂) (Bakolas et al. 1998). Hereunder, the CO₂/H₂O ratio lower than 10 indicated the hydraulic character of lime mortars or plasters. On the other hand, hydraulic index (HI) values higher than 0.1, and cementation index (CI) values higher than 0.3 also demonstrated the hydraulic character of mortar and plaster (Eckel 1905; Boynton 1966).

The CO₂/H₂O ratio of the lime mortars with natural aggregates from Byzantine Bath of Thessaloniki and Castle of Servia was found 2.88–3.08 revealed that they were hydraulic lime mortars. However, one sample were found typical lime mortar (Oğuz, Türker, and Koçkal 2015).

The CO₂/H₂O ratios of the Byzantine lime mortars and plasters produced by using brick aggregates were in the range of 2.91–6.10 in Hagia Sophia Basilica (Bakolas et al. 1998), 5.7–5.9 in St. Katherines Hospice in Rhodes (Moropoulou, Bakolas, and Bisbikou 2000), nearly 3.5–9.5 in Middle Byzantine Monuments in Kiev (Moropoulou, Çakmak, and Lohvyn 2000), approximately 4 in St. Jean Church in Manisa (Oğuz Kılıç et al. 2004), 0.9–5.6 in Hagia Sophia, Hagia Eirine, St. Mary of Chalkoprateia, Church of St. Euphemia, Monastery of Stoudios, Martyrion of Karpos and Papylos, Church of St. Polyeuctus (Gürdal, Kahraman Altaş, and Acun Özgünler 2011), 0.38–2.72 in Yoros Castle (Kurugöl and Güleç 2012), and 3–4 by weight in Istanbul Land Walls and Theodosian Walls (Kahraman Altaş, Acun Özgünler, and Gürdal 2013). The CO₂/H₂O

ratios between 0.38–9.5 indicated that all lime mortar and plasters with brick aggregates possessed hydraulic characteristics.

The hydraulic characteristics were also defined by hydraulic (H.I.) and cementation indices (C.I.) in some studies. Hydraulic index values lower than 0.1, and cementation index values lower than 0.3 show the non-hydraulic character of lime (Eckel 1905; Boynton 1966). Lime mortars with natural aggregates from Archeological site of Kyme had the H.I. values between 0.1–5.89 (Miriello et al. 2011), while lime mortar with brick aggregates from Yoros Castle had H.I. between 2.30–2.31 (Kurugöl and Güleç 2012). The C.I. of lime mortars and plasters with natural aggregates from Byzantine Bath of Thessaloniki and Castle of Servia were in 2.26–4.63 (Stefanidou et al. 2014), when the lime mortars composed of brick aggregates from Yoros Castle were between 13.01–15.76 (Kurugöl and Güleç 2012). These hydraulic and cementation index values demonstrated that, the samples were hydraulic as found by TGA. Therefore, all these methods were compatible with each other.

In addition to that, H.I. values of the lime lumps were determined in Kyme samples and found approximately 0.03 and 0.21 revealing they were as non-hydraulic (Miriello et al. 2011).

Table 2.4. Methods used for the determination of hydraulic and pozzolanic properties of mortars and plasters used in different Byzantine period buildings by recent studies

Area & Reference	Period	Mortar/ Plaster	Aggregate Type		Hydraulic Properties
Fortification Wall of Adana and Kozan Castle in Cilicia (Polat Pekmezci 2012)	Early Byzantine	Mortar	Natural	x	Loss of ignition (105 °C /550 °C / 1050°C)
Synagogue from Andriake Harbour (Oğuz, Türker, and Koçkal 2015)	Byzantine	Mortar	Natural	Electrical conductivity method	Thermogravimetric analysis (200-600 °C /600-900°C)
Archeological Site of Kyme (Miriello et al. 2011)	Early Byzantine	Mortar	Natural	x	Hydraulic Index (HI) via Boynton formula
Serapis Temple/ Kızıl Avlu (Aslan Özkaya 2005)	Early Byzantine	Mortar	Natural	Electrical conductivity method	Thermogravimetric analysis (200-600 °C /600-900°C)
		Plaster	Brick		
Monastery and Churches from Kayseri (Kozlu and Ersen 2011)	Early– Middle Byzantine (4–11 th centuries)	Mortar	Natural	x	x
		Plaster	Natural		
Byzantine Bath of Thessaloniki and Castle of Servia (Stefanidou et al. 2014)	Middle Byzantine (10-13 th centuries)	Mortar Plaster	Natural	High amount of $\text{SiO}_2 + \text{Al}_2\text{O}_3 + \text{Fe}_2\text{O}_3$	Thermogravimetric analysis (200-600 °C /600-800°C) Cementation Index (CI)
Esekap Madrasah (Güleç and Tulun 1996)	Middle Byzantine (11 th century)	Mortar	Natural	x	x
Land Walls of Yedikule in Istanbul (Acun Özgünler, Ersen, and Güleç 2013)	Early Byzantine (5 th century)	Mortar	Brick	x	Loss of ignition (105 °C /550 °C / 1050°C)
Early Byzantine Church in Stratonikeia in Muğla (Caner and Güney 2018)	Early Byzantine (5–7 th centuries)	Mortar	Brick	Electrical conductivity method	x

(cont. on next page)

Table 2.4. (cont.)

Area & Reference	Period	Mortar/ Plaster	Aggregate Type	Pozzolanic Properties	Hydraulic Properties
Hagia Sophia Basilica (Bakolas et al. 1998)	Early Byzantine (6th century)	Mortar	Brick	x	Thermogravimetric analysis (<200 °C / 200-600 °C />600°C)
St. Jean Church in Manisa (Oğuz Kılıç et al. 2004)	Early Byzantine (6th century)	Mortar	Brick	Electrical conductivity method	Thermogravimetric analysis (200-600 °C /600-900°C)
St. Katherines Hospice in Rhodes (Moropoulou, Bakolas, and Bisbikou 2000)	Early– Late Byzantine (6–14 th centuries)	Mortar	Brick	x	Thermogravimetric analysis (120 °C / 200-600 °C />600°C)
Religious Buildings in Istanbul (Gürdal, Kahraman Altaş, and Acun Özgünler 2011)	Early Byzantine	Mortar	Brick	Electrical conductivity method	Loss of ignition (200-600 °C /600-900°C)
Defense Structures in Istanbul (Kahraman Altaş, Acun Özgünler, and Gürdal 2013)	Early Byzantine	Mortar	Brick	Electrical conductivity method	Loss of ignition (200-600 °C /600-900°C)
Middle Byzantine Church in Istanbul (Nežerka et al. 2015)	Middle Byzantine (9 th centuries)	Mortar	Brick	x	x
Middle Byzantine Monuments in Kiev (Moropoulou, Çakmak, and Lohvyn 2000)	Middle Byzantine (11-13 th centuries)	Mortar	Brick	x	Thermogravimetric analysis (200-600 °C />600°C)
Middle Byzantine Chapel in Istanbul (Ulukaya et al. 2017)	Middle Byzantine (11–12 th centuries)	Mortar	Brick	EN 196-5 standard (Fratini test)	Thermogravimetric analysis (200-600 °C /600-900°C)
Yoros Castle in Istanbul (Kurugöl and Güleç 2012)	Late Byzantine (13–14 th centuries)	Mortar	Brick	x	Hydraulic (HI) & Cementation Index (CI) via Boynton formula

CHAPTER 3

KADIKALESİ (ANAIA) AND AYASULUK

General information about the historical background, architectural characteristics, and material use of Kadıkalesi (Anaia) and Ayasuluk are explained in this chapter.

Kadıkalesi (Anaia) is located in Kuşadası-Aydın and Ayasuluk is located in Selçuk-İzmir, in Western Anatolia, 28.6 km from each other (Figure 3.1, 3.2). Kadıkalesi (Anaia) and Ayasuluk are among Byzantine settlements in Western Anatolia.

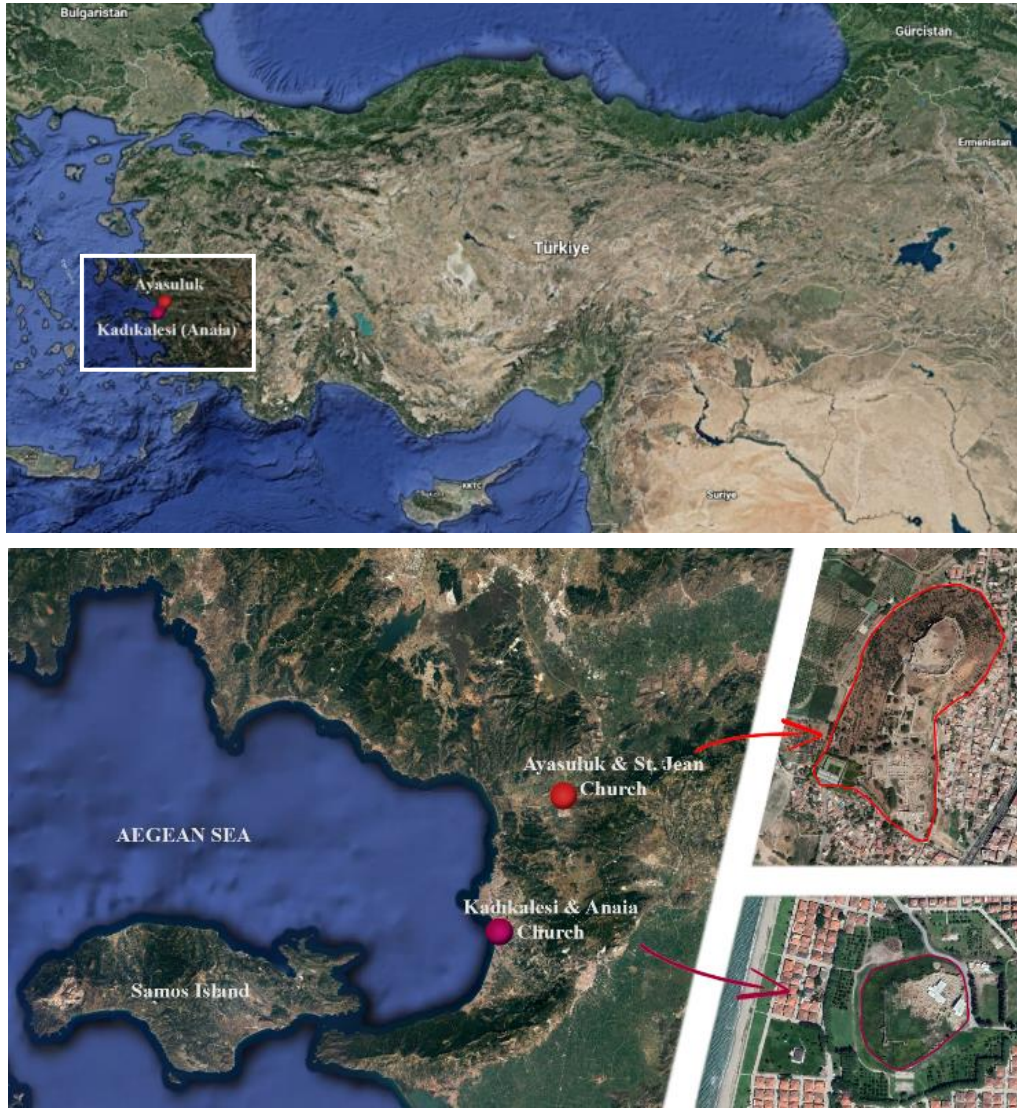


Figure 3.1. Location of Kadıkalesi (Anaia) and Ayasuluk
(Aerial image: Google Earth, May 2022)

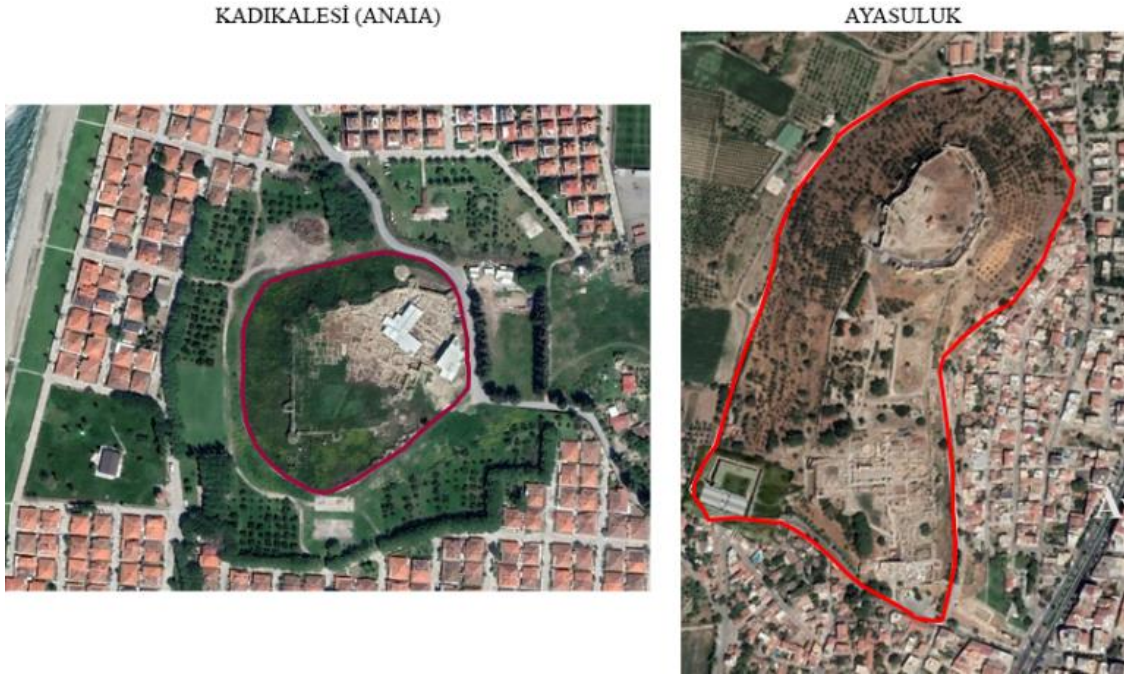


Figure 3.2. Kadikalesi (Anaia) and Ayasuluk
(Aerial image: Google Earth, May 2022)

It is widely accepted that Byzantium began with the establishment of Constantinople in 324 AD and ended with its conquest by the Ottoman Empire in 1453 AD. (Mango 1976). In general, the historians divided Byzantine Period into Early, Middle and Late Byzantine Periods (Mango 1976; Krautheimer 1986) (Figure 3.3):

- 4th – 9th centuries: Early Byzantine Period
- 9th – 13th centuries: Middle Byzantine Period
- 13th – 15th centuries: Late Byzantine Period

In the case areas of Kadikalesi (Anaia) and Ayasuluk, there are structures belonging to these Byzantine periods (Figure 3.3) (Karydis 2015; Kanmaz 2015; Kanmaz and İpekoğlu 2016).

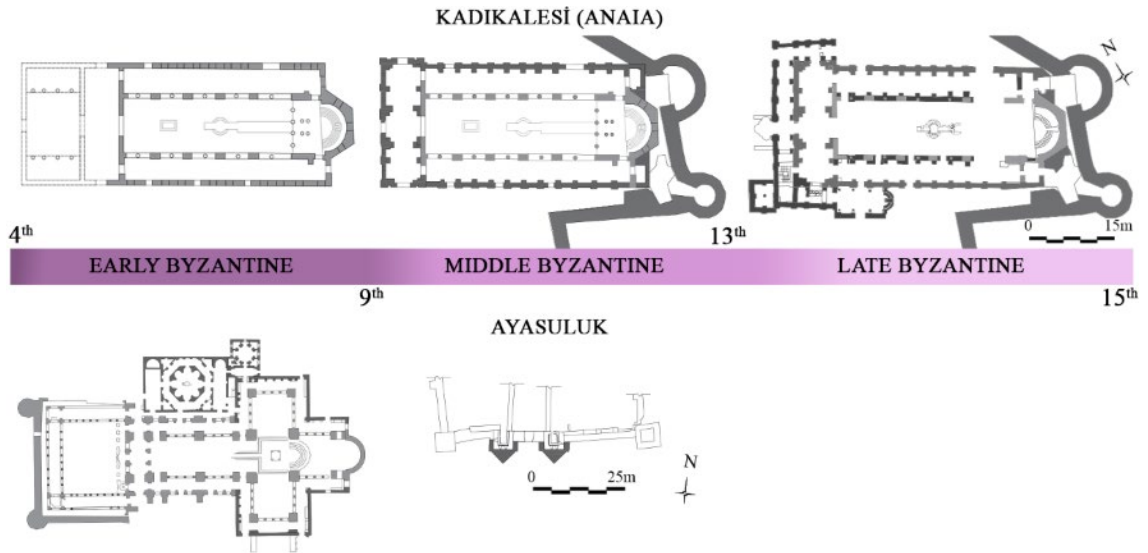


Figure 3.3. Plans of Anaia Church, Kadıkalesi fortification walls and St. Jean Church, Gate of persecution of Ayasuluk in different Byzantine periods (Modified from the drawings from Kanmaz 2016, Karydis 2015)

3.1. Kadıkalesi (Anaia)

Kadıkalesi (Anaia), was located on a prehistoric mound in the south coast of Kuşadası, Aydın province (Figure 3.4). It is approximately 16 km away from Dilek Peninsula, Büyük Menderes Delta National Park and 25 km away from Samos Island.



Figure 3.4. Aerial image of Kadıkalesi (Anaia)
(Source: Kadıkalesi (Anaia) excavation archive, 2020)

3.1.1. Historical Background of Kadıkalesi (Anaia)

Kadıkalesi (Anaia), which was built on a prehistoric mound, had various settlement strata (Akdeniz 2007; Mercangöz 2008). The findings obtained during the excavations revealed that the first settlement started from the Late Chalcolithic Age and continued with the Early, Middle, Late Bronze Ages, Ancient Greek and Roman civilizations, Byzantine, Beyliks and Ottoman settlements (Akdeniz 2007; Mercangöz 2008).

Anaia was first mentioned by Greek author Thucydides in the early fourth century B.C, in “The History of the Peloponnesian War” which narrated the war between 431 and 404 B.C. (Thucydides 2009). The narrative was about the communities involved in the war and their effects on it. Anaia's location and its role in the war were also mentioned in this source. Based on this narrative, Cramer stated that Anaia had a harbor and was in the high lands of the Menderes River between Magnesia and Priene (Cramer 1832). Texier interpreted this information as the land of the Anaian’s continued as far as the shores of Samos (Texier 2002).

The research of Kadıkalesi (Anaia) excavations exposed that the city of Anaia during antiquity and medieval times was located around where Kadıkalesi is situated at the present (Mercangöz 2008). No traces of buildings belonging to the Hellenistic and Roman periods were found within the Kadıkalesi city border (Mercangöz 2002, 2005, 2008; Mercangöz and Tok 2011; Mercangöz, Tok, and Hazinedar Coşkun 2012; Hazinedar Coşkun 2021). However, epigraphs and stone works dated to these periods, which were used in Byzantine buildings as *spolia* (devşirme stones), were unearthed during excavations (Mercangöz and Tok 2011; Mercangöz 2012).

Anaia Church and the baptistery in the northwest were built in the Early Byzantine period (in 5-6th centuries) (Mimaroğlu 2011b, 2011a; Mercangöz, Tok, and Hazinedar Coşkun 2012; Kanmaz and İpekoğlu 2016; Mercangöz 2018; Hazinedar Coşkun 2021) (Figure 3.5).

According to the church registrations, Anaia Church had served as a bishopric of the Ephesus Metropolis between the Early Byzantine to Late Byzantine periods (5-13th centuries) (Foss 1979). From the beginning of the 10th century, the port of Ephesus became unusable for the Byzantine fleet and so the ports of Anaia and Phygela, in the west of Ephesus, gained importance (Foss 1979). During the Lascaris dynasty between

1204–1261 (Middle Byzantine period), Anaia became an *emporion* (trade center), *kommerkion* (customs station) and the Anaia Church ascended to archbishopric (Foss 1979; Mercangöz 2010, 2012, 2013).



Figure 3.5. Aerial image of Anaia Church
(Source: Kadıkalesi (Anaia) excavation archive, 2021)

In the late 13th century, Anaia became a center of piracy consisted of Greeks, Genoese and Turks (Tomaschek 1891; Mercangöz 2008). Anaia was taken by the Turks in 1298, but passed into the hands of the Catalans, who were called for help by Byzantium. It was stated that the Catalans stayed there until 1304 (Tomaschek 1891). However, the excavations revealed the coins of the Rhodes knights dated 1340, thus showing the Christian life in Anaia can be dated to the 14th century (Mercangöz 2012). According to Lemerle, the Anaiaans moved to the inwards where Soğucak Village currently located (Lemerle 1965).

Anaia was dominated by the Aydınoğulları in the 14th century and by the Ottomans in the early 15th century. There is no comprehensive Turkish period structures in the Site, apart from the masjid dated to the Late Ottoman Period (Mercangöz 2008, 2012). While Kuşadası started to gain prominence after the 16th century, Anaia has begun to lose its importance in the region (Onar et al. 2012).

Kadıkalesi (Anaia) was mentioned in "Priene: Ergebnisse der Ausgrabungen und Untersuchungen in den Jahren 1895-1898" written by Wiegand and Schrader. Kadıkalesi

was a fortress built for defending the city of Anaia at end of the 12th or early beginning of 13th centuries (Wiegand and Schrader 1904 cited in Kanmaz 2015; Foss 1979). In the light of these information, Kadıkalesi and Anaia gained their common historical identity.

In 2001, the rescue excavation of Kadıkalesi (Anaia) had started due to the illegal excavations, housing issues in the surrounded area and intense vegetation with the title of “*Kuşadası-Kadıkalesi Kazı ve Restorasyon Projesi*” (Mercangöz 2002). Kadıkalesi (Anaia) was determined as a 1st degree archaeological site with the decision number 1531 in 22.05.2008. The excavations and conservation works continued under the supervision of Prof. Dr. Zeynep Mercangöz from 2001 to 2021, with the support of the Ministry of Culture and Tourism, Kuşadası Municipality and Ege University. Since 2022, it has been continued by the Directorate of Aydın Museum with scientific supervisor of Assoc. Prof. Dr. Suna Çağaptay and honorary head Prof. Dr. Zeynep Mercangöz.

3.1.2. Architectural Features and Material Characteristics of Kadıkalesi and Anaia Church

Within the area surrounded by the Kadıkalesi fortification walls, there are the Anaia Church, Early period baptistery, workshops, a maşjid, and emplacements. Anaia Church was consisted of the apse, bema, baptistery, cisterns, pastophoria, inner and outer narthex, naos, south chapel, and substructure (Figure 3.6).

Spatial organization, construction techniques and materials, and architectural elements of Anaia Church showed that the building had three construction periods (Karabacak 2010; Kanmaz 2015; Kanmaz and İpekoğlu 2016).

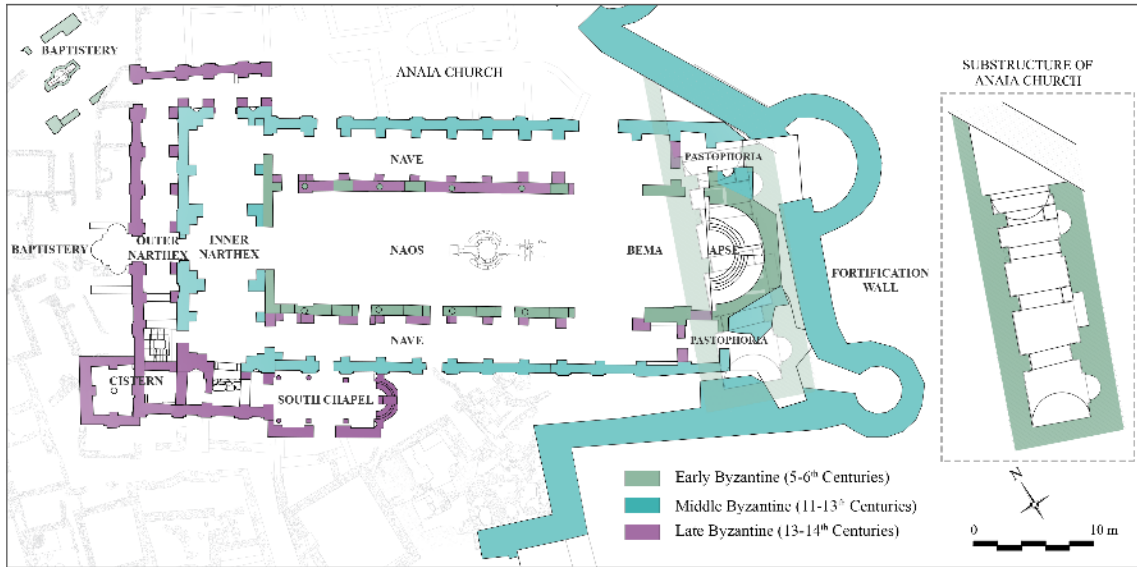


Figure 3.6. Plan showing the spaces and construction periods of Anaia Church (Revised from the drawing by Mehmet Buğra Kanmaz and Umut Kardaşlar, Source: Kadikalesi excavation archive, 2020)

The first construction period of Anaia Church was between 5–6th centuries (Early Byzantine) due to the plan scheme reflecting the characteristics of the period, as well as the architectural elements like the ambo in the naos and the synthronon in the apse (Mercangöz, Tok, and Hazinedar Coşkun 2012; Kanmaz 2015; Kanmaz and İpekoğlu 2016) (Figure 3.7). The church was composed of three naves, a narthex and atrium spaces. According to the traces obtained from the building, it is accepted that the naves and naos were separated from each other with buttresses, marble piers and covered with a wooden hipped roof. Western walls of naos, bema walls and apse still exist in the site from the first construction period. In the naos, traces of marble pavements were also found.



Figure 3.7. a: Ambo in naos as the characteristic of Early Byzantine period, b: Substructure)

The wall of the bema and surface of apse had similar bonding techniques in which brick and stones of different sizes were used alternately in the masonry system. The thickness of the bema walls was in between 90–125 cm, and mortar joints were between 1–2 cm. Remains of mural paintings were found in the apse, bema and baptistery.

The walls of substructure were built in cut stone masonry, while the vault and the arches were constructed of bricks and covered by mural paintings (Figure 3.8). The thickness of the lime mortar joints was generally between 3–6 cm. The buttresses (thickness of 120–130 cm) supporting the arches were in brick and stone masonry with an alternating order and their joints were between 1–6 cm. The Early Byzantine baptistery in the northwest, the baptistery font was covered with ornamented marble by using adhesive lime mortar with natural aggregates (Figure 3.9). The wall of the baptistery was bonded with stone and brick with the thickness of nearly 57 cm. The pavement of the area consisted of opus sectile, marble and brick blocks (Figure 3.9).



Figure 3.8. Mural paintings in substructure



Figure 3.9. Early Byzantine baptistery of Anaia Church

The second construction period was dated to Middle Byzantine Period (11–13th centuries) and *pastophoria* and fortification walls were built in this period. The walls of narthex (thickness of 88–100 cm), south and north walls of naves (70–85 cm) and the buttresses between the naos walls and the narthex (75–140 cm) could be differentiated by the bonding technique of brick and stone masonry using different alignment with joint gaps between 1–5 cm (Figure 3.10). In this bonding system, recessed brick technique which was a characteristic feature of Middle Byzantine period (11–12th centuries) was also observed (Mango 1976; Ousterhout 1999) (Figure 3.11).

Kadıkalesi (Anaia) is on a first-degree seismic zone, and throughout history, it was damaged in three major earthquakes in 1039, 1040 and 1056 (Middle Byzantine periods) with intensities VIII, VII, VIII, respectively, according to the MSK-64 intensity scale (Calvi 1941 cited in Kanmaz 2015, Kanmaz and İpekoğlu 2016; Soysal et al. 1981; MTA 2005) (Table 3.1).

Table 3.1. MSK-64 Intensity scale with its definition
(Soysal et al. 1981)

MSK-64 Intensity Scale	Definition
V	Fairly Strong
VI	Strong
VII	Very Strong
VIII	Damaging
IX	Destructive
X	Devastating

The second construction period also included the repairs and reinforcements of the damages caused by these earthquakes. Determined differences in terms of bonding order of building materials in the walls and discontinuity in joints between western wall of naos and narthex, lead to consider the narthex, and the south and north naves were rebuilt after these earthquake damages (Mercangöz and Tok 2011; Mercangöz, Tok, and Hazinedar Coşkun 2012; Kanmaz 2015; Kanmaz and İpekoğlu 2016). In the narthex and inner surface of the naves, the walls had mural painting traces, but the outer surfaces of the naves were clad with lime-brick plaster by leaving the building materials exposed (Figure 3.11). Cut stone paving were used in both narthex and naves. The atrium was probably not rebuilt after the earthquake (Kanzmaz 2015).



Figure 3.10. Bonding differences and discontinuity in joints between the naos walls and narthex buttresses

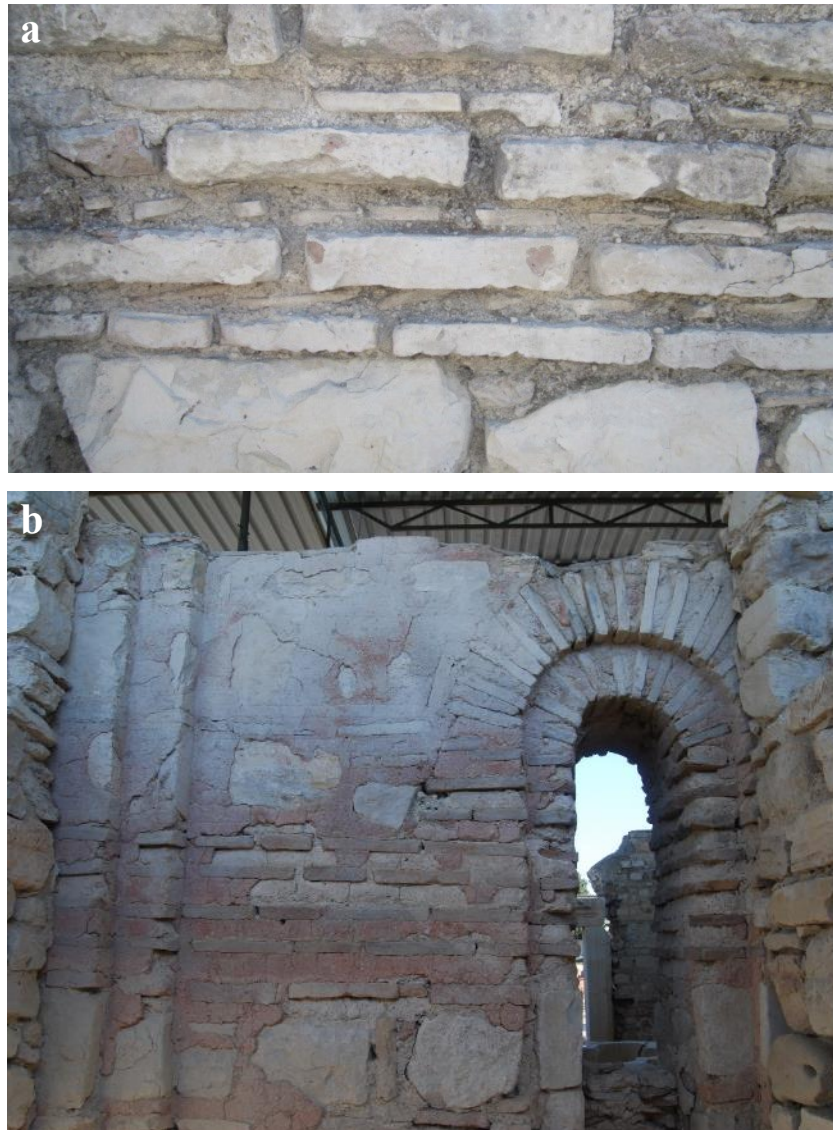


Figure 3.11. a: Recessed brick technique (Source: M.B. Kanmaz 2015), b: Plastering the joints

Rough cut stones and spolia were framed by bricks on the fortification wall which was defined in the literature as *framed technique* (Eyice 1963; Ousterhout 1999). It is a distinctive feature of the Laskaris period (1204–1261) (Mercangöz 2010) (Figure 3.12). Therefore, Kadıkalesi fortification wall is dated to the Middle Byzantine period and it has thought to be built for defending the Anaia City (Foss 1979; Mercangöz 2008, 2010).



Figure 3.12. Kadıkalesi fortification wall

Third construction period of the Church was accepted between 13th and 14th centuries (Late Byzantine period). During this period, it was thought that the structure was strengthened against the destructive effects of earthquakes due to the different bonding techniques observed on the naos walls, buttresses and nave buttresses (Kanmaz 2015; Kanmaz and İpekoğlu 2016). Also, the discontinuity in wall joints and differences in wall bonding techniques indicated that the Church was extended with addition of outer narthex, south chapel, baptistery and two cisterns (Mercangöz and Tok 2011; Kanmaz 2015; Kanmaz and İpekoğlu 2016).

Although inner narthex (second construction period) was bonded with brick-stone alternating order, the outer narthex walls (thickness of 80–85 cm) and buttresses (100–130 cm) were built with rough cut stone. Observing the baptistery in the continuation of the rough-cut stone wall showed that it was also built in the third construction period. Besides, north and south walls (80–90 cm) and buttresses (65–70 cm) of naos were bonded with the rough-cut stone probably to strengthen the structure. Due to the discontinuity between the walls of naves (second construction period) and south chapel, south chapel, and cisterns that continue with also should have been added later. The south chapel walls were approximately 82 cm, while cistern walls were in the range of 70–85 cm.

In the cistern I, two layers of lime plasters with brick aggregates, with thickness of 2 cm for each, were applied on the interior surfaces of walls, whereas in cistern II only one layer of lime plaster with 2 cm thickness was applied. The pavement and the top layer of the arches were also covered with brick- lime plasters.

Horizontal and vertical ornaments were observed on the plasters applied on the walls of cistern II and exterior surfaces of the outer narthex walls (Figure 3.13). The

ornaments were probably done with a red painted rope or a sharp tool to emphasize the joints or to imitate the vertical bricks (Restle 1967; Mango 1976; Ötügen 1990). On the other hand, on the niches and inner walls of outer narthex, only the joints were plastered as can be observed on the exterior surfaces of the nave walls and buttresses. In the baptistery, the mural paintings were determined on the walls. The pavements of outer narthex were coated with brick blocks.



Figure 3.13. Horizontal and vertical ornaments on brick-lime plaster

3.2. Ayasuluk Hill and St. Jean Church

Ayasuluk Hill, which is the first and last settlement of Ephesus, and St. Jean Church are on the UNESCO World Heritage List together with the ancient city of Ephesus, Turkey. It is settled on a prehistoric mound in the present day province of Selçuk, İzmir (Figure 3.14) (Ladstaetter et al. 2015). It is 80 km away from İzmir city center and near to the ancient city of Ephesus, House of Virgin Mary, and Çukuriçi

Mound. Besides, it is on the south of the Küçük Menderes River and it is 9 km away from Küçük Menderes Delta.



Figure 3.14. Aerial image of Ayasuluk
(Source: Selçuk Kent Belleği 2022)

3.2.1. Historical Background of Ayasuluk

A complex and continuous settlement in Ephesus dates back to 3000 B.C. The city site and its harbors were relocated throughout history because of the constant shifting of the shoreline from the east to the west. The first settlement of Ephesus was set on Ayasuluk Hill in the Early Bronze Age (nearly 3000 B.C). During the Hittite dynasty, Ayasuluk was the capital of the Arzawa-Mira Kingdom and was named “*Apasas*” and “*Ephesus*” in the following years (Figure 3.15). In Iron Age, Ephesus was conquered by Lydian King Kroisos, and the city was moved to the plain around the Artemis Temple. The settlement stayed there until the city harbor was silted up. In 300 B.C, the third settlement (Hellenistic city) was established by Lysimakhos, one of the generals of Alexander the Great, between Bülbül and Panayır mountains, where the current ancient city of Ephesus is (Figure 3.15). In the Roman period, Ephesus became the capital of Asian State (Büyükkolancı et al. 2013; Ladstaetter et al. 2015; Selçuk Belediyesi 2022).

Between the years of 37 and 48, St. John, who was one of the apostles of Jesus and also the author of the bible and the apocalypse according to Christian belief, came to

Ephesus with Virgin Mary. He spent his last years in Ayasuluk and was buried here. Because of the importance of St. Jean for Christians, Ayasuluk was a great religious center for pilgrims from 1st century to end of the Byzantine period (Foss 1979).

In the 4th century, a Martyrion (Mausoleum) was built over his tomb. Martyrion was surrounded by a basilica in the time of Theodosius II was (408-450) (Foss 1979; Büyükkolancı 2001; Karydis 2015). The basilica effected from the earthquakes in 468 (Büyükkolancı 2001; MTA 2005). In the Justinian I period (520s), a basilica was built, but some parts of the perimeter walls of the first church were preserved. This structure also collapsed due to a severe earthquake that occurred later. Subsequently, the church was rebuilt in 550s according to the request of Justinian I (Büyükkolancı 2001; Büyükkolancı et al. 2013; Ladstaetter et al. 2015; Karydis 2015; Büyükkolancı 2018). The remains of the first, second and third church belonging to Early Byzantine period have survived to the present (Figure 3.15)

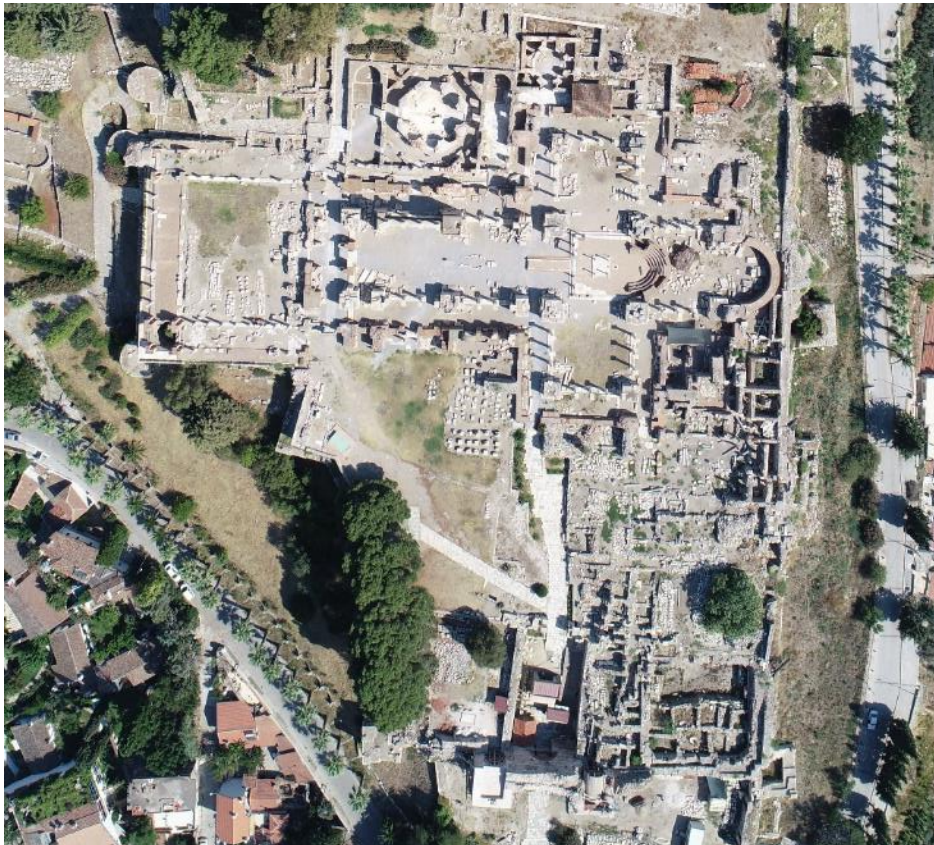


Figure 3.15. Aerial image of St. Jean Church
(Source: Selçuk Kent Belleği, 2022)

During the 6th century, the Ephesus harbour was filled with silt and became a swamp area. Therefore, the inhabitants moved again to the environs of St. Jean Church, Ayasuluk Hill and its slopes (Figure 3.16). In the 7th century, the bishop's palace and the metropolit were moved by St. Jean Church (Büyükkolancı et al. 2013; Ladstaetter et al. 2015; Selçuk Belediyesi 2022). The fortification walls adjacent to the inner walls were built to surround the entire church in the 8th and 9th centuries against the Arab raids (Büyükkolancı 2018).

Ayasuluk, which was attacked and plundered many times until the 11th century, was conquered by a Seljuk Bey, Tengri Birmiş, in 1090. However, it was taken back by the Byzantines in 1096. In approximately 1307, Ayasuluk passed to Turks, Aydınoğulları, and the habitants migrated to Tire. Therefore, the Turkish period started, and Old Ephesus was named as "Ayasuluk" (Büyükkolancı 2001). Under the Turkish rule, several mosques such as İsa Bey Mosque, Masjids, baths and tombs were built in Ayasuluk (Ladstaetter et al. 2015). Fortification walls of the citadel were also built in Seljuks and Ottoman eras. Ayasuluk served as the capital of Aydınoğulları between 1348–1390 and established strong economic and commercial relations with the west. St. Jean Church was used as a mosque in this period, but the church was severely damaged by the earthquakes in the 14th century. After 1390, Ayasuluk came under the control of the Ottomans (Büyükkolancı 2001).

During the 15th century, Ayasuluk was a crowded city where Turks and Rums were lived together (Foss 1979) (Figure 3.16). However, after the 16th century, it lost its importance with the development of İzmir and Kuşadası ports. In 1913, the name of Ayasuluk was changed as Selçuk (Selçuk Belediyesi 2022).



Figure 3.16. Schematic layout plan of Ayasuluk (Ephesus) during the Beyliks Period (Source: Caner Yüksel 2019)

The first archaeological excavation in St. Jean Church was carried out by archaeologist G.A. Sotiriou in 1921 and 1922 (Büyükkolancı 2001). Between 1927 and 1931, the excavations were conducted by H. Hörmann and F. Miltner within the Austrian Archaeological Institute. In 1976, Ayasuluk Hill was registered as a part of “Selçuk-Efes Çevre Düzenleme ve Kazı Onarım Projesi” (Asatekin 1981). Ayasuluk Hill and St. Jean Monument excavations were carried out within the body of Ephesus Museum between 1960–2006. The excavations and repairs were conducted under the supervision of Dr. Mustafa Büyükkolancı on behalf of the Ministry of Culture and Tourism and Pamukkale University between 2007–2020. Since 2020, the excavation and repair studies continue with the head of Assoc. Prof. Dr. Sinan Mimaroğlu, in cooperation with the Ministry of Culture and Tourism, and Hatay Mustafa Kemal University.

3.2.2. Architectural Features and Material Characteristics of Ayasuluk and St. Jean Church

The third church of St. Jean, in its current state, consisted of an apse, atrium, bema, baptistery, naos, narthex, naves, transepts, treasury room, and substructure (Figure 3.17).

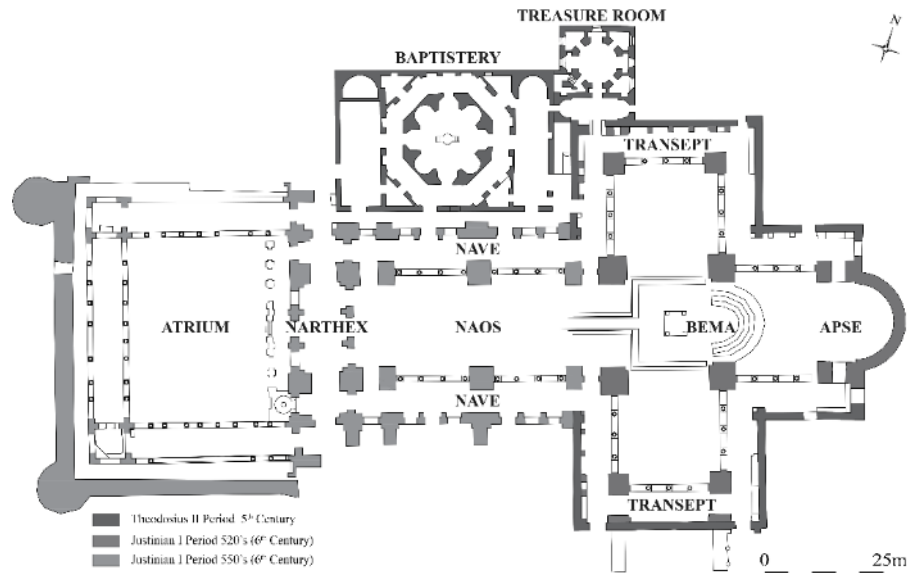


Figure 3.17. Plan showing the spaces and construction periods of St. Jean Church (Revised from the Ayasuluk Hill excavation archive 2020 and Karydis 2015)

Three construction periods were determined due to the foundation traces of the structures and discontinuity in joints.

The first construction period of the church was on a square planned Martyrion which was built over St. Jean's tomb. It was a wooden-roofed basilica with a cross-plan during the time of Theodosius II and accepted as the first construction of the St. Jean Church (408-450) (Hörmann, Keil, and Sotiriou 1951 cited in Büyükkolancı 2001; Foss 1979; Büyükkolancı 2001; Karydis 2015).

The structures that remained from the first church were a baptistery, a treasure room, and north and south walls of transepts (Karydis 2015). The baptistery had a complex plan composed of an octagonal central part surrounded with a corridor, corner rooms and flanked with apsidal halls to the east and west (Figure 3.18). The treasure room also had a complex plan and had corner rooms and niches on the wall (Figure 3.19). Due to the traces of a higher wall, it is evaluated that the treasure room had a second floor (Büyükkolancı 2001).



Figure 3.18. Baptistery in St. Jean Church (a: Baptistery, b: Apsidal hall with tesserae)

The wall bonding system of the baptistery and the treasure room had similar characteristics which were brick and rubble stone adhered with lime mortar, and they had marble pavement. The wall thicknesses of baptistery were between 80–85 cm with 4 cm joint gaps, while the walls of treasure room were in the range of 95–100 cm with 1.5–3.5 cm joint gaps. Due to the construction type of baptistery and the inscription on its entrance, it should have been built in 5th century (Karydis 2015). Constructional similarities between baptistery and treasure room demonstrated that they were constructed in the same period (Karydis 2015).

The transept walls (120–140 cm) and buttresses (nearly 115 cm) on the north and south were built with brick masonry. The joint gaps were between 3–5 cm. On the baptistery wall, marble blocks were used as cladding and apsidal halls' pavements had colored stone tesserae (Figure 3.18). On the other hand, the walls of the treasure room were bonded only with brick masonry and covered with lime plaster with brick aggregates (3–5 cm thickness) (Figure 3.19).

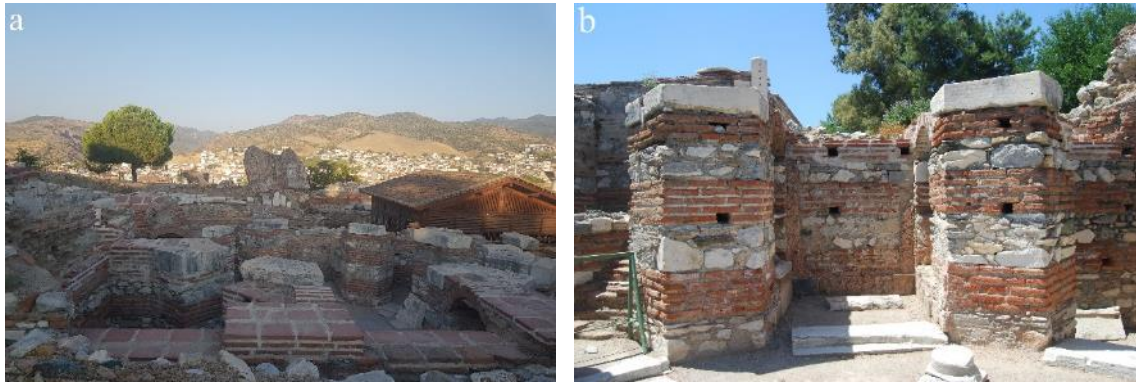


Figure 3.19. Treasure room in St. Jean Church, a: East facing part of the treasure room, b: West wall of the treasure room

During the earthquakes in 468, the first basilica was damaged (Büyükkolancı 2001; Büyükkolancı et al. 2013; Ladstaetter et al. 2015; Büyükkolancı 2018). Therefore, during Justinian period, a church was built on the ruins (Karydis 2015; Büyükkolancı 2001).

In the second construction period, an entirely vaulted, Greek-cross planned basilica was built by preserving the perimeter walls of the first church during the Justinian I era (520s) (Büyükkolancı 2001; Karydis 2015). Some of the buttresses were constructed with brick and rubble stone (thickness of nearly 340 cm with 2–3.5 cm joint gaps) in apse whereas the arches in apse and bema were of brick masonry. The bema buttresses and other two buttresses in apse were built by using cut stone and with a thickness of approximately 455 cm with 2–4 cm joint gaps. After a severe earthquake, the second construction church were damaged (Büyükkolancı 2001; Karydis 2015). The second church remains were apse, bema and buttresses in transepts.

In the third construction period, the church was rebuilt on the remaining structures with the order of Justinian I in 550s. With the addition of the two-bay nave six

domed bays occurred and formed an elongated, directional plan (Büyükkolancı 2001; Büyükkolancı et al. 2013; Karydis 2015; Ladstaetter et al. 2015; Büyükkolancı 2018).

Marble piers were in the naos (Figure 3.20). The buttresses in the naos and transepts were bonded with cut stone and spolia (Figure 3.20), and they were covered with lime plaster composed of brick aggregates. Buttresses and walls (thickness of 120–130 cm with 2–4 cm joint gaps) in the naves were built with brick masonry. The different alignment in the brickwork and discontinuity in joints between the nave and the transept can be considered as the features of the third construction period (Figure 3.21) (Karydis 2015). The Justinian I monograms in the nave also supported the evaluation of the belonged period (Figure 3.21) (Karydis 2015). On the nave wall, traces of lime plaster with brick aggregates were observed. In the substructure, vault was built with brick, but the walls were consisted of brick and rubble stone. The substructure walls covered with double layer of lime plaster.

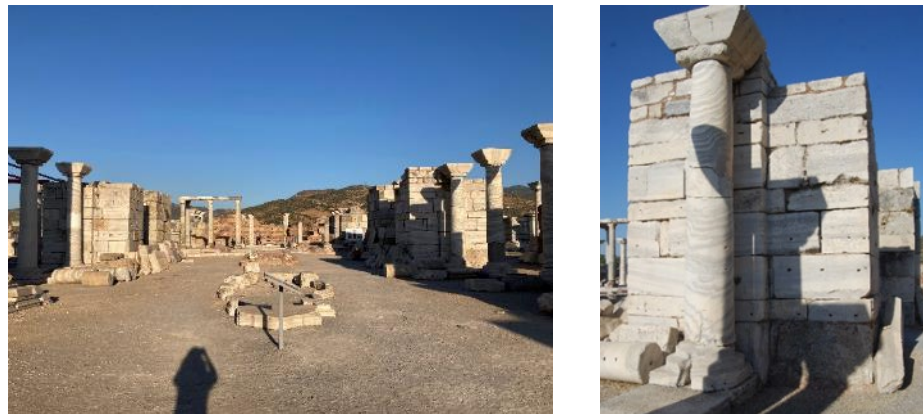


Figure 3.20. West side of naos in the St. Jean Church

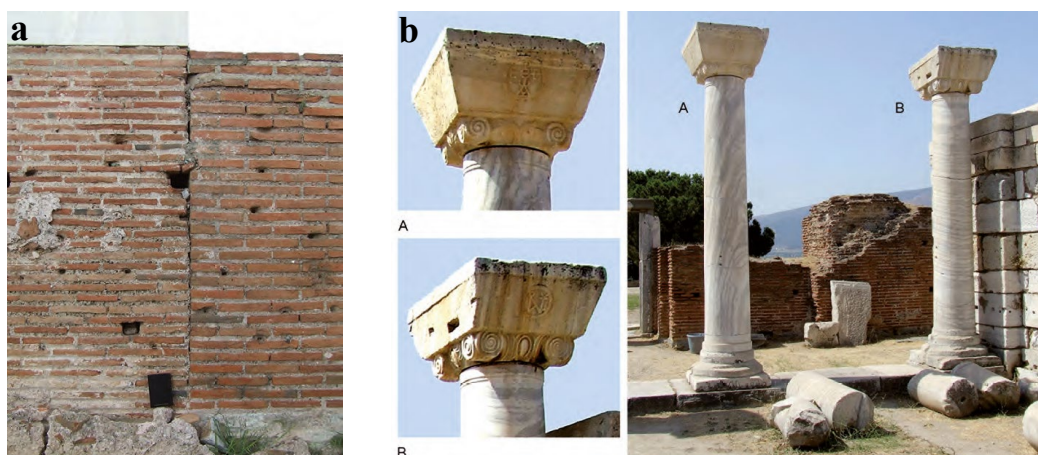


Figure 3.21. a: Discontinuity of the nave and transept walls, b: Monograms of Justinian (B) and Theodora (A) (Source: Karydis 2015)

The inner walls of fortification walls were built as a supporting wall together with the St. Jean Church of Justinian I. There are niches in the east and west of the church and the walls were built with brick-stone alternating order. Gate of persecution of fortification wall belonged to Early Byzantine period bonded with cut stone and brick masonry adhered with lime mortar composed of natural aggregates. In contrast, the Middle Byzantine period buttress addition was bonded with rubble stone and lime mortar with brick aggregate (Figure 3.22).



Figure 3.22. Gate of Persecution Wall a: Early Byzantine, b: Middle Byzantine

CHAPTER 4

EXPERIMENTAL METHODS

In this chapter, sampling and experimental methods used for the characterization of the Byzantine period lime mortars and plasters from Kadıkalesi, Anaia Church, and Ayasuluk, St. Jean Church were described. Experimental studies were carried out to determine the basic physical properties, raw material compositions, and hydraulic properties of lime mortars and plasters; mineralogical and chemical compositions, microstructural properties of binders, aggregates, and limes; and pozzolanic activities of aggregates. The data collection was done by using standard test methods, scanning electron microscopy coupled with energy-dispersive X-ray spectrometry (SEM-EDX), X-ray diffraction (XRD), and thermogravimetric analysis (TGA).

4.1. Sampling

Samples were taken from Anaia Church and fortification wall of Kadıkalesi (Anaia), and St. Jean Church and Persecution Gate in Ayasuluk. Sampling was carried out with the permission of the directorates of the archeological excavation teams, the Aydın Archeological Museum, and the Ephesus Archeological Museum in July 2020.

Lime mortars and plasters were collected from undeteriorated parts of the buildings regarding their different construction periods which were determined by previous archaeological studies (Mercangöz 2008, 2012, 2010; Karabacak 2010; Mimaroglu 2011b; Büyükkolancı et al. 2013; Ladstaetter et al. 2015; Büyükkolancı 2001; Kanmaz 2015; Karydis 2015; Kanmaz and İpekoğlu 2016; Mercangöz 2018; Hazinedar Coşkun 2021; Mimaroglu and Karabacak 2021) . Nevertheless, putlog holes or the surfaces that had been already cracked were preferred to avoid damaging the integrity of the remains.

In the field studies, it was determined that the mortars had a grayish or pinkish color, and the plasters had a pinkish color depending on the type of the aggregates they contained. Particularly, grayish mortars consisted of natural aggregates, while pinkish mortars and plasters contained brick aggregates. In both Kadıkalesi (Anaia) and Ayasuluk, some of the lime mortars with natural aggregates contain of small amount of

brick aggregates whereas some of lime mortars or plasters with brick aggregates consist of a few natural aggregates.

In Kadıkalesi (Anaia), mortars were produced using natural aggregates and plasters were produced using brick aggregates. On the other hand, in Ayasuluk, there are two types of mortars: produced natural or brick aggregates; and all plasters have brick aggregates.

Ten mortar and five plaster samples from Kadıkalesi; and twelve mortar and four plaster samples from Ayasuluk were collected to carry out the experimental studies. The types of the collected samples according to their aggregate types and periods are given in Table 4.1:

Table 4.1. Distribution of collected samples according to the sites, periods, and aggregate types

	Kadıkalesi (Anaia)			Ayasuluk	
	Early Byzantine Period	Middle Byzantine Period	Late Byzantine Period	Early Byzantine Period	Middle Byzantine Period
Brick Aggregate	-	1 Plaster	4 Plasters	5 Mortars 4 Plasters	1 Mortar
Natural Aggregate	6 Mortars	3 Mortars	1 Mortar	6 Mortars	-

Samples were labeled, respectively according to the name of the site, location of the sample, type, and the number of samples taken from the same location (Table 4.2).

Table 4.2. Abbreviations used for labeling the collected samples

Case Areas	Location	Type	Number
A: Ayasuluk	B: Bema	M: Mortar	○ 1
K: Kadıkalesi (Anaia)	Ba: Baptistery	P: Plaster	+ 2
	C: Cistern		3
	F: Fortification Wall		4
	G: Gate		
	N: Naos		
	O: Outer Narthex		
	R: Treasure Room		
	S: Substructure		
	T: Transept		

4.1.1. Kadıkalesi (Anaia)

In Kadıkalesi (Anaia), samples were collected from baptistery, walls of the naos, and substructure dated to the Early Byzantine period; from inner narthex, north and south nave and the fortification dated to the Middle Byzantine period (11th-13th centuries)(Müller-Wiener 1961); and from the outer narthex, cisterns, and some of walls and buttresses in naos dated to the Late Byzantine period (13th and 14th centuries) (Figure 4.1, 4.2).

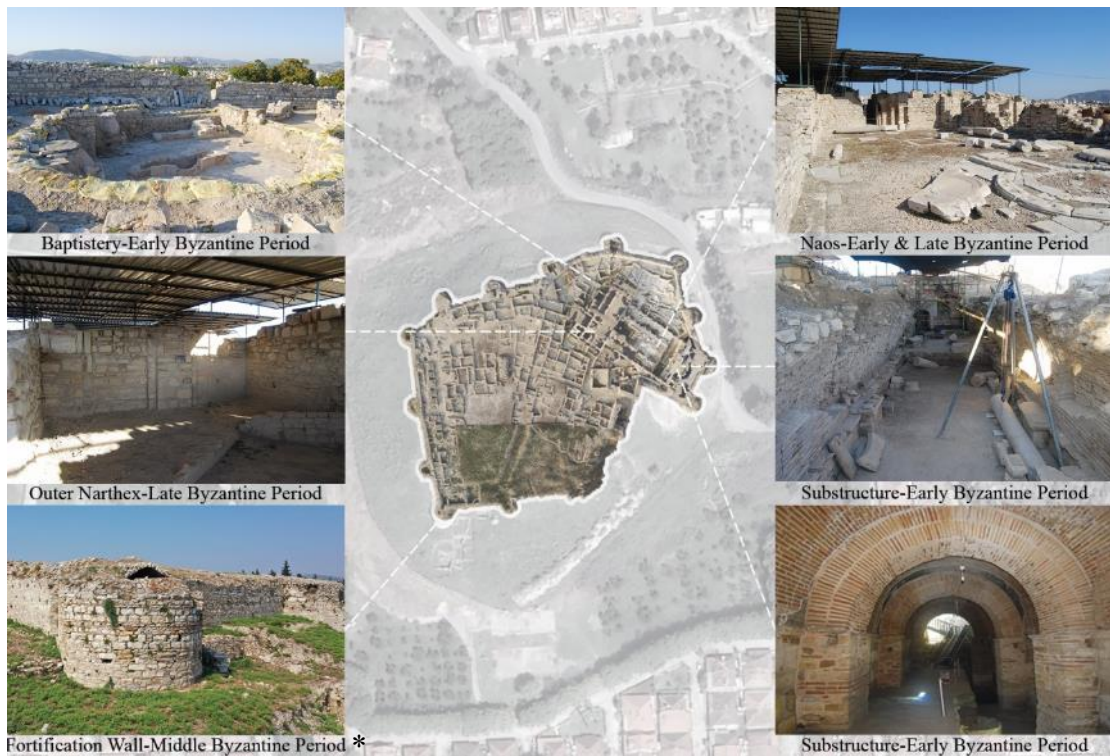


Figure 4.1 Site plan of Kadıkalesi (Anaia) and Anaia Church with the photographs of the relevant areas (Aerial photo: Google Earth Pro 2021, Kadıkalesi 37°47'29.00"N, 27°16'14.87"W, and Kadıkalesi excavation achieve, Photos from the site: T. Işık 2020, and Kadıkalesi excavation achieve*)

Six lime mortar samples from baptistery, naos, and substructure dated to Early Byzantine period; three lime mortars from fortification wall of Kadıkalesi, and naos dated to Middle Byzantine period; and one lime mortar from naos dated to Late Byzantine were collected (Figure 4.2) (Table 4.3). Also, one lime plaster sample from outer narthex dated to Middle Byzantine period, whereas four lime plasters from outer narthex and cistern I and cistern II dated to Late Byzantine period were collected.

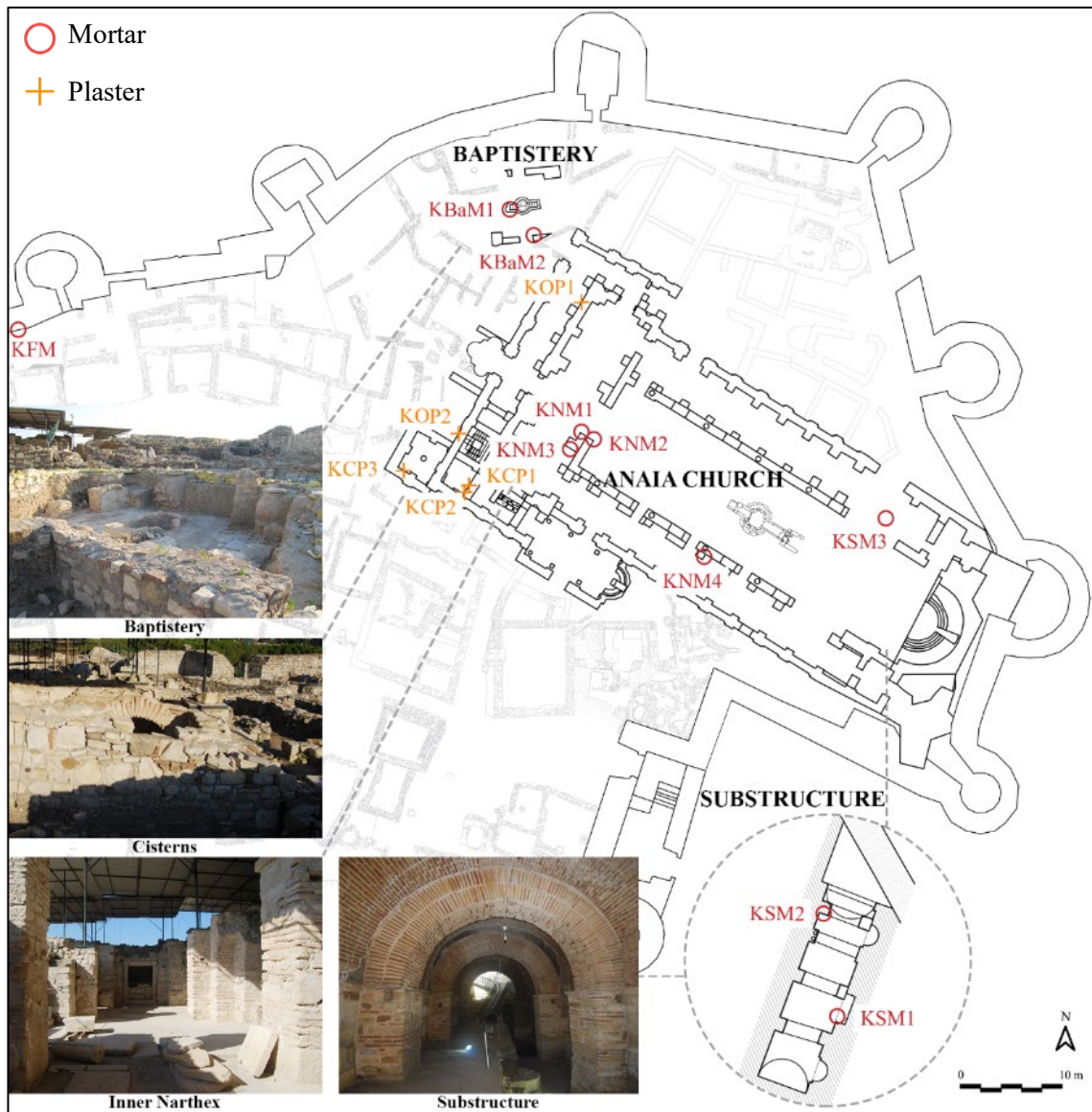


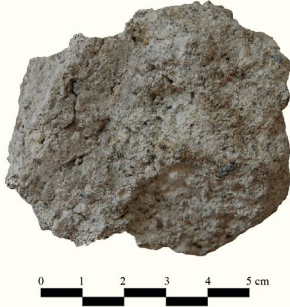







Figure 4.2. The plan of the Kadıkalesi, Anaia Church and the Substructure showing the locations of samples (Revised from the drawing by Mehmet Buğra Kanmaz and Umut Kardaşlar, Source: Kadıkalesi excavation archive 2020, Photos from the site: T. Işık 2020)

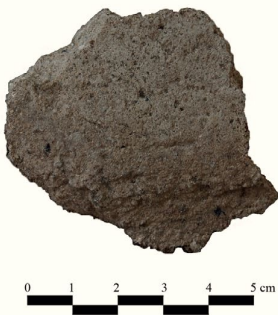

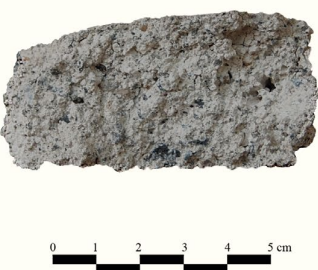

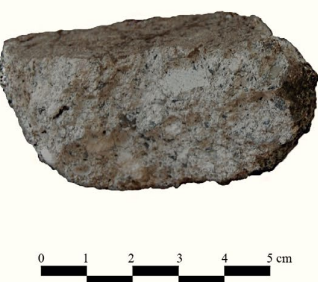



Table 4.3. Samples of lime mortars and plasters from Kadıkalesi (Supplementary aggregates in samples *- Brick Aggregate, °- Natural Aggregate)

Sample	Location	Definition
 <p>KBaM1</p>	 <p>Baptistry of Anaia Church</p>	<p>Mortar from Baptismal Pool bonding bricks</p> <p>Natural Aggregate *</p>
 <p>KBaM2</p>	 <p>Baptistry of Anaia Church</p>	<p>Mortar from Baptistry wall bonding bricks and ashlars</p> <p>Natural Aggregate *</p>
 <p>KNM2</p>	 <p>Naos of Anaia Church</p>	<p>Mortar from entrance wall bonding bricks and ashlars</p> <p>Natural Aggregate</p>
 <p>KSM1</p>	 <p>Substructure of Anaia Church</p>	<p>Mortar from the arch constructed of bricks</p> <p>Natural Aggregate</p>

Early Byzantine Period
First Construction (5-6th Centuries)

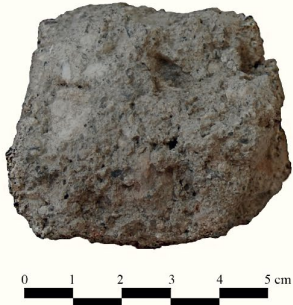







(cont. on next page)

Table 4.3. (cont.)

	Sample	Location	Definition
Early Byzantine Period First Construction (5-6 th Centuries)	 <p>KSM2</p>	 <p>Substructure of Anaia Church</p>	<p>Mortar from buttress which was constructed out of bricks and rubble stones</p> <p>Natural Aggregate</p>
	 <p>KSM3</p>	 <p>Substructure of Anaia Church</p>	<p>Mortar from the vault that was constructed of bricks</p> <p>Natural Aggregate</p>
Middle Byzantine Period Second Construction (11-13 th Centuries)	 <p>KNM1</p>	 <p>Naos of Anaia Church</p>	<p>Mortar from first buttress of entrance that was constructed of bricks and ashlars</p> <p>Natural Aggregate *</p>
	 <p>KFM</p>	 <p>Fortification Wall of Kadikalesi</p>	<p>Mortar from north side of the fortification wall which was constructed of bricks and rubble stones</p> <p>Natural Aggregate</p>







(cont. on next page)

Table 4.3. (cont.)

	Sample	Location	Definition
Middle Byzantine Period Second Construction (11-13 th Centuries)	 <p style="text-align: center;">KNM3</p>	 <p style="text-align: center;">Naos of Anaia Church</p>	Mortar from second buttress of entrance that was constructed of bricks and ashlars Natural Aggregate
	 <p style="text-align: center;">KOP1</p>	 <p style="text-align: center;">Outer Narthex of Anaia Church</p>	Plaster from the east wall Brick Aggregate
Late Byzantine Period Third Construction (13-14 th Centuries)	 <p style="text-align: center;">KOP2</p>	 <p style="text-align: center;">Outer Narthex of Anaia Church</p>	Plaster from the west wall Brick Aggregate
	 <p style="text-align: center;">KCP1</p>	 <p style="text-align: center;">Cistern I of Anaia Church</p>	Plaster covering the inner surface of the east wall Brick Aggregate °

(cont. on next page)

Table 4.3. (cont.)

	Sample	Location	Definition
Late Byzantine Period Third Construction (13-14 th Centuries)	 <p style="text-align: center;">KCP2</p>	 <p style="text-align: center;">Cistern I of Anaia Church</p>	<p>Plaster covering the outer surface of the south wall</p> <p style="text-align: center;">Brick Aggregate °</p>
	 <p style="text-align: center;">KCP3</p>	 <p style="text-align: center;">Cistern II of Anaia Church</p>	<p>Plaster covering the inner surface of the south wall</p> <p style="text-align: center;">Brick Aggregate °</p>
	 <p style="text-align: center;">KNM4</p>	 <p style="text-align: center;">Naos of Anaia Church</p>	<p>Mortar from buttress of south wall which was constructed of bricks and ashlars</p> <p style="text-align: center;">Natural Aggregate *</p>

4.1.2. Ayasuluk

Gate of Persecution in Ayasuluk consists of two construction periods which are the Early (4th and 6th centuries), and the Middle (10th-12th centuries) Byzantine periods, whereas St. Jean Church was built in the Early Byzantine period (4th and 6th centuries) (Büyükkolancı 2001; Büyükkolancı et al. 2013; Ladstaetter et al. 2015; Karydis 2015; Büyükkolancı 2018). Baptistry, bema, naos, transept, treasure room, and substructure were built during the Early Byzantine period (Figure 4.3). The first stage of the gate of persecution was dated to Early Byzantine period, whereas the second stage is dated to the Middle Byzantine period (Figure 4.3).



Figure 4.3. Site plan of Ayasuluk and St. Jean Church with the photographs of the relevant areas (Aerial photo: Google Earth Pro (2021) Ayasuluk Tepesi 37°57'07.51"N, 27°22'08.93"W, Photos from the site: T. Işık 2020)

Sixteen samples were collected from the Gate of persecution and different sections of St. Jean Church (Figure 4.4). Six lime mortars with natural aggregates were

taken from transept, treasure room, bema, substructure, and gate of persecution wall whereas, five lime mortars consisted of brick aggregates were taken from baptistery, transept, bema, and naos dated to Early Byzantine period (Table 4.4). One lime mortar with brick aggregates were collected from gate of persecution wall that belong to Middle Byzantine period (Table 4.4). Lime plasters were taken from the treasure room, substructure and naos dated to Early Byzantine period (Table 4.4).

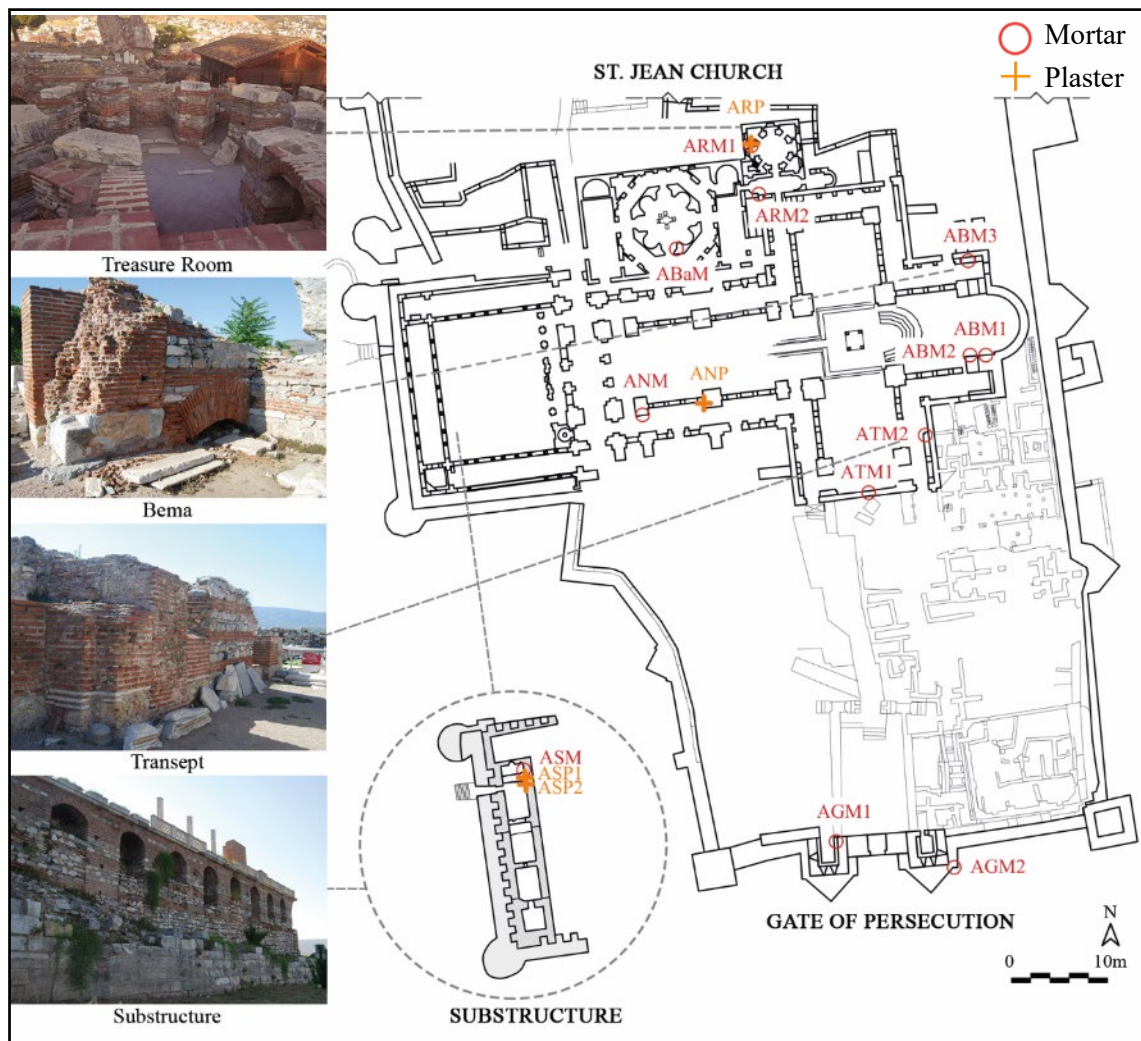
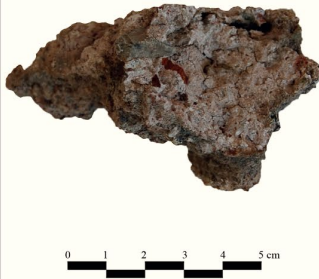

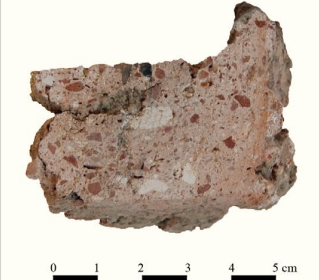

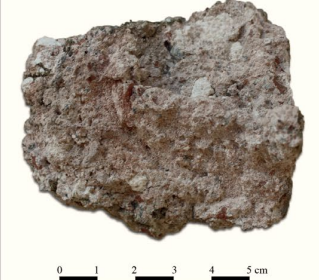

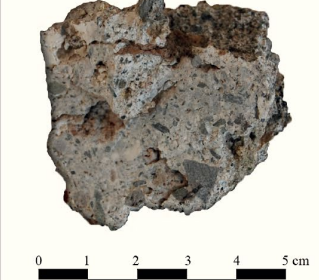



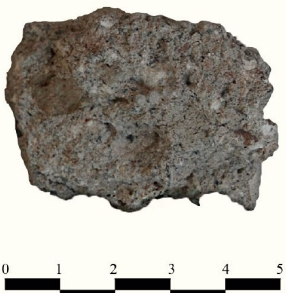

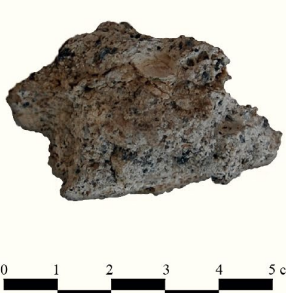



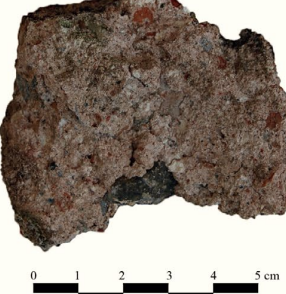

Figure 4.4. Plan of St. Jean Church, its Substructure and Gate of Persecution (Drawing: Ayasuluk excavation team, Source: Ayasuluk excavation archive, Photos from the site: T. Işık 2020)

Table 4.4. Samples of lime mortar and plaster samples from Ayasuluk (Supplementary aggregates in samples *-Brick Aggregate, °-Natural Aggregate)

	Sample	Location	Definition
Early Byzantine Period First Construction (4-5 th Centuries)	 <p style="text-align: center;">ARP</p>	 <p style="text-align: center;">Treasure Room of St. Jean Church</p>	Plaster covering the niche in the north wall that was constructed with bricks in western cell of treasury Brick Aggregate °
	 <p style="text-align: center;">ABaM</p>	 <p style="text-align: center;">Baptistry of St. Jean Church</p>	Mortar from the southeast wall bonding bricks Brick Aggregate
	 <p style="text-align: center;">ATM1</p>	 <p style="text-align: center;">Transept of St. Jean Church</p>	Mortar from the south wall bonding bricks in South Transept Brick Aggregate °
	 <p style="text-align: center;">ATM2</p>	 <p style="text-align: center;">Transept of St. Jean Church</p>	Mortar from the east wall bonding bricks in South Transept Natural Aggregate *

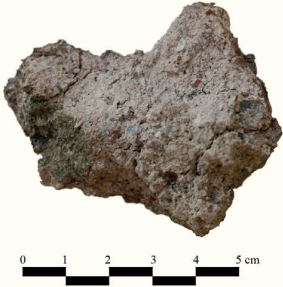






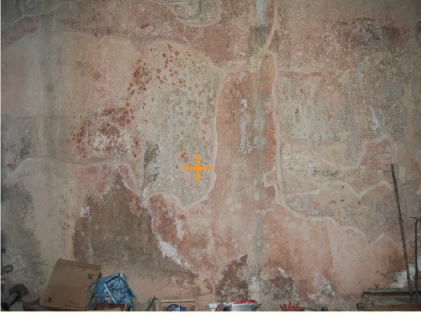
(cont. on next page)

Table 4.4. (cont.)

	Sample	Location	Definition
Early Byzantine Period First Construction (4-5 th Centuries)	 <p style="text-align: center;">ARM1</p>	 <p style="text-align: center;">Treasure Room of St. Jean Church</p>	<p>Mortar from the niche in the north wall bonding bricks In western cell of treasury</p> <p style="text-align: center;">Natural Aggregate *</p>
	 <p style="text-align: center;">ARM2</p>	 <p style="text-align: center;">Transition Space of St. Jean Church</p>	<p>Mortar from the niche bonding bricks</p> <p style="text-align: center;">Natural Aggregate</p>
	 <p style="text-align: center;">ABM3</p>	 <p style="text-align: center;">Bema of St. Jean Church</p>	<p>Mortar from the inner surface of the brick arch in the south</p> <p style="text-align: center;">Natural Aggregate *</p>
	 <p style="text-align: center;">ABM1</p>	 <p style="text-align: center;">Bema of St. Jean Church</p>	<p>Mortar from the buttress that constructed of ashlars</p> <p style="text-align: center;">Brick Aggregate °</p>


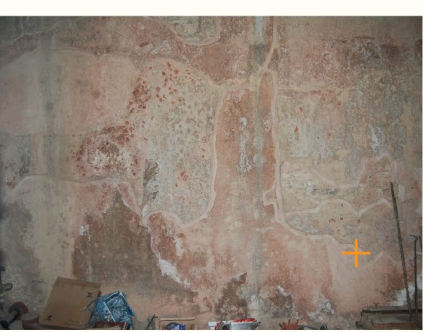
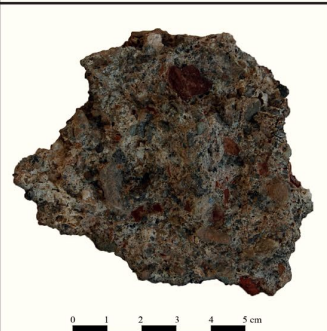
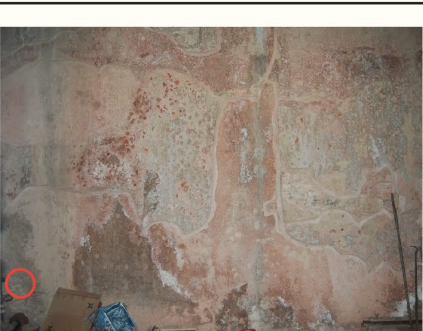
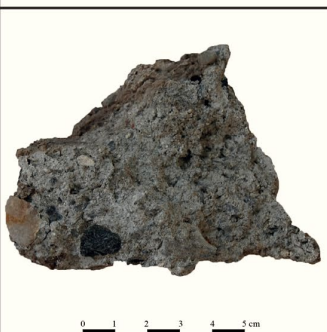
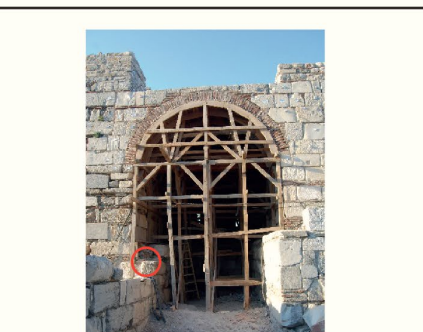
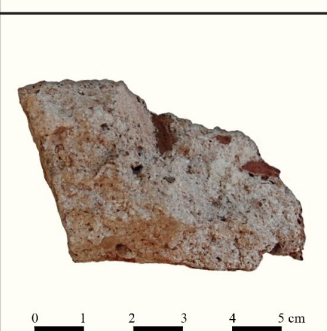
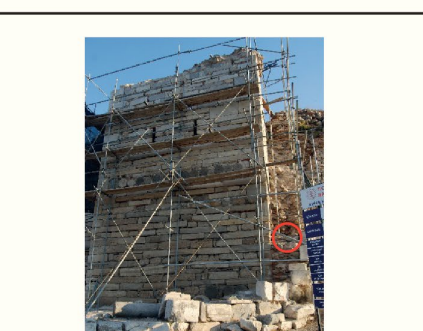
(cont. on next page)

Table 4.4. (cont.)

	Sample	Location	Definition
Early Byzantine Period Second Construction (Early 6 th Century)	 <p style="text-align: center;">ABM2</p>	 <p style="text-align: center;">Bema of St. Jean Church</p>	<p>Mortar from the buttress that was constructed with bricks and rubble stones</p> <p style="text-align: center;">Brick Aggregate °</p>
	 <p style="text-align: center;">ANM</p>	 <p style="text-align: center;">Naos of St. Jean Church</p>	<p>Mortar from the southwest buttress that was constructed with ashlars</p> <p style="text-align: center;">Brick Aggregate °</p>
	 <p style="text-align: center;">ANP</p>	 <p style="text-align: center;">Naos of St. Jean Church</p>	<p>Plaster from the south buttress that was constructed with ashlars</p> <p style="text-align: center;">Brick Aggregate</p>
	 <p style="text-align: center;">ASP1</p>	 <p style="text-align: center;">Substructure of St. Jean Church</p>	<p>First layer of plaster covering on the east wall</p> <p style="text-align: center;">Brick Aggregate</p>

(cont. on next page)

Table 4.4. (cont.)

	Sample	Location	Definition
Early Byzantine Period Third Construction (Mid 6 th Century)	 <p>ASP2</p>	 <p>Substructure of St. Jean Church</p>	<p>Second layer of plaster covering on the east wall</p> <p>Brick Aggregate</p>
	 <p>ASM</p>	 <p>Substructure of St. Jean Church</p>	<p>Mortar from the east wall</p> <p>Natural Aggregate *</p>
	 <p>AGM1</p>	 <p>Ayasuluk's Gate of Persecution</p>	<p>Mortar from the West Tower bonding bricks and ashlars</p> <p>Natural Aggregate</p>
Middle Byzantine Period (10-12 th Centuries)	 <p>AGM2</p>	 <p>Ayasuluk's Gate of Persecution</p>	<p>Mortar from the East Tower's east facade bonding rubble stones</p> <p>Brick Aggregate</p>

4.2. Experimental Studies

The following properties of the collected lime mortars and plasters were investigated by experimental studies:

- Basic physical properties
 - Density
 - Porosity
- Raw material compositions
 - Lime-aggregate ratios
 - Particle size distributions of aggregates
 - Maximum aggregate sizes
 - Roundness scale
- Mineralogical compositions
- Chemical compositions
- Pozzolanic activities of aggregates
- Hydraulic properties of binders
- Microstructural properties

4.2.1. Determination of Basic Physical Properties

The basic physical properties of the mortar and plaster samples which are described by density and porosity values were determined by RILEM standard test methods (RILEM 1980). The bulk density is expressed by the ratio of the dry sample mass to the bulk volume (g/cm^3), whereas the porosity is expressed as a percentage (%) of the ratio of the pore volume to the bulk volume of the sample.

Two parallel specimens of each mortar and plaster sample were used to determine the density and porosity values. Firstly, the samples were dried in an oven at 40°C for at least 24 hours in order to vaporize the trapped moisture (Teutonico 1988). Thereafter, dry weights (M_{dry}) were measured by a precision balance (AND HF-3000G) (Figure 4.5). Then, the samples were placed in plastic beakers and filled with distilled water until it reached about 2 cm above the samples. They were put in a vacuum oven (Lab-Line 3608-6CE Vacuum Oven) and saturated entirely for 24 hours at -25 kPa (Figure 4.5). The

saturated weights (M_{sat}) and the Archimedes weights (M_{arch}) that were determined with hydrostatic weighting in distilled water by measuring with the precision balance (Figure 4.5, 4.6). After all, bulk densities (D) (4.1) and porosities (P) (4.2) of the mortar and plaster specimens were calculated with the following formulas in accordance with the data of the dry, saturated, and Archimedes weights:

$$D \text{ (g/cm}^3\text{)} = M_{dry} / (M_{sat} - M_{arch}) \quad (4.1)$$

$$P \text{ (\%)} = [(M_{sat} - M_{dry}) / (M_{sat} - M_{arch})] \times 100 \quad (4.2)$$

where;

D: Density (g/cm³) M_{dry} : Dry Weight (g) $M_{sat} - M_{dry}$: Pore Volume (g)

P: Porosity (%) M_{sat} : Saturated Weight (g) $M_{sat} - M_{arch}$: Bulk Volume (g)

M_{arch} : Archimedes Weight (g)



Figure 4.5. a: weighing the dry and saturated samples by precision balance, b: the samples in vacuum oven to saturate them entirely



Figure 4.6. Measurement of Archimedes weight

4.2.2. Determination of Raw Material Compositions

The raw material compositions of the mortar and plasters were defined by the lime-aggregate ratio and the particle size distribution of aggregates.

Carbonated lime (CaCO_3) of mortars and plasters were dissolved by using dilute hydrochloric acid. Firstly, the specimens were dried in the oven at 40°C for 24 hours and weighed (M_{sam}) by a precision balance. Then, they were put in beakers and filled with dilute (5%) hydrochloric acid solution and left until the carbonated lime dissolved entirely. Lastly, the insoluble part was filtered, washed with distilled water until all chlorine ions remove (Figure 4.7) and it was dried one day at room temperature, then dried in the oven at 40°C and weighed (M_{agg}) by the precision balance.

The percentage of the acid-soluble and insoluble parts were determined by the following formulas:

$$\text{Insoluble (\%)} = [(M_{\text{sam}} - M_{\text{agg}}) / (M_{\text{sam}})] \times 100 \quad (4.3)$$

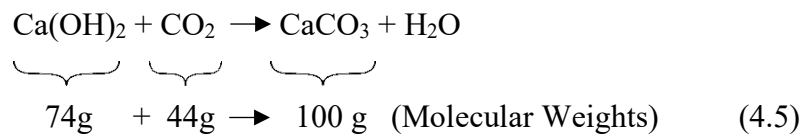
$$\text{Acid Soluble (\%)} = 100 - \text{Insoluble (\%)} \quad (4.4)$$

where;

M_{sam} = Dry weight of the sample (g)

M_{agg} = Dry weight of the aggregates (g)

The exact lime ratio of the mortars and plasters are calculated according to the lime ($\text{Ca}(\text{OH})_2$) which had been used in the preparation of them. However, since the acid-soluble ratio is calculated with the dissolved carbonated lime (CaCO_3), the chemical formula of carbonation given below is considered for the exact ratio.



$$\text{Aggregate (\%)} = (100 \times \text{Insoluble}) / [((\text{Acid Soluble (\%)} \times \text{M.W.}_{\text{Ca}(\text{OH})_2}) / \text{M.W.}_{\text{CaCO}_3}) + \text{Insoluble (\%)}] \quad (4.6)$$

$$\text{Lime (\%)} = 100 - \text{Aggregate (\%)} \quad (4.7)$$

where;

$M.W._{CaCO_3}$ = Molecular weight of $CaCO_3$ which is 100.

$M.W._{Ca(OH)_2}$ = Molecular weight of $Ca(OH)_2$ which is 74.

The dried residue which is the aggregates that purified from the lime was sieved through a series of sieves with 1180 μm , 500 μm , 250 μm , 125 μm , and 53 μm , respectively to determine the particle sizes by shaking the obtained aggregates in an analytical sieve shaker (Retsch AS200) (Figure 4.7). The remaining particles on each sieve surface were weighed by a precision balance and calculated their percentages.



Figure 4.7. a: Filtering of the insoluble parts while washing with distilled water,
b: Shaking the aggregates and so eliminating them from series of sieves

The physical properties of the obtained aggregates were determined by macro-observations in terms of the maximum aggregate sizes and roundness scale of coarse aggregates.

The sharpness of a particle's edges and corners determines its roundness regardless of its shape. The roundness scale was defined in six classes from very angular to well-rounded (Powers 1953) (Figure 4.8). The average roundness scale of investigated aggregates was defined by macroscopic observations using these classes.

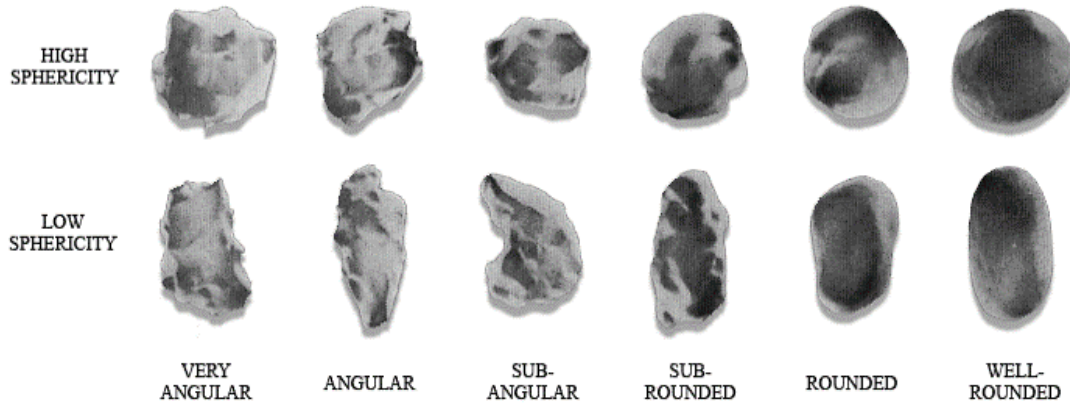


Figure 4.8. Roundness scale
(Source: Powers 1953)

4.2.3. Determination of Mineralogical Compositions

The mineralogical compositions of the finely ground aggregates, binders and lime lumps less than 53 μm were detected by using X-ray diffraction (XRD). The XRD analyses were done by using a Philips X-Pert Pro X-Ray Diffractometer and the instrument was operated on $\text{CuK}\alpha$ radiation with Ni filter, at 40 kV and 40 mA in the range of 5-60° with a scan speed of 0.08°/s. X'Pert High Score Plus Analysis software program was used to determine the mineral phases in each sample.

4.2.4. Determination of Chemical Compositions

The chemical compositions of aggregates, binders and lime lumps were determined by a Philips XL 30S FEG Scanning Electron Microscope (SEM) coupled with Energy Dispersive X-ray Spectroscopy (EDS). The SEM-EDS analyses were carried out by a Philips XL 30S FEG on pellets obtained from powder samples (<53 μm) pressed with a pressure of 10 tons/cm². The chemical compositions were determined via an X-ray detector and by using the averages of the data derived from three distinct areas of the samples.

Hydraulic (H.I.) and cementation (C.I.) indices of lime lumps (Eckel 1905; Boynton 1966) were calculated by the below equations (Eq. 4.8, 4.9) to identify the hydraulic of character of the lime used in the production of mortars and plasters.

$$\text{H.I.} = (\% \text{Al}_2\text{O}_3 + \% \text{Fe}_2\text{O}_3 + \% \text{SiO}_2) / (\% \text{CaO} + \% \text{MgO}) \quad (4.8)$$

$$\text{C.I.} = (2.8 \% \text{SiO}_2 + 1.1 \% \text{Al}_2\text{O}_3 + 0.7 \% \text{Fe}_2\text{O}_3) / (\% \text{CaO} + 1.4 \% \text{MgO}) \quad (4.9)$$

Hydraulic index values lower than 0.1, and cementation index values lower than 0.3 indicate the non-hydraulic character of lime (Eckel 1905; Boynton 1966).

4.2.5. Determination of Microstructural Properties

Microstructural and morphological characteristics were identified by using a Philips XL 30S FEG Scanning Electron Microscope (SEM) coupled with Energy Dispersive X-Ray Analysis (EDX).

The microstructural properties of the mortars, aggregates and lime lumps were determined by scanning electron detector (SE); while the property of the reaction rims at the interfaces between the binder and pozzolanic aggregates and reaction rims around the limestone aggregates were defined by backscattered electron detector (BSE) at different magnifications (100x, 250x, 500x, 1000x, 2500x, 5000x, 10000x). These analyses were done on polished thin sections and gold coated broken surfaces of mortars and lime lumps.

4.2.6. Determination of Pozzolanic Activities of Aggregates

The pozzolanic activities of the natural and artificial aggregates were determined by using the electrical conductivity method (Luxan, Madruga, and Saavedra 1989). In this method, electrical conductivity differences of dilute calcium hydroxide solutions ($\text{Ca}(\text{OH})_2$) before and after the addition of finely ground (<53 micron) aggregates were measured. The differences of two measurements indicate the reaction between aggregates and lime.

The electrical conductivity of the 20 ml saturated calcium hydroxide solution ($\text{Ca}(\text{OH})_2$) was measured by a conductivity meter (WTW MultiLine P3), then 500 mg finely ground aggregates (<53 micron) were added to the solution, and stirred by a magnetic stirrer (IKAMAG RH) for 2 minutes (Figure 4.9). After stirring, electrical conductivity of the solution was measured by the conductivity meter (Figure 4.9). If the

electrical conductivity difference is found more than 1.2 mS/cm, it reveals that aggregates are pozzolan (Luxan, Madruga, and Saavedra 1989).



Figure 4.9. a: magnetic stirrer to mix the $\text{Ca}(\text{OH})_2$ and fine aggregate, b: electrical conductivity analysis by conductivity meter

4.2.7. Determination of Hydraulic Properties

The hydraulic properties of the mortars and plasters were determined with measuring of the weight losses between 200–600°C and 600–900°C by thermogravimetric analysis (Shimadzu TGA-21).

The weight losses between 200–600°C occurred due to the loss of chemically bound water (H_2O) of hydraulic compounds, whereas at the weight losses between 600–900°C were due to the loss of carbon dioxide gas (CO_2) released during the decomposition of CaCO_3 . Mortars and plasters can be evaluated as hydraulic if the ratio of $\text{CO}_2/\text{H}_2\text{O}$ (chemically bound water) is found below 10 (Bakolas et al. 1998; Moropoulou, Bakolas, and Bisbikou 2000).

CHAPTER 5

RESULTS AND DISCUSSIONS

In this chapter, results of the experimental studies carried out to determine basic physical properties, raw material compositions, mineralogical and chemical compositions, hydraulic and microstructural properties of the lime mortars and plasters, and mineralogical and chemical compositions, pozzolanic activities and microstructural properties of aggregates were presented and discussed. The results were evaluated by considering the sites, construction periods, function and aggregate types used in lime mortars and plasters.

5.1. Basic Physical Properties

Basic physical properties of the mortars and plasters were defined by their density (g/cm^3) and total porosity (%) values.

In Kadikalesi (Anaia), all lime mortar samples were composed of natural aggregates, and lime plaster samples were produced by using brick aggregates. Lime mortars were measured to be denser and less porous than lime plasters. Density values of the lime mortars were between $1.54\text{--}1.86 \text{ g/cm}^3$ and the porosity values were between $27.74\text{--}36.90 \%$. Density and porosity values of the lime plasters were found in the range of $1.30\text{--}1.42 \text{ g/cm}^3$ and $43.03\text{--}47.49 \%$, respectively (Table 5.1). It was determined that basic physical properties did not differ according to the construction periods and the locations of the samples.

Double layered plaster was only used in Cistern I which dates to the Late Byzantine Period. Basic physical properties of both inner (KCP1) and outer (KCP2) layers were different from other plaster samples with comparatively lower density (1.34 g/cm^3 and 1.36 g/cm^3 , respectively) and higher porosity (47.49% and 43.62% , respectively) values (Table 5.1).

In Ayasuluk, lime mortars were composed of either brick aggregates or natural aggregates, whereas all lime plasters were produced with brick aggregates. The density and porosity values did not differ according to the construction periods though differences

were identified due to the type of aggregate. Lime mortars with natural aggregates had higher density and lower porosity values of 1.65–1.92 g/cm³ and 25.15–34.75 %, respectively (Table 5.2). However, lime mortars with brick aggregates that were taken from buttresses (ANM, ABM1, ABM2, AGM2), walls (ABaM, ATM1) were slightly less dense and high porous with values in the range of 1.23–1.67 g/cm³ and 36.47–50.95% (Table 5.2).

In the substructure, double layered plaster was applied on the wall surface. The inner plaster layer (ASP1) had a lower density (1.38 g/cm³) and higher porosity (42.22 %) than the outer plaster layer (ASP2) (1.70 g/cm³ and 23.14 %, respectively) (Table 5.2). In Naos buttress (ANP) and Treasure Room wall (ARP), single plaster layers were used, and their basic physical properties were similar to the inner plaster layer of the substructure (ASP1) (Table 5.2).

The physical properties of lime mortars and plasters from Kadıkalesi (Anaia) and Ayasuluk did not demonstrate significant differences according to the construction periods and location. The results showed that the differences between the basic physical properties depend on the aggregate types. All lime mortar samples produced by natural aggregates had higher density and lower porosity values than the lime mortars with brick aggregates which were used only in Ayasuluk. The physical properties of lime plasters from Ayasuluk and Kadıkalesi (Anaia) were in the same range, and they had lower density and higher porosity values compared to lime mortars. These differences may be explained by the porous structure of brick aggregates (Uğurlu and Böke 2009).

Similarly, recent studies on Byzantine period lime mortars and plasters from historic buildings belonging to different sub-periods, with different functions and in different locations like monuments in Kiev, the Serapis Temple in Pergamon, religious buildings in İstanbul, Fortification Wall of Adana and Kozan Castle in Cilicia, defense structures in İstanbul, Middle Byzantine Chapel in İstanbul and Early Byzantine Church in Southwest Anatolia demonstrated that mortars prepared with natural aggregates had higher density (1.62–2.00 g/cm³) and lower porosity (22–38 %) than mortars or plasters prepared with brick aggregates (1.04–1.90 g/cm³, 28–54 %, respectively) (Moropoulou, Bakolas, and Bisbikou 2000; Oğuz Kılıç et al. 2004; Özkaya and Böke 2009; Gürdal, Kahraman Altaş, and Acun Özgünler 2011; Kozlu and Ersen 2011; Kurugöl and Güleç 2012; Polat Pekmezci 2012; Kahraman Altaş, Acun Özgünler, and Gürdal 2013; Acun Özgünler, Ersen, and Güleç 2013; Stefanidou et al. 2014; Ulukaya et al. 2017; Caner and Güney 2018) (Table 5.3).

Table 5.1. Basic physical properties of lime mortars and plasters from Kadikalesi

Period	Sample	Location	Function	Aggregate Type	Density (g/cm ³)	Porosity (%)	
Early Byzantine	First Construction	KBaM1	Baptistery Wall	Mortar	Natural	1.72	30.89
		KBaM2	Baptistery Wall	Mortar	Natural	1.63	36.15
		KNM2	Naos Wall	Mortar	Natural	1.66	33.48
		KSM1	Substructure Arch	Mortar	Natural	1.62	36.70
		KSM2	Substructure Buttress	Mortar	Natural	1.72	31.66
		KSM3	Substructure Vault	Mortar	Natural	1.58	36.90
Middle Byzantine	Second Construction	KFM	Fortification Wall	Mortar	Natural	1.86	27.74
		KNM1	Naos Buttress	Mortar	Natural	1.67	35.25
		KNM3	Naos Buttress	Mortar	Natural	1.73	31.38
		KOP1	Outer Narthex Wall	Plaster	Brick	1.31	43.03
Late Byzantine	Third Construction	KOP2	Outer Narthex Wall	Plaster	Brick	1.42	44.20
		KCP1	Cistern I Wall	Plaster	Brick	1.34	47.49
		KCP2	Cistern I Wall	Plaster	Brick	1.36	43.62
		KCP3	Cistern II Wall	Plaster	Brick	1.30	46.14
		KNM4	Naos Buttress	Mortar	Natural	1.54	33.71

Table 5.2. Basic physical properties of lime mortars and plasters from Ayasuluk

Period	Sample	Location	Function	Aggregate Type	Density (g/cm ³)	Porosity (%)		
Early Byzantine	First Construction	ARP	Treasure Room Wall	Plaster	Brick	1.30	47.40	
		ABaM	Baptistery Wall	Mortar	Brick	1.23	50.95	
		ATM1	Transept Wall	Mortar	Brick	1.50	41.11	
		ATM2	Transept Buttress	Mortar	Natural	1.88	26.96	
		ARM1	Treasure Room Niche	Mortar	Natural	1.68	34.75	
		ARM2	Treasure Room Wall	Mortar	Natural	1.88	25.62	
	Second Construction	ABM3	Bema Arch	Mortar	Natural	1.73	31.37	
		ABM1	Bema Buttress	Mortar	Brick	1.63	37.75	
		ABM2	Bema Buttress	Mortar	Brick	1.50	39.21	
		Third Construction	ANM	Naos Buttress	Mortar	Brick	1.67	36.47
			ANP	Naos Buttress	Plaster	Brick	1.27	46.23
			ASP1	Substructure Wall	Plaster	Brick	1.38	42.22
ASP2	Substructure Wall		Plaster	Brick	1.70	23.14		
ASM	Substructure Wall		Mortar	Natural	1.65	31.14		
AGM1	Gate of Persecution Wall		Mortar	Natural	1.92	25.15		
Middle Byzantine	AGM2	Gate of Persecution Buttress	Mortar	Brick	1.45	42.60		

Table 5.3. Basic physical properties of mortars and plasters used in different Byzantine period buildings

Area & Reference	Period	Mortar/ Plaster	Aggregate Type	BASIC PHYSICAL PROPERTIES	
				Density (g/cm ³)	Porosity (%)
Fortification Wall of Adana and Kozan Castle in Cilicia (Polat Pekmezci 2012)	Early Byzantine	Mortar	Natural	1.75–1.94	24–30
Serapis Temple/ Kızıl Avlu (Özkaya and Böke 2009)	Early Byzantine	Mortar	Natural	1.7	34
		Plaster	Brick	1.3	48
Monastery and Churches from Kayseri (Kozlu and Ersen 2011)	Early– Middle Byzantine (4–11 th centuries)	Mortar	Natural	1.24–1.70	32–53
		Plaster	Natural	1.08–1.70	48–54
Byzantine Bath of Thessaloniki and Castle of Servia (Stefanidou et al. 2014)	Middle Byzantine (10–13 th centuries)	Mortar	Natural	1.74–1.90	14–19
		Mortar	Brick	1.45–1.58	23–28
Land Walls of Yedikule in Istanbul (Acun Özgünler, Ersen, and Güleç 2013)	Early Byzantine (5 th century)	Mortar	Brick	1.62–2.00	22–38
St. Jean Church in Manisa (Oğuz Kılıç et al. 2004)	Early Byzantine (6 th century)	Mortar	Brick	1.5–1.6	33–40

(cont. on next page)

Table 5.3. (cont.)

Area & Reference	Period	Mortar/ Plaster	Aggregate Type	BASIC PHYSICAL PROPERTIES	
				Density (g/cm ³)	Porosity (%)
Early Byzantine Church in Southwest Anatolia (Caner, Güney 2018)	Early Byzantine (5–7 th centuries)	Mortar	Brick	1.04–1.19	41–48
		Plaster	Brick	1.19–1.21	40–41
Defense Structures in Istanbul (Kahraman Altaş, Acun Özgünler and Gürdal 2013)	Early Byzantine	Mortar	Brick	1.14–1.90	28–52
Religious Buildings in Istanbul (Gürdal, Kahraman Altaş and Acun Özgünler 2011)	Early Byzantine	Mortar	Brick	1.23–1.66	32–48
Monuments in Kiev (Moropoulou et al. 2000)	Middle Byzantine (11–13 th centuries)	Mortar	Brick	1.49–1.51	42–46
Middle Byzantine Chapel in Istanbul (Ulukaya et al. 2016)	Middle Byzantine (11–12 th centuries)	Mortar	Brick	1.2	54
Yoros Castle in Istanbul (Kurugöl and Güleç 2012)	Late Byzantine (13–14 th centuries)	Mortar	Brick	1.57–1.82	29–35

5.2. Raw Material Compositions

Raw material compositions of lime mortars and plasters were defined by their lime/aggregate ratios, particle size distribution of aggregates, and physical properties of aggregates in terms of maximum aggregate sizes and roundness scale of coarse aggregates.

Lime plasters from Kadıkalesi (Anaia) had lime/aggregate ratios between $1/3$ – $4/3$ (Table 5.4). Lime/aggregate ratios of the lime mortars were between $1/2$ – $1/1$ in samples from walls (KBaM1, KBaM2, KNM2, KFM), an arch (KSM1), a vault (KSM3) and a buttress (KSM2); while they were between $4/3$ – $5/3$ in samples from buttresses (KNM1, KNM3 and KNM4) (Table 5.4). Accordingly, it was determined that the second construction period samples KNM1, KNM3, and third construction period sample KNM4 had higher lime content than first construction period samples.

However, calcareous aggregates such as limestone, shells, marble fragments may dissolve in acidic solutions. Hence, in the mortars or plasters in which calcareous aggregates were contained, after dissolution in dilute hydrochloric acid, calcareous aggregates would have been lost and only siliceous aggregates would remain which may result in a higher lime/aggregate ratio. Therefore, the difference between lime/aggregate ratios of second and third construction period mortars used in buttresses (KNM1, KNM3 and KNM4) could be explained by the existence of calcareous aggregates (Casadio, Chiari, and Simon 2005).

In Ayasuluk, lime/aggregate ratio of lime plasters were between $3/4$ and $5/3$ (Table 5.5). Plasters applied on wall surfaces (ARP, ASP1, ASP2) had higher lime/aggregate ratios ($4/3$ – $5/3$) than lime plaster on a buttress in naos (ANP) with a ratio of $3/4$ (Table 5.5). The lime/aggregate ratio of the lime mortars from Early and Middle Byzantine periods had mostly resembled and were in the range of $1/3$ and $5/3$. On the other hand, ANM sample from naos buttress, and ABM3 from bema arch were found to have a lower lime/aggregate ratio of $1/2$ and $2/3$, respectively (Table 5.5). The differences in the lime/aggregate ratios of the samples can be explained by the presence of calcareous aggregates in their contents.

Kadıkalesi (Anaia) and Ayasuluk samples had slightly higher lime/aggregate ratios in average compared to the results of previous studies (Table 5.6). Lime/aggregate ratios of different Byzantine period buildings in Istanbul were determined between $1/4$ –

1/5 in a Middle Byzantine Chapel (Ulukaya et al. 2016), 2/3–1/3 in Yoros Castle (Kurugöl and Güleç 2012), 2/3–3/2 in Yedikule Landswall (Acun Özgünler, Ersen, and Güleç 2013), 2/3 in a Middle Byzantine Church (Nežerka et al. 2015), 1/3 in Istanbul Land Walls and Theodosian Walls (Kahraman Altaş, Acun Özgünler, and Gürdal 2013), between 1/2–1/4 in Hagia Sophia, Hagia Eirine, St. Mary of Chalkoprateia, Church of St. Euphemia, Monastery of Stoudios, Martyrion of Karpos and Papylos, Church of St. Polyeuctus (Gürdal, Kahraman Altaş, and Acun Özgünler 2011), and between 1/2–1/4 in Hagia Sophia Basilica (Moropoulou et al. 2002) (Table 5.6). In other regions, the lime/aggregate ratios were found as 1/1 in St. Jean Church in Manisa (Oğuz Kılıç et al. 2004), 1/5–1/2.6 in Serapis Temple, Pergamon (Aslan Özkaya 2005), 1/4–5/2 in Monastery and Churches from Kayseri (Kozlu and Ersen 2011), 2/1–3/1 in archeological site of Kyme (Miriello et al. 2011), 1/3 in Fortification Wall of Adana and Kozan Castle, Cilicia (Polat Pekmezci 2012), 1/9–1/5 in the Synagogue from Andriake Harbour in Lycia (Oğuz, Türker, and Koçkal 2015), and 1/3 in Middle Byzantine Monuments, Ukraine (Moropoulou, Bakolas, and Bisbikou 2000) (Table 5.6). The differences might be related to the geological features and raw material resources in different regions.

Table 5.4. Lime and aggregate percentages and lime/aggregate ratios of lime mortars and plasters from Kadıkalesi (Anaia)

Period	Sample	Location	Func.	Aggregate Type	Lime (%)	Aggregate (%)	<u>Lime</u> <u>Agg.</u>	
Early Byzantine	First Construction	KBaM1	Baptistery Wall	Mortar	Natural	43.88	56.12	0.78
		KBaM2	Baptistery Wall	Mortar	Natural	52.39	47.61	1.10
		KNM2	Naos Wall	Mortar	Natural	46.10	53.90	0.86
		KSM1	Substructure Arch	Mortar	Natural	53.20	46.80	1.14
		KSM2	Substructure Buttress	Mortar	Natural	33.71	66.29	0.51
		KSM3	Substructure Vault	Mortar	Natural	53.23	46.77	1.14
Middle Byzantine	Second Construction	KFM	Fortification Wall	Mortar	Natural	34.48	65.52	0.53
		KNM1	Naos Buttress	Mortar	Natural	59.09	40.91	1.44
		KNM3	Naos Buttress	Mortar	Natural	62.37	37.63	1.66
		KOP1	Outer Narthex Wall	Plaster	Brick	53.43	46.57	1.15
Late Byzantine	Third Construction	KOP2	Outer Narthex Wall	Plaster	Brick	51.02	48.98	1.04
		KCP1	Cistern I Wall	Plaster	Brick	42.02	57.98	0.72
		KCP2	Cistern I Wall	Plaster	Brick	57.91	42.09	1.38
		KCP3	Cistern II Wall	Plaster	Brick	27.20	72.80	0.37
		KNM4	Naos Buttress	Mortar	Natural	57.59	42.41	1.36

Table 5.5. Lime and aggregate percentages and lime/aggregate ratios of lime mortars and plasters from Ayasuluk

Period	Sample	Location	Func.	Aggregate Type	Lime (%)	Aggregate (%)	<u>Lime</u> <u>Agg.</u>	
Early Byzantine	First Construction	ARP	Treasure Room Wall	Plaster	Brick	55.16	44.84	1.23
		ABaM	Baptistery Wall	Mortar	Brick	64.69	35.31	1.83
		ATM1	Transept Wall	Mortar	Brick	55.02	44.98	1.22
		ATM2	Transept Buttress	Mortar	Natural	64.34	35.66	1.80
		ARM1	Treasure Room Niche	Mortar	Natural	Not determined		
		ARM2	Treasure Room Wall	Mortar	Natural	62.94	37.06	1.70
	Second Construction	ABM3	Bema Arch	Mortar	Natural	41.00	59.00	0.69
		ABM1	Bema Buttress	Mortar	Brick	61.64	38.36	1.61
		ABM2	Bema Buttress	Mortar	Brick	60.82	39.18	1.55
	Third Construction	ANM	Naos Buttress	Mortar	Brick	35.67	64.33	0.55
		ANP	Naos Buttress	Plaster	Brick	43.41	56.59	0.77
		ASP1	Substructure Wall	Plaster	Brick	59.28	40.72	1.46
ASP2		Substructure Wall	Plaster	Brick	61.74	38.26	1.61	
ASM		Substructure Wall	Mortar	Natural	60.68	39.32	1.54	
AGM1		Gate of Persecution Wall	Mortar	Natural	49.55	44.90	1.23	
Middle Byzantine	AGM2	Gate of Persecution Buttress	Mortar	Brick	56.16	43.84	1.28	

Table 5.6. Comparison of the raw material compositions with the literature

Area & Reference	Period	Mortar/ Plaster	Aggregate Type	RAW MATERIAL COMPOSITIONS
				Lime /Aggregate
Fortification Wall of Adana and Kozan Castle in Cilicia (Polat Pekmezci 2012)	Early Byzantine	Mortar	Natural	1/3–2/3
Synagogue from Andriake Harbour (Oğuz, Türker, and Koçkal 2015)	Byzantine	Mortar	Natural	1/9–1/5
Archeological Site of Kyme (Miriello et al. 2011)	Early Byzantine	Mortar	Natural	2/1–3/1
Monastery and Churches from Kayseri (Kozlu and Ersen 2011)	Early– Middle Byzantine (4–11 th centuries)	Mortar	Natural	1/4–5/2
		Plaster	Natural	1/3–2/1
Serapis Temple/ Kızıl Avlu (Özkaya 2005)	Early Byzantine	Mortar	Natural	1/5
		Plaster	Brick	1/2.6
Defense Structures in Istanbul (Acun Özgünler, Gürdal, Kahraman 2013)	Early Byzantine	Mortar	Brick	1/3
Religious Buildings in Istanbul (Gürdal, Kahraman Altaş, Acun Özgünler 2011)	Early Byzantine	Mortar	Brick	1/4–1/2
Land Walls of Yedikule in Istanbul (Acun Özgünler, Ersen, and Güleç 2013)	Early Byzantine (5 th century)	Mortar	Brick	2/3–3/2
St. Jean Church in Manisa (Oğuz Kılıç et al. 2004)	Early Byzantine (6 th century)	Mortar	Brick	1/1
Hagia Sophia Basilica (Moropoulou et al. 2002)	Early and Middle Byzantine (6 th to 10 th centuries)	Mortar	Brick	1/4–1/2
Middle Byzantine Monuments in Kiev (Moropoulou et al. 2000)	Middle Byzantine (11–13 th centuries)	Mortar	Brick	1/3
Middle Byzantine Chapel in Istanbul (Ulukaya et al. 2016)	Middle Byzantine (11–12 th centuries)	Mortar	Brick	1/5–1/4
Middle Byzantine Church in Istanbul (Nežerka et al. 2014)	Middle Byzantine (9 th century)	Mortar	Brick	2/3
Yoros Castle in Istanbul (Kurugöl and Güleç 2012)	Late Byzantine (13–14 th centuries)	Mortar	Brick	2/3–1/3

Particle size distribution of aggregates is another important feature in defining the raw material compositions of lime mortars and plasters since it is known that a particle sizes of aggregates effect the physical properties, durability and mechanical strength of mortars (Lanas et al. 2004; Pavía and Toomey 2008).

In general, the aggregates with particle sizes greater than 1180 μm constituted the major fraction and formed 13.41–23.15% of total aggregates by weight in all investigated mortars and plasters (Table 5.7, 5.8). Similarly, the studies about Byzantine lime mortars demonstrated that largest fraction of aggregates were the sizes greater than 1000 μm (Aslan Özkaya 2005; Gürdal, Kahraman Altaş, and Acun Özgünler 2011; Polat Pekmezci 2012; Acun Özgünler, Ersen, and Güleç 2013; Kahraman Altaş, Acun Özgünler, and Gürdal 2013; Ulukaya et al. 2017; Caner and Güney 2018) (Table 5.9).

In Ayasuluk, the particle size distributions of the natural aggregates were similar to brick aggregates. The percentages of the aggregates decreased gradually from coarse aggregates ($>1180 \mu\text{m}$) (19–23 %) to fine aggregates ($<53 \mu\text{m}$) (0.6–1 %) (Table 5.8) (Figure 5.1–5.4). In addition to these, the aggregates with particle sizes 1180–500 μm , 500–250 μm , 250–125 μm and 125–53 μm sieves were found 7–11%, 5–9%, 4–5%, 4–5% by weight, respectively (Table 5.8) (Figure 5.1–5.4).

However, in Kadikalesi, the particle size distributions of natural and brick aggregates were different from each other. Natural aggregates of Kadikalesi had higher amounts of aggregates with sizes of $>1180 \mu\text{m}$ (4–37%), 1180–500 μm (8–21%), 500–250 μm (5–32%), 250–125 μm (3–14%) and 125–53 μm (2–7%) by weight and less amount of aggregates $<53 \mu\text{m}$ (0.5–2 %) by weight (Table 5.8) (Figure 5.1–5.4). Within the distribution of brick aggregates, the weight percentages of aggregates of sizes $>1180 \mu\text{m}$ (10–19%), 500–250 μm (9–17%), 1180–500 μm (4–12 %) were lower; and the weight percentages of aggregates of sizes 250–125 μm (5–12%), 125–53 μm (6–12%) and $<53 \mu\text{m}$ (0.5–5%) were higher when compared with the distribution of natural aggregates (Table 5.8) (Figure 5.1–5.4).

Physical properties of the coarse aggregates with sizes greater than 1180 μm were defined in terms of maximum aggregate size and roundness scale by macro-observations (Powers 1953).

Lime mortars were composed of natural aggregates with a maximum aggregate size were between ~ 5 –38 mm in Kadikalesi (Anaia), and ~ 4 –35 mm in Ayasuluk (Table 5.7, 5.8). Brick aggregates had maximum aggregate sizes between ~ 2 –12 mm in Kadikalesi (Anaia) and between ~ 3 –23 mm in Ayasuluk (Table 5.7, 5.8). The aggregates

in lime mortars had coarser sizes than lime plasters. Mean roundness of brick aggregates in Kadıkalesi (Anaia) and Ayasuluk were sub-angular and angular, while the natural aggregates were sub-angular, angular and very-angular (Table 5.7, 5.8).

The angular form of aggregates makes possible interlocking among aggregates and provides a higher surface area (McGennis et al. 1995; McCarthy and Dyer 2019). Also, it is known that angularity of aggregates leads to increase bulk density and decrease porosity (Holmes and Wingate 1997; Pavía and Toomey 2008).

Maximum aggregate size values and mean roundness properties were similar in different periods and locations. Therefore, it can be interpreted that the Byzantine masters knew the advantages of the angularity of aggregates. They probably used relevant quarries as raw material sources instead of stream beds for natural aggregates; and prepared the brick aggregates taking this advantage into account.

Table 5.7. Particle size distributions, mean roundness of aggregates and maximum aggregate size from Kadıkalesi (Anaia)

Period	Sample	Location	Func.	Aggregate Type	%						Max. Agg. Size	Mean Roundness	
					1180 μm	500 μm	250 μm	125 μm	53 μm	<53 μm			
Early Byzantine	First Construction	KBaM1	Baptistery Wall	Mortar	Natural	36.4	7.6	5.3	3.5	3.4	0.5	~38 mm	Sub-Angular
		KBaM2	Baptistery Wall	Mortar	Natural	21.9	10.5	10.4	5.4	3.1	0.2	~9 mm	Sub-Angular
		KNM2	Naos Wall	Mortar	Natural	24.1	12.5	6.9	5.2	2.9	0.6	~21 mm	Sub-Angular
		KSM1	Substructure Arch	Mortar	Natural	13.2	10.2	19.2	7.7	3.5	0.5	~10 mm	Very Angular
		KSM2	Substructure Buttress	Mortar	Natural	15.2	12.3	15.2	13.6	6.6	1.5	~7 mm	Sub-Angular
		KSM3	Substructure Vault	Mortar	Natural	19.0	12.5	14.0	4.0	2.5	0.5	~11 mm	Sub-Angular
Middle Byzantine	Second Construction	KFM	Fortification Wall	Mortar	Natural	37.1	16.8	6.0	2.1	2.0	0.5	~13 mm	Angular
		KNM1	Naos Buttress	Mortar	Natural	11.3	12.1	40.0	4.2	2.0	0.4	~10 mm	Sub-Angular
		KNM3	Naos Buttress	Mortar	Natural	9.5	9.3	25.2	3.7	2.6	0.4	~8 mm	Sub-Angular
		KOP1	Outer Narthex Wall	Plaster	Brick	27.4	18.3	4.9	24.5	11.2	0.7	~7 mm	Sub-Angular
Late Byzantine	Third Construction	KOP2	Outer Narthex Wall	Plaster	Brick	11.1	8.8	5.4	10.5	12.2	1.2	~2 mm	Sub-Angular
		KCP1	Cistern I Wall	Plaster	Brick	10.1	10.2	11.2	4.8	5.8	5.1	~2 mm	Sub-Angular
		KCP2	Cistern I Wall	Plaster	Brick	10.6	14.7	5.5	12.1	10.3	1.5	~6 mm	Sub-Angular
		KCP3	Cistern II Wall	Plaster	Brick	19.0	16.8	7.7	14.7	9.9	1.7	~12 mm	Angular
		KNM4	Naos Buttress	Mortar	Natural	3.6	20.5	5.0	2.6	2.7	0.4	~5 mm	Very Angular

Table 5.8. Particle size distributions, mean roundness of aggregates and maximum aggregate size from Ayasuluk

Period	Sample	Location	Func.	Aggregate Type	%						Max. Agg. Size	Mean Roundness	
					1180 μm	500 μm	250 μm	125 μm	53 μm	<53 μm			
Early Byzantine	First Construction	ARP	Treasure Room Wall	Plaster	Brick	24.6	6.0	4.6	3.0	4.8	2.9	~15 mm	Sub-Angular
		ABaM	Baptistery Wall	Mortar	Brick	10.9	8.3	6.2	5.5	6.1	0.4	~11 mm	Sub-Angular
		ATM1	Transept Wall	Mortar	Brick	25.4	6.7	12.6	4.0	2.4	1.7	~23 mm	Angular
		ATM2	Transept Buttress	Mortar	Natural	18.1	6.6	13.0	3.3	2.0	0.2	~35 mm	Very Angular
		ARM1	Treasure Room Niche	Mortar	Natural	35.3	17.8	4.6	6.2	5.7	1.0	~13 mm	Angular
		ARM2	Treasure Room Wall	Mortar	Natural	11.4	10.4	6.5	2.6	2.6	0.4	~4 mm	Angular
	Second Construction	ABM3	Bema Arch	Mortar	Natural	28.1	11.6	11.7	4.9	6.4	0.5	~18 mm	Sub-Angular
		ABM1	Bema Buttress	Mortar	Brick	16.0	6.7	5.0	4.8	3.6	1.1	~16 mm	Angular
		ABM2	Bema Buttress	Mortar	Brick	21.9	8.4	8.1	2.4	1.3	0.8	~12 mm	Angular
	Third Construction	ANM	Naos Buttress	Mortar	Brick	25.9	13.9	7.0	10.5	4.3	0.2	~8 mm	Sub-Angular
		ANP	Naos Buttress	Plaster	Brick	15.8	3.7	3.7	3.8	3.6	0.2	~12 mm	Angular
		ASP1	Substructure Wall	Plaster	Brick	11.6	5.0	1.7	3.9	5.1	0.9	~3 mm	Angular
		ASP2	Substructure Wall	Plaster	Brick	6.6	6.5	0.3	6.6	12.1	1.1	~3 mm	Angular
		ASM	Substructure Wall	Mortar	Natural	16.4	10.4	10.6	3.1	2.6	0.8	~8 mm	Angular
	Middle Byzantine	AGM1	Gate of Persecution Wall	Mortar	Natural	29.6	6.8	6.4	4.3	3.8	0.7	~30 mm	Sub-Angular
AGM2		Gate of Persecution Buttress	Mortar	Brick	29.4	3.1	1.9	3.0	5.4	1.0	~21 mm	Angular	

Table 5.9. Comparison of the raw material compositions with the literature

Area & Reference	Period	Mortar/ Plaster	Aggregate Type	RAW MATERIAL COMPOSITIONS
				Particle Size Distributions
Fortification Wall of Adana and Kozan Castle in Cilicia (Polat Pekmezci 2012)	Early Byzantine	Mortar	Natural	>1000 μm largest fraction
Synagogue from Andriake Harbour (Oğuz, Türker, and Koçkal 2015)	Byzantine	Mortar	Natural	>1000 μm largest fraction
Serapis Temple/ Kızıl Avlu (Özkaya 2005)	Early Byzantine	Mortar	Natural	>1000 μm largest fraction
		Plaster	Brick	
Defense Structures in Istanbul (Acun Özgünler, Gürdal, Kahraman 2013)	Early Byzantine	Mortar	Brick	4000 μm largest fraction
Religious Buildings in Istanbul (Gürdal, Kahraman Altaş, Acun Özgünler 2011)	Early Byzantine	Mortar	Brick	4000 μm largest fraction
Land Walls of Yedikule in Istanbul (Acun Özgünler, Ersen, and Güleç 2013)	Early Byzantine (5th century)	Mortar	Brick	>1000 μm largest fraction
Early Byzantine Church in Stratonikeia in Muğla (Caner and Güney 2018)	Early Byzantine (5–7th centuries)	Mortar	Brick	>1000 μm largest fraction
		Plaster	Brick	
Middle Byzantine Chapel in Istanbul (Ulukaya et al. 2016)	Middle Byzantine (11–12 th centuries)	Mortar	Brick	>4000 μm largest fraction

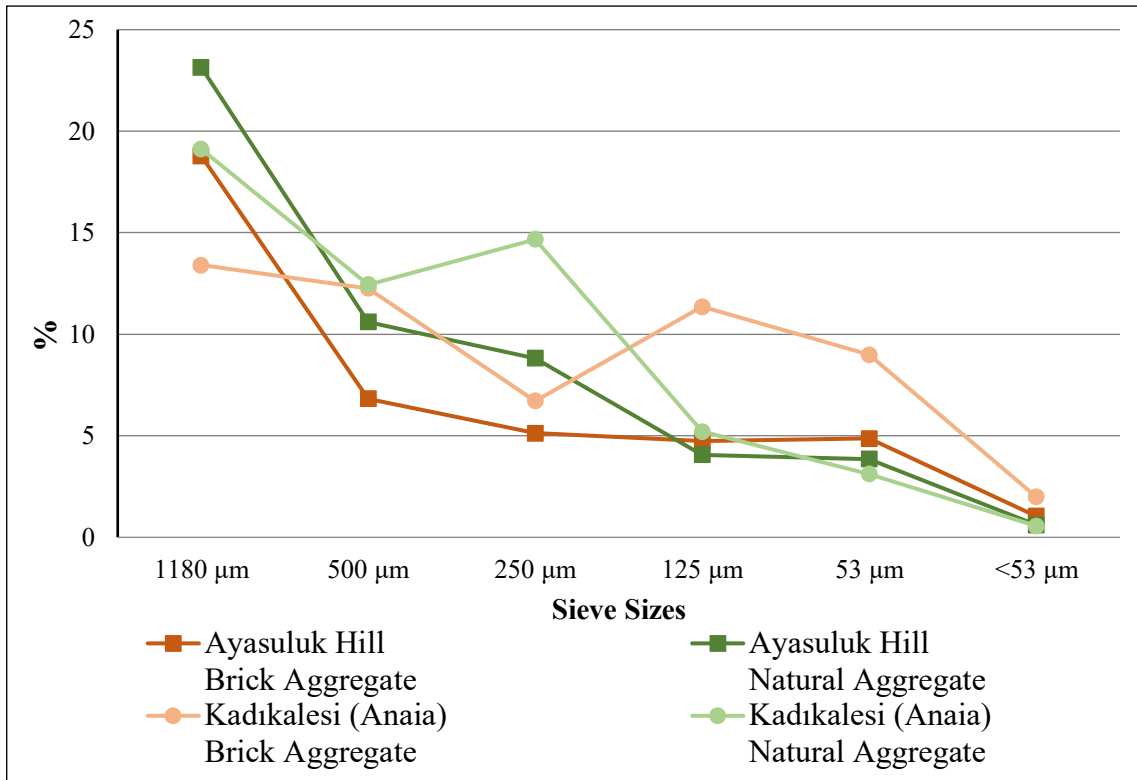


Figure 5.1. Particle size distributions of aggregates from Kadıkalesi (Anaia) and Ayasuluk Hill

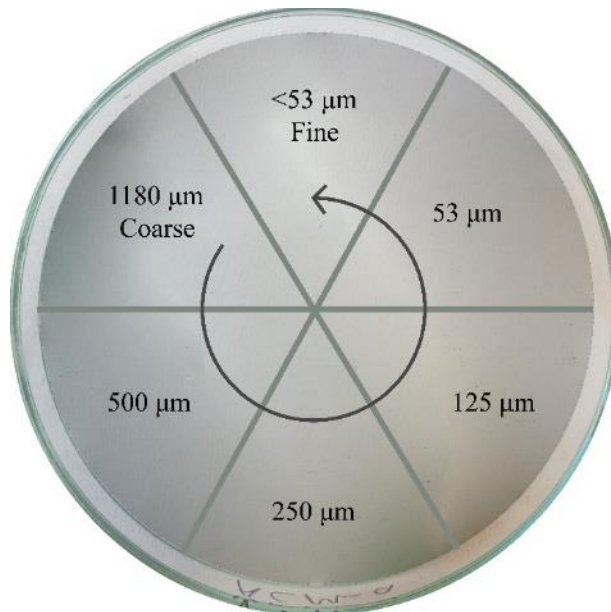
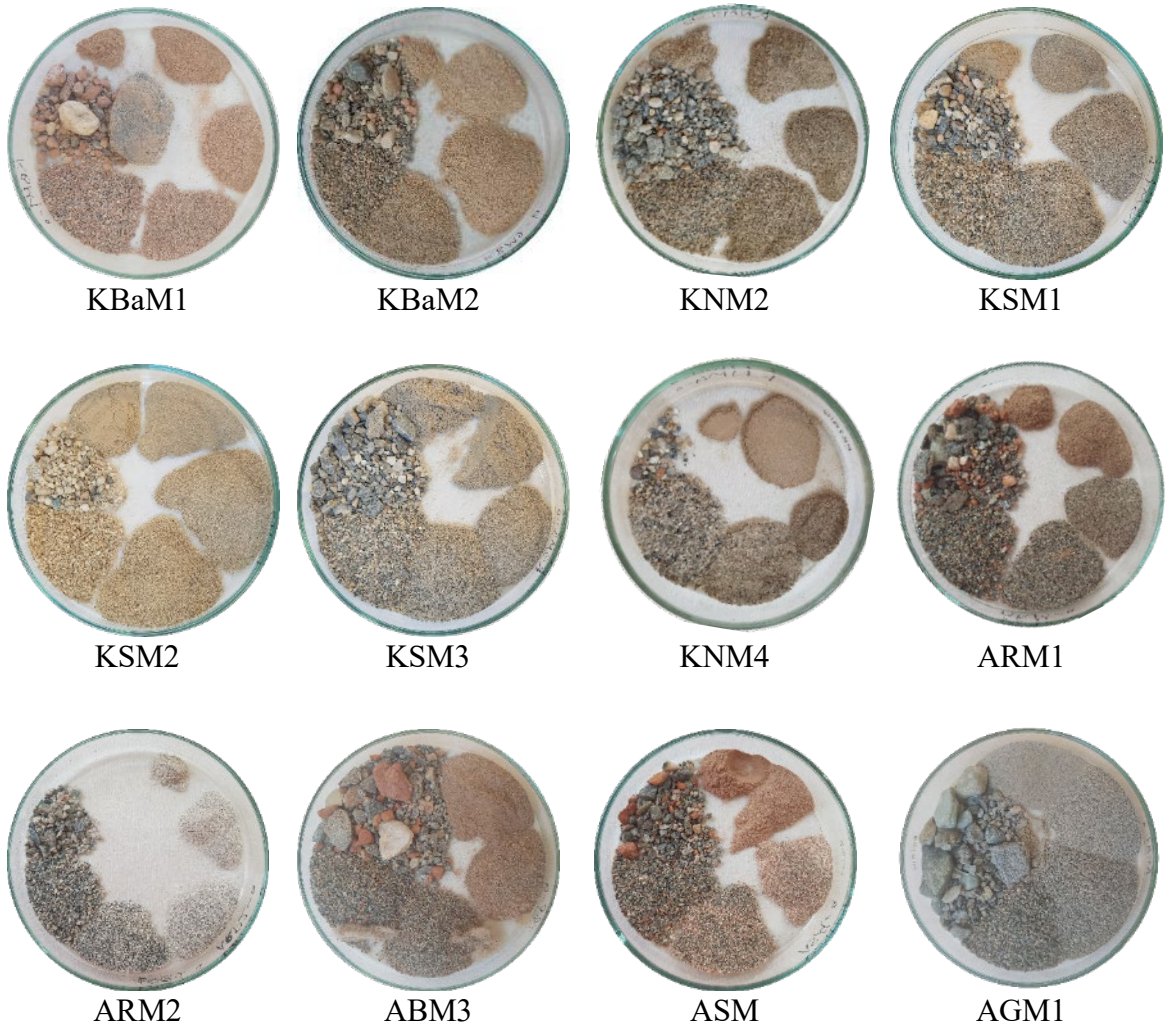


Figure 5.2. Distribution of the aggregates from coarse to fine in samples indicated in Figure 5.3 and 5.4

EARLY BYZANTINE



MIDDLE BYZANTINE

LATE BYZANTINE

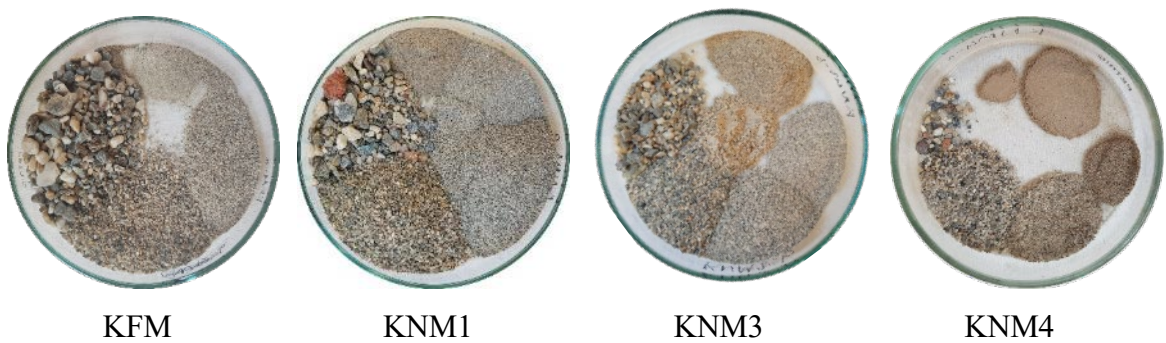


Figure 5.3. Natural aggregates used in lime mortars from Kadıkalesi (Anaia) and Ayasuluk

EARLY BYZANTINE



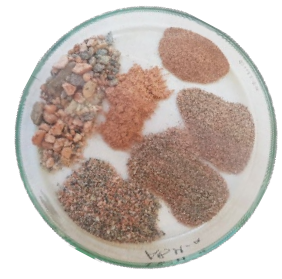
ARP



ABaM



ATM1



ABM1



ABM2



ANM



ANP



ASP1

MIDDLE BYZANTINE



AGM2



KOP1

LATE BYZANTINE



KOP2



KCP1



KCP2



KCP3

Figure 5.4. Brick aggregates used in lime mortars from Kadikalesi (Anaia) and Ayasuluk

5.3. Possible Provenance of Natural Aggregates

Since the study areas are in the Western Aegean Region, the region's geological features were examined to determine the possible provenance and formation of natural aggregates. Geologically, rock and mineral formations in the area are associated with the older rocks of Menderes Massif and younger Neogene and Quaternary graben fill units (Figure 5.5).

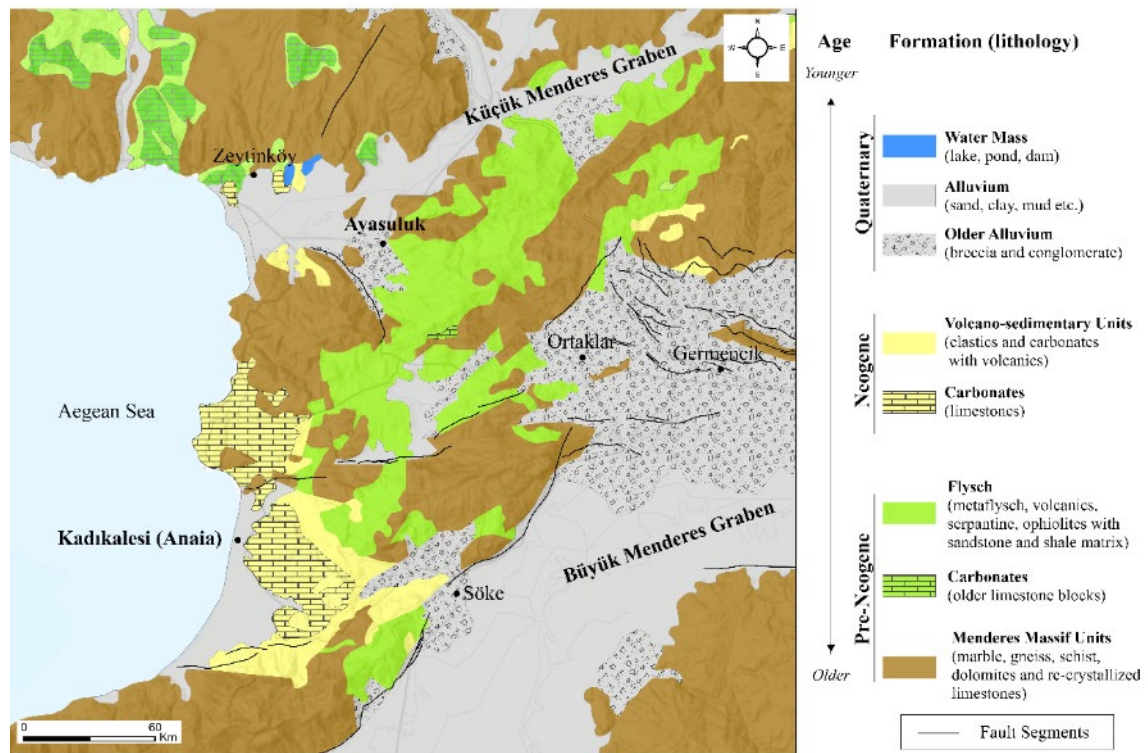


Figure 5.5. Geological map of the Kadıkalesi (Anaia), and Ayasuluk environs (Modified after Akbaş et al. 2011 by using ArcGIS Pro software by Taygun Uzelli)

Macro-observations revealed that coarse aggregates were constituted of different types of rocks with white, grey, brown, green, colors (Figure 5.6). In the literature, the clasts were defined according to their colors, hereunder the grayish-green or whitish cream-colored are schists, orangish/red-browns are gneisses, green colored are clinocllore and white, red and dark tones are quartz fragments (Koçyiğit 2015). Metamorphic schists (mostly mica schists) glowing in the light and similar fragments of gneisses with thicker foliate plates were determined in macro samples. In general, quartz-dominated aggregates were observed in samples (Figure 5.3, 5.4, 5.6).

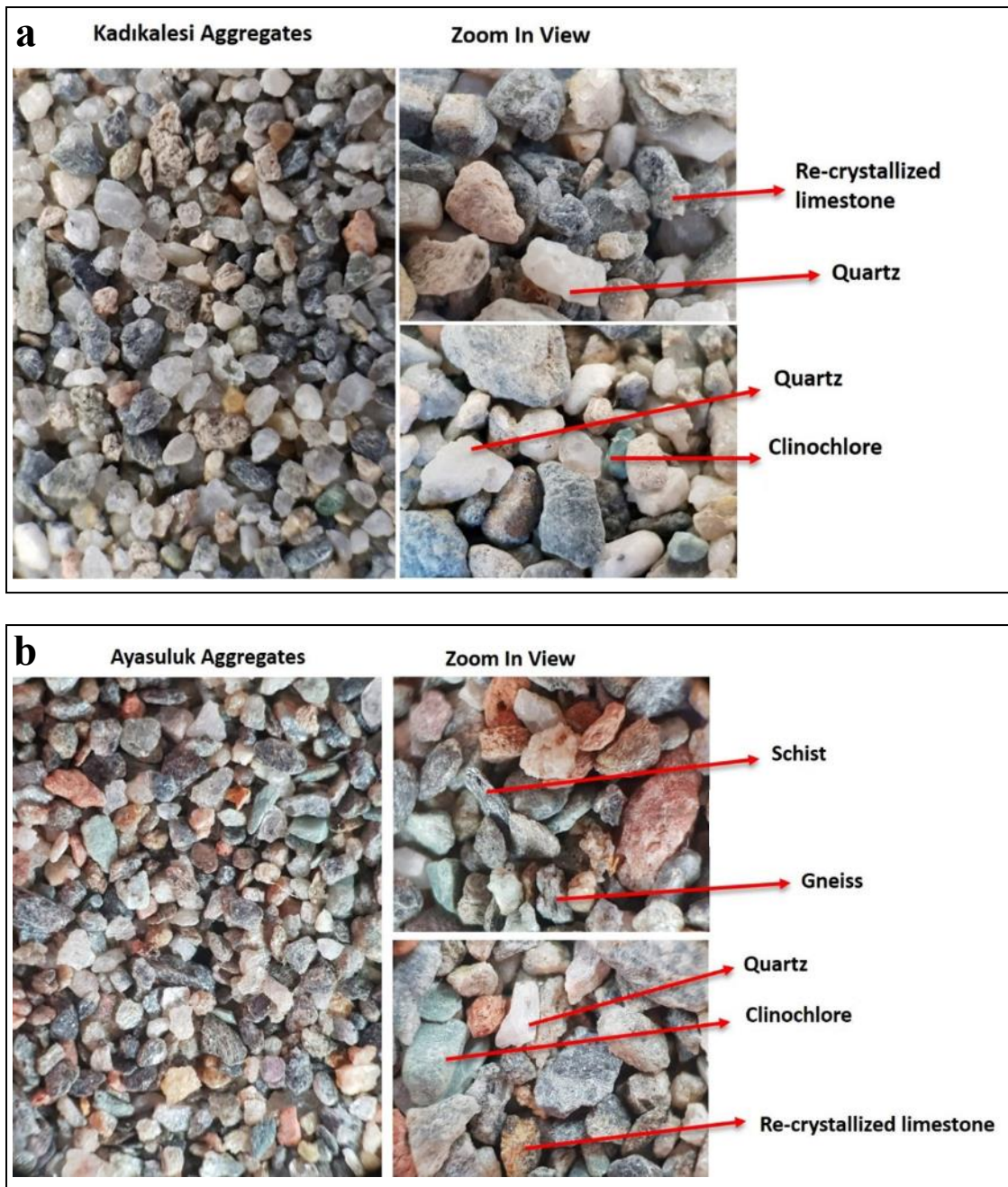


Figure 5.6. Macro-observations of natural aggregates from Kadıkalesi (Anaia) (a) and Ayasuluk (b)

These observations indicated that the aggregates may have been derived from Menderes Massif, where older rock assemblages form the higher topographies, mountains, and horsts in the Aegean Region (Bozkurt and Oberhänsli 2001; Erdoğan and Güngör 2004; Seyitoğlu and Işık 2009). Erosion, tectonic activity and fluvial processes affect the metamorphic rocks of the Menderes Massif which cause disintegration and crumbling from their surfaces, and so the disintegrated fragments are transported and deposited around graben-horst systems (Figure 5.7). These deposits are called as breccias

and conglomerates in the literature which composed of a finely ground matrix such as clay, volcanic rock fragments. Breccias and conglomerates can be differentiated and identified by their roundness scales formed due to their proximity to valleys and stream beds (Figure 5.7).

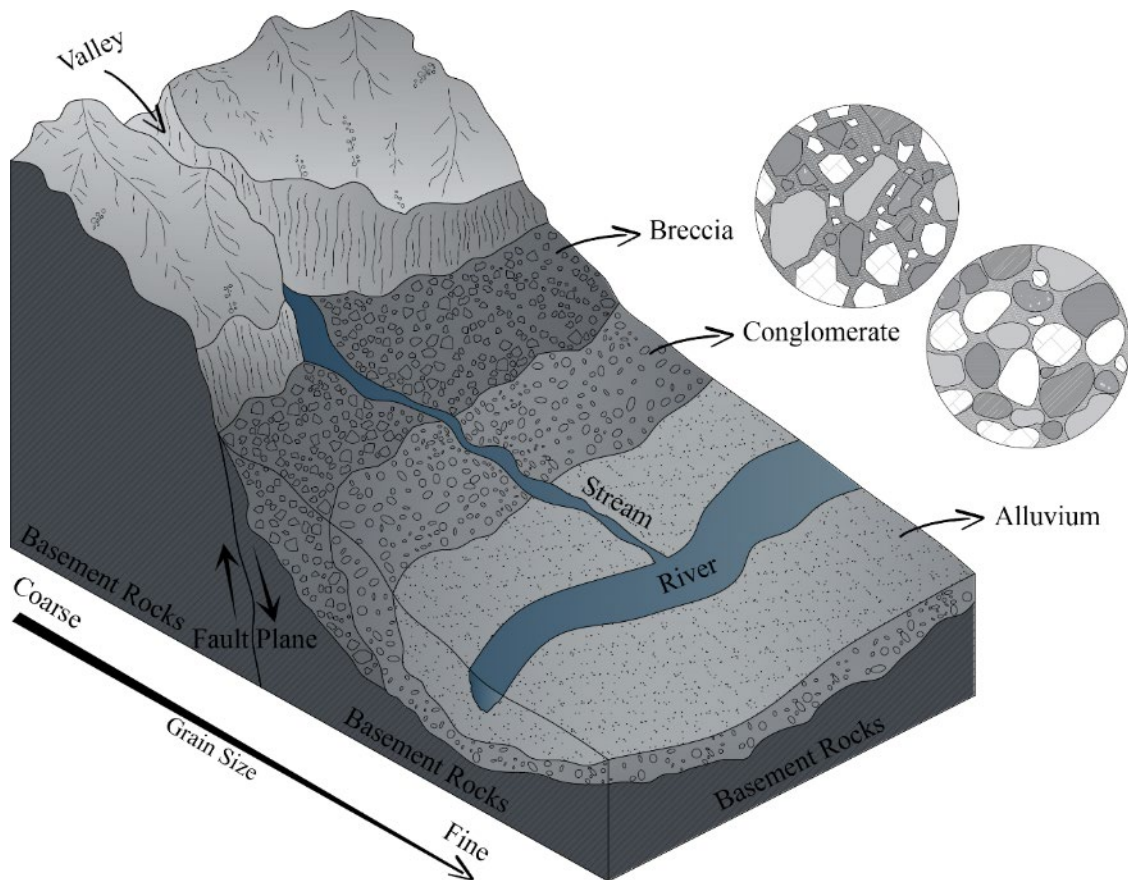


Figure 5.7. Schematic determination of the possible places of natural aggregate sources (Modified from Halдар and Tišljар 2014)

Different igneous, sedimentary, or metamorphic clasts (rock fragments) may be found in conglomerates (rounded to sub-rounded fragment form) and breccias (angular fragment forms) due to the sedimentation and accumulation process of sediments (Pettijohn 1957; Boggs Jr. 2009). The roundness of the fragments may provide information about their transportation distance before the deposition and the correlation of the deposited layers (Powers 1953; Pettijohn 1957; Boggs Jr. 2009).

Conglomerates have been exposed to longer transportation distances at rivers, streams, and coastlines resulting in a rounded and sub-rounded forms; whereas breccias

might be obtained from mountain slopes and fault zones with angular forms (Boggs Jr. 2009) (Figure 5.7, 5.8).

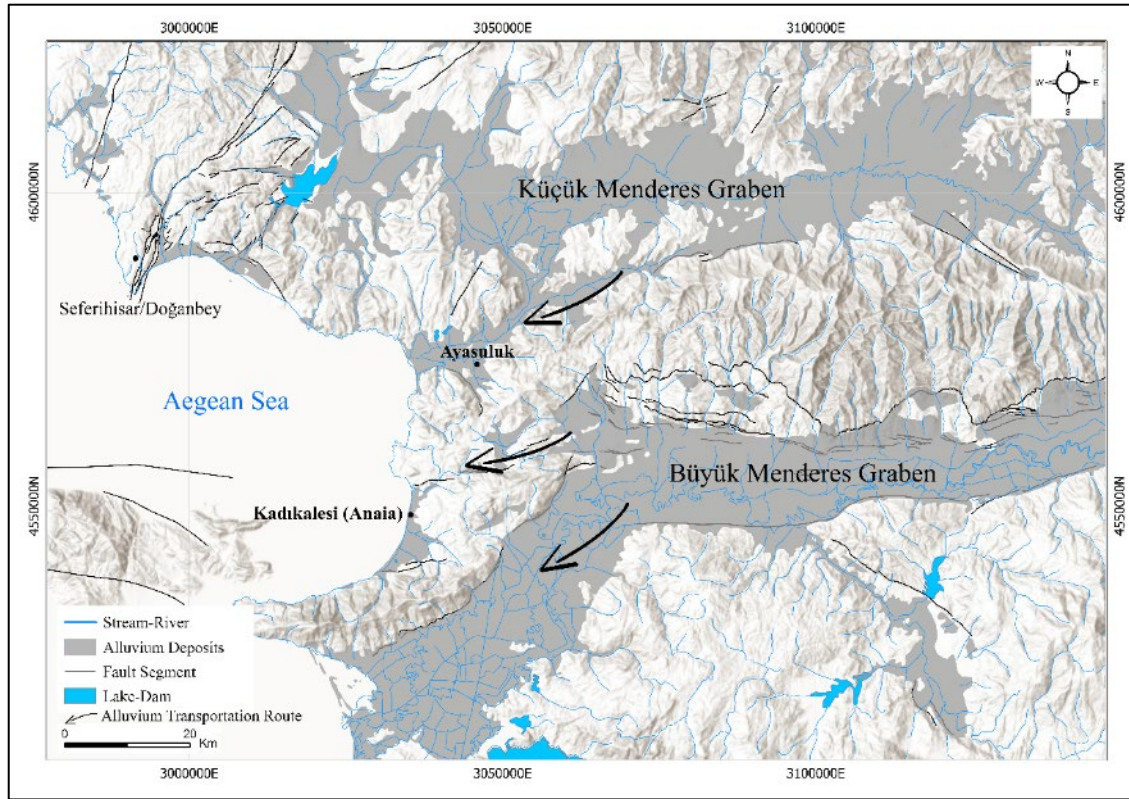


Figure 5.8. Possible sediment transportation and accumulation directions of Büyük and Küçük Menderes rivers (Produced via ArcGIS Pro by Taygun Uzelli 2022)

The examined coarse aggregates in Kadıkalesi (Anaia) and Ayasuluk had sub-angular, angular, and very angular forms indicating breccia (Table 5.7, 5.8) (Figure 5.3, 5.4, 5.6).

The possible sources for the breccia in the region were the mountain slopes of Büyük Menderes Grabens (most likely Söke, Germencik district) which is close to Kadıkalesi (Anaia), and Küçük Menderes Grabens (most probably Selçuk) which is nearby Ayasuluk (Figure 5.5, 5.8). The angular forms of the investigated breccia aggregates indicated alluvial materials, rich in gneiss, schist and quartzite, deposited on the mountainous slopes of the Grabens as their provenance. These sources were surrounded by Neogene-aged volcanic units and volcano-sedimentary units which affected the compositions of breccia matrices (Figure 5.5) (Bozkurt and Oberhänsli 2001; Bozkurt 2001; Şengör and Bozkurt 2013). The Pre-Neogene volcanic-containing units in the east and north of Ayasuluk (Seferihisar-Doğanbey) were generally consisted of old

oceanic flysch and sandstone-shale with volcanic-containing units in their matrix. However, Neogene limestones and volcanics were found more around Kadıkalesi (Eşder 1988; Erdoğan 1990; Erdoğan and Güngör 2004; Akbaş et al. 2011). These geological differences resulted in the existence of more volcanic materials in the matrices of Ayasuluk aggregates and more carbonate content of Kadıkalesi aggregates.

5.4. Characteristics of Fine Aggregates

The pozzolanic activities, mineralogical and chemical compositions, microstructural properties of the natural and brick aggregates with particle sizes finer than 53 μm were determined to define their characteristics. The finest aggregates were chosen for characterization because the parts of the binder parts of the mortars which were consisted of small grain-sized silica and carbonated lime, are accepted as the most important parts in terms of providing hydraulic properties and strength to the mortars (Moropoulou, Bakolas, and Bisbikou 1995; Middendorf et al. 2005).

Pozzolanic activities of aggregates were determined via electrical conductivity differences and ASTM C618-03. Electrical conductivity differences were measured before and after the addition of fine aggregates (<53 μm) into the saturated calcium hydroxide solution ($\text{Ca}(\text{OH})_2$) (Luxan, Madruga, and Saavedra 1989). Electrical conductivity differences higher than 1.2 mS/cm demonstrated the pozzolanic property of aggregates (Luxan, Madruga, and Saavedra 1989). According to ASTM C618-03 standard, $\text{SiO}_2 + \text{Al}_2\text{O}_3 + \text{Fe}_2\text{O}_3$ content of the material should be above 70 % to consider it as pozzolanic (ASTM C618-03 2003).

Mineralogical compositions of the aggregates were analyzed via XRD on fine aggregates (<53 μm). The chemical compositions of the pelletized fine aggregates and microstructural properties of the polished and broken surfaces were specified via SEM-EDS.

5.4.1. Characteristics of Fine Natural Aggregates

The results of SEM-EDS analysis showed that fine natural aggregates in lime mortars from Kadıkalesi (Anaia) were mainly composed of large amounts of SiO_2 (66.80–75.77 %), moderate amounts of Al_2O_3 (11.26–16.87 %) and smaller amounts of Fe_2O_3

(4.39–8.05 %), MgO (1.80–4.39 %), K₂O (2.25–3.40 %), Na₂O (0.37–2.34 %), CaO (0.63–1.81 %) and TiO₂ (0.64–1.46 %) (Table 5.10). Similarly, fine natural aggregates of lime mortars from Ayasuluk were comprised of mostly large amounts of SiO₂ (64.16–81.35 %), moderate amounts of Al₂O₃ (7.48–18.34 %) and smaller amounts of Fe₂O₃ (3.70–9.13 %), MgO (3.57–8.81 %), K₂O (1.09–3.18 %), Na₂O (0.50–1.05 %), CaO (0.82–1.84 %) and TiO₂ (0.67–1.28 %) (Table 5.10).

Chemical compositions of aggregates were also used to estimate their pozzolanic activity as defined by the standard ASTM C618-03. SiO₂+Al₂O₃+Fe₂O₃ content of natural aggregates in Kadıkalesi were 89.75–92.47 while in Ayasuluk the values were between 84.69–93.05 (Table 5.10). Electrical conductivity differences of natural aggregates of Kadıkalesi (Anaia) and Ayasuluk in saturated calcium hydroxide solution were measured between 1.51–8.03 mS/cm and 2.65–7.61 mS/cm, respectively (Table 5.10). According to these results, all fine aggregates in the Byzantine lime mortars from Kadıkalesi (Anaia) and Ayasuluk were found to possess highly active pozzolanic properties. Highly reactive pozzolanic properties of the fine natural aggregates can be attributed to the volcanoclastic matrix of the breccia (Figure 5.5).

Recent studies showed that, the natural aggregates used in Serapis Temple (Aslan Özkaya 2005), archeological site of Kyme (Miriello et al. 2011) and some Cilicia Buildings (Polat Pekmezci 2012) were also found reactive pozzolans (Table 5.11). Natural aggregates of Serapis Temple and Archeological site of Kyme in Western Anatolia were more similar with Kadıkalesi (Anaia) and Ayasuluk in terms of chemical compositions than natural aggregates of Cilicia buildings which contained less SiO₂, but more Al₂O₃ and CaO (Aslan Özkaya 2005; Miriello et al. 2011; Polat Pekmezci 2012) (Table 5.11).

Table 5.10. Chemical compositions and pozzolanic activities of the natural aggregates in Kadikalesi (Anaia) and Ayasuluk

Period	Sample	Location	Func.	Chemical Compositions (%)								Pozzolanic Activity	
				Na ₂ O	MgO	Al ₂ O ₃	SiO ₂	K ₂ O	CaO	TiO ₂	Fe ₂ O ₃	Electrical Conductivity Difference (mS/cm)	SiO ₂ +Al ₂ O ₃ +Fe ₂ O ₃ (%)
Early Byzantine	KBaM1	Baptistery Wall	Mortar	0.60	2.29	11.26	75.77	2.25	1.55	0.84	5.44	7.13	92.47
	KBaM2	Baptistery Wall	Mortar	1.86	2.23	12.71	73.47	2.77	1.81	0.76	4.39	7.97	90.57
	KNM2	Naos Wall	Mortar	0.62	4.21	16.07	66.90	3.20	0.74	1.04	7.23	5.53	90.20
	KSM1	Substructure Arch	Mortar	0.66	4.39	15.47	66.80	3.19	1.06	0.94	7.48	1.51	89.75
	KSM2	Substructure Buttress	Mortar	2.34	1.80	16.87	69.53	2.83	0.63	0.71	5.29	1.64	91.69
	KSM3	Substructure Vault	Mortar	0.63	3.02	12.54	74.38	2.79	0.83	0.64	5.18	8.03	92.10
	ATM2	Transept Buttress	Mortar	0.50	3.57	7.48	80.85	1.09	1.31	0.75	4.46	7.61	92.79
	ARM1	Treasure Room Niche	Mortar	0.96	8.81	18.34	57.22	3.18	1.42	0.94	9.13	2.65	84.69
	ARM2	Treasure Room Wall	Mortar	0.52	3.72	8.00	81.35	1.23	0.82	0.67	3.70	7.58	93.05
	ABM3	Bema Arch	Mortar	0.87	7.48	13.89	64.96	2.22	1.51	1.09	7.97	5.66	86.82
Middle Byz.	ASM	Substructure Wall	Mortar	0.88	6.86	13.20	66.74	2.05	1.38	1.22	7.68	7.28	87.62
	AGM1	Gate of Persecution Wall	Mortar	1.05	7.85	14.30	64.16	2.72	1.84	1.28	6.80	6.04	85.26
	KFM	Fortification Wall	Mortar	0.67	3.24	15.83	67.44	3.12	0.88	0.78	8.05	3.84	91.32
	KNM1	Naos Buttress	Mortar	0.78	3.27	14.11	69.74	3.40	0.99	1.22	6.51	4.33	90.36
	KNM3	Naos Buttress	Mortar	0.80	3.02	13.56	71.53	3.11	1.17	1.00	5.82	7.90	90.91
Late Byz.	KNM4	Naos Buttress	Mortar	0.37	2.24	15.27	71.14	3.27	0.85	1.46	5.40	3.08	91.81

Table 5.11. Comparison of chemical compositions and pozzolanic activity of natural aggregates with the literature

Area & Reference	Period	Chemical Compositions								Pozzolanic Activity	
		Na ₂ O	MgO	Al ₂ O ₃	SiO ₂	K ₂ O	CaO	TiO ₂	Fe ₂ O ₃	Electrical Conductivity Difference (mS/cm)	SiO ₂ + Al ₂ O ₃ + Fe ₂ O ₃ (%)
Fortification Wall of Adana and Kozan Castle in Cilicia (Polat Pekmezci 2012)	Early Byzantine	1.42	2.86–4.29	21.78–25.54	41.8–51.75	3.81–7.43	6.53–11.22	0.00	8.73–10.80	-	74.04–82.90
Archeological Site of Kyme (Miriello et al. 2010)	Early Byzantine	1.79–5.01	0.91–2.81	12.63–21.35	60.33–76.71	2.85–4.84	0.96–5.92	0.10–0.88	0.12–5.24	-	84.03–90.83
Serapis Temple/ Kızıl Avlu (Özkaya 2005)	Early Byzantine	1.3–2.3	1.4–2.1	5.6–6.8	80.1–83.9	1.0–1.1	-	0.7–1.3	6.8–11.4	7.72	94.8–95.2

Chemical compositions of fine natural aggregates were evaluated through the ternary diagram which was plotted according to their silica and alumina, carbonate, and alkali phase contents. Ternary diagrams were generally used to exhibit the compositional differences of the materials and to discuss their possible provenances (Strazzera, Dondi, and Marsigli 1997; Böke et al. 2006; Grimoldi et al. 2014). The ternary diagram clearly showed that all fine natural aggregates were rich in silica and alumina; but poor in carbonate and alkali phases (Figure 5.9). On the diagram, it was observed that the fine aggregates formed three distinct groups. The first group was consisted of all the fine natural aggregates of Kadıkalesi (Anaia), and the second group was from Ayasuluk which composed of first construction period wall (ARM2) and buttress (ATM2). Natural aggregate from a first construction period niche (ARM1), a second construction period arch (ABM3), and third construction period walls (ASM, AGM1) consisted of the third group.

The distinctions in the chemical compositions revealed that natural aggregates used in Kadıkalesi and Ayasuluk mortars were probably obtained from different sources. Most likely, Kadıkalesi aggregates were obtained from the same quarry for centuries, while two different sources were used for Ayasuluk aggregates.

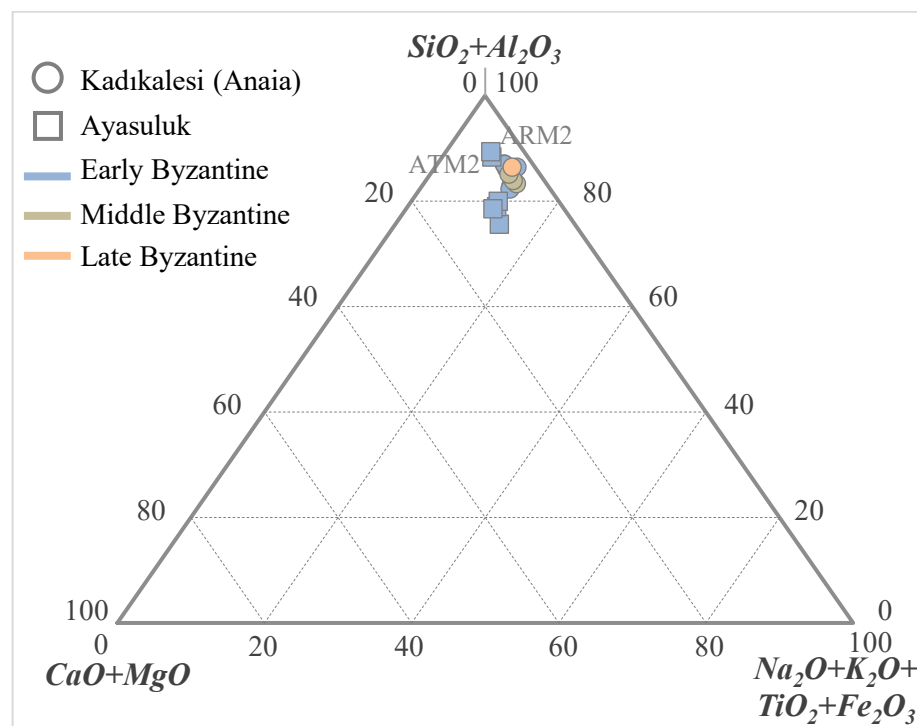


Figure 5.9. Ternary Diagram ($SiO_2 + Al_2O_3 - CaO + MgO - Na_2O + K_2O + TiO_2 + Fe_2O_3$) of chemical compositions of natural aggregate

Chemical compositions of fine natural aggregates were also evaluated by the total alkali-silica (TAS) diagram in order to assign possible geochemical origins of volcanic fragments contained in the deposit matrix of breccia (Le Maitre et al. 2002). The fine volcanic fragments in aggregates of Kadıkalesi had varying silica content (SiO_2) between 66.80–74.38% and alkali content ($\text{Na}_2\text{O}+\text{K}_2\text{O}$) in the range of 2.85–5.17% (Figure 5.10). In Ayasuluk aggregates, the silica content varied between 57.22–81.35%, whereas the alkali contents were between 1.59–4.14% (Figure 5.10). Predominant igneous rocks found in natural aggregates were dacite and rhyolite in both areas. Nevertheless, natural aggregates of Early Byzantine period samples from Ayasuluk were consisted of andesite, dacite or rhyolite fragments. In Kadıkalesi, natural aggregate fragments used in Middle and Late Byzantine period lime mortars were composed of dacite fragments, whereas Early Byzantine period aggregates had dacite or rhyolite fragments. (Figure 5.10).

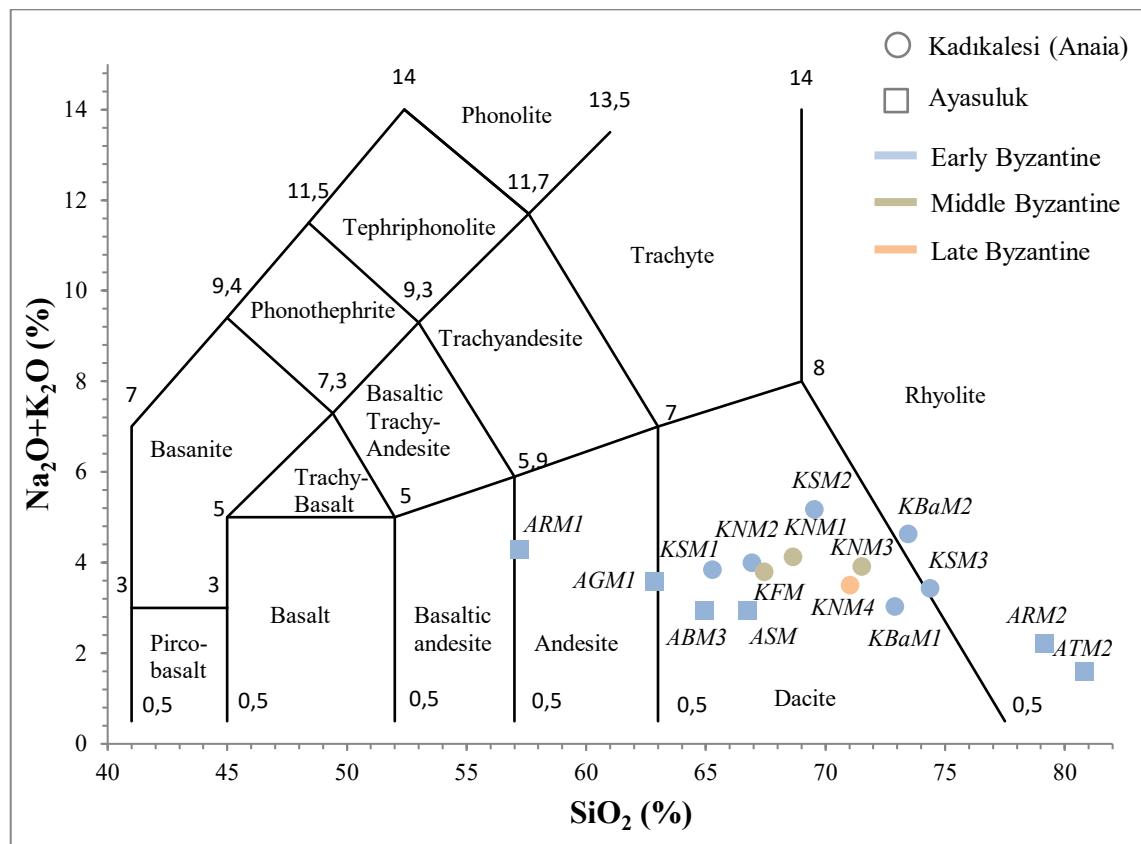


Figure 5.10. Total Alkali Silica (TAS) diagram (Le Maitre et al. 2002) showing the geochemical origins of fine aggregates

Mineralogical compositions of the rhyolite, dacite, and andesite were defined in “Igneous Rocks: A Classification and Glossary of Terms” (Le Maitre et al. 2002). Rhyolite is composed of mainly quartz, alkali feldspar (orthoclase, sanidine, microcline, anorthoclase), with a minor amount of plagioclase (albite, anorthite, labradorite, bytownite, andesine, plagioclase) and biotite; whereas dacite mainly consists of quartz, plagioclase, and trace amount of biotite, hornblende, or pyroxene; andesite is composed of mostly plagioclase and pyroxene, hornblende, or biotite (Le Maitre et al. 2002).

The mineralogical compositions of fine natural aggregates determined by XRD analysis were compatible with the geochemical classes found with TAS diagram. XRD results revealed that the fine natural aggregates of Kadıkalesi (Anaia), determined to be in the rhyolite class, were composed of quartz (SiO_2), orthoclase ($\text{K(AlSi}_3\text{O}_8)$), albite ($\text{Na(AlSi}_3\text{O}_8)$), muscovite ($\text{KAl}_2(\text{Si}_3\text{Al})\text{O}_{10}(\text{OH,F})_2$) and, clinochlore ($(\text{Mg,Fe})_5\text{Al(Si}_3\text{Al})\text{O}_{10}(\text{OH})_8$) (Figure 5.11). Natural aggregates consisted of dacite fragments, and andesite fragments had quartz, albite, muscovite and clinochlore minerals (Figure 5.11). In Kadıkalesi (Anaia), only KSM1, and KSM2 samples that belonged to Early Byzantine period did not contain clinochlore mineral. KBaM2 and KSM3 samples from Early Byzantine period had orthoclase mineral different from other samples due to the contain rhyolite fragments.

In Ayasuluk, fine natural aggregates in rhyolite origin had quartz, orthoclase, albite, muscovite, clinochlore, phillipsite ($(\text{KCa(Si}_5\text{Al}_3)\text{O}_{16.6}\text{H}_2\text{O})$) and hornblende ($(\text{Ca,Na})_2(\text{Mg,Fe,Al})_5(\text{Al,Si})_8\text{O}_{22}(\text{OH})_2$) minerals (Figure 5.12) on their XRD patterns. Fine natural aggregates of dacite and andesite origins had similar mineralogical compositions with rhyolite, except the orthoclase minerals (Figure 5.12). ATM2 and ARM2 samples differed from other Early Byzantine samples by having orthoclase minerals because of rhyolite fragments in the matrix.

The differences determined in the mineralogical compositions of the fine aggregates of Kadıkalesi and Ayasuluk mortars may indicate that different raw material sources were used in these two areas. Since Ayasuluk was located closer to older volcanic units, and close to the volcanics such as Seferihisar-Doğanbey, the hornblende and phillipsite minerals detected in natural aggregates of Ayasuluk might be originated from these volcanic units. The absence of these hornblende and phillipsite minerals in Kadıkalesi (Anaia) can be the indicator of the use of different raw material sources.

Natural aggregates of Serapis Temple in Pergamon, Western Anatolia showed similar mineralogical compositions in terms of including quartz, albite, feldspar, and mica

minerals (Aslan Özkaya 2005). Further investigations should be carried out in order to determine the possibility of the use of Menderes Massif as a common raw material source in Western Anatolia.

On the XRD patterns of some natural aggregates from Kadıkalesi (Anaia) and Ayasuluk, the peaks of pozzolanic minerals such as amorphous silicates with a diffuse band between 20–30 °2θ were moderately observed. These bands were observed more clearly on the natural aggregate samples with higher pozzolanic activities such as KSM3 (8.03 mS/cm) and ATM2 (7.61 mS/cm) (Figure 5.13).

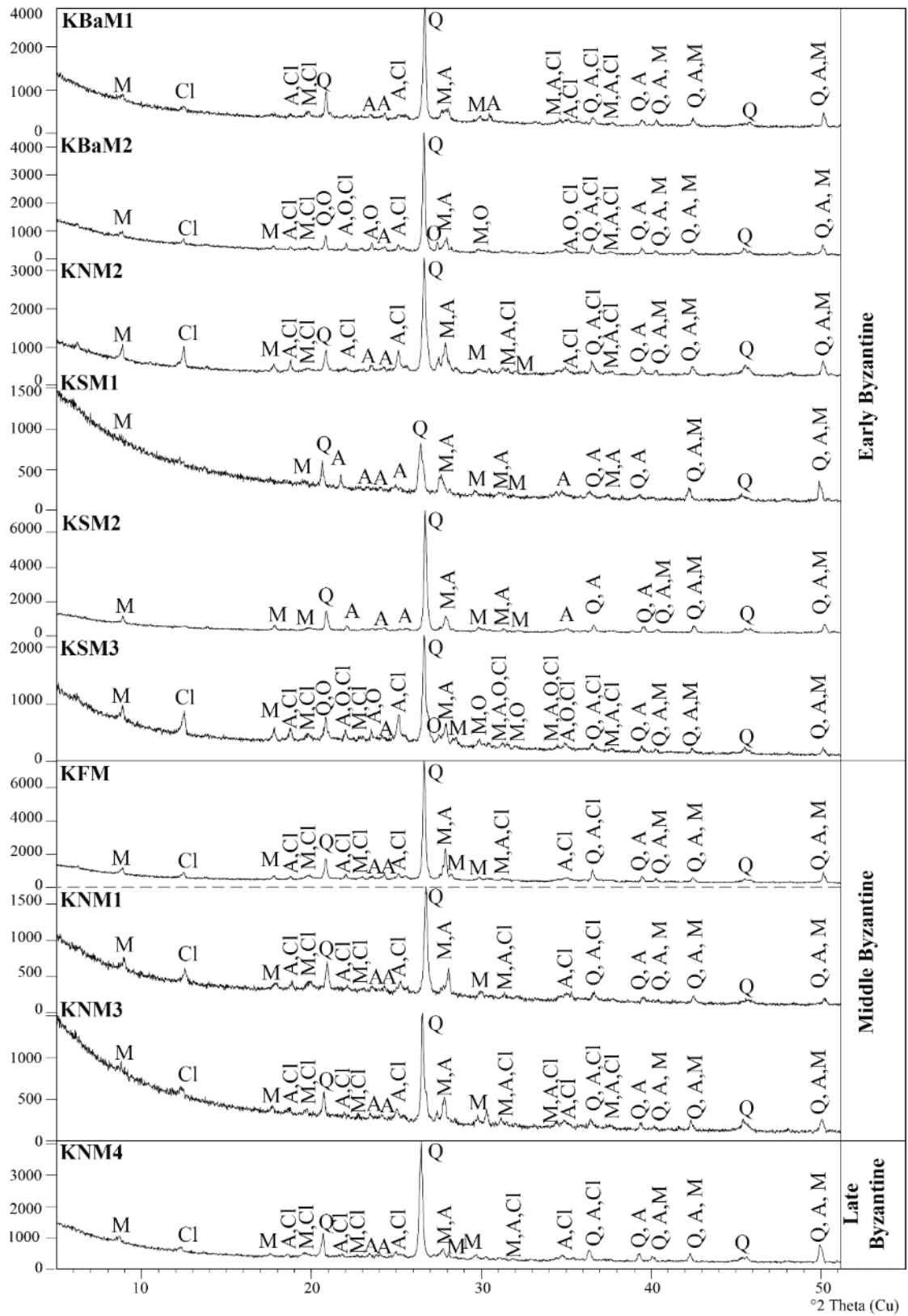


Figure 5.11. XRD patterns of natural aggregates in lime mortars from Kadikalesi (Anaia) (A: Albite 76-1819, Cl: Clinocllore 79-1270, M: Muscovite 84-1302, O: Orthoclase 31-0966, Q: Quartz 85-0798)

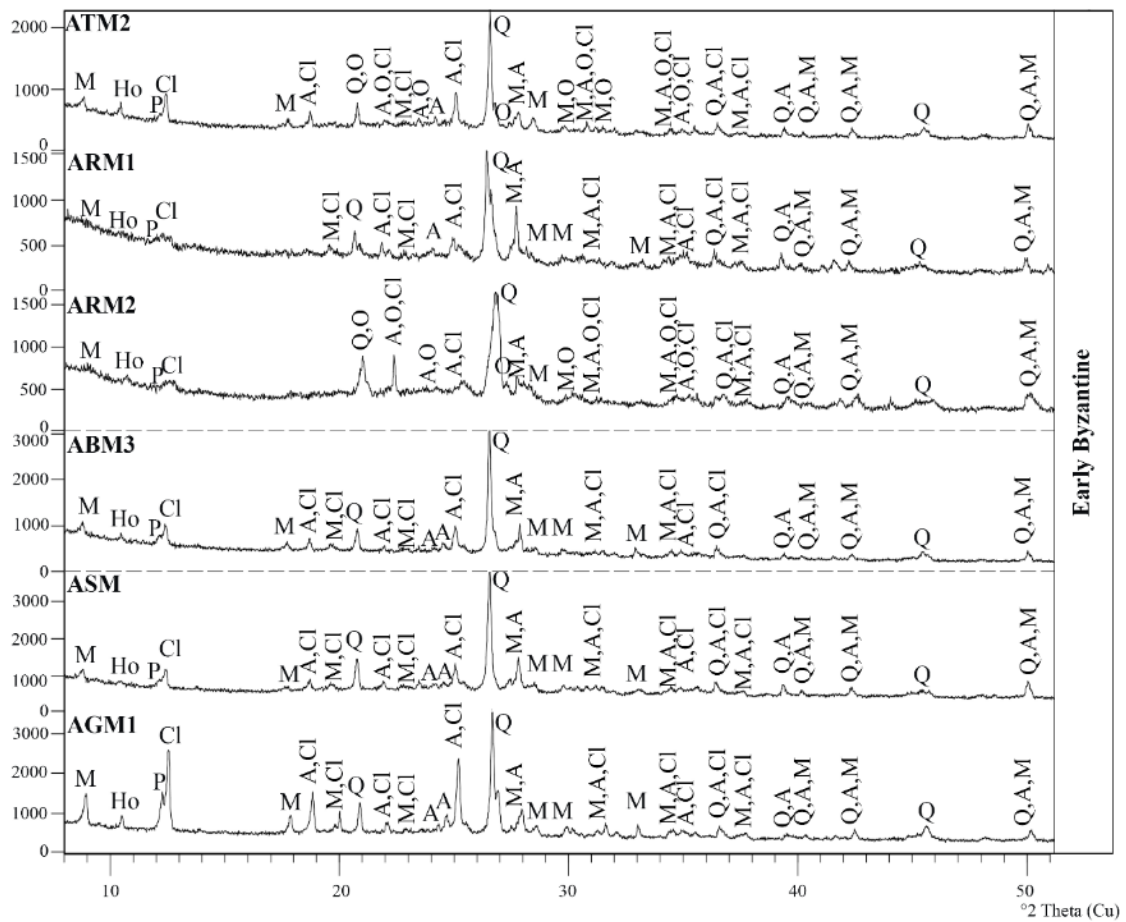


Figure 5.12. XRD patterns of natural aggregates in lime mortars from Ayasuluk (A: Albite 76-1819, Cl: Clinocllore 79-1270, Ho: Hornblende 71-1060, M: Muscovite 84-1302, O: Orthoclase 31-0966, P: Phillipsite 39-1375, Q: Quartz 85-0798)

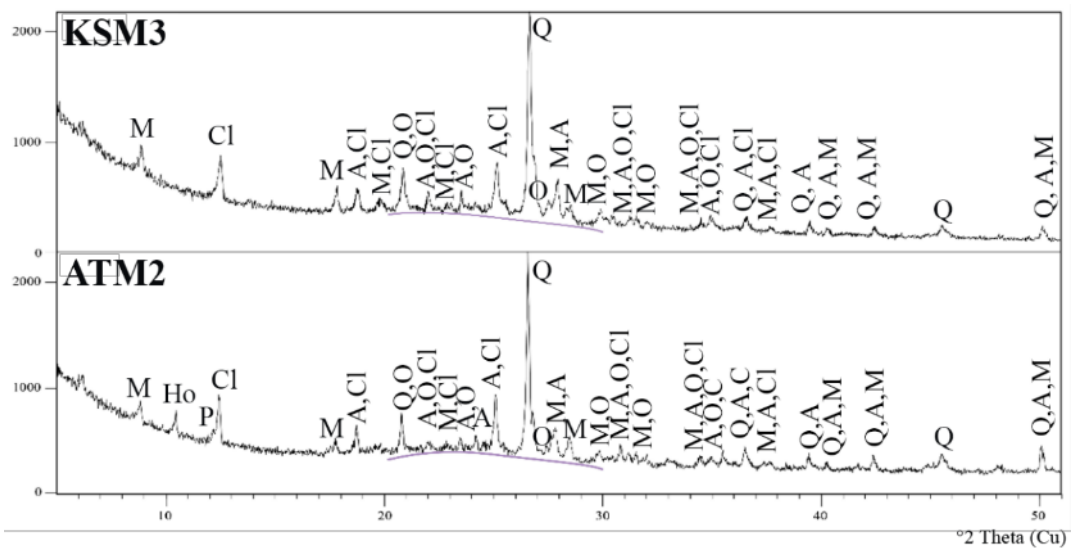


Figure 5.13. The existence of amorphous silicates with a diffuse band between the 20–30 $^{\circ}2\theta$ in XRD pattern

SEM images demonstrated that mostly natural aggregates had angular forms and a non-porous microstructure (Figure 5.14, 5.15). The angularity provided higher surface area, and enhanced the interlocking between binder and the aggregate (McGennis et al. 1995; McCarthy and Dyer 2019). (Figure 5.15).

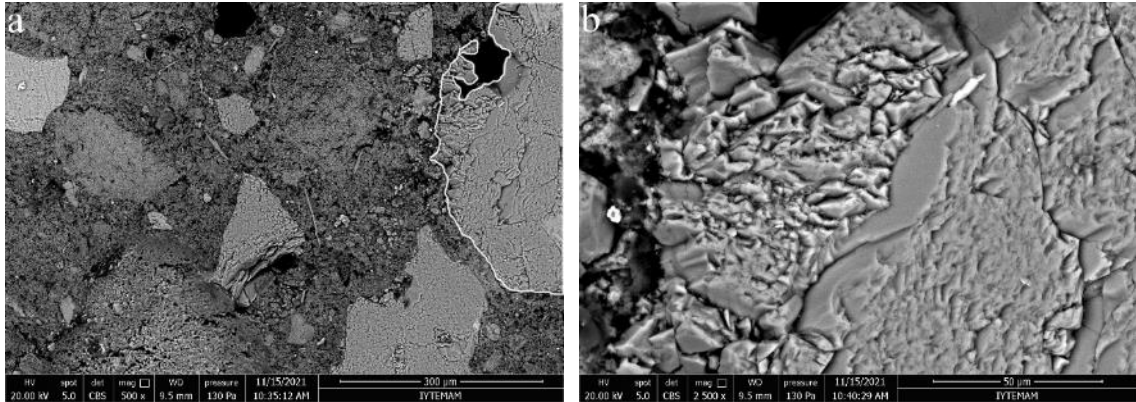


Figure 5.14. SEM images showing the angular forms of natural aggregates within the mortar matrix from Kadikalesi (Anaia) (a: KNM2 x500, b: KNM2 x2500)

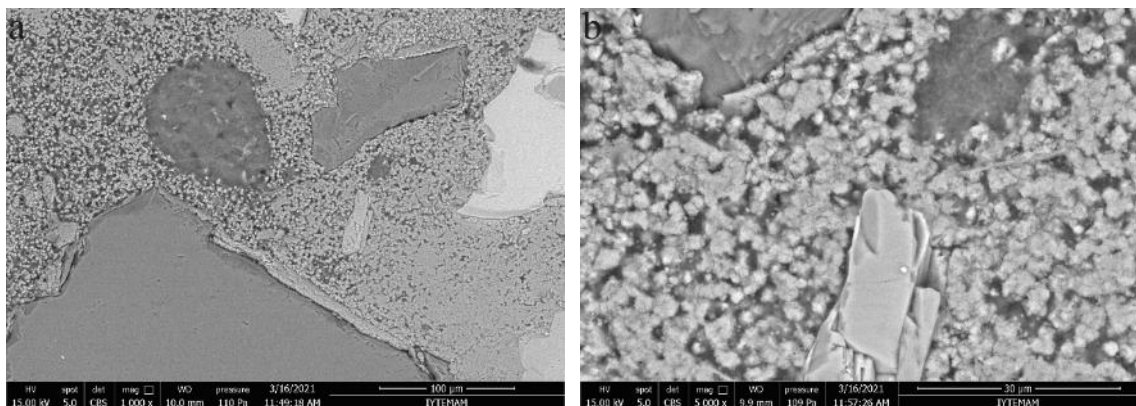
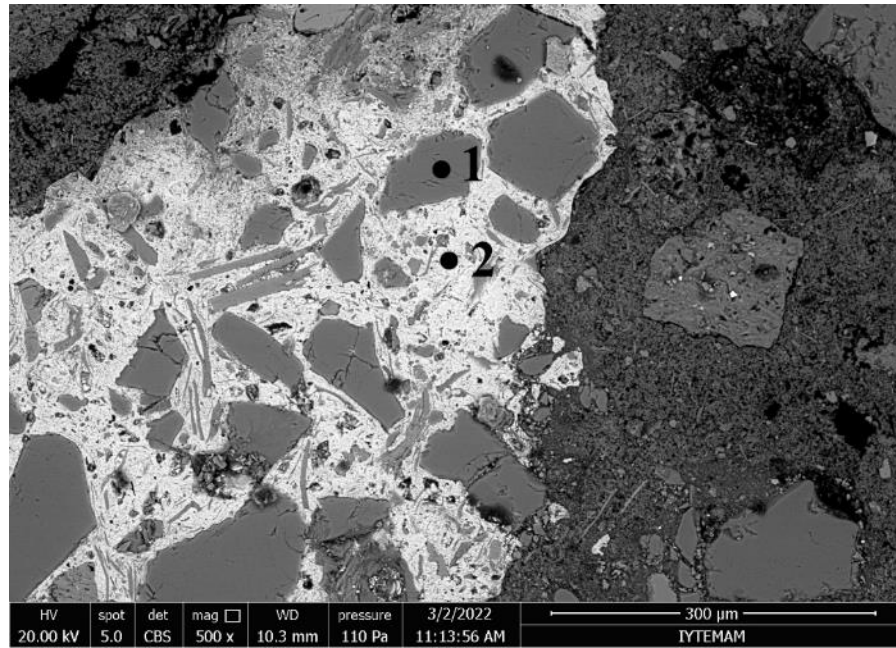


Figure 5.15. Less porous structure of the natural aggregates and strong adhesion between binder and the aggregate from Ayasuluk (a: ATM2 x1000, b: ATM2 x5000)

In the SEM images, the breccia fragments were also observed. The clasts in the angular forms were composed of mainly SiO_2 (91.05 %), while the matrix was consisted of mostly Fe_2O_3 (71.63 %) and moderate amount of SiO_2 (18.88 %) (Figure 5.16).



Chemical Composition (%)								
	Na ₂ O	MgO	Al ₂ O ₃	SiO ₂	K ₂ O	CaO	TiO ₂	Fe ₂ O ₃
1	0.06	0.25	0.78	91.05	0.21	2.32	0.00	5.33
2	0.25	1.21	4.16	18.88	0.55	3.21	0.11	71.63

Figure 5.16. SEM image and EDS analysis of breccia in lime mortar (KNM3) from Kadikalesi (Anaia)

5.4.2. Characteristics of Fine Brick Aggregates

Brick aggregates used in Kadikalesi (Anaia) were mainly comprised of large amounts of SiO₂ (66.12–78.15 %), moderate amounts of Al₂O₃ (10.41–16.76 %), and smaller amounts of Fe₂O₃ (4.04–7.83 %), MgO (1.35–3.07 %), K₂O (2.13–3.76 %), Na₂O (0.49–0.99 %), CaO (0.83–4.10 %) and TiO₂ (0.58–1.03 %) (Table 5.12). Likewise, brick aggregates of lime mortars and plasters from Ayasuluk were primarily composed of large amounts of SiO₂ (59.19–81.62 %), moderate amounts of Al₂O₃ (6.78–17.14 %), Fe₂O₃ (5.53–9.92 %) and smaller amounts of MgO (3.68–7.98 %), K₂O (0.90–2.82 %), Na₂O (0.20–0.85 %), CaO (0.71–2.12 %) and TiO₂ (0.58–1.54 %) (Table 5.12). Results of SEM-EDS analyses indicated that all brick aggregates were produced from Ca-poor clays (Table 5.12).

The chemical compositions of brick aggregates do not differ according to the periods or locations in both sites except the multi-layered plasters. It was determined that

of aggregates outer plaster layers KCP2 and ASP2 had larger amounts of Fe_2O_3 (7.83 and 9.97%) than inner layers KCP1 and ASP1 (4.04 and 7.29%) (Figure 5.17).

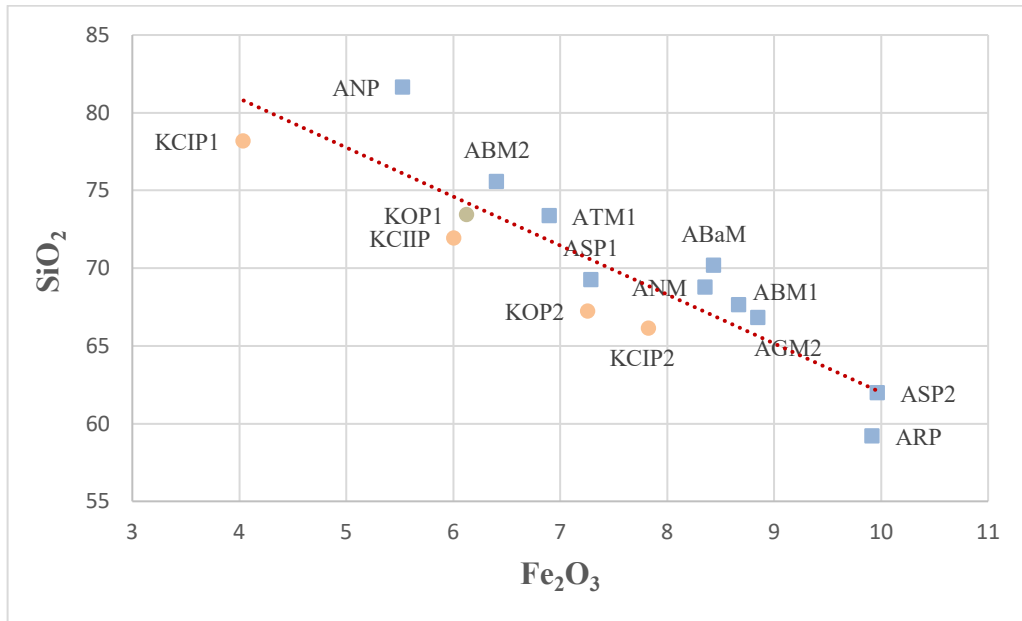


Figure 5.17. SiO_2 and Fe_2O_3 contents of brick aggregates

Among the major oxides Fe_2O_3 , MgO , and Al_2O_3 were determined as distinctive oxides in grouping the brick aggregates according to the sites (Figure 5.18). Brick aggregates of Ayasuluk were richer in MgO (3.7–8.0%) and Fe_2O_3 (5.5–9.9%), and poorer in Al_2O_3 (6.8–17.1 %) on average, while the brick aggregates of Kadikalesi (Anaia) were richer in Al_2O_3 (10.4–16.8 %), and poorer in MgO (1.6–3.1%) and Fe_2O_3 (6.0–7.8%) (Figure 5.18) (Table 5.12). The ternary diagram depicted this clear distinction between brick aggregates from Kadikalesi (Anaia) and Ayasuluk (Figure 5.18). This distinction may indicate that different clay sources were used for the production of brick aggregates in two sites over centuries. The use of local sources for bricks and brick aggregates was probably a common practice in the Byzantine period, which has also been reported by different studies (Baronio, Binda, and Lombardini 1997; Binda, Baronio, and Tedeschi 1999; Aslan Özkaya 2005; Stefanidou et al. 2014; Ulukaya et al. 2017; Taranto et al. 2019; Pérez-Monserrat et al. 2022).

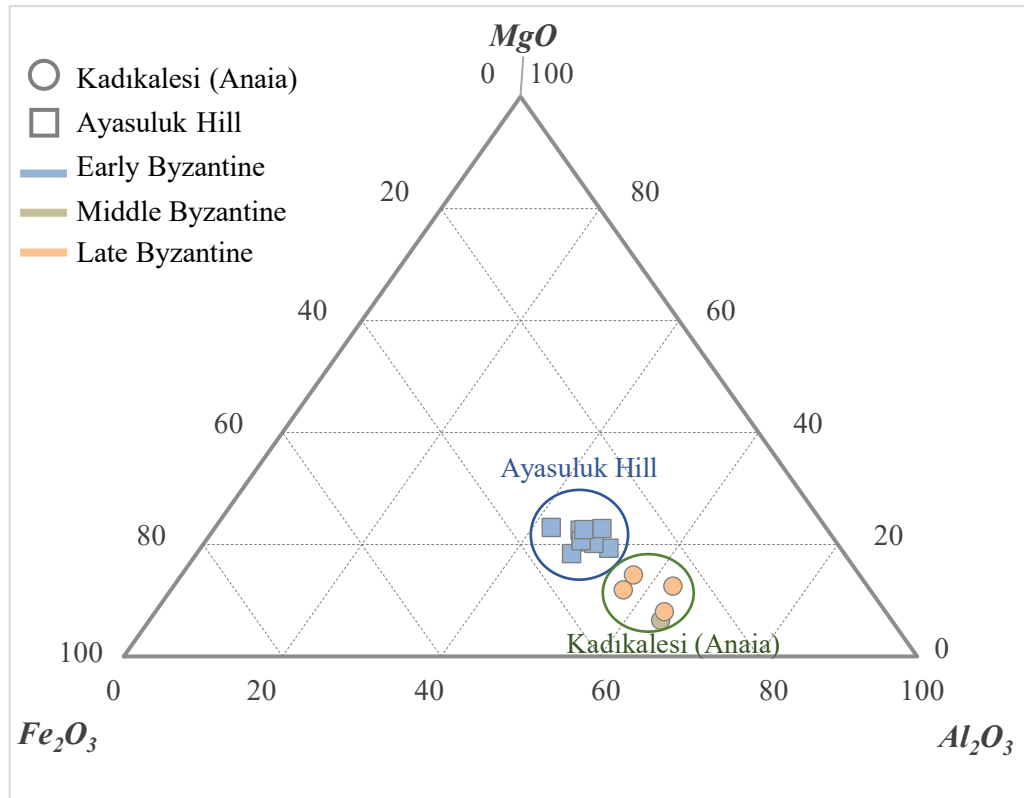


Figure 5.18. Ternary plot showed the Fe_2O_3 - MgO - Al_2O_3 compositions of brick aggregates

Chemical compositions of brick aggregates were also used to estimate the requirements for the pozzolans according to ASTM C618-03 standard (ASTM C618-03 2003), where the sum of SiO_2 , Al_2O_3 , and Fe_2O_3 should be greater than 70 %. The sum of SiO_2 , Al_2O_3 , and Fe_2O_3 was calculated between 91.22–93.14 % for brick aggregates of Kadikalesi (Anaia) samples, and between 86.25–93.93 % for brick aggregates of Ayasuluk samples (Table 5.12).

In addition to this, electrical conductivity differences before and after the addition of brick aggregates into saturated calcium hydroxide solution was measured between 5.68–7.85 mS/cm in Kadikalesi (Anaia) samples and between 5.07–8.00 mS/cm in Ayasuluk samples (Table 5.12). Similar electrical conductivity differences were determined in Kadikalesi (Anaia) and Ayasuluk samples, and these differences did not vary according to the belonged periods or locations.

The results obtained both by the ASTM C618-03 standard and the electrical conductivity method were found to be compatible and demonstrated that all brick aggregates in lime plasters or mortars from Kadikalesi (Anaia) and Ayasuluk possessed

highly reactive pozzolanicity. Pozzolanic properties of brick aggregates can be associated with high clay content of their raw materials and low firing temperatures ($< 900\text{ }^{\circ}\text{C}$) during their production (Baronio and Binda 1997; Böke, Akkurt, and İpekoğlu 2004).

Similar results were obtained for brick aggregates of Serapis Temple, Pergamon (Aslan Özkaya 2005), San Michele in Africisco (Baronio, Binda, and Lombardini 1997), a Middle Byzantine Chapel in İstanbul (Ulukaya et al. 2017) and Early Byzantine Church in Southwest Anatolia (Caner and Güney 2018) (Table 5.13).

Table 5.12. Chemical compositions and pozzolanic activities of the brick aggregates in Kadıkalesi (Anaia) and Ayasuluk

Period	Sample	Location	Func.	Chemical Compositions (%)								Pozzolanic Activity	
				Na ₂ O	MgO	Al ₂ O ₃	SiO ₂	K ₂ O	CaO	TiO ₂	Fe ₂ O ₃	Electrical Conductivity Difference (mS/cm)	SiO ₂ + Al ₂ O ₃ + Fe ₂ O ₃ (%)
Early Byzantine	ARP	Treasure Room Wall	Plaster	0.66	7.98	17.14	59.19	2.82	1.54	0.74	9.92	5.76	86.25
	ABaM	Baptistery Wall	Mortar	0.36	4.49	11.62	70.17	1.82	2.12	0.99	8.44	8.00	90.23
	ATM1	Transept Wall	Mortar	0.68	4.51	10.25	73.36	1.27	1.82	1.20	6.90	7.66	90.51
	ABM1	Bema Buttress	Mortar	0.85	5.58	12.84	67.61	1.90	1.56	1.00	8.67	5.07	89.12
	ABM2	Bema Buttress	Mortar	0.20	4.74	9.79	75.55	1.29	1.14	0.88	6.41	7.30	91.75
	ANM	Naos Buttress	Mortar	0.46	6.03	12.43	68.75	1.77	1.35	0.85	8.36	7.96	89.54
	ANP	Naos Buttress	Plaster	0.20	3.68	6.78	81.62	0.90	0.71	0.58	5.53	7.65	93.93
	ASP1	Substructure Wall	Plaster	0.51	4.82	12.91	69.24	2.04	1.65	1.54	7.29	7.65	89.44
	ASP2	Substructure Wall	Plaster	0.55	6.58	16.06	61.96	2.47	1.51	0.92	9.97	Not determined	87.99
Middle Byz.	AGM2	Gate of Persecution Buttress	Mortar	0.25	6.00	14.06	66.79	1.71	1.37	0.98	8.85	7.45	89.70
	KOP1	Outer Narthex Wall	Plaster	0.99	1.35	13.60	73.41	2.89	0.83	0.80	6.13	7.57	93.14
Late Byz.	KOP2	Outer Narthex Wall	Plaster	0.99	2.08	16.76	67.20	3.76	1.23	0.73	7.26	5.68	91.22
	KCP1	Cistern I Wall	Plaster	0.52	2.07	10.41	78.15	2.13	2.09	0.58	4.04	7.69	92.60
	KCP2	Cistern I Wall	Plaster	0.49	2.98	14.40	66.12	3.04	4.10	1.03	7.83	7.85	88.35
	KCP3	Cistern II Wall	Plaster	0.47	3.07	12.06	71.90	2.60	2.96	0.93	6.01	7.85	89.97

Table 5.13. Comparison of chemical compositions of brick aggregates with the literature

Area & Reference	Period	Chemical Compositions								Pozzolanic Activity	
		Na ₂ O	MgO	Al ₂ O ₃	SiO ₂	K ₂ O	CaO	TiO ₂	Fe ₂ O ₃	Electrical Conductivity Differences (mS/cm)	SiO ₂ +Al ₂ O ₃ +Fe ₂ O ₃ (%)
San Michele in Africisco (Baronio, Binda, and Lombardini 1997)	Early Byzantine (6 th century)	0.58	1.00	7.48-Fe ₂ O ₃	40.83	1.25	26.45	-	7.48-Al ₂ O ₃	-	-
Serapis Temple/ Kızıl Avlu (Aslan Özkaya 2005)	Early Byzantine	0.00	1.6–2.0	6.7–7.7	50.5–53.7	0.9	1.1–1.3	0.00	3.9–6.1	3.23-5.90	-
Early Byzantine Church in Southwest Anatolia (Caner and Güney 2018)	Early Byzantine (5–7 th centuries)	-	-	-	-	-	-	-	-	3.1–5.7	-
Middle Byzantine Chapel in Istanbul (Ulukaya et al. 2017)	Middle Byzantine (11–12 th centuries)	1.1–1.3	2.4–2.7	14.0–14.4	48.4–49.5	2.0–2.3	23.1–23.9	0.00	7.7–8.2	-	-

Mineralogical compositions of the brick aggregates were determined by XRD analysis. All brick aggregates were mainly composed of quartz (SiO_2), albite ($\text{Na}(\text{AlSi}_3\text{O}_8)$), hematite (Fe_2O_3) and muscovite ($\text{KAl}_2(\text{Si}_3\text{Al})\text{O}_{10}(\text{OH},\text{F})_2$) (Figure 5.19, 5.20).

The firing temperatures of the brick aggregates can be estimated using the results of XRD analysis according to the existence of different mineral phases. At high firing temperatures ($>900^\circ\text{C}$), amorphous substances disappear; high temperature minerals like mullite ($\sim 1000^\circ\text{C}$), cristobalite ($\sim 1200^\circ\text{C}$) and wollastonite ($\sim 900\text{--}1050^\circ\text{C}$) are formed; and pozzolanic activities are lost (Lee and Moon 2004, Cardiano et al. 2004). Therefore, the absence of these high temperature minerals and the pozzolanic character of aggregates indicated that the firing temperature did not exceed $\sim 900^\circ\text{C}$. Also, presence of albite appearing nearly at 800°C , and hematite forming at nearly 850°C , shows the minimum firing temperature of brick aggregates (Lee, Kim, and Moon 1999; Cardiano et al. 2004; Tekin and Kurugöl 2011). Existence of albite and/or hematite and absence of high-temperature minerals demonstrated that brick aggregates from Kadıkalesi (Anaia) and Ayasuluk were fired between $800\text{--}900^\circ\text{C}$ (Figure 5.19, 5.20). The low firing temperatures of bricks produced from clay-rich raw materials allowed the formation of pozzolanic amorphous substances. However, these amorphous substances could not be determined on the XRD patterns since their non-crystalline structure did not give indicative peaks.

In recent studies, high firing temperature minerals were also not detected in brick aggregates (Moropoulou, Bakolas, and Bisbikou 2000; Oğuz Kılıç et al. 2004; Aslan Özkaya 2005; Gürdal, Kahraman Altaş, and Acun Özgünler 2011; Acun Özgünler, Ersen, and Güleç 2013; Kahraman Altaş, Acun Özgünler, and Gürdal 2013; Ulukaya et al. 2017; Caner and Güney 2018) (Table 5.14). The fact that all samples were fired at low temperatures can be explained by the similar firing technology of the brick kilns of the Byzantine period.

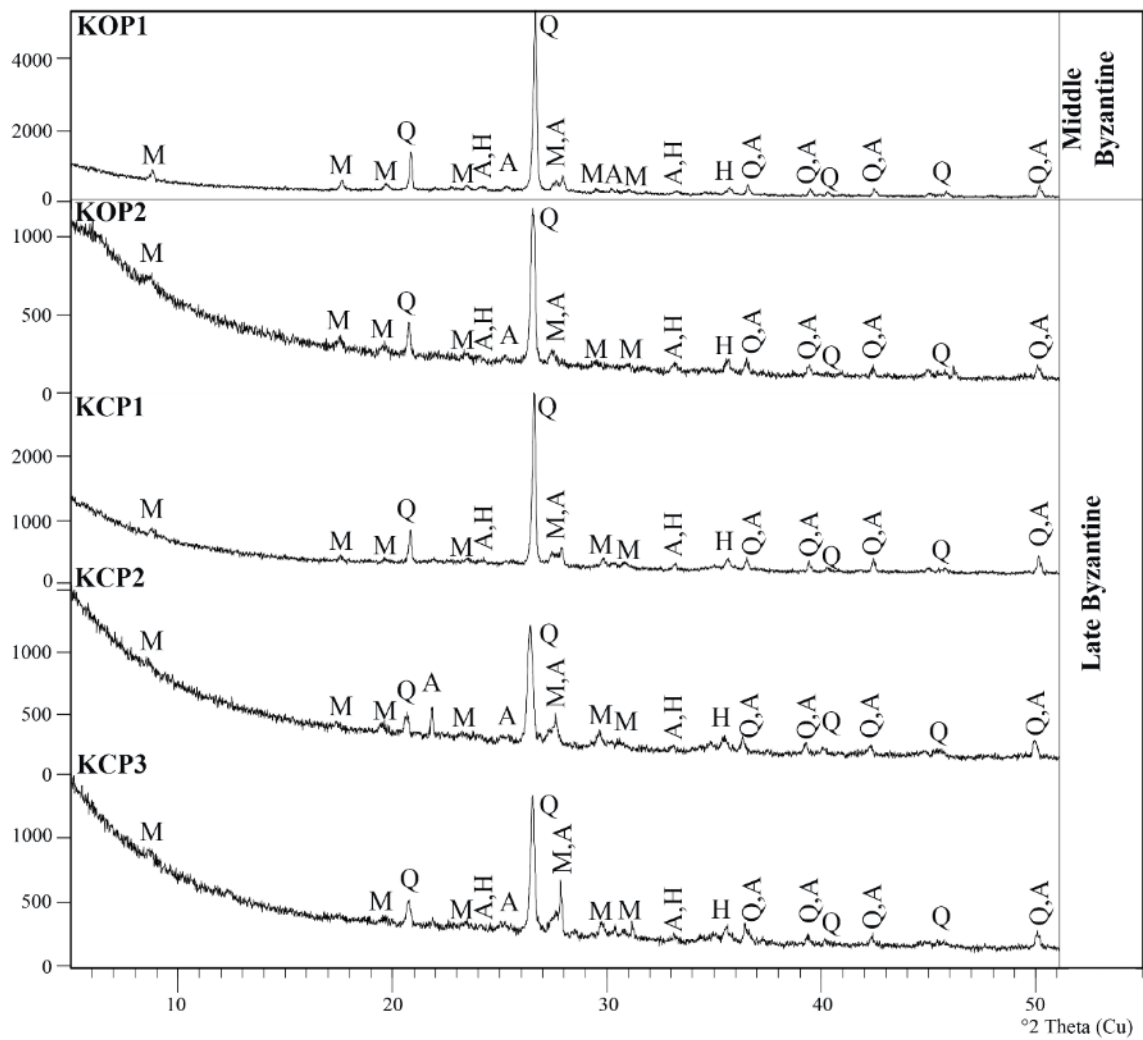


Figure 5.19. XRD patterns of brick aggregates in lime plasters from Kadıkalesi (Anaia)
 (A: Albite 84-0982, H: Hematite 87-1166, M: Muscovite 84-1302,
 Q: Quartz 85-0798)

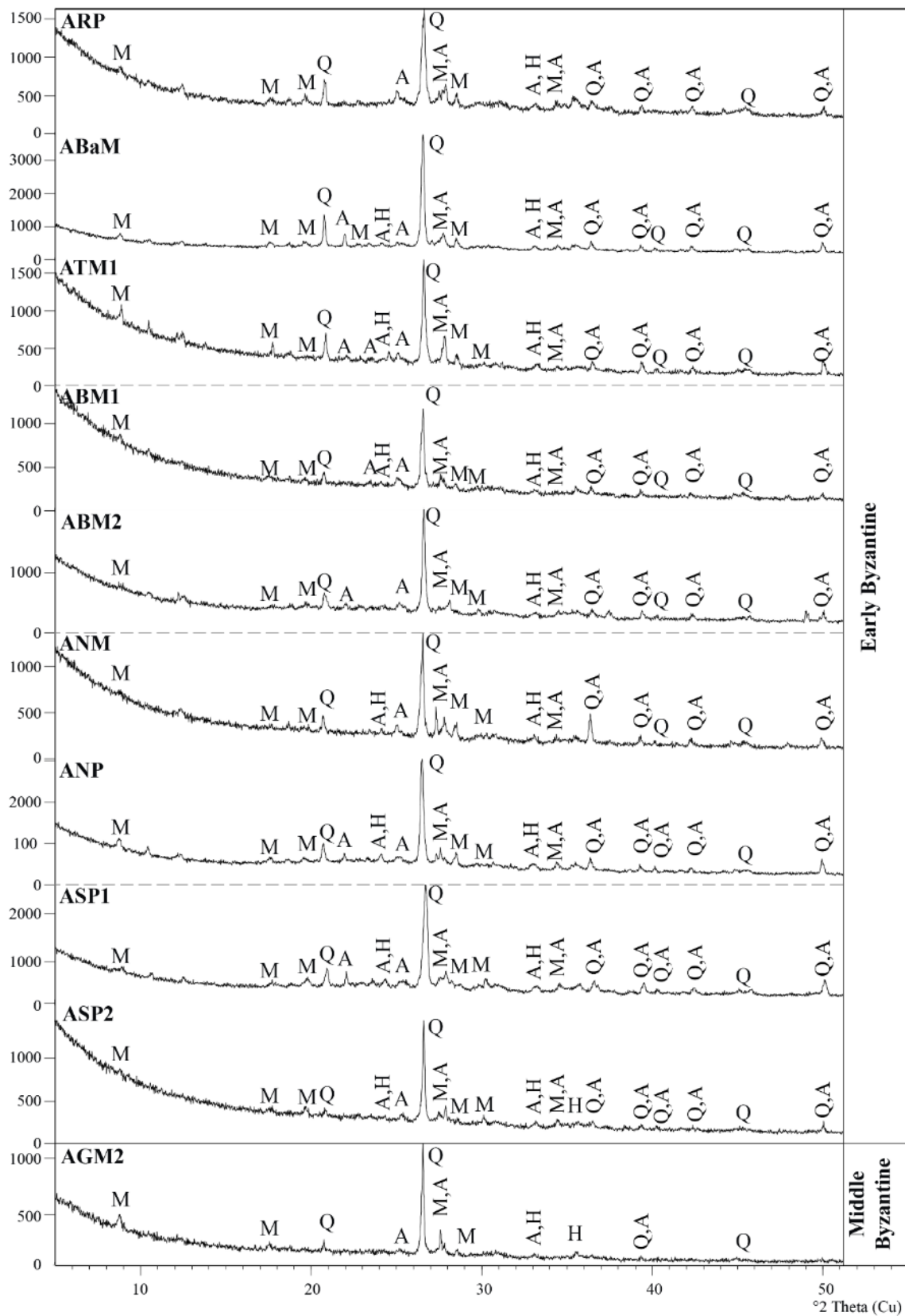


Figure 5.20. XRD patterns of brick aggregates in lime mortars and plasters from Ayasuluk (A: Albite 84-0982, H: Hematite 87-1166, M: Muscovite 84-1302, Q: Quartz 85-0798)

Table 5.14. Comparison of mineralogical compositions of brick aggregates with the literature

Area & Reference	Period	Mineralogical Compositions												
		Quartz	Calcite	Albite	Anorthite	Illite	Orthoclase	Muscovite	Hematite	Feldspar	Aragonite	Dolomite	Magnetite	
Serapis Temple/ Kızıl Avlu (Özkaya 2005)	Early Byzantine	+++		+++					++	+	+++			
Defense Structures in Istanbul (Kahraman Altaş, Acun Özgünler, and Gürdal 2013)	Early Byzantine	+++	+++											
Religious Buildings in Istanbul (Gürdal, Kahraman Altaş, and Acun Özgünler 2011)	Early Byzantine	+++	+++				+							
St. Jean Church in Manisa (Oğuz Kılıç et al. 2004)	Early Byzantine (6th century)	+++	+			+					+			
Early Byzantine Church in Southwest Anatolia (Caner, Güney 2018)	Early Byzantine (5–7 th centuries)	+++	+++	++		+								++
St. Katherines Hospice in Rhodes (Moropoulou, Bakolas, and Bisbikou 2000)	Early– Late Byzantine (6–14th centuries)	+++	+++						+					
Monuments in Kiev (Moropoulou et al. 2000)	Middle Byzantine (11–13 th centuries)	++	+++							+	++		++	
Middle Byzantine Chapel in Istanbul (Ulukaya et al. 2016)	Middle Byzantine (11–12 th centuries)	+++				++				++				

The porous structures of brick aggregates allowed the calcite crystals which were dissolved by the effect of the humidity to precipitate inside the pores, and so enhanced the durability to deterioration problems (Figure 5.22) (Uğurlu and Böke 2006; Uğurlu and Böke 2009).

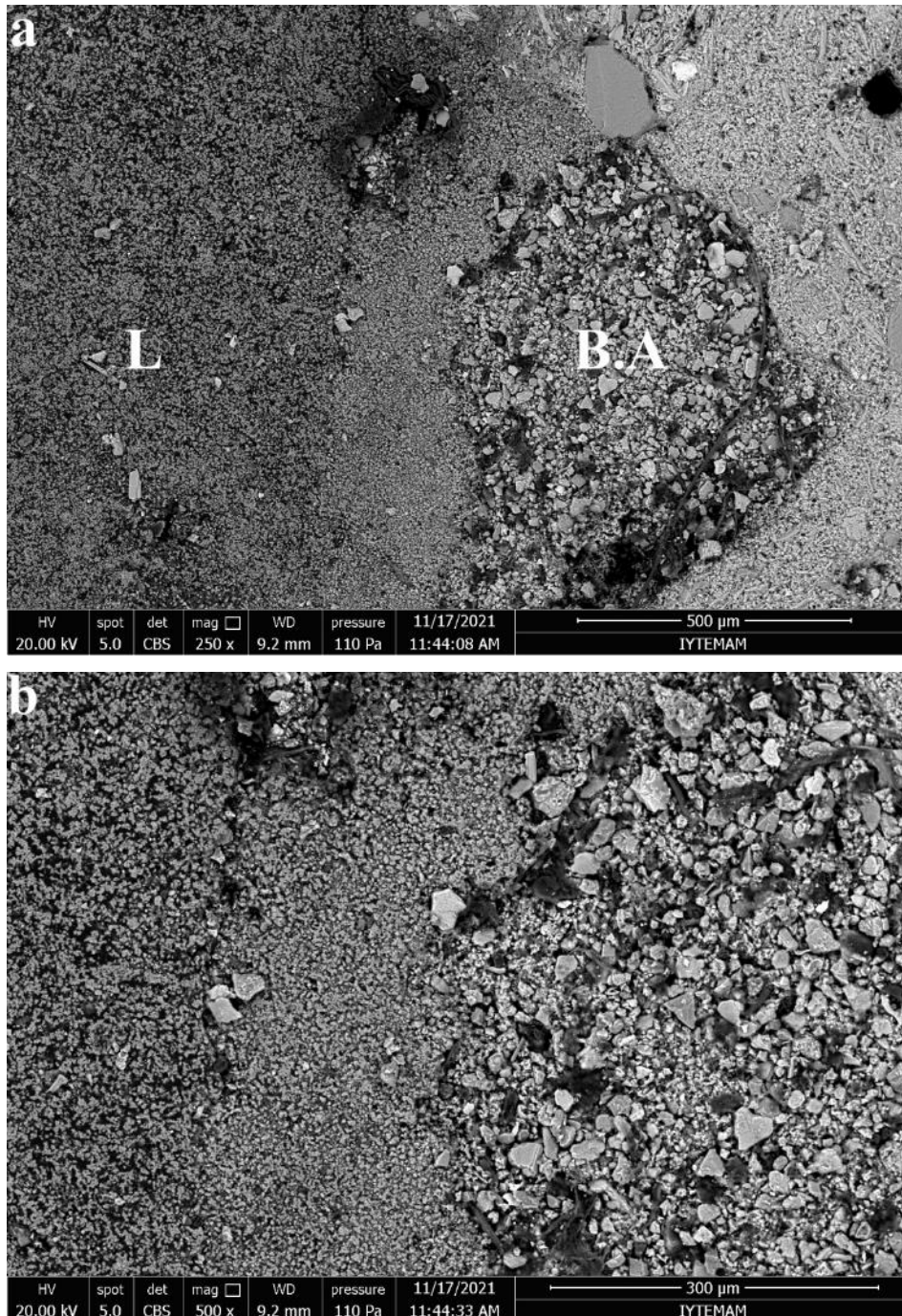


Figure 5.22. Precipitated calcite crystals in the pores of brick aggregate from Kadıkalesi (Anaia) (a: KOP1 x250, b: KOP1 x500; B.A: Brick aggregate, L: Lime lump)

Brick aggregates in lime mortars of Ayasuluk were comprised of clay layers showing no vitrification that indicated the brick aggregate fired at low temperatures (<950°C) (Figure 5.23) (Böke et al. 2006).

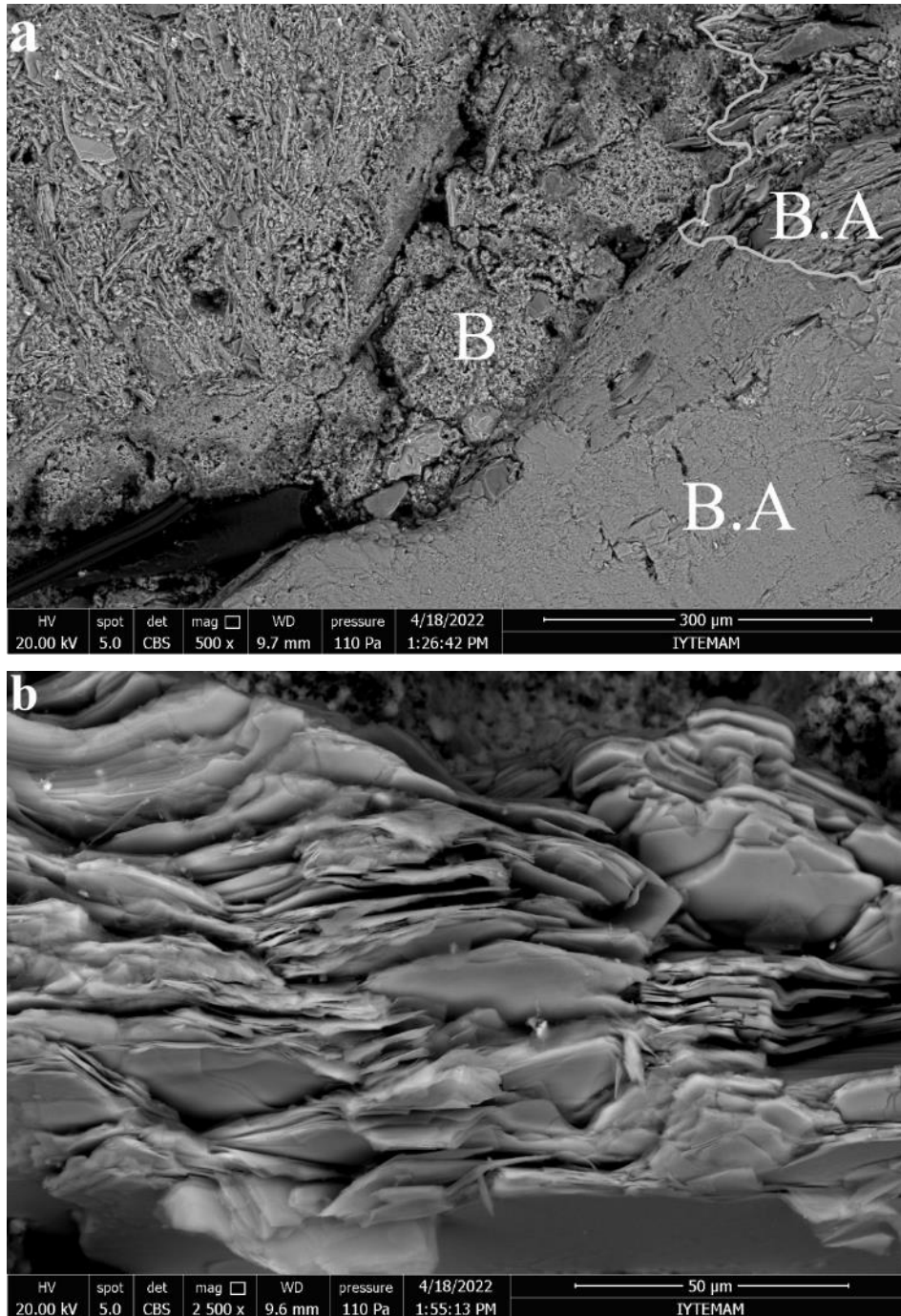


Figure 5.23. Clay layers of brick aggregates from Ayasuluk

(a: AGM2 x500, b: AGM2 x2500; B: Binder, B.A: Brick aggregate)

Hematite (Fe_2O_3) mineral which forms in Ca-poor clays at approximately 850°C were detected in the SEM images. EDS analysis performed on the bright areas of the SEM image demonstrated the high Fe_2O_3 (73.71%) content and confirmed the existence of hematite (Figure 5.24) (Table 5.15). This result also supported the XRD analysis (Figure 5.20). Therefore, the firing temperatures might around 850°C (Lee, Kim, and Moon 1999).

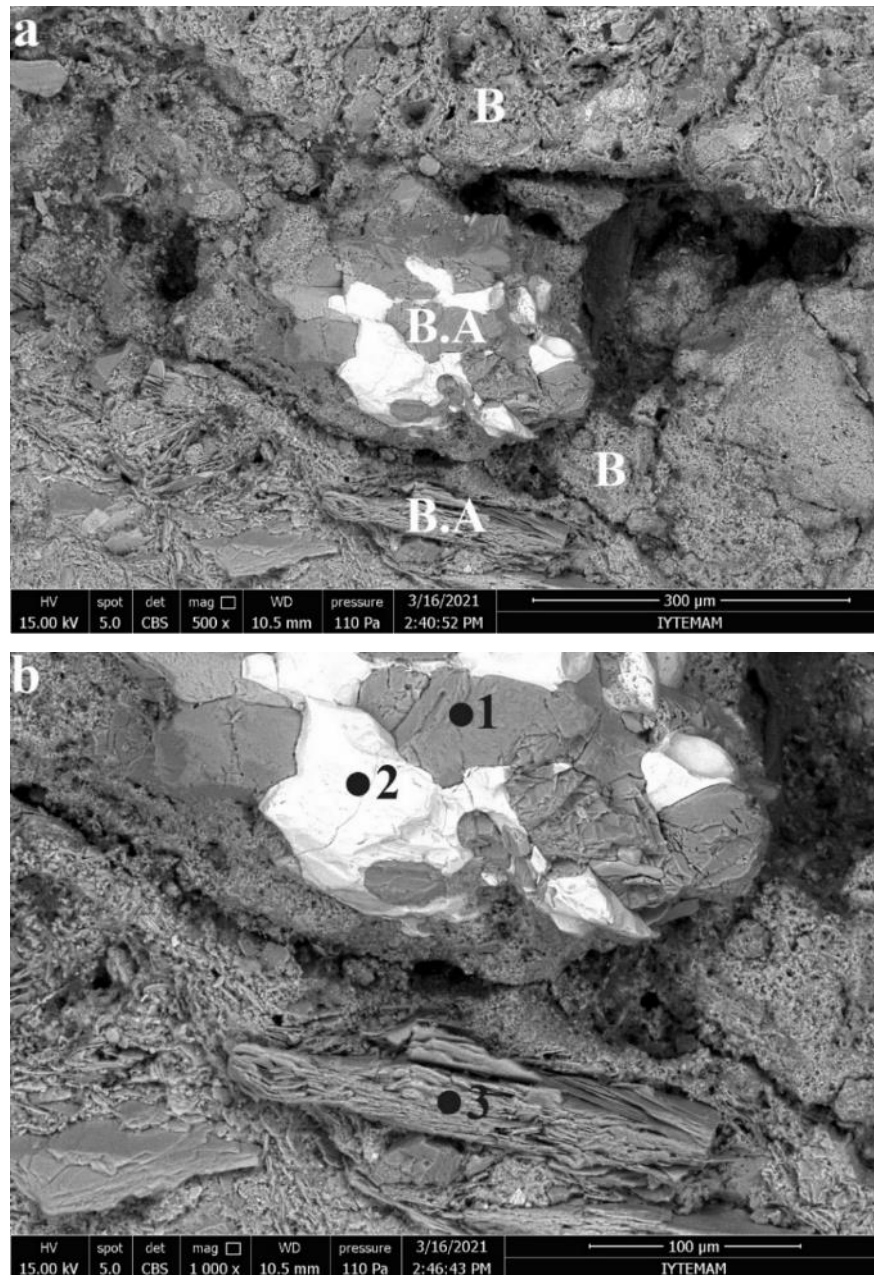


Figure 5.24. Hematite existence in the brick aggregates from Ayasuluk
(a: ABM1 x500, b: ABM1 x1000; B: Binder, B.A: Brick aggregate)

Table 5.15. Chemical composition of the brick aggregate in ABM matrix

	Na ₂ O	MgO	Al ₂ O ₃	SiO ₂	K ₂ O	CaO	TiO ₂	Fe ₂ O ₃
1	11.54	-	18.58	61.27	0.37	2.93	-	5.30
2	1.33	1.12	3.63	8.84	0.58	3.16	7.64	73.71
3	0.57	3.13	29.76	46.91	9.27	4.77	-	5.59

5.5. Characteristics of Lime Used as Binding Material

The white nodules with a few millimeters to 2 cm in the lime mortars and plasters were called as “white lumps” (Bakolas et al. 1995; Bruni et al. 1997). White lumps were considered to represent the lime used as binder and had same chemical and mineralogical composition with the raw material (Bakolas et al. 1995; Bruni et al. 1997; Barba et al. 2009). Therefore, the characteristics of the lime used in mortars and plasters were determined by examining the lime lumps in the samples (KNM2, KSM3, KNM3, ABaM, ATM2, ABM1).

The mineralogical compositions of lumps from Kadıkalesi (Anaia) and Ayasuluk were analyzed via XRD. On the XRD patterns, only sharp calcite peaks were detected indicating the carbonated lime (Figure 5.25).

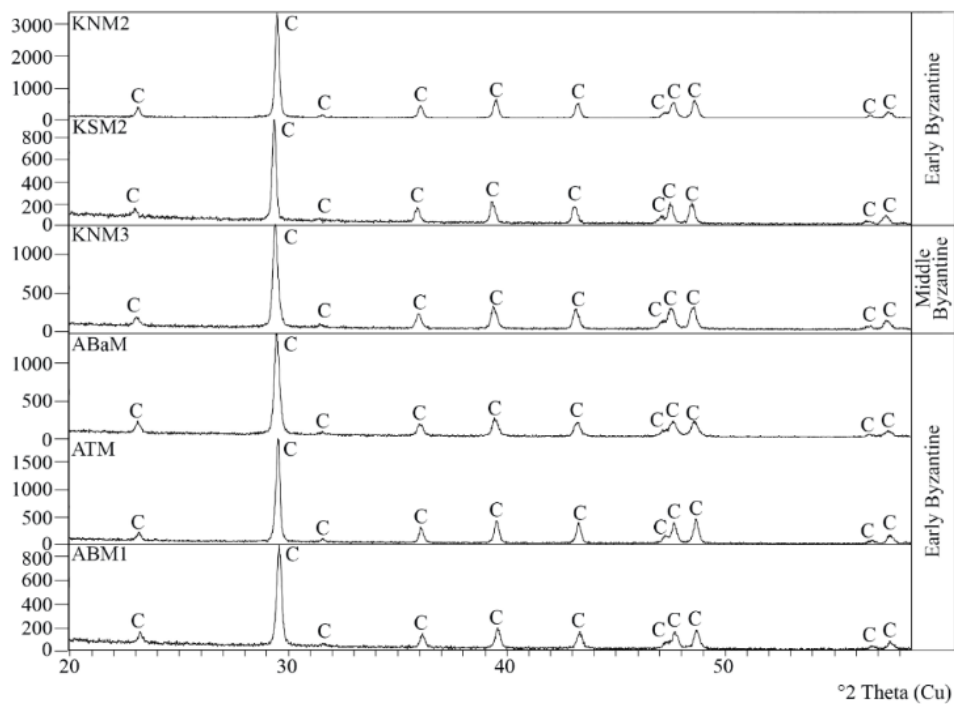


Figure 5.25. XRD patterns of lime lumps (C: Calcite 86-2334)

The chemical compositions of the lime lumps were determined via SEM-EDS analysis. In Ayasuluk samples, lime lumps were comprised of mainly CaO (95.93–98.61 %) and smaller amounts of SiO₂ (0.30–1.54 %), MgO (0.29–1.26 %), Na₂O (0.00–0.63 %), Al₂O₃ (0.52–0.62 %), K₂O (0.05–0.38 %), TiO₂ (0.00–0.27 %), Fe₂O₃ (0.00–0.11 %) (Table 5.16). Likewise, lime lumps from mortars of Kadikalesi (Anaia) were consisted of mainly CaO (97.17–98.16 %) and smaller amounts of SiO₂ (0.63–1.24 %), MgO (0.61–0.90 %), Na₂O (0.00–0.11 %), Al₂O₃ (0.37–0.62 %), K₂O (0.00–0.20 %), TiO₂ (0.00 %), Fe₂O₃ (0.00–0.03 %) (Table 5.16). The chemical compositions of the lumps of different period mortars were found to be similar to each other. The high content of CaO in the lumps showed that fat lime was used during the production of mortars and plasters (Cowper 1998).

Table 5.16. The chemical compositions (%), hydraulic (H.I.) and cementation indices (C.I.) of lime lumps

Sample	Period	Na ₂ O	MgO	Al ₂ O ₃	SiO ₂	K ₂ O	CaO	TiO ₂	Fe ₂ O ₃	H.I.	C.I.
KNM2	Early	0.00	0.61	0.37	0.77	0.07	98.16	0.00	0.03	0.01	0.03
	Byzantine										
KSM2	Early	0.11	0.90	0.53	0.63	0.20	97.62	0.00	0.00	0.01	0.02
	Byzantine										
KNM3	Middle	0.05	0.70	0.62	1.24	0.00	97.38	0.00	0.00	0.02	0.04
	Byzantine										
ABaM	Early	0.00	1.26	0.62	1.54	0.38	95.93	0.27	0.00	0.02	0.05
	Byzantine										
ATM1	Early	0.02	0.29	0.52	0.30	0.05	98.61	0.10	0.11	0.01	0.02
	Byzantine										
ABM1	Early	0.63	0.49	0.52	1.48	0.27	96.59	0.00	0.03	0.02	0.05
	Byzantine										

Chemical compositions of lime lumps were used to calculate their hydraulic indices (HI) (4.1) and cementation indices (CI) (4.2) according to Boynton formula (Eckel 1905; Boynton 1966). Hydraulic index values lower than 0.1, and cementation index values lower than 0.3 demonstrate non-hydraulic character of lime (Eckel 1905; Boynton 1966).

$$\text{H.I.} = (\% \text{Al}_2\text{O}_3 + \% \text{Fe}_2\text{O}_3 + \% \text{SiO}_2) / (\% \text{CaO} + \% \text{MgO}) \quad (4.1)$$

$$\text{C.I.} = (2.8 \% \text{SiO}_2 + 1.1 \% \text{Al}_2\text{O}_3 + 0.7 \% \text{Fe}_2\text{O}_3) / (\% \text{CaO} + 1.4 \% \text{MgO}) \quad (4.2)$$

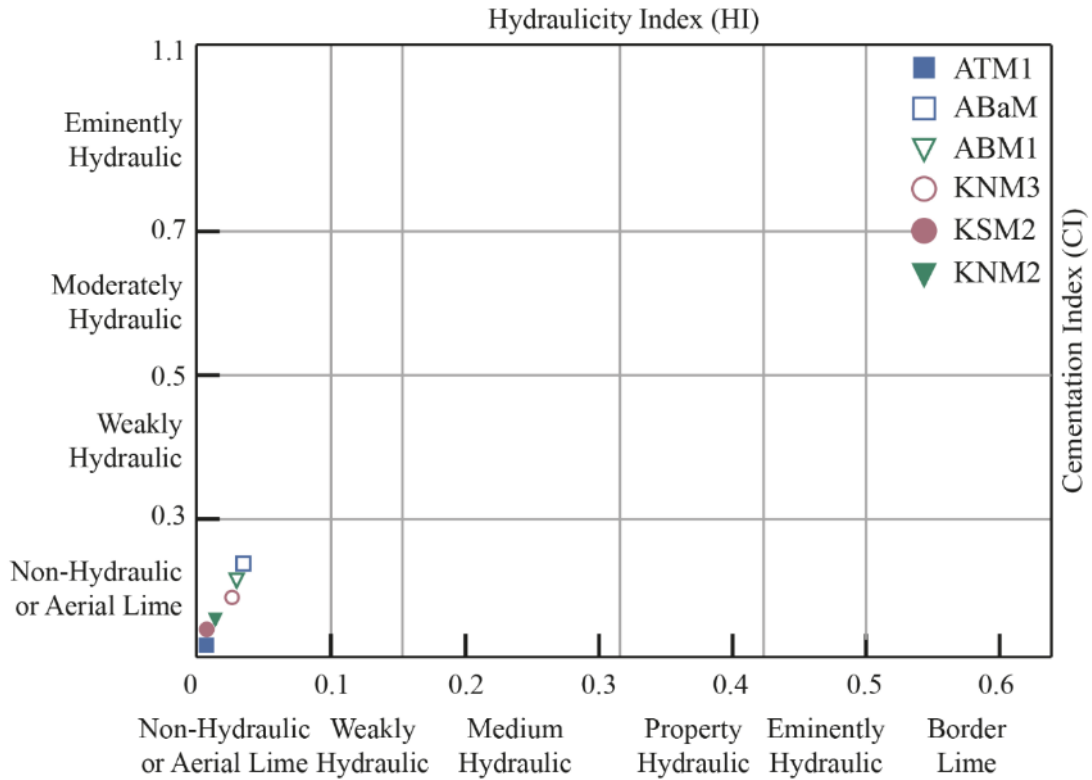


Figure 5.26. The hydraulicity ranges of the lime lumps

In Kadıkalesi (Anaia) samples, hydraulicity and cementation indices of the lime lumps were between 0.01–0.02 and 0.03–0.04, respectively (Table 5.16, Figure 5.26). Similarly, the lime lumps from Ayasuluk, the hydraulicity indices were between 0.01–0.02 and cementation indices were between 0.02–0.05 (Table 5.16, Figure 5.26). These results showed that all the lime lumps, which represented lime used as a binder, could be classified as non-hydraulic and fat lime.

Likewise, in Middle Byzantine Chapel in İstanbul, the mineralogical composition of lime lumps showed only calcite peaks (Ulukaya et al. 2017). The chemical compositions of lime lumps in Byzantine buildings in Kyme were mainly CaO (91.52–95.82 %) and smaller amounts of SiO₂ (0.68–3.47 %), MgO (0.89–1.16 %), Na₂O (0.20–1.09 %), Al₂O₃ (0.41–1.51 %), K₂O (0.00–0.24 %), TiO₂ (0.09–0.27 %), Fe₂O₃ (0.22–0.62 %) exhibiting hydraulic indices between 0.01–0.06 and cementation indices between 0.03–0.10 (Miriello et al. 2011). The lime mortars from Middle Byzantine Chapel and

Byzantine buildings in Kyme revealed that they were produced using non-hydraulic lime as determined in Kadıkalesi (Anaia) and Ayasuluk lime mortars.

SEM images demonstrated that lime lumps were consisted of small sized ($<5\mu\text{m}$) micritic calcite crystals (Figure 5.27, 5.28). These calcite crystals may be pointing out that the lime had been used after a long aging (Zamba et al. 2007). Since ancient times, it had been recommended to use aged lime for preparing lime mortars and plasters to increase the plasticity and carbonation rate of lime (Vitruvius 1960; Rodriguez-Navarro, Hansen, and Ginell 1998). SEM images of calcite crystals revealed that this ancient knowledge was transferred for centuries and also used by the Byzantine masters.

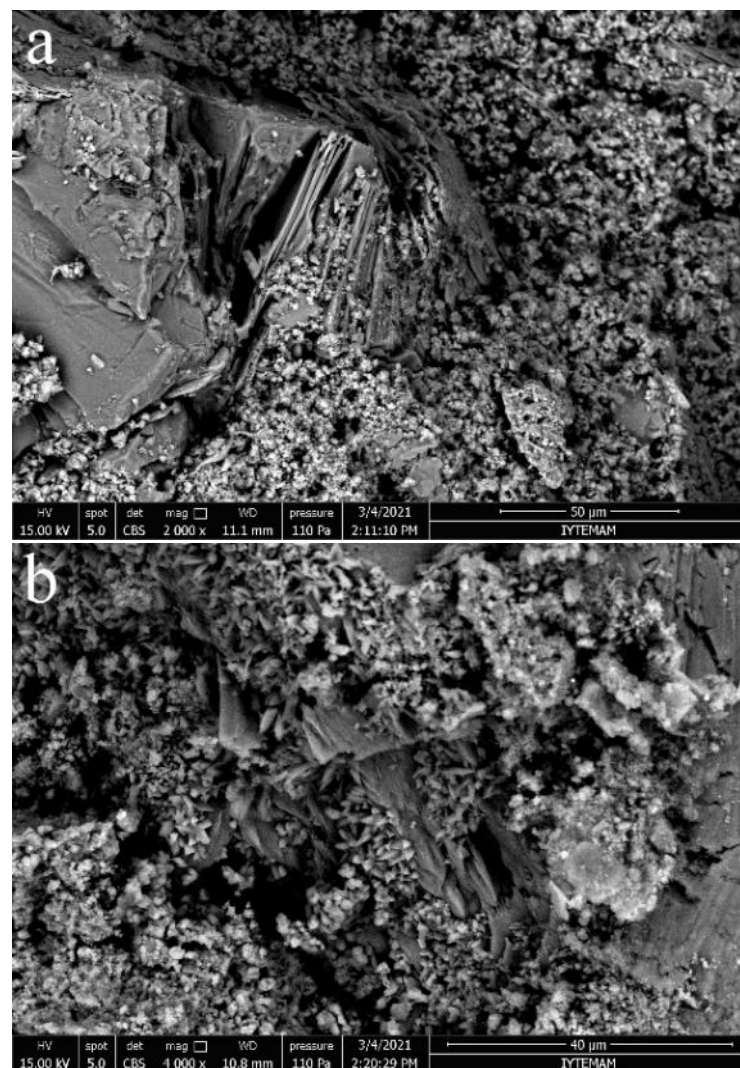


Figure 5.27. SEM images of lime lumps from Ayasuluk
(a: AGM1 x2000, b: AGM2 x4000)

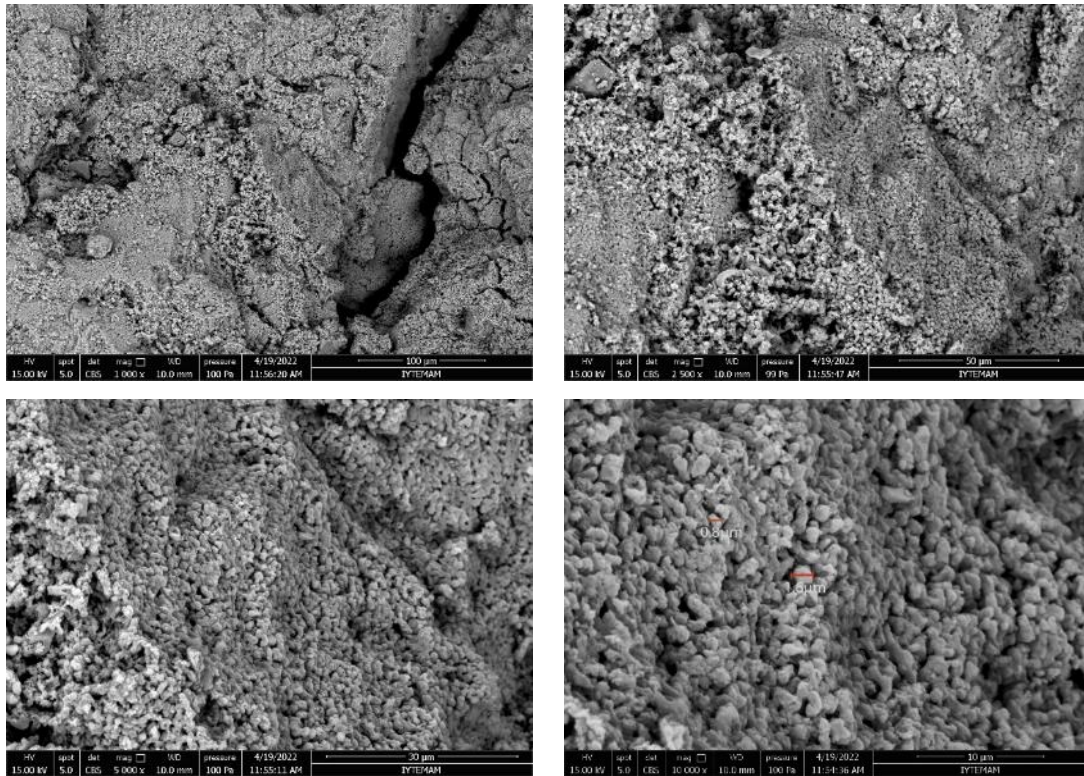


Figure 5.28. SEM images of lime lumps from Kadıkalesi (Anaia)

(a: KSM2 x1000, b: KSM2 x2500, c: KSM2 x5000, d: KSM2 x10000)

5.6. Characteristics of Binders

Fine mortar and plaster matrices comprised of carbonated lime (CaCO_3) and small grain-sized aggregates were defined as “binder” (Bakolas et al. 1995; Middendorf et al. 2005). The hydraulic characteristics and high strength of the mortars and plasters were considered to be mainly achieved by binders (Bakolas et al. 1995; Middendorf et al. 2005).

Chemical compositions of binders and microstructural properties of polished section of samples were determined by SEM-EDS analysis. Mineralogical compositions of binders were specified via XRD.

Weight losses of the binder parts of mortars and plasters (<53 micron) at between 200–600°C and 600–900°C were measured by thermogravimetric analysis (TGA) to define the hydraulic properties of the binders. When the temperature is between 200–600°C, structurally bound water (H_2O) of hydraulic products releases; and decomposition of carbonated lime releases carbon dioxide (CO_2) at 600–900°C (Moropoulou, Bakolas,

and Bisbikou 1995; Bakolas et al. 1998, 1995). Lime mortars and plasters are considered as hydraulic, if the ratio of the percent of weight losses due to $\text{CO}_2/\text{H}_2\text{O}$ ratio is less than 10 (Moropoulou, Bakolas, and Anagnostopoulou 2005).

5.6.1. Characteristics of Binders with Natural Aggregates

SEM-EDS analysis demonstrated that binders with natural aggregates from Kadıkalesi (Anaia) were comprised of large amounts of CaO (66.95–87.24 %), moderate amounts of SiO_2 (6.85–20.25 %), and smaller amounts of Al_2O_3 (2.19–6.41 %), MgO (1.40–3.65 %), Fe_2O_3 (0.72–2.97 %), K_2O (0.37–1.30 %), Na_2O (0.00–0.46 %), TiO_2 (0.00–0.49 %) (Table 5.17).

Ayasuluk binders with natural aggregates were consisted of large amounts of CaO (37.43–62.95%), SiO_2 (18.43–33.80 %), moderate amounts of Al_2O_3 (7.06–10.74 %), MgO (3.38–9.36 %), and smaller amounts of Fe_2O_3 (2.96–6.10 %), K_2O (1.24–4.62 %), Na_2O (0.45–2.49 %), TiO_2 (0.18–0.82 %) (Table 5.17).

Mortars from transept, bema, substructure and gate of persecution (ASM, AGM1, ABM3, ATM2) had lower CaO+ MgO content (37.43–50.60%); however, mortars from treasure room (ARM1, ARM2) and all the Kadıkalesi samples (KBaM1, KBaM2, KSM1, KSM2, KSM3, KNM1, KNM2, KNM3, KNM4) had higher CaO+ MgO content (61.45–87.24%) (Table 5.17, Figure 5.29). The differentiation between the Ayasuluk and Kadıkalesi (Anaia) in terms of CaO+ MgO might be due to the limestone or dolostone aggregates which specified in SEM images of Kadıkalesi (Anaia) (Figure 5.29, 5.36), and the difference of Al_2O_3 + Fe_2O_3 may be caused by the pozzolans in the matrix. Higher amount of SiO_2 , Al_2O_3 and Fe_2O_3 content in Ayasuluk binder may be due to the hydraulic reactions as well as the presence of pozzolanic aggregates (Figure 5.29).

Table 5.17. Chemical compositions of the binders with natural aggregates in Kadikalesi (Anaia) and Ayasuluk

Period	Sample	Location	Func.	Chemical Compositions (%)								Hydraulic Properties			
				Na ₂ O	MgO	Al ₂ O ₃	SiO ₂	K ₂ O	CaO	TiO ₂	Fe ₂ O ₃	200-600°C H ₂ O	600-900°C CO ₂	$\frac{CO_2}{H_2O}$	H.I
Early Byzantine	KBaM1	Baptistery Wall	Mortar	0.22	3.65	6.18	19.08	1.30	66.95	0.35	2.28	4.9	28.7	5.8	0.39
	KBaM2	Baptistery Wall	Mortar	0.00	1.41	2.69	7.45	0.65	86.47	0.05	1.28	4.1	36.8	9.1	0.13
	KNM2	Naos Wall	Mortar	0.33	2.47	6.40	20.25	1.16	67.14	0.35	1.90	5.8	29.8	5.2	0.41
	KSM1	Substructure Arch	Mortar	0.46	1.95	2.83	9.45	0.87	83.54	0.00	0.90	4.2	35.7	8.5	0.15
	KSM2	Substructure Buttress	Mortar	0.43	2.68	4.94	16.12	1.25	72.50	0.16	1.92	4.3	30.8	7.2	0.31
	KSM3	Substructure Vault	Mortar	0.29	1.91	2.19	6.85	0.37	87.24	0.12	1.02	4.7	38.3	8.1	0.11
	ATM2	Transept Buttress	Mortar	0.68	3.54	7.56	33.80	1.24	49.89	0.33	2.96	4.5	27.5	6.2	0.83
	ARM1	Treasure Room Niche	Mortar	0.83	3.38	7.27	22.49	1.29	61.45	0.18	3.10	4.2	22.5	5.4	0.51
	ARM2	Treasure Room Wall	Mortar	0.45	4.52	7.06	18.43	1.51	62.95	0.82	4.25	6.0	28.6	4.7	0.44
	ABM3	Bema Arch	Mortar	2.49	5.85	10.31	26.16	4.62	45.21	0.69	4.67	6.8	21.9	3.2	0.81
Middle Byz.	ASM	Substructure Wall	Mortar	2.44	9.36	10.74	30.92	2.35	37.43	0.66	6.10	4.5	18.2	4.0	1.02
	AGM1	Gate of Persecution Wall	Mortar	1.07	5.56	7.71	29.94	1.40	50.60	0.26	3.47	4.2	22.4	5.3	0.73
	KFM	Fortification Wall	Mortar	0.44	3.18	6.41	18.44	1.02	67.05	0.49	2.97	4.4	31.1	7.1	0.40
	KNM1	Naos Buttress	Mortar	0.23	1.40	2.99	9.69	0.44	84.53	0.00	0.72	3.1	31.1	10.0	0.16
	KNM3	Naos Buttress	Mortar	0.42	2.01	5.13	18.95	0.85	71.51	0.00	1.13	4.0	33.3	8.3	0.34
Late Byz.	KNM4	Naos Buttress	Mortar	0.21	1.40	3.62	13.56	0.69	79.22	0.24	1.05	4.1	34.8	8.4	0.23

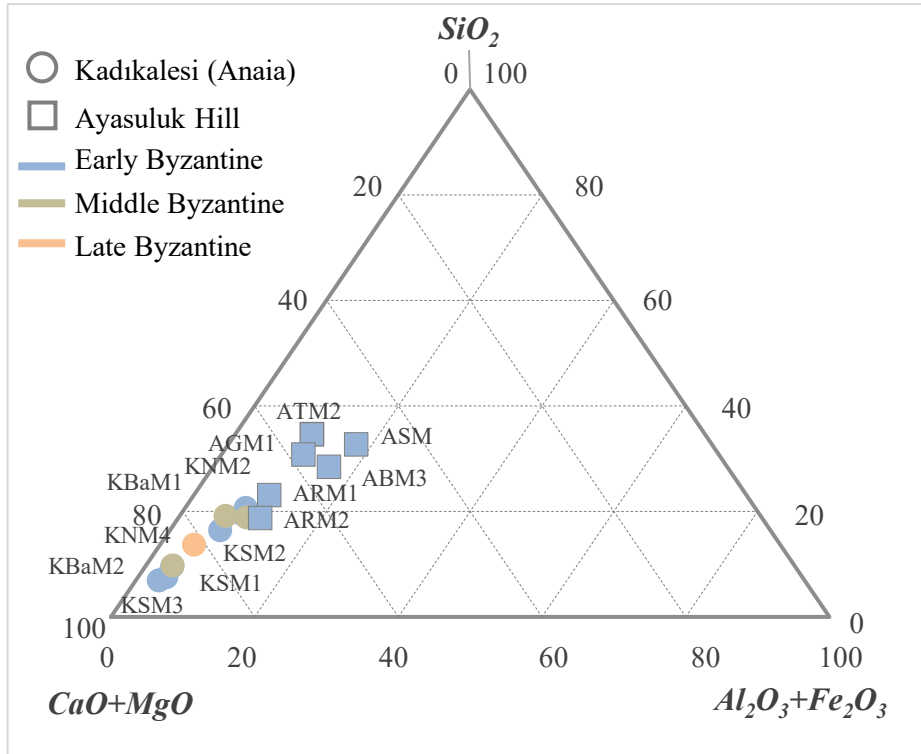


Figure 5.29. (CaO+MgO)-(Al₂O₃+Fe₂O₃)-SiO₂ diagram representing the composition of the binders with natural aggregates

Hydraulic properties of binders were determined by both TGA and hydraulic index values. The ratio of the weight losses between 200–600°C and 600–900°C which were associated with to the loss of structurally bound water of hydraulic products (H₂O) and CO₂ loss due to the decomposition of calcite were calculated. CO₂/H₂O ratios were found between 5.2–10.0 for Kadikalesi (Anaia) samples and between 3.2–6.2 for Ayasuluk samples (Table 5.17). Since all the CO₂/H₂O ratios were found between 1 and 10, all investigated lime mortars with natural aggregates were accepted to possess hydraulic properties.

In addition to TGA, hydraulic indices of binders were calculated according to the Boynton formula (4.4). The H.I. values greater than 0.1 indicate hydraulicity.

$$\text{H.I.} = (\% \text{SiO}_2 + \% \text{Al}_2\text{O}_3 + \% \text{Fe}_2\text{O}_3) / (\% \text{CaO} + \% \text{MgO}) \quad (4.4)$$

H.I. values were in the range of 0.11–0.41 for the binders of Kadikalesi (Anaia) samples and were in the range of 0.44–1.02 for the binders of Ayasuluk samples (Table 5.17). These values also indicated the hydraulic character of the binders.

It was determined by both methods that all the examined binders had hydraulic properties, regardless of the place they were used and the construction periods. Hydraulic properties of the binders could be attributed to the pozzolanic aggregates since it was determined that the lime lumps did not have hydraulic properties (Table 5.16, Figure 5.26). By the fact that, the lime lumps from mortars with natural aggregates only obtained from Kadıkalesi (Anaia), comparison of the $(\text{SiO}_2 + \text{Al}_2\text{O}_3 + \text{Fe}_2\text{O}_3)$ to $(\text{CaO} + \text{MgO})$ meaning the H.I. values of lime lumps and the binders of Kadıkalesi (Anaia) were depicted in figure 5.30.

Nevertheless, it should be noted that the $\text{CO}_2/\text{H}_2\text{O}$ ratios and the H.I. values of Ayasuluk binders revealed higher hydraulic character than the Kadıkalesi (Anaia) binders. Pozzolanic activity values of fine natural aggregates were found in the similar ranges for both sites (1.51–8.03 mS/cm) (Table 5.10, 5.12). The type of the natural aggregates was specified as breccia, and their possible sources were estimated as mountain slopes of Küçük Menderes for Ayasuluk and mountain slopes of Büyük Menderes for Kadıkalesi. The possible natural aggregate provenance of Ayasuluk is closer to the Seferihisar-Doğanbey volcanic region than Kadıkalesi. Although the pozzolanic activities of fine aggregates ($< 53\mu\text{m}$) were similar for both sites, the amount of volcanic originated particles possessing pozzolanic properties in the breccia used in the production of the mortars may have been higher in Ayasuluk mortars.

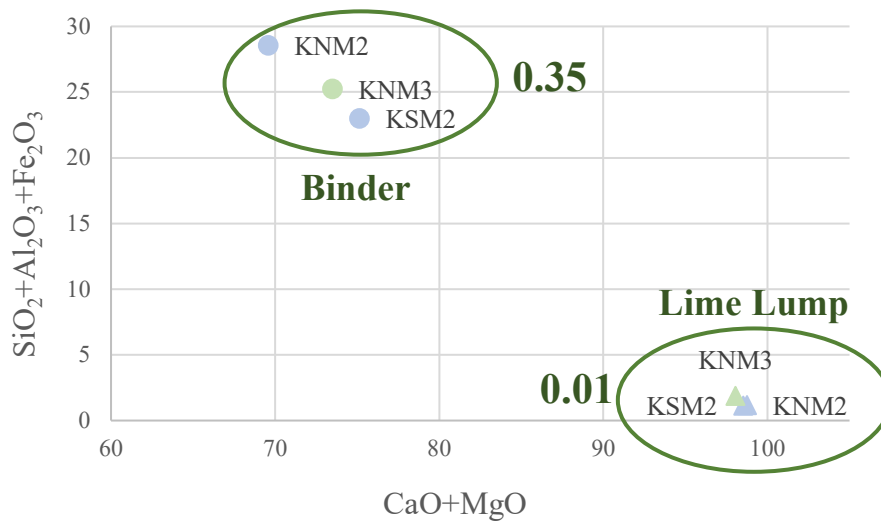


Figure 5.30. $\text{SiO}_2 + \text{Al}_2\text{O}_3 + \text{Fe}_2\text{O}_3 / \text{CaO} + \text{MgO}$ diagrams of binder and lime lumps in the lime mortars of Kadıkalesi (Anaia)

Mineralogical compositions of the binders with natural aggregates were determined via XRD. Kadikalesi (Anaia) binders with natural aggregates were composed of calcite (CaCO_3), quartz (SiO_2), and albite ($\text{Na(AlSi}_3\text{O}_8)$) (Figure 5.31). Ayasuluk binders were consisted of calcite, quartz, albite and hornblende ($(\text{Ca,Na})_2(\text{Mg,Fe,Al})_5(\text{Al,Si})_8\text{O}_{22}(\text{OH})_2$) minerals (Figure 5.32). Calcite was derived from carbonated lime; whereas quartz, albite, and hornblende minerals were from aggregates. Calcium silicate hydrate (CSH) and calcium aluminate hydrate (CAH) which were formed as a result of the hydraulic reaction between lime and pozzolanic aggregates were not detected on the XRD patterns. The amorphous structures of these formations or the fact that their main peaks coincide with the main peak of calcite can be shown as the reasons why they could not be determined on the XRD patterns (Luxán and Dorrego 1996; Haga et al. 2002).

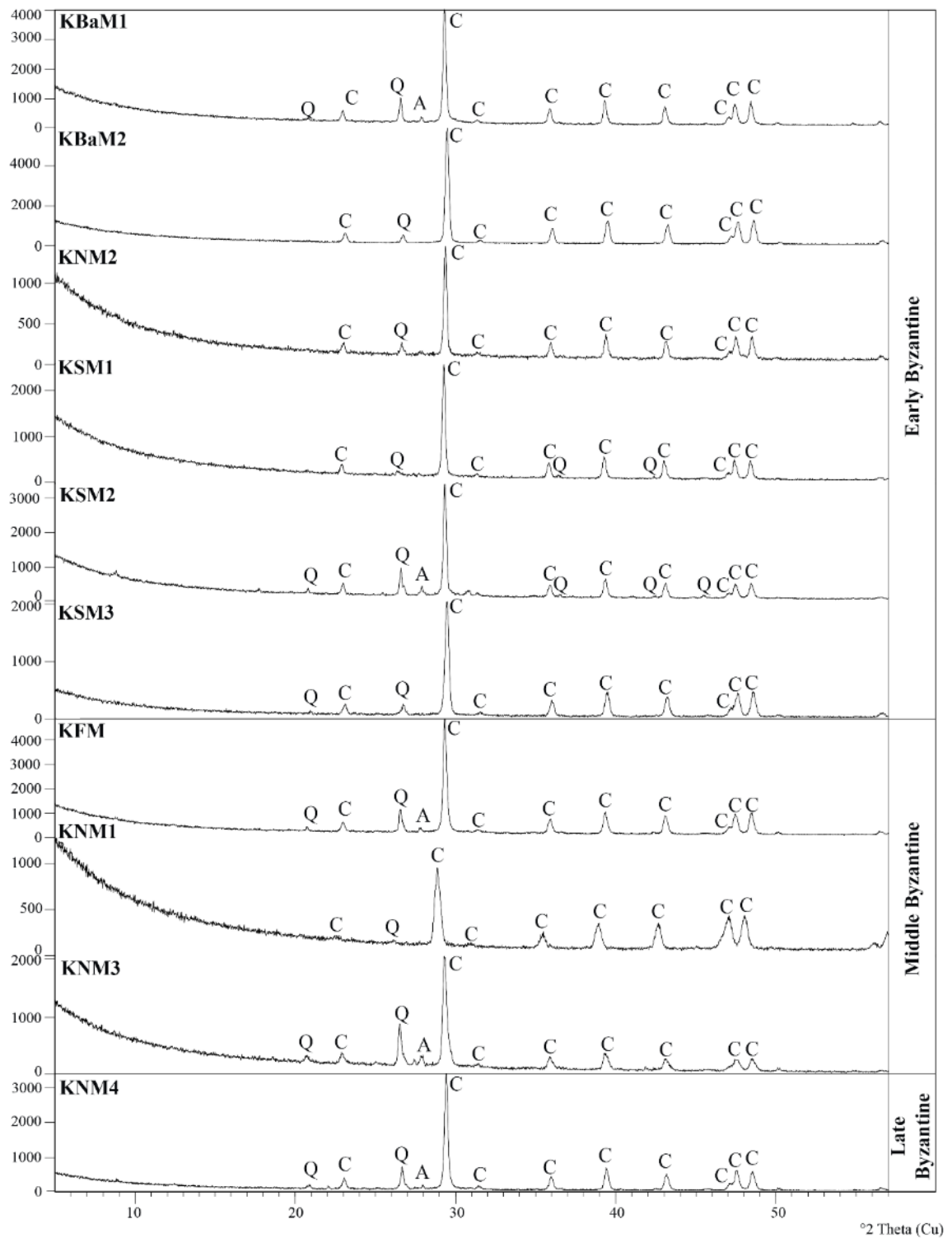


Figure 5.31. XRD patterns of the binders with natural aggregates from Kadıkalesi (Anaia) (A: Albite 76-1819, C: Calcite 86-2334, Q: Quartz 85-0798)

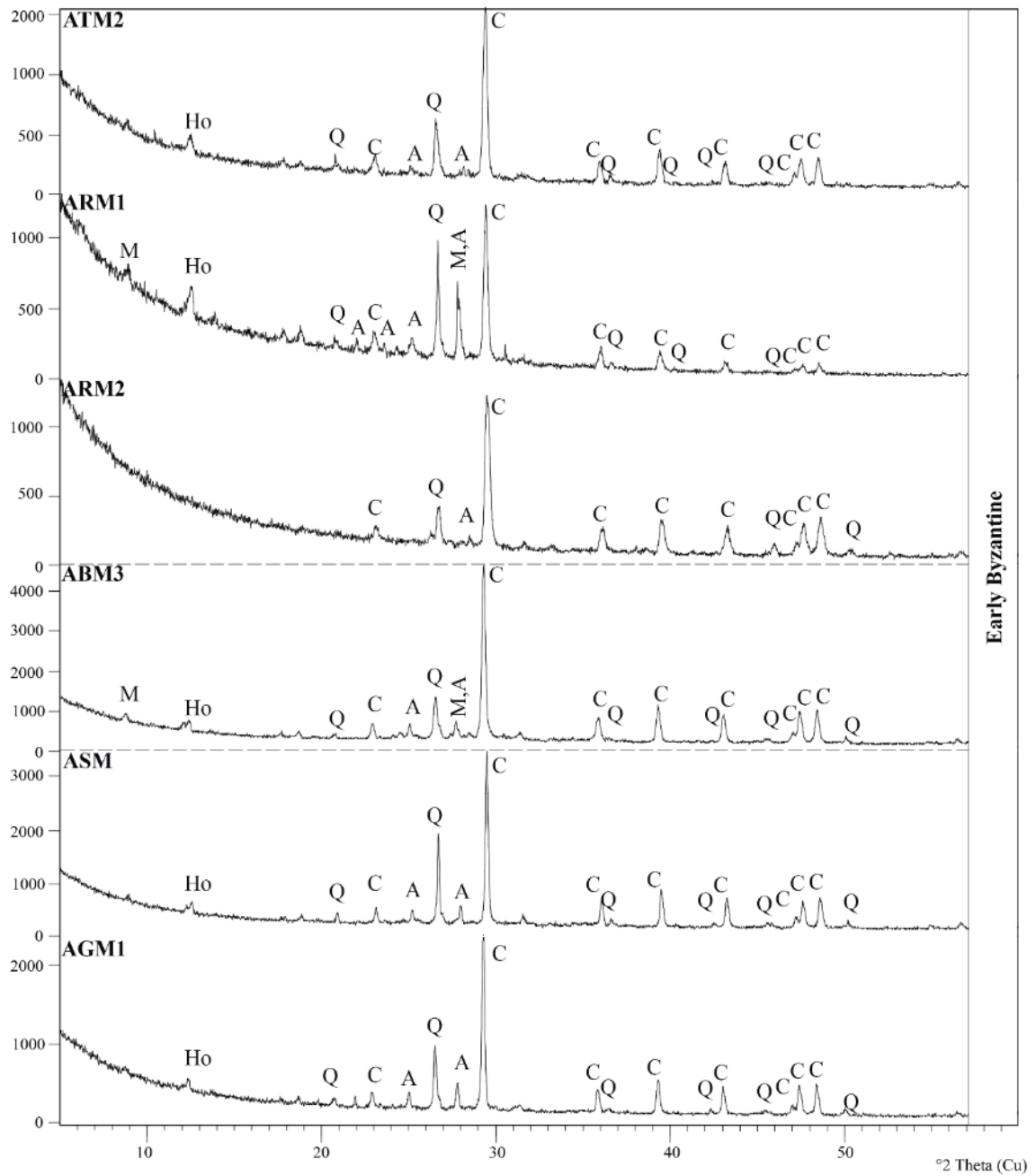


Figure 5.32. XRD patterns of the binders with natural aggregates from Ayasuluk (A: Albite 76-1819, C: Calcite 86-2334, Ho: Hornblende 71-1060, M: Muscovite 84-1302, Q: Quartz 85-0798)

Microstructural properties of binders were investigated via SEM-EDS. Micro cracks and some irregularities between aggregates and binder were observed in Kadıkalesi samples, whereas they presented a stronger adhesion with no microcracks in Ayasuluk samples (Figure 5.33). This adhesion may be due to the higher hydraulic properties and also a better mixing process of the pozzolans and lime during the manufacturing process that provided mortars to be more compact, stiff and hard (Uğurlu Sağın, Duran, and Böke 2021).

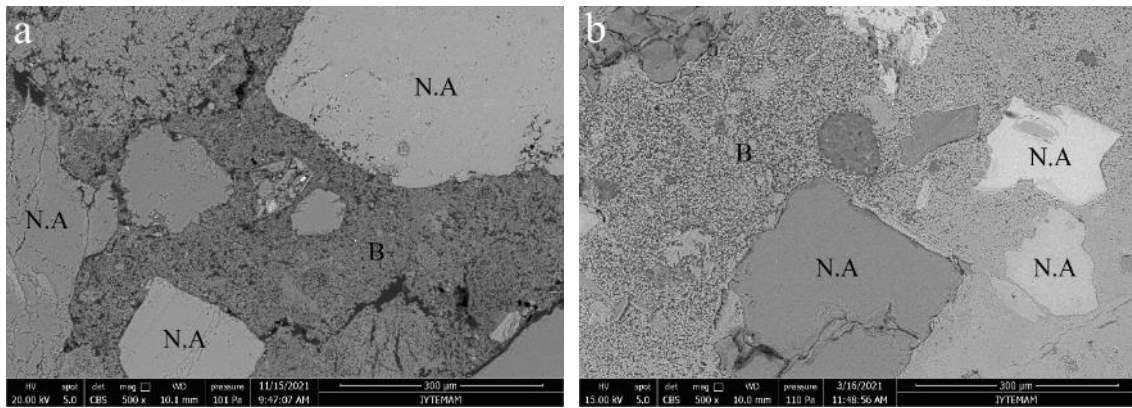
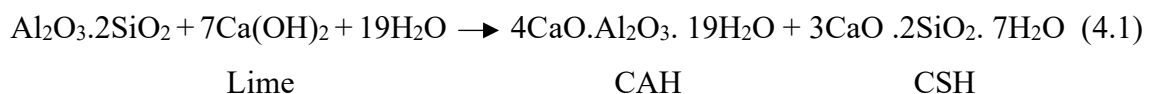


Figure 5.33. Binder matrix of Kadıkalesi (Anaia) and Ayasuluk

(a: KNM1 x500, b: ATM2 x500) (B: Binder, N.A: Natural aggregate)

Within the binders, needle-like amorphous structures mainly comprised of SiO_2 (39.83–64.09%), CaO (23.88–30.65%) and Al_2O_3 (8.45–14.93 %) were observed (Figure 5.34, 5.35) (Table 5.18). These structures were the indicators of the reaction between the lime and pozzolans. In an alkaline environment, silica and alumina in the aggregates reacts with lime and produced tetra calcium aluminate hydrate (CAH) and calcium silicate hydrate (CSH) (4.1) (Prince, Castanier, and Giafferi 2001; Böke and Akkurt 2003). They are the products that give the hydraulic property to the mortars and plasters.



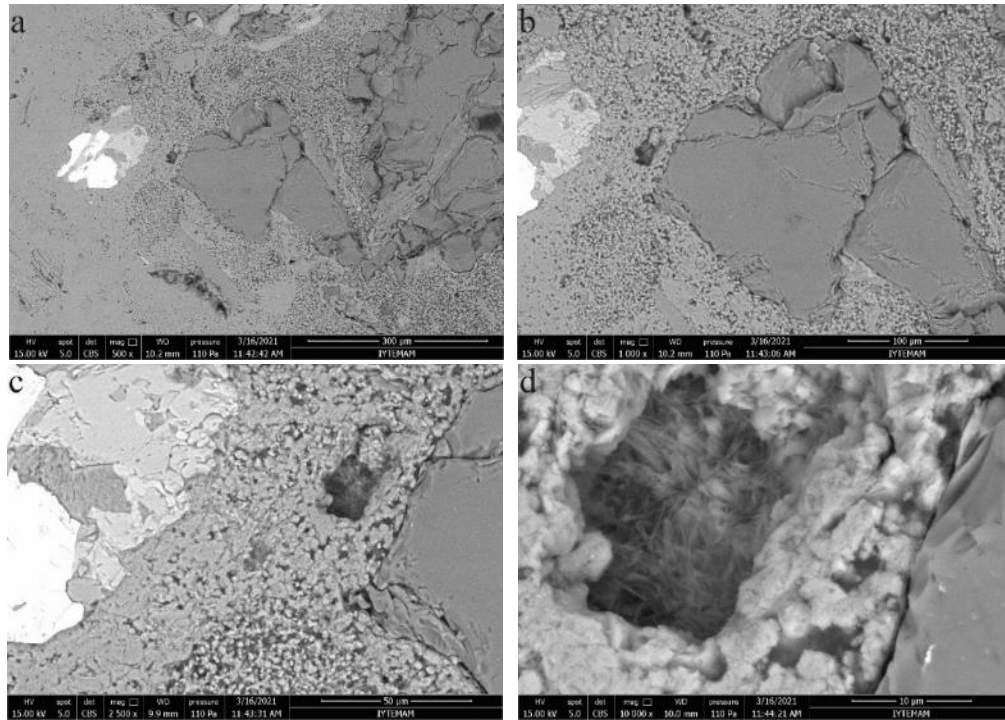


Figure 5.34. SEM images of CSH and CAH formations detected in Ayasuluk binders (a:ATM2 x500, b:ATM2 x1000, c:ATM2 x2500, d:ATM2 x1000)

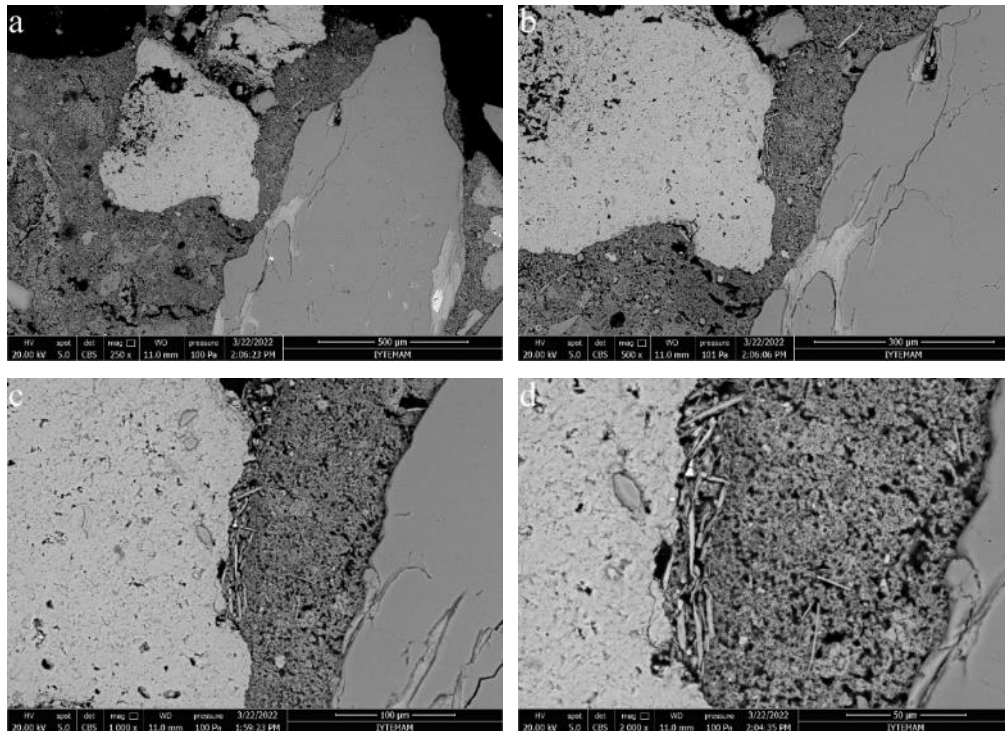
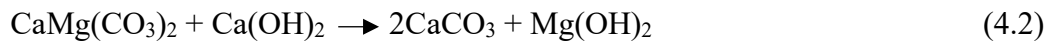


Figure 5.35. SEM images of CSH and CAH formations detected in Kadikalesi (Anaia) binders (a:KNM1 x250, b:KNM1 x500, c:KNM1 x1000, d:KNM1 x2000)

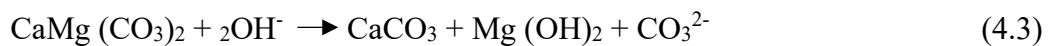
Table 5.18. Chemical compositions of CSH and CAH formations observed in ATM2 and KNM1 mortar matrices

Chemical Composition (%)					
MgO	Al ₂ O ₃	SiO ₂	K ₂ O	CaO	Fe ₂ O ₃
1.03–5.99	8.45–14.93	39.83–64.09	1.25–3.02	23.88–30.65	1.31–4.98

SEM-EDS analysis also demonstrated that lime mortars from Kadıkalesi (Anaia) contained dolomitic aggregates which were surrounded by reaction rims in terms of thicker (T.R) and narrow (N.R) reaction rims and halo (H) (Figure 5.36). The dolomitic aggregate was mostly composed of CaO (53.74%), MgO (23.57%) and SiO₂ (15.79%). The narrow reaction rim contained CaO (37.03%), SiO₂ (29.99%), MgO (16.58%) and Al₂O₃ (12.84%). The surrounded thicker reaction rim was consisted of CaO (53.37%), MgO (12.67%) and SiO₂ (15.79%), whereas in the halo formation CaO was sharply increased to 80.09%, but MgO was decreased to 4.53%. The increase of CaO and decrease of MgO revealed that the chemical reactions occurred because of the dedolomitization of dolomitic aggregates (Busenberg and Plummer 1982; García et al. 2003; Ponce-Antón et al. 2020). The dedolomitization process starts with the reaction of the dolomite (CaMg(CO₃)₂) with slaked lime (Ca(OH)₂), calcite (CaCO₃) and brucite (Mg(OH)₂); and the products precipitated as the reaction rim (4.2) (Busenberg and Plummer 1982; García et al. 2003; Ponce-Antón et al. 2020).

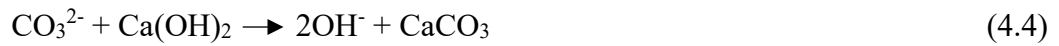


Dissolution of dolomitic aggregates happens in alkaline environments and also it is affected from temperature. In alkaline environment, which caused by the lime in mortar, the dolomitic aggregate reacts with OH⁻ and so; calcite, brucite and carbonate ions (CO₃²⁻) produce (4.3) (Busenberg and Plummer 1982; Moropoulou et al. 2002; García et al. 2003; Ponce-Antón et al. 2020).



The carbonate ions (CO₃²⁻) react with slaked lime and produce calcite and OH⁻ ions, so the halo forms within the binder in contact with the outer part of the dolomitic

aggregate (4.4) (Busenberg and Plummer 1982; García et al. 2003; Ponce-Antón et al. 2020).



The formation of siliceous rim can be attributed to the reaction of alkaline environment with phyllosilicates being in dolostones, and small amount of silicate gel (ASSR-gel) occurs. The ASSR-gel reacts with brucite in the thicker reaction rim and form into “chlorite-like” phases, which may explain the clinochlore peaks on the XRD patterns (Figure 5.11).

The existence of these dolomitic aggregates may have affected the lime/aggregate ratios of mortars and plasters (Table 5.4, 5.5) since dilute hydrochloric acid used during the determination of raw materials compositions to dissolve the lime parts of the samples probably also caused the dissolution of dolomitic aggregates.

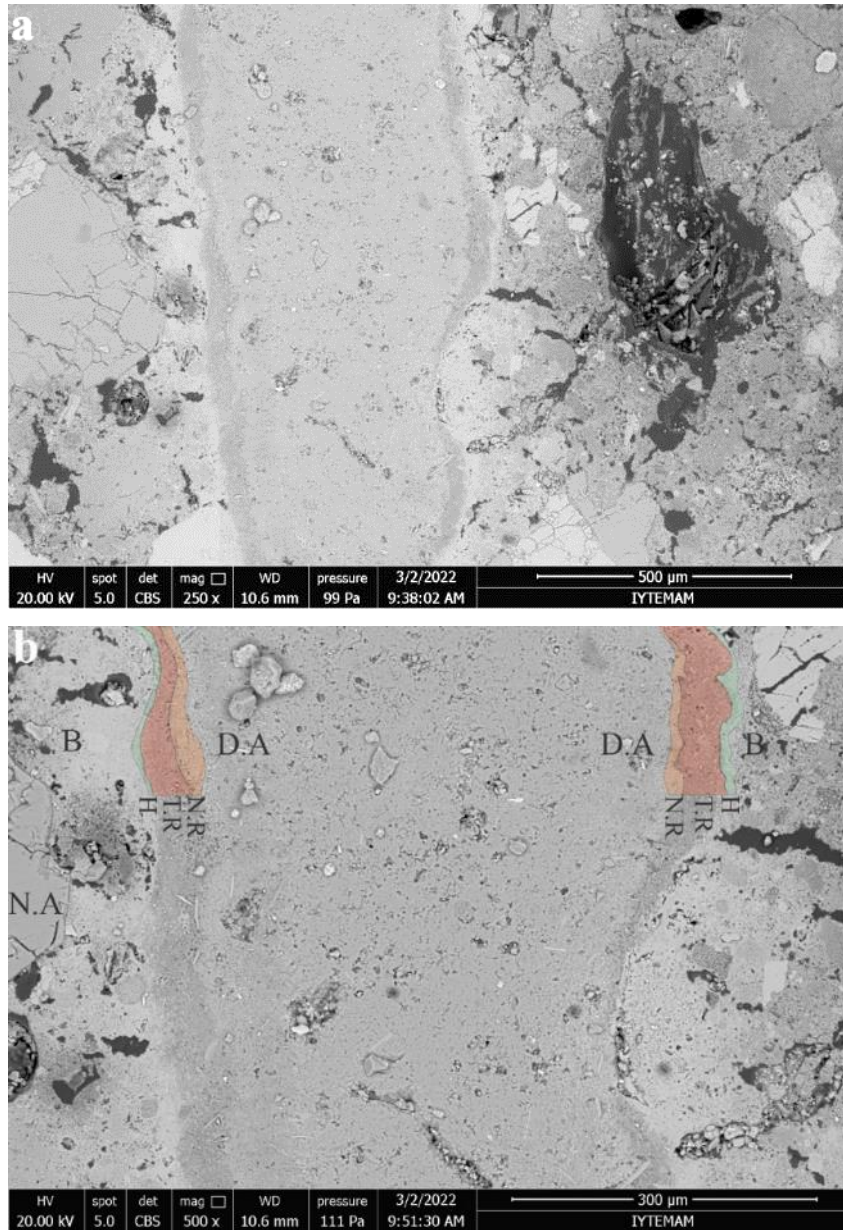


Figure 5.36. SEM images that showed the dedolomitization of dolomitic aggregate in lime mortar sample of Kadıkalesi (Anaia) (a: KNM2 x250, b: KNM2 x500; B: Binder, D.A: Dolomitic aggregate, H: Halo, N.A: Natural aggregate, N.R: Narrow reaction rim, T.R: Thicker reaction rim)

5.6.2. Characteristics of Binders with Brick Aggregates

Binders with brick aggregates from Kadıkalesi (Anaia) were composed of large amounts of CaO (36.42–64.86%), SiO₂ (19.49–34.51 %), moderate amounts of Al₂O₃ (9.15–14.05 %), and smaller amounts of MgO (1.80–6.67 %), Fe₂O₃ (2.59–4.87 %), K₂O (1.18–2.53 %), Na₂O (0.42–0.70 %), TiO₂ (0.40–0.58 %) (Table 5.19). Similarly, binders with brick aggregates from Ayasuluk were consisted of large amounts of CaO (41.18–75.21%), SiO₂ (13.96–30.10 %), moderate amounts of Al₂O₃ (4.72–12.58 %), and smaller amounts of MgO (2.34–6.83 %), Fe₂O₃ (2.17–4.88 %), K₂O (1.06–3.55 %), Na₂O (0.19–2.22 %), TiO₂ (0.18–0.64 %) (Table 5.19).

The hydraulic characteristics of the binders with brick aggregates were also defined by TGA and hydraulic index (H.I.) calculations.

CO₂/H₂O ratios due to the weight losses between 200–600°C and 600–900°C were determined in the range of 2.7–4.8 in Kadıkalesi (Anaia) samples and 3.1–9.0 in Ayasuluk samples (Table 5.19). All binders could be accepted as hydraulic according to the TGA results since all the CO₂/H₂O ratios were below 10 (Bakolas et al. 1998; Moropoulou, Bakolas, and Bisbikou 2000).

Also, H.I. of the binders calculated as $(\%SiO_2 + \%Al_2O_3 + \%Fe_2O_3) / (\% CaO + \% MgO)$ were found between 0.47–1.24 for Kadıkalesi (Anaia) and between 0.27–1.03 for Ayasuluk samples. TGA analysis and the hydraulic index calculations both showed that all binders with brick aggregates possessed hydraulic properties.

The hydraulic indices of the lime lumps and the binders from only Ayasuluk (ABM1, ABaM, ATM1) were compared and depicted in Figure 5.37. Lime lumps of Kadıkalesi (Anaia) lime plasters could not be separated and investigated. The mean hydraulic index values of were 0.39 in binders revealing the hydraulic character; whereas it was 0.02 in lime lumps meaning as they were non-hydraulic. Because of this, hydraulic properties of binders could be attributed to the pozzolanic character of brick aggregates (Table 5.10, 5.12, 5.19). The reaction between pozzolanic brick aggregates with lime and the formation of hydraulic products (CSH, CAH) provided the hydraulic character to the mortars and plasters (Taylor 1997; Hodgkinson and Hughes 1999; Miriello et al. 2011).

Table 5.19. Chemical compositions of binders with brick aggregates in Kadikalesi (Anaia) and Ayasuluk

Period	Sample	Location	Func.	Chemical Compositions (%)								Hydraulic Properties			
				Na ₂ O	MgO	Al ₂ O ₃	SiO ₂	K ₂ O	CaO	TiO ₂	Fe ₂ O ₃	200-600°C H ₂ O	600-900°C CO ₂	$\frac{CO_2}{H_2O}$	H.I
Early Byzantine	ARP	Treasure Room Wall	Plaster	0.20	3.39	7.24	17.41	1.53	66.72	0.22	3.29	3.9	30.2	7.7	0.40
	ABaM	Baptistery Wall	Mortar	0.29	3.24	5.52	15.28	1.83	71.13	0.37	2.34	5.5	29.2	5.3	0.31
	ATM1	Transept Wall	Mortar	0.34	2.34	4.72	13.96	1.06	75.21	0.18	2.20	4.2	30.3	7.2	0.27
	ABM1	Bema Buttress	Mortar	0.25	4.20	8.85	23.01	1.76	57.57	0.48	3.90	3.2	29.0	9.0	0.58
	ABM2	Bema Buttress	Mortar	0.19	3.18	7.17	25.21	1.12	60.42	0.54	2.17	5.4	27.8	5.2	0.54
Middle Byz.	ANM	Naos Buttress	Mortar	0.83	3.43	8.18	25.42	1.22	56.65	0.32	3.94	3.9	22.3	5.7	0.62
	ANP	Naos Buttress	Plaster	0.94	3.43	9.76	27.80	2.53	50.77	0.56	4.21	3.7	24.9	6.7	0.77
	ASP1	Substructure Wall	Plaster	2.22	5.01	12.58	30.10	3.55	41.18	0.49	4.88	4.4	19.4	4.4	1.03
	ASP2	Substructure Wall	Plaster	1.68	5.35	10.66	24.32	2.05	50.92	0.64	4.38	3.6	15.8	4.3	0.70
	AGM2	Gate of Persecution Buttress	Mortar	1.12	6.83	9.74	22.57	1.89	53.01	0.45	4.40	7.9	24.7	3.1	0.61
Late Byz.	KOP1	Outer Narthex Wall	Plaster	0.42	6.67	14.05	34.51	2.48	36.42	0.58	4.87	5.3	17.8	3.4	1.24
	KOP2	Outer Narthex Wall	Plaster	0.61	5.66	11.20	32.34	2.53	42.56	0.40	4.70	6.1	16.4	2.7	1.00
	KCP1	Cistern I Wall	Plaster	0.47	3.28	12.82	33.21	2.31	43.30	0.53	4.07	5.3	14.2	2.7	1.08
	KCP2	Cistern I Wall	Plaster	0.70	3.30	12.49	29.57	2.32	46.81	0.42	4.37	3.7	17.9	4.8	0.93
	KCP3	Cistern II Wall	Plaster	0.50	1.80	9.15	19.49	1.18	64.86	0.43	2.59	6.4	19.7	3.1	0.47

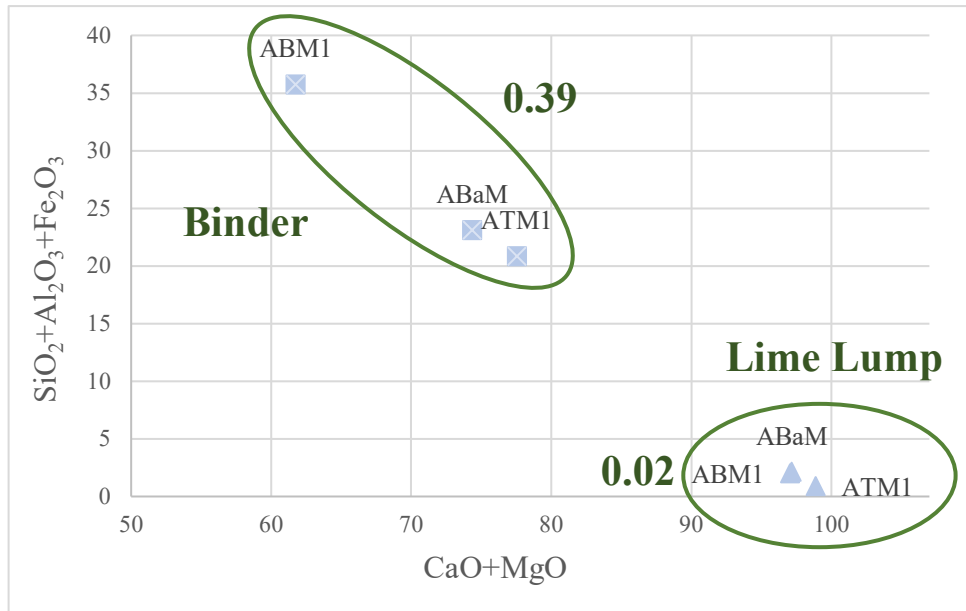


Figure 5.37. $\text{SiO}_2 + \text{Al}_2\text{O}_3 + \text{Fe}_2\text{O}_3 / \text{CaO} + \text{MgO}$ diagrams of binder and lime lumps in the lime mortars of Ayasuluk

XRD analysis were conducted to determine the mineralogical compositions of the binders with brick aggregates. Binders from both Kadıkalesi (Anaia) and Ayasuluk were comprised of calcite (CaCO_3), quartz (SiO_2) and albite ($\text{Na(AlSi}_3\text{O}_8)$) (Figure 5.38, 5.39). Only KOP2 which belonged to Late Byzantine period cistern had also muscovite ($\text{KAl}_2(\text{Si}_3\text{Al})\text{O}_{10}(\text{OH},\text{F})_2$) mineral additionally (Figure 5.38). Calcite was originated from carbonated lime; whereas quartz, albite, and muscovite minerals were from brick aggregates. Calcium silicate hydrate (CSH) and calcium aluminate hydrate (CAH) which could be expected in the mineralogical compositions were not observed due to their amorphous structures (Luxán and Dorrego 1996; Haga et al. 2002).

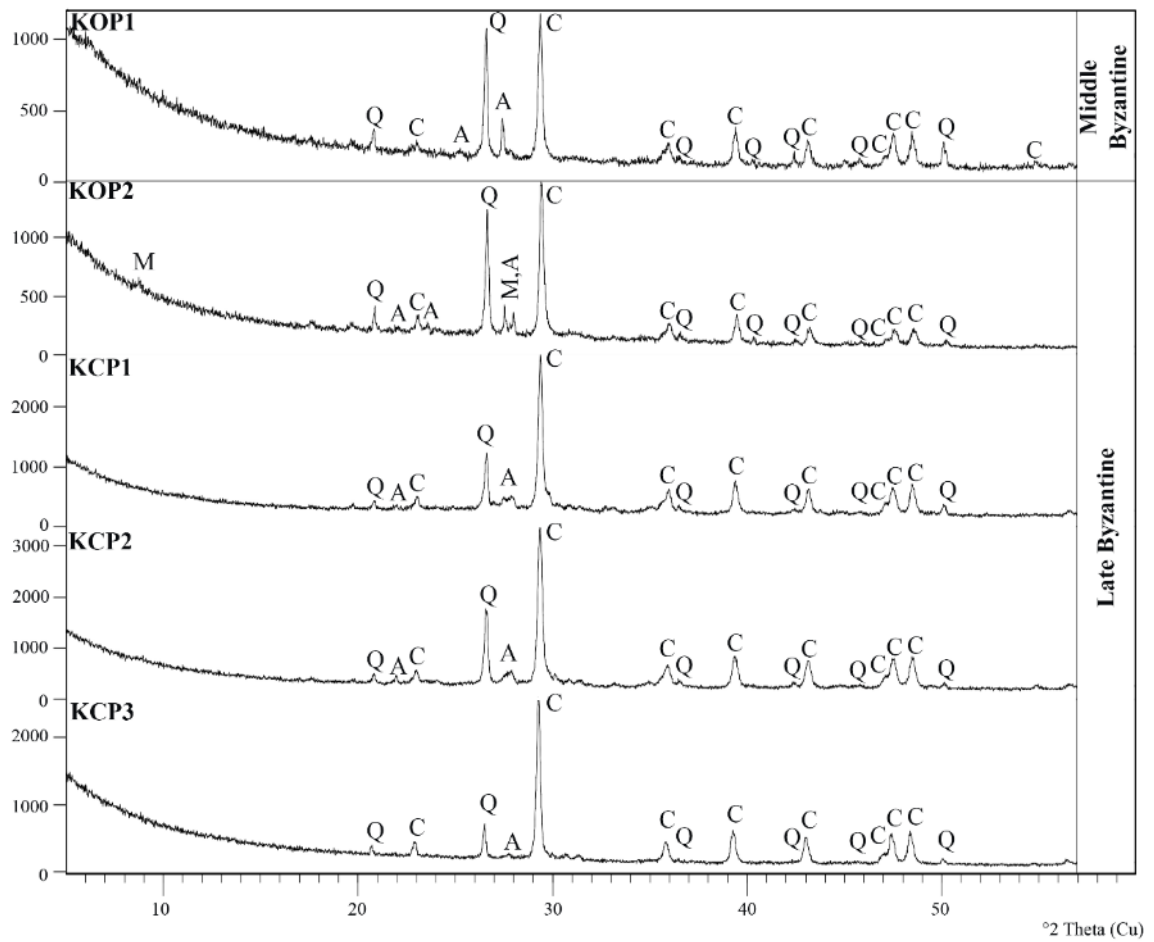


Figure 5.38. XRD patterns of binders with brick aggregates from Kadıkalesi (Anaia)

(A: Albite 76-1819, C: Calcite 86-2334, M: Muscovite 84-1302, Q: Quartz 85-0798)

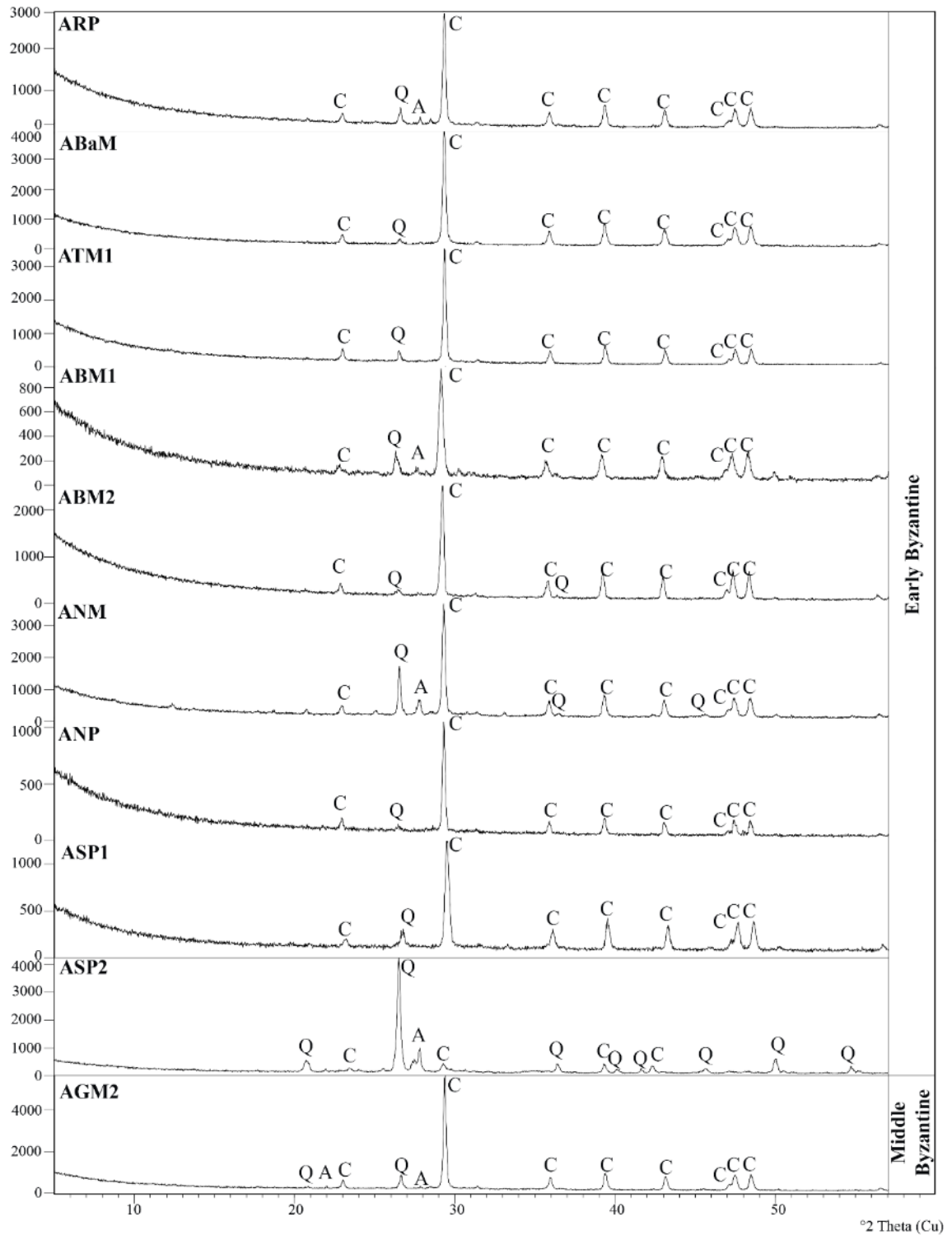


Figure 5.39. XRD patterns of binders with brick aggregates from Ayasuluk
(A: Albite 76-1819, C: Calcite 86-2334, Q: Quartz 85-0798)

SEM images demonstrated that the lime crystals and the pozzolanic brick aggregates were well mixed and provided a uniform structure in the matrix (Figure 5.40).

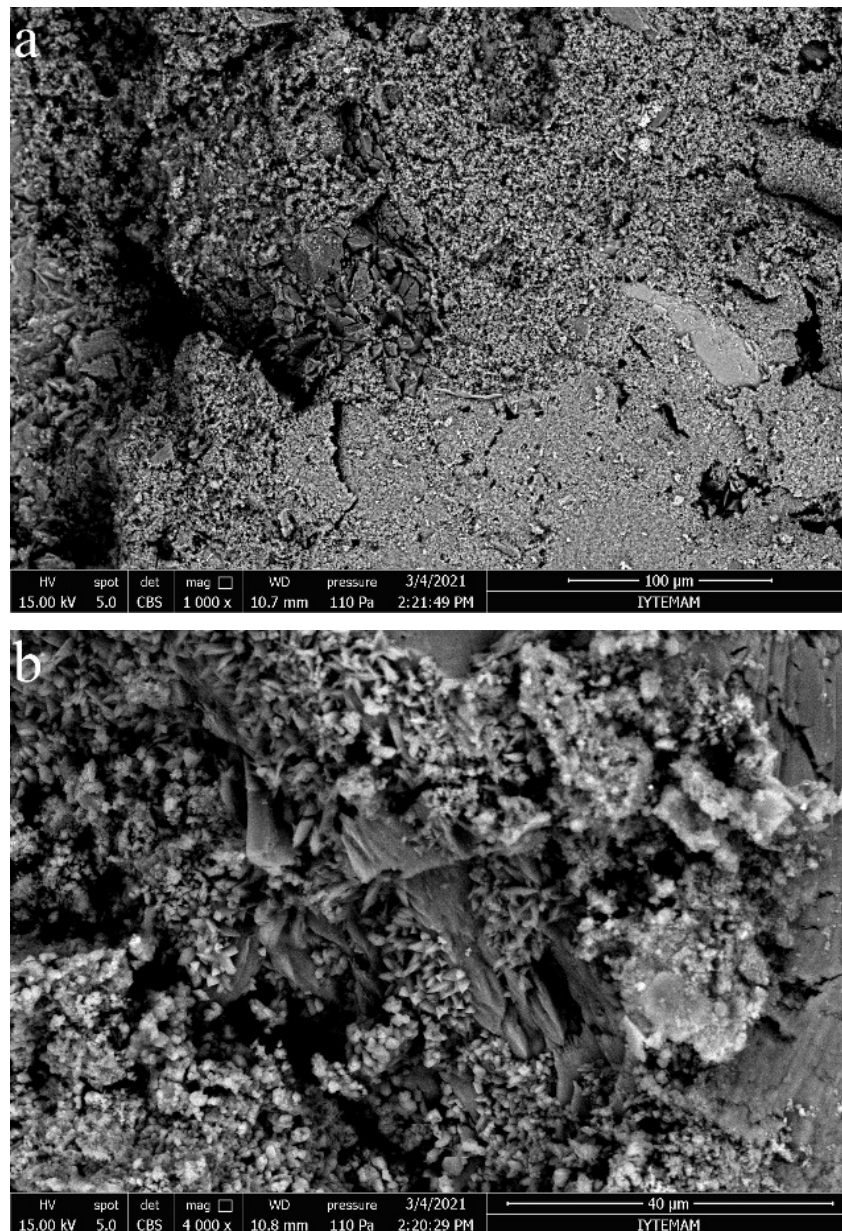


Figure 5.40. SEM images showed the strong adhesion between pozzolans and lime detected in lime mortar sample from Ayasuluk (a: AGM2 x1000, b: AGM2 x4000)

Rod-like crystals were determined in the matrices of the lime mortar of Ayasuluk (AGM2) and lime plaster of Kadıkalesi (Anaia) (KOP1) (Figure 5.41, 5.42). These formations were mainly composed of SiO_2 (38.7–42.9%), Al_2O_3 (19.1–21.4%), CaO (12.14–14.44%), MgO (6.05–12.55%), and Fe_2O_3 (10.1–11.9%). The shapes and the chemical compositions of these crystals indicated that they were calcium silicate hydrate (CSH) and calcium aluminate hydrates (CAH) which were the hydraulic products of the brick aggregate and the lime reaction.

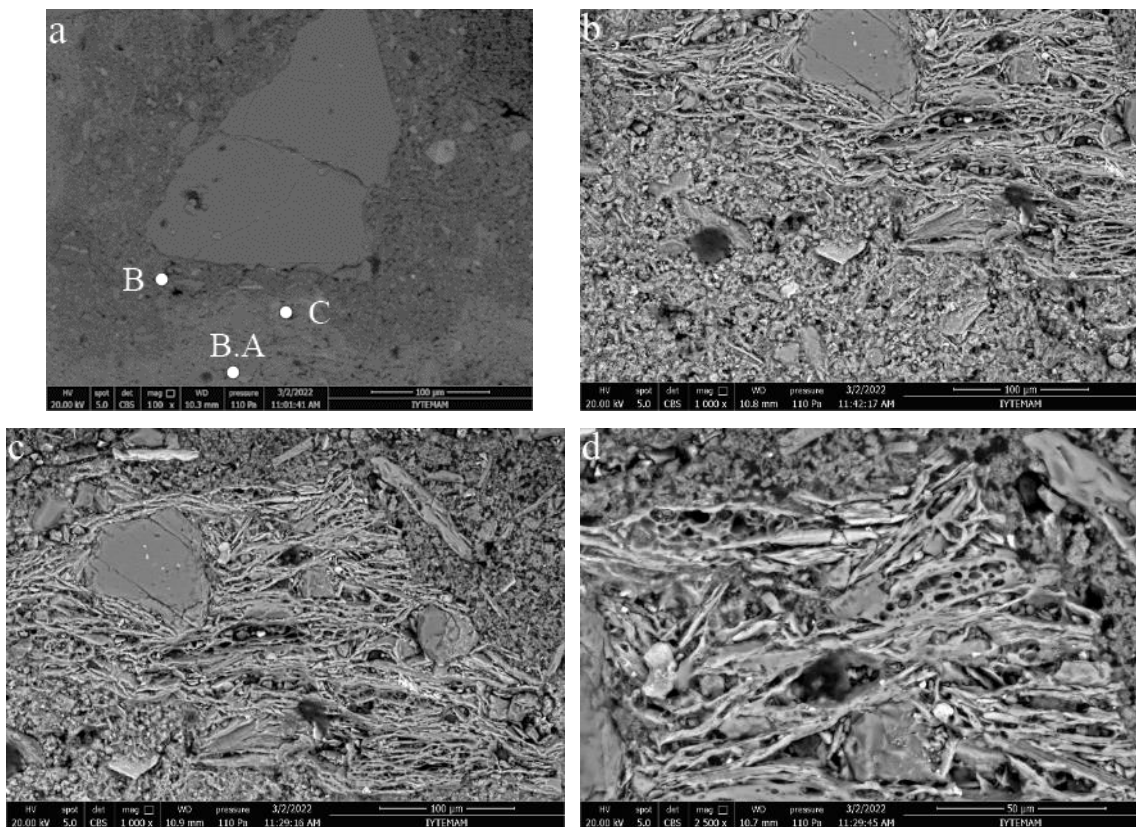


Figure 5.41. SEM images of CSH/CAH formations specified in Kadıkalesi (Anaia) lime plaster (B: Binder, B.A: Brick aggregate, C: CSH/CAH formations; a: KOP1 x100, b: KOP1 x1000, c: KOP1 x1000, d: KOP1 x2500)

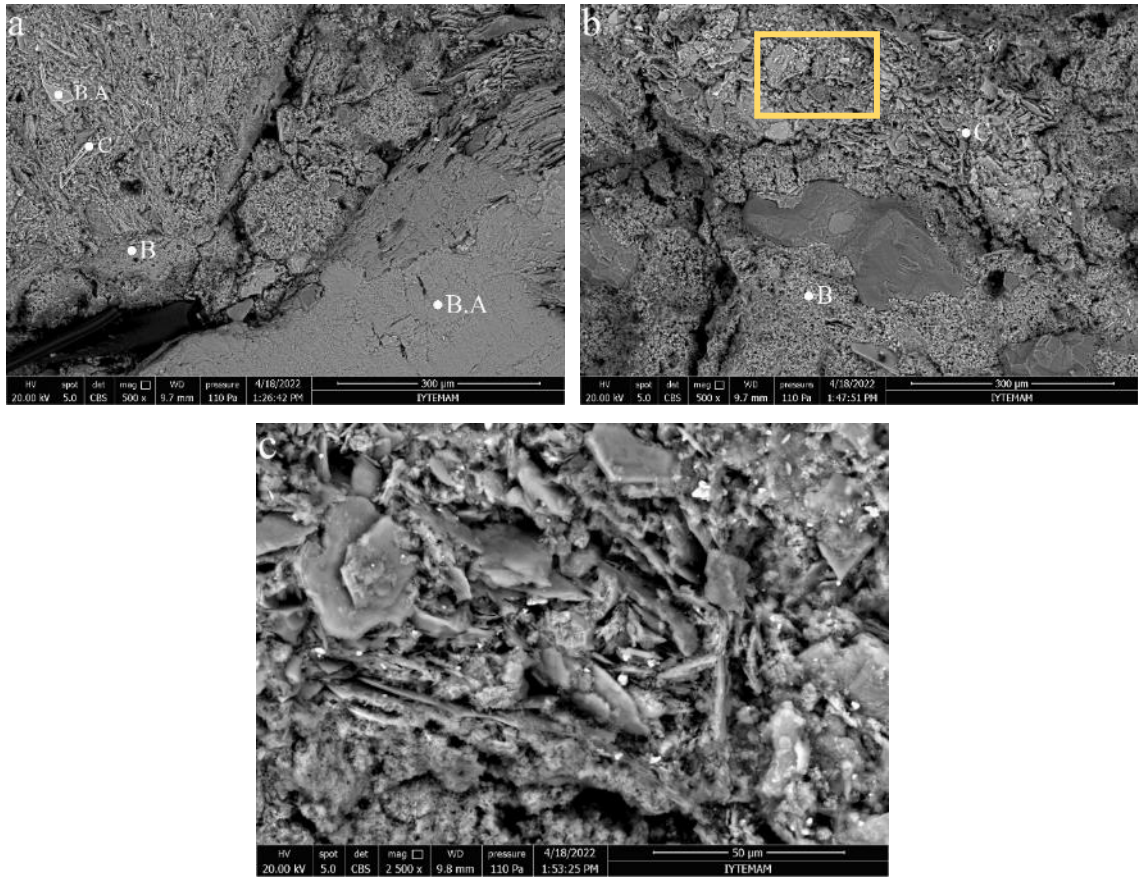


Figure 5.42. SEM images of CSH/CAH formations determined in Ayasuluk lime mortar (B: Binder, B.A: Brick aggregate, C: CSH/CAH formations; a: AGM2 x500, b: AGM2 x500, c: AGM2 x2500)

CHAPTER 6

CONCLUSION

In this study, characteristics of lime mortars and plasters produced with natural and brick aggregates used in Byzantine period buildings from Kadıkalesi (Anaia) and Ayasuluk were determined in order to investigate the continuity of lime mortar technology over centuries and the possible provenance of raw materials.

Within this context, basic physical properties, raw material compositions, and hydraulic properties of lime mortars and plasters; mineralogical, chemical compositions, microstructural properties of binders, aggregates, and limes; pozzolanic activities of natural and brick aggregates were examined through several analytical methods.

Lime plasters applied in both Kadıkalesi (Anaia) and Ayasuluk were consisted of brick aggregates; whereas, lime mortars were mainly composed of natural aggregates, except for a few examples from Ayasuluk. The lime mortars and plasters with brick aggregates were found to be less dense and more porous than lime mortars with natural aggregates due to the porous structure of the brick aggregates. Overall, the basic physical properties did not show significant differences in terms of their use in different construction periods and their location of use in the buildings.

In the production of lime mortars and plasters, high calcium lime and pozzolanic aggregates were used in both areas. The lime/aggregate ratios of lime plasters were between 1/3-4/3 in Kadıkalesi (Anaia) and 3/4-5/3 in Ayasuluk. In Kadıkalesi (Anaia) lime/aggregate ratios were between 1/2-1/1 for the Early Byzantine lime mortars, and between 4/3-5/3 for the Middle and Late Byzantine mortars. The lime/aggregate ratios of Early and Middle Byzantine lime mortars from Ayasuluk were in the range of 1/3-5/3. The higher lime content of the mortars may be caused by the calcareous particles.

Non-hydraulic and fat lime was used in lime mortars and plasters. Also, it has been determined that both natural and brick aggregates had a wide range of particle sizes. Mean-roundness of these aggregates were from sub-angular to very-angular which makes possible interlocking among aggregates and provided a higher surface area. These formal properties indicated that quarries were utilized as raw material sources rather than stream beds for natural aggregates, and brick aggregates were manufactured and processed accordingly. In macro-observations, the different types of rock fragments and the angular

forms of the natural aggregates revealed that they were obtained from the older brecciated alluviums from the Menderes Massif units. Therefore, the possible sources for the breccia in the region were the mountain slopes of Büyük Menderes Grabens (most probably Söke, Germencik district) for Kadıkalesi (Anaia) and Küçük Menderes Grabens (most likely Selçuk) for Ayasuluk.

Fine natural aggregates possessed highly reactive pozzolanic properties due to the volcaniclastic matrix of breccia. Mineralogical compositions of fine natural aggregates were mainly consisted of quartz, albite, muscovite and clinocllore. However, natural aggregates of Ayasuluk also contained volcanic originated hornblende and phillipsite minerals due to the vicinity of volcanic units such as Seferihisar-Doğanbey. All fine natural aggregates were rich in silica and alumina, but poor in carbonate and alkali phases. Determined compositional differences by ternary diagram and mineralogical compositions revealed that Kadıkalesi (Anaia) and Ayasuluk natural aggregates must have been obtained from different sources, and also two different sources must have been used for Ayasuluk aggregates. The microstructures of these natural aggregates were non-porous and had angular forms that strengthen the interlocking with binder.

Brick aggregates were mainly consisted of mainly quartz, albite, hematite and muscovite minerals. They were composed of large amounts of SiO_2 , moderate amounts of Al_2O_3 , Fe_2O_3 , and smaller amounts of MgO , CaO , Na_2O , K_2O and TiO_2 . Brick aggregates of Kadıkalesi and Ayasuluk were distinctively separated by their MgO , Al_2O_3 , Fe_2O_3 contents which may indicate the use of different clay sources. Brick aggregates from both sites were manufactured from Ca-poor clays at low firing temperatures between 800–900 °C. They were highly reactive pozzolans due to the use of clay-rich raw materials and low firing temperatures. Their microstructure was porous where calcite crystals could precipitate and so enhanced the durability to deterioration problems.

Fine mortar and plaster matrices comprised of carbonated lime (CaCO_3) and small grain-sized aggregates were defined as “binder”. The binders were the parts that provided hydraulic properties and high strength to mortars and plasters. The binders with natural aggregates from Kadıkalesi (Anaia) were composed of larger amounts of CaO , MgO ; while binders of Ayasuluk had higher Al_2O_3 , Fe_2O_3 content; so binders of sites was consisted of calcite originated mainly from lime; and quartz, albite and hornblende derived from the aggregates. All binders possessed hydraulic properties which were attributed to the highly pozzolanic properties of natural aggregates. Kadıkalesi (Anaia) is near to the Neogene carbonates, while Ayasuluk is close to the volcanic region of

Seferihisar-Doğanbey. Accordingly, the higher hydraulic properties of Ayasuluk lime mortars with natural aggregates were due to the higher amount of volcanic particles possessing pozzolanic properties in the breccia. Besides, higher CaO, MgO content of the lime mortars with natural aggregates from Kadıkalesi (Anaia) were due to the limestone and/or dolostone aggregates obtained from Neogene carbonates. Since the amounts of pozzolanic aggregates were higher, and mortars and plasters had higher hydraulic properties, Ayasuluk mortars were more compact, stiff and hard than Kadıkalesi mortars.

The binders with brick aggregates from both Kadıkalesi (Anaia) and Ayasuluk were consisted of large amounts of CaO and SiO₂, moderate amounts of Al₂O₃ and smaller amounts of MgO, CaO, Na₂O, K₂O, Fe₂O₃ and TiO₂. They were mostly composed of calcite, quartz and albite minerals, and possessed hydraulic property originated from pozzolanic brick aggregates. Lime mortars and plasters consisted of brick aggregates were well mixed and provided a uniform structure in the matrix.

Consequently, the basic physical properties, raw material compositions, and chemical and mineralogical compositions of the lime mortars and plasters were similar in terms of use in different construction periods and locations. Chemical and mineralogical compositions, hydraulic and microstructural properties varied according to the type of aggregate and the differences in raw material provenances of natural aggregates. Finding suitable raw material sources to produce hydraulic mortars and plasters and the use of mortar and plaster with similar properties in different periods revealed that the knowledge of local raw material resources and mortar production technology was transferred over the centuries.

New lime mortars and plasters, that will be manufactured for the future conservation projects in Kadıkalesi (Anaia) and Ayasuluk, should be physically, chemically, and mineralogically compatible with the original mortar and plaster properties determined by this study. Possible local lime, natural aggregate, and clay sources from Söke and Germencik districts for Kadıkalesi (Anaia) and Selçuk district for Ayasuluk should be investigated in detail, and their suitability for use in mortar and plaster manufacturing should be assured. The brick aggregates should have been produced by firing raw material containing high amounts of clay at low temperatures (< 900 °C). Moreover, the aged fat lime and a wide range of particle sizes of aggregates should have been used, and homogeneous mixing procedure should be ensured during the production.

REFERENCES

- Acun Özgünler, S., A. Ersen, and A. Güleç. 2013. "A Research About Characterization Of Lime Mortars Used in the Early Byzantine Period in The Land Walls of Constantinople, Yedikule." *Restorasyon ve Konservasyon Çalışmaları*, 31–39.
- Adam, J.P. 2005. *Roman Building Materials and Techniques*. (First pub. London and New York: Routledge.
- Akbaş, B., N. Akdeniz, A. Aksay, İ. E. Altun, V. Balcı, E. Bilginer, T. Bilgiç, M. Duru, T. Ercan, and İ. Gedik. 2011. "1: 1.250. 000 Ölçekli Türkiye Jeoloji Haritası." *Maden Tetkik ve Arama Genel Müdürlüğü Yayını, Ankara-Türkiye*.
- Akdeniz, E. 2007. "Kadıkalesi Kazısı Miken Buluntuları." *Arkeoloji Dergisi* 9 (1): 35–70.
- Akman, M. S., A. Güner, and I. H. Aksoy. 1986. "The History and Properties of Khorasan Mortar and Concrete." *Turkish and Islamic Science and Technology in the 16th Century, ITU Research Centre of History of Science and Technology* 1: 101–12.
- Asatekin, G. 1981. "Selçuk-Efes Çevre Düzenleme ve Kazı-Onarım Projesi. III. Kazı Sonuçları Toplantısı." Ankara.
- Aslan Özkaya, Ö. 2005. "Properties of Roman Bricks and Mortars Used in Serapis Temple in Bergama." İzmir Institute of Technology.
- ASTMC618-03. 2003. "Standard Specification for Coal Fly Ash and Raw or Calcined Natural Pozzolan for Use in Concrete." *ASTM International*.
<https://doi.org/10.1520/C0618-03>.
- Bakolas, A., G. Biscontin, A. Moropoulou, and E. Zendri. 1995. "Characterization of the Lumps in the Mortars of Historic Masonry." *Thermochimica Acta* 269 (270): 809–16.
- Bakolas, A., G. Biscontin, A. Moropoulou, and E. Zendri. 1998. "Characterization of Structural Byzantine Mortars by Thermogravimetric Analysis." *Thermochimica Acta* 321: 151–60. [https://doi.org/10.1016/s0040-6031\(98\)00454-7](https://doi.org/10.1016/s0040-6031(98)00454-7).

- Barba, L., J. Blancas, L. R. Manzanilla, A. Ortiz, D. Barca, G. M. Crisci, D. Miriello, and A. Pecci. 2009. "Provenance of the Limestone Used in Teotihuacan (Mexico): A Methodological Approach." *Archaeometry* 51 (4): 525–45. <https://doi.org/10.1111/j.1475-4754.2008.00430.x>.
- Baronio, G., and L. Binda. 1997. "Study of the Pozzolanicity of Some Bricks and Clays." *Construction and Building Materials* 11 (1): 41–46. [https://doi.org/10.1016/S0950-0618\(96\)00032-3](https://doi.org/10.1016/S0950-0618(96)00032-3).
- Baronio, G., L. Binda, and N. Lombardini. 1997. "The Role of Brick Pebbles and Dust in Conglomerates Based on Hydrated Lime and Crushed Bricks." *Construction and Building Materials* 11 (1): 33–40. [https://doi.org/10.1016/S0950-0618\(96\)00031-1](https://doi.org/10.1016/S0950-0618(96)00031-1).
- Binda, L., G. Baronio, and C. Tedeschi. 1999. "Experimental Study on the Mechanical Role of Thick Mortar Joints in Reproduced Byzantine Masonry." In *International RILEM Workshop on Historic Mortars: Characteristics and Tests*, edited by P. Bartos, C. Groot, and J. Hughes, 227–47. RILEM Publications SARL.
- Boggs Jr., S. 2009. *Petrology of Sedimentary Rocks*. 2nd ed. Cambridge: Cambridge University Press.
- Böke, H., and S. Akkurt. 2003. "Ettringite Formation in Historic Bath Brick-Lime Plasters." *Cement and Concrete Research* 33 (9): 1457–64. [https://doi.org/10.1016/S0008-8846\(03\)00094-2](https://doi.org/10.1016/S0008-8846(03)00094-2).
- Böke, H., S. Akkurt, and B. İpekoğlu. 2004. "Investigation of the Pozzolanic Properties of Bricks Used in Horasan Mortars and Plasters in Historic Buildings." *Key Engineering Materials* 264–268: 2399–2402. <https://doi.org/10.4028/www.scientific.net/kem.264-268.2399>.
- Böke, H., S. Akkurt, B. İpekoğlu, and E. Uğurlu. 2006. "Characteristics of Brick Used as Aggregate in Historic Brick-Lime Mortars and Plasters." *Cement and Concrete Research* 36: 1115–22. <https://doi.org/10.1016/j.cemconres.2006.03.011>.
- Boynton, R.S. 1966. *Chemistry and Technology of Lime and Limestone*. John Wiley & Sons.
- Bozkurt, E. 2001. "Neotectonics of Turkey—a Synthesis." *Geodinamica Acta* 14 (1–3): 3–30. <https://doi.org/10.1080/09853111.2001.11432432>.

- Bozkurt, E., and R. Oberhänsli. 2001. "Menderes Massif (Western Turkey): Structural, Metamorphic and Magmatic Evolution - A Synthesis." *International Journal of Earth Sciences* 89 (4): 679–708. <https://doi.org/10.1007/s005310000173>.
- Bruni, S., F. Cariati, P. Fermo, P. Cairati, G. Alessandrini, and L. Toniolo. 1997. "White Lumps in Fifth- to Seventeenth-Century AD Mortars from Northern Italy." *Archaeometry* 39 (1): 1–7. <https://doi.org/10.1111/j.1475-4754.1997.tb00786.x>.
- Busenberg, E., and L. N. Plummer. 1982. "The Kinetics of Dissolution of Dolomite in CO₂-H₂O Systems at 1.5 to 65°C and 0 to 1 Atm PCO₂." *American Journal of Science*. <https://doi.org/10.2475/ajs.282.1.45>.
- Büyükkolancı, M. 2001. *St. John*. İstanbul: Efes 2000 Foundation.
- Büyükkolancı, M. 2018. "Efes'te Hıristiyanlık, Aziz Yuhanna ve Kilisesi." *Arkeoloji Kültür Sanat Dergisi*, 18–27.
- Büyükkolancı, M., B. Duman, P. Ulusoy, and Ö. Aytek. 2013. "Ayasuluk Tepesi ve St. Jean Anıtı Kazısı Takip Kapısı Projesi." Denizli.
- Calvi, V.S. 1941. "Erdbebenkatalog Der Turkei Und Einiger Benaehbarter Gebiete." Ankara.
- Caner, E., and B. A. Güney. 2018. "Investigation of Mortars and Plasters of a Byzantine Church in Southwest Anatolia with Emphasis on Possible Pozzolan Use." *Medziagotyra* 24 (3): 327–31. <https://doi.org/10.5755/j01.ms.24.3.18590>.
- Caner Yüksel, Ç. 2019. "A Tale of Two Port Cities: Ayasuluk (Ephesus) and Balat (Miletus) during the Beyliks Period." *Journal of the Medieval Mediterranean* 31 (3): 338–65.
- Cardiano, P., S. Ioppolo, C. De Stefano, A. Pettignano, S. Sergi, and P. Piraino. 2004. "Study and Characterization of the Ancient Bricks of Monastery of 'San Filippo Di Fragalà' in Frazzanò (Sicily)." *Analytica Chimica Acta* 519: 103–11. <https://doi.org/10.1016/j.aca.2004.05.042>.
- Casadio, F, G Chiari, and S Simon. 2005. "Evaluation Of Binder/Aggregate Ratios In Archaeological Lime Mortars With Carbonate Aggregate: A Comparative Assessment Of Chemical, Mechanical And Microscopic Approaches." *Archaeometry* 47: 671–89.

- Columbu, S., F. Sitzia, and G. Ennas. 2017. *The Ancient Pozzolan Mortars and Concretes of Heliocaminus Baths in Hadrian's Villa (Tivoli, Italy)*. *Archaeological and Anthropological Sciences*. Vol. 9. Archaeological and Anthropological Sciences. <https://doi.org/10.1007/s12520-016-0385-1>.
- Cowper, A. D. 1998. *Lime and Lime Mortars*. *Lime and Lime Mortars*. 1st publis. Shaftesbury: Donhead Publishing. <https://doi.org/10.4324/9781315538303>.
- Cramer, J. A. 1832. *A Geographical and Historical Description of Asia Minor; with a Map*. Oxford at the University Press. <https://books.google.fr/books?id=KsnlF-f4ZtAC&hl=fr>.
- Davey, N. 1961. *A History of Building Materials*. London: Phoenix House. <https://doi.org/10.2307/3100831>.
- Degryse, P., J. Elsen, and M. Waelkens. 2002. "Study of Ancient Mortars from Sagalassos (Turkey) in View of Their Conservation." *Cement and Concrete Research* 32 (9): 1457–63. [https://doi.org/10.1016/S0008-8846\(02\)00807-4](https://doi.org/10.1016/S0008-8846(02)00807-4).
- Eckel, E. C. 1905. *Cements, Limes, and Plasters: Their Materials, Manufacture, and Properties*. First Edit. New York: John Wiley & Sons.
- Erdoğan, B. 1990. "İzmir- Ankara Zonunun İzmir İle Seferihisar Arasındaki Bölgede Stratigrafi Özellikleri ve Tektonik Evrimi." *Türkiye Petrol Jeologları Derneği Bülteni* 2 (1): 1–20.
- Erdoğan, B., and T. Güngör. 2004. "The Problem of the Core-Cover Boundary of the Menderes Massif and an Emplacement Mechanism for Regionally Extensive Gneissic Granites, Western Anatolia (Turkey)." *Turkish Journal of Earth Sciences* 13 (1): 15–36.
- Eşder, T. 1988. "Gümüldür-Cumaovası (İzmir) Alanının Jeolojisi ve Jeotermal Enerji Olanaklarının Araştırılması." İstanbul Üniversitesi.
- Eyice, S. 1963. *Son Devir Bizans Mimarisi*. İstanbul: İstanbul Üniversitesi Edebiyat Fakültesi Yayınları.
- Foss, C. 1979. *Ephesus after Antiquity: A Late Antique, Byzantine and Turkish City*. New York: Cambridge University Press.

- Freidin, C., and I. A. Meir. 2005. "Byzantine Mortars of the Negev Desert." *Construction and Building Materials* 19 (1): 19–23. <https://doi.org/10.1016/j.conbuildmat.2004.05.001>.
- García, E., P. Alfonso, E. Tauler, and S. Galí. 2003. "Surface Alteration of Dolomite in Dedolomitization Reaction in Alkaline Media." *Cement and Concrete Research* 33 (9): 1449–56. [https://doi.org/10.1016/S0008-8846\(03\)00096-6](https://doi.org/10.1016/S0008-8846(03)00096-6).
- Granger, F. 1931. *Vitruvius on Architecture*. Edited fro. London: William Heineman/ New York: G. P. Putnam's Sons.
- Grimoldi, A., M. P. Riccardi, M. Cantu', M. Cofani, A. Landi, and S. C. Tarantino. 2014. "Earthen Mortars in Cremona: Characterization and First Hypothesis of Dating." *9th International Masonry Conference 2014 in Guimaraes*, 1–8.
- Güleç, A., and T. Tulun. 1996. "Studies of Old Mortars and Plasters from the Roman, Byzantine, and Ottoman Period of Anatolia." *Architectural Science Review* 39 (1): 3–13. <https://doi.org/10.1080/00038628.1996.9697352>.
- Gürdal, E., G. Kahraman Altaş, and S. Acun Özgünler. 2011. "The Investigation of the Properties of the Khorasan Mortars Used in Early-Age Byzantine Religious Buildings in Istanbul." *Vakıf Restorasyon Yıllığı*, 63–72.
- Haga, K., M. Shibata, M. Hironaga, S. Tanaka, and S. Nagasaki. 2002. "Silicate Anion Structural Change in Calcium Silicate Hydrate Gel on Dissolution of Hydrated Cement." *Journal of Nuclear Science and Technology* 39 (5): 540–47. <https://doi.org/10.1080/18811248.2002.9715232>.
- Haldar, S. K., and J. Tišljär. 2014. *Introduction to Mineralogy and Petrology*. Elsevier. <https://doi.org/10.1016/C2012-0-03337-6>.
- Hazinedar Coşkun, T. 2021. "Byzantine Glass Samples Belonging to Seasons of 2017-2020 in Kuşadası, Kadıkalesi Excavation." *Sanat Tarihi Dergisi* 30 (2): 1019–37. <https://doi.org/https://doi.org/10.29135/std.901513>.
- Hodgkinson, E. S., and C. R. Hughes. 1999. "The Mineralogy and Geochemistry of Cement/Rock Reactions: High- Resolution Studies of Experimental and Analogue Materials." *Geological Society Special Publication* 157: 195–211. <https://doi.org/10.1144/GSL.SP.1999.157.01.15>.

- Holmes, S., and M. Wingate. 1997. *Building with Lime: A Practical Introduction*. 2nd ed. London.
- Hörmann, H., J. Keil, and G. A. Sotiriou. 1951. “Die Johanneskirche (Forschungen in Ephesos IV. 3).” Vienna.
- ICOMOS. 1964. “International Charter for the Conservation and Restoration of Monuments and Sites (The Venice Charter).”
- ICOMOS. 2013. “Mimari Mirası Koruma Bildirgesi.”
- Kahraman Altaş, G., S. Acun Özgünler, and E. Gürdal. 2013. “Investigation of the Properties of the Khorasan Mortar Used in the Defense Structures in Istanbul.” *Vakıf Restorasyon Yıllığı* 6.
- Kanmaz, M. B. 2015. “Evaluation of Conservation Problems of Anaia Byzantine Church, Kadıkalesi, Kuşadası.” Izmir Institute of Technology. <http://openaccess.iyte.edu.tr:8080/handle/11147/4578>.
- Kanmaz, M. B., and B. İpekoğlu. 2016. “Restorations Due to Earthquakes in the Ancient Cities: Anaia Byzantine Church.” *Kargir Yapılarda Koruma ve Onarım Semineri VIII*, 189–205.
- Karabacak, E. 2010. “Kuşadası, Kadıkalesi Kazısında Ortaya Çıkan Kilise/ Manastır Kompleksinin Mimarisi.” Ege University.
- Karydis, N. 2015. *Jahreshefte Des Österreichischen Archäologischen Institutes in Wien*. Austria: Verlag Holzhausen GmbH.
- Koçyiğit, A. 2015. “An Overview on the Main Stratigraphic and Structural Features of a Geothermal Area: The Case of Nazilli-Buharkent Section of the Büyük Menderes Graben, SW Turkey.” *Geodinamica Acta* 27 (2–3): 85–109.
- Kozlu, H., and A. Ersen. 2011. “Kayseri’ de Roma, Bizans, Selçuklu ve Osmanlı Dönemi Yapıları Harçlarının Özellikleri ve Onarım Harçları Tasarımı.” *ITU Journal Series A: Architecture, Planning, Design* 10 (1): 125–36. <http://search.ebscohost.com/login.aspx?direct=true&db=a9h&AN=64925288&site=ehost-live>.

- Krautheimer, R. 1986. *Early Christian and Byzantine Architecture. Jubulon*. 4th ed. New Haven and London: Yale University Press.
<https://www.ancient.eu/image/8974/church-of-the-holy-apostles-athens/>.
- Kurugöl, S., and A. Güleç. 2012. “Physico-Chemical, Petrographic, and Mechanical Characteristics of Lime Mortars in Historic Yoros Castle (Turkey).” *International Journal of Architectural Heritage* 6 (3): 322–41.
<https://doi.org/10.1080/15583058.2010.540072>.
- Ladstaetter, S., M. Büyükkolancı, E. Uluşan, U. Özdemir, and B. Sayar. 2015. “Ephesus-Nomination File.”
<https://whc.unesco.org/uploads/nominations/1018rev.pdf>.
- Lanas, J., J. L. Pérez Bernal, M. A. Bello, and J. I. Alvarez Galindo. 2004. “Mechanical Properties of Natural Hydraulic Lime-Based Mortars.” *Cement and Concrete Research* 34 (12): 2191–2201. <https://doi.org/10.1016/j.cemconres.2004.02.005>.
- Lazell, E. W. 1915. *Hydrated Lime*. Pittsburgh: Jackson-Remlinger PTG. CO.
- Lee, S., Y. J. Kim, and H. S. Moon. 1999. “Phase Transformation Sequence from Kaolinite to Mullite Investigated by an Energy-Filtering Transmission Electron Microscope.” *Journal of the American Ceramic Society*.
<https://doi.org/10.1111/j.1151-2916.1999.tb02165.x>.
- Lemerle, P. 1965. *Travaux Et Mémoires*.
- Luxán, M. P., and F. Dorrego. 1996. “Ancient XVI Century Mortar from the Dominican Republic: Its Characteristics, Microstructure and Additives.” *Cement and Concrete Research* 26 (6): 841–49. [https://doi.org/10.1016/0008-8846\(96\)00073-7](https://doi.org/10.1016/0008-8846(96)00073-7).
- Luxan, M. P, F Madruga, and J Saavedra. 1989. “Rapid Evaluation of Pozzolanic Activity of Natural Products by Conductivity Measurement.” *Cement and Concrete Research* 19: 63–68.
- Macdonald, W. L. 1965. *The Architecture of the Roman Empire*. New Haven and London: Yale University Press.
- Maitre, R. W. Le, A Streckeisen, B Zanettin, M. J. Le Bas, B. Bonin, P. Bateman, G Bellieni, et al. 2002. *Igneous Rocks. A Classification and Glossary of Terms*. 2nd Editio. New York: Cambridge University Press.

- Mango, Cyril. 1976. *Byzantine Architecture*. London: Faber and Faber Limited.
- Maria, S. 2016. "Use of Natural Pozzolans with Lime for Producing Repair Mortars." *Environmental Earth Sciences* 75 (9). <https://doi.org/10.1007/s12665-016-5444-5>.
- McCarthy, M. J., and T. D. Dyer. 2019. "Pozzolanas and Pozzolanic Materials." In *Lea's Chemistry of Cement and Concrete*, edited by Peter C. Hewlett and Martin Liska, 5th ed., 363–467. Elsevier.
- McGennis, R.B., R.M. Anderson, T.W. Kennedy, and S. M. 1995. "Background of Superpave Asphalt Mixture Design and Analysis."
- Mercangöz, Z. 2002. "Kuşadası Kadı Kalesi Kazısı 2001 Yılı Çalışmaları." *24. Kazı Sonuçları Toplantısı 2. Cilt*, 125–38.
- Mercangöz, Z. 2005. "Kuşadası, Kadıkalesi in Its 4th Year/Anaia Kazısı" 1 (April): 205–23.
- Mercangöz, Z. 2008. "Kuşadası, Kadıkalesi Kazısı 2006 Yılı Çalışmaları." *29. Kazı Sonuçları Toplantısı 3: 449–70*.
- Mercangöz, Z. 2010. "The Variable Historical Destiny of Anaia as Emporion and Kommerkion." *I. Uluslararası Sevgi Gönül Bizans Araştırmaları Sempozyumu*, 279–92.
- Mercangöz, Z. 2012. *Kuşadası, Kadıkalesi (Anaia)*. Edited by Altan Çilingiroğlu, Zeynep Mercangöz, and Gürcan Polat. 1st ed. İzmir: Ege Üniversitesi Yayınları.
- Mercangöz, Z. 2013. *Byzantine Craftsman-Latin Patrons*. Ege Üniversitesi Yayınları.
- Mercangöz, Z. 2018. "Doğu Akdeniz İslam Topraklarından Bir Bizans Kalesine: Kuşadası, Kadıkalesi'nde Orta Çağ İslam Seramikleri" *17 (93): 93–117*. <https://doi.org/10.22520/tubaked.2018.17.006>.
- Mercangöz, Z., and E. Tok. 2011. "Kuşadası Kadıkalesi 2010 Kazı Sezonu Çalışmaları." *33. Kazı Sonuçları Toplantısı 2. Cilt*, 353–71.
- Mercangöz, Z., E. Tok, and T. Hazinedar Coşkun. 2012. "Kuşadası, Kadıkalesi Kazısı

2011 Yılı Çalışmaları.” 34. Kazı Sonuçları Toplantısı 2. Cilt, 2013–15.

- Middendorf, B., J. J. Hughes, K. Callebaut, G. Baronio, and I. Papayianni. 2005. “Investigative Methods for the Characterisation of Historic Mortars - Part 2: Chemical Characterisation.” *Materials and Structures/Materiaux et Constructions* 38 (282): 771–80. <https://doi.org/10.1617/14282>.
- Mimaroğlu, S. 2011. “Kadıkalesi/Anaia Bizans Dönemi Amphoraları.” *Sanat Tarihi Dergisi*, 63–92.
- Mimaroğlu, S. 2011. “Kuşadası, Kadıkalesi/ Anaia Kazısı’nda Ele Geçen Bizans Dönemi Günlük Kullanım Seramikleri.” Ege University.
- Mimaroğlu, S., and E. Karabacak. 2021. “Examples of Phiale from the Basilica of St. John at Ephesus.” *Sanat Tarihi Dergisi* 30 (1): 661–77.
- Miriello, D., A. Bloise, G.M. Crisci, C. Apollaro, and A. La Marca. 2011. “Characterisation of Archaeological Mortars and Plasters from Kyme (Turkey).” *Journal of Archaeological Science* 38 (4): 794–804. <https://doi.org/10.1016/j.jas.2010.11.002>.
- Moropoulou, A., A. Bakolas, and E. Aggelakopoulou. 2001. “The Effects of Limestone Characteristics and Calcination Temperature to the Reactivity of the Quicklime.” *Cement and Concrete Research* 31 (4): 633–39. [https://doi.org/10.1016/S0008-8846\(00\)00490-7](https://doi.org/10.1016/S0008-8846(00)00490-7).
- Moropoulou, A., A. Bakolas, and S. Anagnostopoulou. 2005. “Composite Materials in Ancient Structures.” *Cement and Concrete Composites* 27 (2): 295–300. <https://doi.org/10.1016/J.CEMCONCOMP.2004.02.018>.
- Moropoulou, A., A. Bakolas, and K. Bisbikou. 1995. “Characterization of Ancient, Byzantine and Later Historic Mortars by Thermal and X-Ray Diffraction Techniques.” *Thermochimica Acta* 269–270 (C): 779–95. [https://doi.org/10.1016/0040-6031\(95\)02571-5](https://doi.org/10.1016/0040-6031(95)02571-5).
- Moropoulou, A., A. Bakolas, and K. Bisbikou. 2000. “Investigation of the Technology of Historic Mortars.” *Journal of Cultural Heritage* 1: 45–58. [https://doi.org/10.1016/S1296-2074\(99\)00118-1](https://doi.org/10.1016/S1296-2074(99)00118-1).
- Moropoulou, A., A. S. Cakmak, G. Biscontin, A. Bakolas, and E. Zendri. 2002.

- “Advanced Byzantine Cement Based Composites Resisting Earthquake Stresses: The Crushed Brick/Lime Mortars of Justinian’s Hagia Sophia.” *Construction and Building Materials* 16: 543–52. [https://doi.org/10.1016/S0950-0618\(02\)00005-3](https://doi.org/10.1016/S0950-0618(02)00005-3).
- Moropoulou, A., A. S. Cakmak, and N. Lohvyn. 2000. “Earthquake Resistant Construction Techniques and Materials on Byzantine Monuments in Kiev.” *Soil Dynamics and Earthquake Engineering* 19 (8): 603–15. [https://doi.org/10.1016/S0267-7261\(00\)00021-X](https://doi.org/10.1016/S0267-7261(00)00021-X).
- Moropoulou, A., K. Labropoulos, P. Moundoulas, and A. Bakolas. 2007. “The Contribution of Historic Mortars on the Earthquake Resistance of Byzantine Monuments.” *Measuring, Monitoring and Modeling Concrete Properties*, 643–52. https://doi.org/10.1007/978-1-4020-5104-3_78.
- MTA. 2005. “İzmir Yakın Çevresinin Diri Fayları ve Deprem Potansiyelleri (Rapor No. 10754).” Ankara.
- Müller-Wiener, Wolfgang. 1961. “Zur Frage Der Stadtbefestigung von Byzantion.” *Bonner Jahrbücher* 161: 165–75.
- Nežerka, V., J. Němeček, Z. Sližková, and P. Tesárek. 2015. “Investigation of Crushed Brick-Matrix Interface in Lime-Based Ancient Mortar by Microscopy and Nanoindentation.” *Cement and Concrete Composites* 55: 122–28. <https://doi.org/10.1016/j.cemconcomp.2014.07.023>.
- Oates, J.A.H. 1998. *Lime and Limestone: Chemistry and Technology, Production and Uses. Lime and Limestone*. Weinheim: Wiley-VCH. <https://doi.org/10.1002/9783527612024>.
- Oğuz, C., F. Türker, and N. U. Koçkal. 2015. “Properties of Roman, Byzantine and Seljuk Period Mortar in Andriake Harbour.” *İMO Teknik Dergi*, 6993–7014.
- Oğuz Kılıç, D., H. Böke, S. Akkurt, and B. İpekoğlu. 2004. “Microstructural and Pozzolanic Characteristics of Bricks Used in Horasan Mortars of Historic St. Jean Church.” *Proceedings of the 10th International Congress on Deterioration and Conservation of Stone*.
- Onar, V., Z. Mercangöz, L. Kutbay, and E. Tok. 2012. *Kuşadası Kadıkalesi (Anaia) Kazısında Ortaya Çıkarılan İşlenmiş Kemik Kalıntıları*. 28. Arkeometri Sonuçları Toplantısı. Çorum: T.C. Kültür ve Turizm Bakanlığı.

- Ötüken, Y. 1990. "Bizans Duvar Tekniğinde Tektonik ve Estetik Çözümler." *Vakıflar Dergisi* 21: 395–410.
- Ousterhout, R. 1999. *Master Builders of Byzantium*. 1st ed. Philadelphia: Princeton University Press.
- Özdoğan, A. 2007. *12000 Yıl Önce Uygarlığın Anadolu'dan Avrupa'ya Yolculuğunun Başlangıcı Neolitik Dönem*. Edited by N. Başgelen. İstanbul: Yapı Kredi Kültür Sanat Yayıncılık.
- Özkaya, Ö. A., and H. Böke. 2009. "Properties of Roman Bricks and Mortars Esed in Serapis Temple in the City of Pergamon." *Materials Characterization* 60 (9): 995–1000. <https://doi.org/10.1016/j.matchar.2009.04.003>.
- Öztan, A. 2009. "Arkeoloji ve Sanat Tarihi Eski Anadolu Uygarlıkları Neolitik Çağ (Yeni Taş/ Cilalı Taş Çağı)." *T.C. Kültür ve Turizm Bakanlığı Türkiye Kültür Portalı Projesi*. Ankara. <https://doi.org/10.1038/132817a0>.
- Pasley, C. W. 1997. *Observations on Limes*. Edited by Wingate Michael. First publ. Donhead.
- Pavía, S., and B. Toomey. 2008. "Influence of the Aggregate Quality on the Physical Properties of Natural Feebly-Hydraulic Lime Mortars." *Materials and Structures/Materiaux et Constructions* 41 (3): 559–69. <https://doi.org/10.1617/s11527-007-9267-4>.
- Pérez-Monserrat, E. M., M. A. Causarano, L. Maritan, A. Chavarria, G. P. Brogiolo, and G. Cultrone. 2022. "Roman Brick Production Technologies in Padua (Northern Italy) along the Late Antiquity and Medieval Times: Durable Bricks on High Humid Environs." *Journal of Cultural Heritage* 54: 12–20. <https://doi.org/10.1016/j.culher.2022.01.007>.
- Pettijohn, F. J. 1957. *Sedimentary Rocks*. 2nd ed. Bombay, Calcutta, Madras: Orient Longmans Private Ltd.
- Polat Pekmezci, I. 2012. "Characterization of Historic Mortars and Plasters in Çukurova Region (Cilicia) and Proposals for Repair Mortara." İstanbul Technical University.
- Ponce-Antón, G., M. C. Zuluaga, L. A. Ortega, and J. A. Mauleon. 2020. "Multi-Analytical Approach for Chemical-Mineralogical Characterization of Reaction

- Rims in the Lime Mortars from Amaiur Castle (Navarre, Spain).” *Microchemical Journal* 152: 1–8. <https://doi.org/10.1016/J.MICROC.2019.104303>.
- Powers, M. C. 1953. “A New Roundless Scale for Sedimentary Particles.” *Journal of Sedimentary Petrology* 23 (2): 117–19.
- Prince, W., G. Castanier, and J. L. Giafferi. 2001. “Similarity Between Alkali-Aggregate Reaction and the Natural Alteration of Rocks.” *Cement and Concrete Research* 31 (2): 271–76. [https://doi.org/10.1016/S0008-8846\(00\)00478-6](https://doi.org/10.1016/S0008-8846(00)00478-6).
- Restle, Marcell. 1967. *Byzantine Wall Painting in Asia Minor*. Vol. 1. New York graphic society.
- RILEM. 1980. “Tests Defining the Structure.” *Materials and Construction*. Vol. 13.
- Rodriguez-Navarro, C., E. Hansen, and W. S. Ginell. 1998. “Calcium Hydroxide Crystal Evolution upon Aging of Lime Putty.” *Journal of the American Ceramic Society* 81 (11): 3032–34. <https://doi.org/10.1111/j.1151-2916.1998.tb02735.x>.
- Selçuk Belediyesi. 2022. “Selçuk Belediyesi.” 2022. <http://www.selcuk.gov.tr/ilcemizin-tarihcesi>.
- Selçuk Kent Belleği. 2022.
- Şengör, A. M. C., and E. Bozkurt. 2013. “Layer-Parallel Shortening and Related Structures in Zones Undergoing Active Regional Horizontal Extension.” *International Journal of Earth Sciences* 102 (1): 101–19. <https://doi.org/10.1007/s00531-012-0777-0>.
- Seyitoğlu, G., and V. Işık. 2009. “Meaning of the Küçük Menderes Graben in the Tectonic Framework of the Central Menderes Metamorphic Core Complex (Western Turkey).” *Geologica Acta* 7 (3): 323–32.
- Soysal, H, S Sipahioğlu, D Kolçak, and Y Altınok. 1981. *Historical Earthquake Catalog of Turkey and Its Surroundings (B.C 2100-A.C 1900)*. İstanbul: Tübitak Yayınları.
- Stefanidou, M., V. Pachta, S. Konopissi, F. Karkadelidou, and I. Papayianni. 2014. “Analysis and Characterization of Hydraulic Mortars from Ancient Cisterns and Baths in Greece.” *Materials and Structures/Materiaux et Constructions* 47 (4):

571–80. <https://doi.org/10.1617/s11527-013-0080-y>.

Strazzera, B., M. Dondi, and M. Marsigli. 1997. “Composition and Ceramic Properties of Tertiary Clays from Southern Sardinia (Italy).” *Applied Clay Science* 12: 247–66.

Taranto, M., L. Barba, J. Blancas, A. Bloise, M. Cappa, F. Chiaravalloti, G. M. Crisci, et al. 2019. “The Bricks of Hagia Sophia (Istanbul, Turkey): A New Hypothesis to Explain Their Compositional Difference.” *Journal of Cultural Heritage* 38: 136–46. <https://doi.org/10.1016/j.culher.2019.02.009>.

Taşcı, B. 2021. “Properties of Lime Binders and Aggregates of Roman Mortars in Western Anatolia.” Izmir Institute of Technology.

Taşcı, B., and H. Böke. 2018. “Properties of Roman Lime Mortars in Ancient Lycia Region.” *AIP Conference Proceedings* 2022. <https://doi.org/10.1063/1.5060692>.

Taylor, H. F. W. 1997. *Cement Chemistry*. Edited by Thomas Telford. Vol. 2. London: Thomas Telford London.

Tekin, Ç., and S. Kurugöl. 2011. “Physicochemical and Pozzolanic Properties of the Bricks Used in Certain Historic Buildings in Anatolia.” *Gazi University Journal of Science* 24 (4): 959–72.

Teutonico, J. M. 1988. *A Laboratory Manual for Architectural Conservators*. Vol. 168. ICCROM Rome.

Texier, C. 2002. *Küçük Asya Coğrafyası, Tarihi ve Arkeolojisi*. Translated by Suat Ali. Ankara: Enformasyon ve Dokümantasyon Hizmetleri Vakfı.

Thucydides. 2009. *The Peloponnesian War*. Translated by Martin Hammond. New York: Oxford University Press.

Tomaschek, W. 1891. *Zur Historischen Topographie von Kleinasien Im Mittelalter*. Edited by F. Tempsky. Vienna.

Tranmer, J. 2015. “AlmaVerde’s Traditional, Working Lime Kiln.” 2015. <https://www.almaverde.com/blog/sustainability/almaverdes-traditional-working-lime-kiln-2/>.

- Uğurlu, E., and H. Böke. 2006. "Osmanlı Dönemi Hamam Yapılarında Kullanılan Horasan Sıvaların Özellikleri." 3. *Ulusal Yapı Malzemesi Kongresi ve Sergisi*, 585–96.
- Uğurlu, E., and H. Böke. 2009. "The Use of Brick–Lime Plasters and Their Relevance to Climatic Conditions of Historic Bath Buildings." *Construction and Building Materials* 23 (6): 2442–50. <https://doi.org/10.1016/J.CONBUILDMAT.2008.10.005>.
- Uğurlu Sağın, E., H. E. Duran, and H. Böke. 2021. "Lime Mortar Technology in Ancient Eastern Roman Provinces." *Journal of Archaeological Science: Reports* 39 (July). <https://doi.org/10.1016/j.jasrep.2021.103132>.
- Ulukaya, S., A. B. Hazar Yoruç, N. Yüzer, and D. Oktay. 2017. "Material Characterization of Byzantine Period Brick Masonry Walls Revealed in Istanbul (Turkey)." *Periodica Polytechnica Civil Engineering* 61 (2): 209–15. <https://doi.org/10.3311/PPci.8868>.
- Vicat, L. J. 1837. *Mortars and Cements*. 1997 Editi. Shaftesbury: Donhead Publishing. <https://doi.org/10.1038/scientificamerican12021905-25016bsupp>.
- Vitruvius, P. 1960. *The Ten Books on Architecture*. Edited by M.H. Morgan. First publ. New York: Dover Publications.
- Ward-Perkins, J. B. 1970. *Roman Imperial Architecture*. Yale University Press.
- Wiegand, T., and H. Schrader. 1904. *Priene: Ergebnisse Der Ausgrabungen Und Untersuchungen in Den Jahren 1895-1898*. Berlin: Georg Reimer.
- Zacharopoulou, G. 1998. "The Renascence of Lime Based Mortars Technology an Appraisal of a Bibliography Study," 89–114.
- Zamba, I. C., M. G. Stamatakis, F. A. Cooper, P. G. Themelis, and C. G. Zambas. 2007. "Characterization of Mortars Used for the Construction of Saithidai Heroon Podium (1st Century AD) in Ancient Messene, Peloponnesus, Greece." *Materials Characterization* 58: 1229–39. <https://doi.org/10.1016/j.matchar.2007.07.004>.